Dedicated to Prof. György L. Balázs for his 65th birthday

2023

Vol. 24

Biner 12. 2020 – concrete coloured in
its materil and painted

100 x 51 x 35 cm

Prepared by: Csurgai Ferenc, Hungarian
sculptor

CONTENT

HISTORY OF FIB INTERNATIONAL PHD SYMPOSIA IN CIVIL ENGINEERING

György L. Balázs

The International PhD Symposia in Civil Engineering were developed to increase the international exposure of young researchers preparing their PhD Theses. It has been realised that the PhD students needed a particular forum above their PhD programmes to present and discuss the results of their ongoing research and to collect pieces of advice on how to continue the research. This forum should have been very similar to what we generally have for technical or scientific presentations and to collect opinions on a large scale. It is called PhD Symposium. Many thanks for the continuous support of CEB (Committeé Euro- International du Béton) then to fib (International Fedération du Béton).

The PhD Symposium in Civil Engineering system was initiated by the Faculty of Civil Engineering at the Budapest University of Technology (BME) in 1996. Many universities have successfully followed this idea in Europe, North America and Asia:

1996 Budapest Univ. of Techn. (BME), Budapest, Hungary	2012 Karlsruhe Institute of Techn. (KIT), Karslruhe, Germany
1998 Budapest Univ. of Techn. (BME), Budapest, Hungary	2014 Université Laval, Quebec City, Canada
2000 University of Applied Sciences, Vienna, Austria	2016 The Tokyo University, Tokyo, Japan
2002 Technical Univ. of Münich and Univ. of Federal Armed Forces Münich, Münich Germany	2018 Technical Univ. of Prague, Prague, Czechia
2004 Research School Structural Eng., Delft University of Technology, Delf, The Nederlands	2020 University Gustave Eiffel, Paris, France
	2021 University Gustave Eiffel, Paris, France
2006 ETH Zürich, Zürich, Switzerland	2022 University of Rome, Tor Vergata,Rome, Italy
2008 University Stuttgart, Stuttgart, Germany	2024 Budapest University of Techology and Economics (BME), Budapest, Hungary
2010 Tech. Univ. of Denmark, Lyngby, Denmark	

1. IMPORTANCE OF PHD

The highest level in the university curriculum is PhD research. The objective of the PhD system is to provide highly qualified engineers who can lead research and teach, on the one hand, or realise special applications, on the other hand.

The PhD research should always include a wide knowledge of related basic subjects and a deep knowledge of specific research areas.

Every PhD system requires a synthesis of results with clarification of a new and promising field of development. These new developments are essential for universities' future activities and for proceeding with technical solutions in the industry.

The selection of PhD candidates is a careful process at universities to ensure successful PhD research. Key factors for the success of PhD research are the selection of the PhD topic, the dedication of the PhD student to the topic, the ability of the PhD student to synthesise results, and the supervision of the PhD research.

The system of PhD studies differs slightly from different universities. Still, the basic requirements are practically the same: a high-level PhD Thesis should be submitted within a limited period.

The pressure on the PhD students is high, especially in recognition of the level of results.

The general rule for the PhD candidate is to defend the Thesis in front of a PhD Committee of experts from the own university or outside of the university.

The organisation of the PhD Thesis is not the same in various universities: there could be a limit on the number of pages.

A PhD degree from anywhere is considered to be ready to solve complex questions.

2. IDEA OF PHD SYMPOSIA

It is a pleasure to summarise the intentions and the successes of the PhD Symposia.

The principal intention of developing the first idea for an international PhD Symposia was to increase the international exposure of young researcher preparing their PhD Thesis. This is a challenging time for them with a lot of effort before the synthesis of results provides the final conclusions to submit the PhD Thesis.

You can find the locations of the International PhD Symposia in Civil Engineering in *Fig. 1,* and also which has already been planned for the next year.

The Faculty of Civil Engineering at the Budapest University of Technology (BME) initiated the system of the International PhD Symposium in Civil Engineering in 1996 (the present name is Budapest University of Technology and

Fig. 1: Locations of the International PhD Symposia in Civil Engineering 1996-2024 (Courtesy to *fib*) (*Table 1*)

PhD Symposia locations

1996 in Budapest, Hungary
1998 in Budapest, Hungary
2000 in Vienna, Austria
2002 in München, Germany
2004 in Delft, The Netherlands
2006 in Zurich, Switzerland
2008 in Stuttgart, Germany
2010 in Lyngby, Denmark
2012 in Karlsruhe, Germany
2014 in Quebec, Canada
2016 in Tokyo, Japan
2018 in Prague, Czech Republic
2020-21 in Paris, France
2022 in Rome, Italy

Next Symposium: 2024 in Budapest, Hungary

Economics, BME). At Openings, it is often mentioned that „Prof. György L. Balázs developed the concept, and the first edition took place in 1996 in Budapest".

The reason for initiating such a special Symposium was to help the PhD students succeed with their PhD research and their PhD defence.

It finally realised that the PhD students needed a *special forum* above their PhD programmes to present and discuss the results of their ongoing research and to collect advice on how to continue the research. This forum should have been very similar to what we generally have for technical or scientific presentations and to gather opinions on a large scale. It is called PhD Symposium.

Fig. 2: The Symbolic Stone of the PhD Symposia at the events at Karlsruhe Institute of Techn. (KIT), PhD Symposium 2012 and at Université Laval, Quebec City, Canada, PhD Symposium 2014
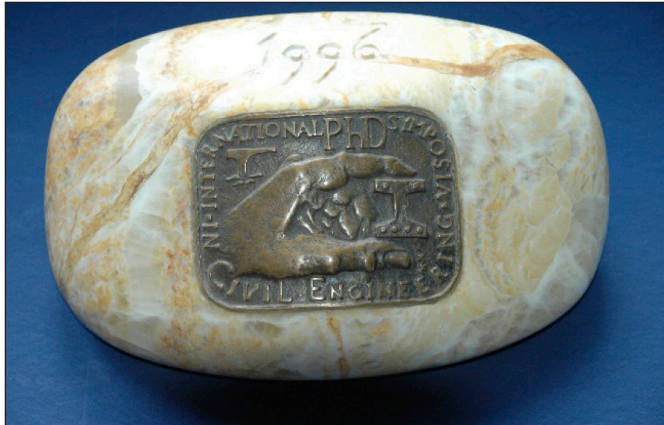
Bronze relief at the front of the Symbolic stone
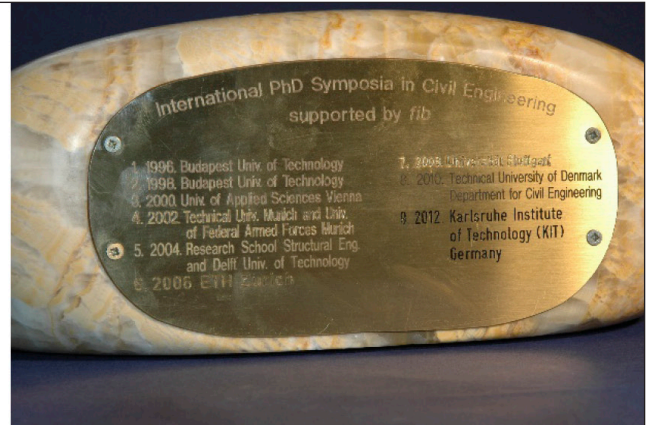
Back plate at the Symbolic stone to include the names of organizing universities

A Symbol of the PhD Symposia – short name: PhD stone – was developed at the beginning as a piece of Onyx natural stone of 11 kg with a bronze relief in front and a copper plate indicating the names of the subsequent who organised it (*Fig. 2*).

3. STRUCTURE OF PHD SYMPOSIA

The system of the PhD Symposia is to have oral presentations by the PhD students themselves. Then, the presentations are discussed immediately afterwards. The main results of the study are summarised in the Symposium Proceedings.

3.1 Obligatory discussion time after every presentation

An essential role of the PhD Symposium is to help the PhD students prepare for the defence of the Thesis. During the defence of the Thesis, the PhD candidate has to answer complex questions orally concerning the technical content of the Thesis.

One important speciality of the PhD Symposium is to have *20 minutes of presentation time and an obligatory 10 minutes of discussion time after every presentation, or alternatively, 15 minutes of presentation time and an obligatory 15 minutes of discussion time* after every presentation. In any case, define a block of 30 minutes for every presentation. The Chairmen are responsible for reasonably using the discussion time. The audience is, of course, allowed to ask questions too.

The unique characteristics of the PhD Symposia are summarised in the following:
1. *Only PhD candidates and not their supervisors are allowed to give the presentation*s.
2. Ample time is given for discussions after every presentation. Discussions are essential parts of these Symposia. This way, we want to help our young colleagues proceed with their research. Chairmen and charladies are reasonable to stimulate discussions.
3. *The Symposia provides good opportunities to meet other researchers from the same or similar fields to* your research fields.
4. Finally, at these Symposia, *the registration fee must be low* (I suggest not more than 200 EURs as the early bird) in order not to stop any young colleagues from participating.

These objectives were established in 1996 during the 1st International PhD Symposium.

The international character of the PhD Symposia has been created by the 1st PhD Symposium in Budapest owing to the immediate support of an international association the Committeé Euro- International du Béton (CEB). Then it was supported by *fib*. CEB merged with FIP in 1998 and formed *fib* = International Fedération du Béton.

3.2 Charpersons

Chairpersons of the Sessions are always invited from an internationally recognised university. Co-chairs are also professors or colleagues from the industry with PhD degrees.

A new idea that successful works – established at the PhD Symposium 2020 Paris – to have a third Co-chair carefully selected from young engineers (with or without PhD degree).

3.3 Evaluations and Prizes

All written and oral presentations are evaluated by the Chairpersons and discussed by the Scientific Committee.

Fig. 3: *Opening speech of Prof. Josée Bastien during the PhD Symosium 2014 at Université Laval in Quebec City*

Prizes are delivered by the Closing ceremony for the best presentations.

3.4 Organising universities

It is always organised by an important university in civil engineering by Professors in Civil Engineering. There is always a preliminary list of interested universities to organise in the future.

There is a unique process to deliver the Symbolic Stone of the event from one organiser to the other. *Fig. 3* indicates the delivery from Quebec City to Tokyo.

3.5 Proceedings

For every PhD Symposia in Civil Engineering the written form of presentations are published in the Proceedings that are available free of charge on the internet (list appended).

3.6 Organising universities

It is always organised by an important university in civil engineering by Professors in Civil Engineering. Many thanks for the professor colleagues for offering their time and efforts to organize the PhD Symposia at their universities and in the same time for helping the PhD students. The collaboration of universities was excellent. The collaboration of the Karlsruhe Institute of Technology (KIT) as organizer for 2012 and the Université Laval, Quebec City as organizer for 2014 is symbolicaly indicated in Fig, 3 form the speech of Prof. Josée Bastien at the Opening of the PhD Symosium 2014 at Université Laval in Quebec City.

There is a unique process to deliver the Symbolic Stone of the event from one organiser to the other. Fig. 3 indicates the delivery e.g. from the
- Technical University of Denmark, Lungby (2010) to the Karlsruhe Institute of Technology (2012) *(Fig. 4.a)*,
- the Karlsruhe Institute of Technology (2012) to the Université Laval, Quebec City (2014) *(Fig. 4.b)*
- the Université Laval, Quebec City (2014) to The University of Tokyo *(Fig. 4.c)*

4. PARTICIPATING UNIVERSITIES

Typically, 40-60 universities are represented by PhD Symposia. This indicates an interest from many countries and many universities.

Participation from BME, Hungary, was always considerably high, with 6 to 15 participants. An example of Karlsruhe in 2012 is shown in *Fig. 5* for 10 BME participants.

5. LEVEL OF PHD SYMPOSIA

The general opinion of the previous PhD Symposia about the level of presentations is very high based on the following reasons:

Fig. 4.a: *The Scientific Committee of Professors for the Technical University of Denmark, Lungby (2010) and delivery of the Symbolic Stone to the Karlsruhe Institute of Technology (2012)*

Fig. 5: *Participants from BME, Hungary, at the PhD Symposium 2012 KIT Karlsruhe, Germany*

Fig. 4.b: *The Scientific Committee of Professors for the Karlsruhe Institute of Technology (2012) and delivery of the Symbolic Stone to the Université Laval, Quebec City (2014)*

- only PhD candidates are allowed to give presentations who work hard on an interesting research topic to reach significant, reliable results,
- the PhD candidates prepared for an extended discussion time (longer than any other conferences) after every presentation. That means the speakers must be prepared very carefully,
- the PhD candidates intend to understand the topic fully; hence, they go into many details experimentally, analytically, or numerically respectively.

6. PROFESSORSHIP RELATED TO THE PHD SYMPOSIA

To receive a professorship is difficult at any university in the world. It requires a high quality of research and teaching capacity and successful coordination in research work to be recognised internationally. It means that our research is embedded into a judgement of the international research community and, in this way, the evaluation of the professorships, too.

We intend to establish a collection of names of colleagues who participated as a PhD students at any of the PhD Symposia and completed their career as Profs. or Assoc. Profs.

7. CONCLUSIONS

The ***fib*** International PhD Symposium is a special forum for PhD students in civil engineering to help to finalise their PhD Thesis and defend it.

The unique characteristics of the PhD Symposia are summarised in the following:
a. *Only PhD candidates and not their supervisors are allowed to give the presentations.*
b. Ample time is given for discussions after every presentation. Discussions are essential parts of these Symposia. This

Fig. 4.c: *The Scientific Committee of Professors for PhD Symp 2014 Quebec City and delivery of the Symbolic Stone for PhD Symp 2016 Tokyo*

way, we want to help our young colleagues proceed with their research. Chairpersons are reasonable to stimulate discussions.

c. *The Symposia provides good opportunities to meet other researchers from the same or similar fields to* your research fields.

d. Finally, at these Symposia, *the registration fee must be low* (I suggest not more than 200 EURs as the early bird) in order not to stop any young colleagues from participating.

These objectives were established exactly in the same way in 1996 during the 1st International PhD Symposium and kept all along.

8. ACKNOWLEDGEMENTS

Table 1: *PhD Symposia in Civil Engineering 1996 – Organising universities and the names of main organizers*

Nr.	Year	Organising universities	Country	Name of main organisers
1.	1996	Budapest University of Technology (BME)	Hungary	Prof. György L. Balázs
2.	1998	Budapest University of Technology (BME)	Hungary	Prof. György L. Balázs
3.	2000	University of Applied Sciences, Wien	Austria	Prof. Konrad Bergmeister
4.	2002	Technical University of München and Univ. of Federal Armed Forces Münich	Germany	Prof. Peter Schiessl Prof. Norbert Gebbeken Prof. Manfred Keuse Prof. Konrad Zilch
5.	2004	Research School Structural Eng., Delft University of Technology	The Netherlands	Prof. Joost Walraven Prof. Johan Blaauwendraad Prof. Tom Scarpas Prof. Bert Snijder
6.	2006	ETH Zürich	Switzerland	Prof. Peter Marti
7.	2008	University Stuttgart	Germany	Prof. Rolf Eligehausen Prof. Christoph Gehlen
8.	2010	Technical University of Denmark (DTU), Lyngby	Denmark	Prof. Gregor Fischer Assoc. Prof. Mette Geiker Assoc. Prof. Ole Hededal Assoc. Prof. Lisbeth Ottosen Prof. Henrik Stang
9.	2012	Karlsruhe Institute of Technology (KIT)	Germany	Prof. Harald Müller Assoc. Prof. Michael Haist Assoc. Prof. Fernando Acosta
10.	2014	Université Laval, Quebec City	Canada	Prof. Josée Bastien Prof. Nicolas Rouleau Prof. Mathieu Fiset Prof. Mathieu Thomassin
11.	2016	The Tokyo University	Japan	Prof. Koich Maekawa Dr. Akio Kasuga
12.	2018	Chech Technical University, Prague	Chechia	Prof. Petr Hajek Prof. Jan Vítek
13.	2020 & 2021	Gustav Eiffel University, Paris	France	Prof. Jean-Michel Torrenti Prof Fabrice Gatuingt
14.	2022	University of Rome, La Torre Vergata, Roma	Italy	Prof. Marco di Prisco Prof. Alberto Meda
15.	2024	Budapest University of Technology	Hungary	Prof. György L. Balázs Dr. Sándor Sólyom

INTERNATIONAL PHD SYMPOSIA IN CIVIL ENGINEERING SUPPORTED BY *fib*

1996 Budapest Univ. of Techn. (BME)
1998 Budapest Univ. of Techn. (BME)
2000 University of Applied Sciences, Vienna
2002 Technical Univ. of Münich and Univ.
  of Federal Armed Forces Münich
2004 Research School Structural Eng.,
  Delft University of Technology

2006 ETH Zürich
2008 Universität Stuttgart
2010 Tech. Univ. of Denmark, Lyngby
2012 Karlsruhe Institute of Techn. (KIT)
2014 Université Laval, Quebec City
2016 The Tokyo University
2018 Technical Univ. of Prague
2020 University Gustave Eiffel, Paris
2021 University Gustave Eiffel, Paris
2022 Uni. of Rome" Tor Vergata
2024 Budapest Univ. of Technology and Economics (BME)

PHD SYMPOSIA PROCEEDINGS
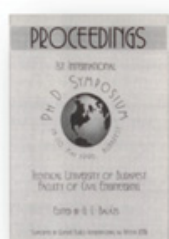
1st *fib* International PhD Symposium in Civil Engineering

May 1996, Technical University of Budapest, Budapest, Hungary

order info:
  Balázs, György (Ed.)
  Sokszorositotta a Muegyetemi Kiado
  Risograph technologiaval
  Fedelos vezeto: Veress Janos
  Munkaszam: 96-Mk10
  E-Mail: *fib*@eik.bme.hu
  ISBN 963 420 504 6

2nd *fib* International PhD Symposium in Civil Engineering

August 1998, Technical University of Budapest, Budapest, Hungary

order info:
  Balázs, György (Ed.)
  ISBN 963 420 560 7
  Publishing Company of Technical University of Budapest
  Head: Janos Veress
  Offset printing No: 98-0134
  E-Mail: *fib*@eik.bme.hu

3rd *fib* International PhD Symposium in Civil Engineering

October 2000, University of Agricultural Sciences Vienna, Vienna, Austria

order info:
  IKI - Institute for Structural Engineering,
  BOKU - University of Agricultural Sciences,
  Peter Jordanstr. 82, A-1190 Vienna, Austria
  Phone: +43 1 47654 5250
  Fax: +43 1 47654 5292
  E-mail: lilo@iki.boku.ac.at
  ISSN 1028-5334

4th *fib* International PhD Symposium in Civil Engineering

September 2002, Technische Universität München, Universität der Bundeswehr München, München, Germany

order info:
  Springer-VDI-Verlag GmbH & Co. KG
  Düsseldorf, Germany
  ISBN 3-935065-09-4

5th *fib* International PhD Symposium in Civil Engineering

2004, Delft University of Technology, Delft, The Netherlands

order info:
W. Sutjiadi
Faculty of Civil Engineering and Geosciences
Delft Univ. of Technology
Stevinweg 1, 2628 CN Delft, The Netherlands
Tel: +31 15 278 4665
Fax: +31 15 278 7313
E-mail: w.sutjiadi@ct.tudelft.nl
ISBN Vol 1: 90 5809 677 7
ISBN Vol 2: 90 5809 678 5

6th *fib* International PhD Symposium in Civil Engineering

August 2006, ETH Zurich, Zurich, Switzerland

order info:
fib secretariat
Case Postale 88,
CH-1015 Lausanne, Switzerland
Phone: + 41 21 693 2747
Fax: + 41 21 693 6245
E-mail: fib@epfl.ch

7th *fib* International PhD Symposium in Civil Engineering

September 2008, University of Stuttgart, Stuttgart, Germany

order info:
PhD Symposium Secretariat
IWB Universität Stuttgart
Pfaffenwaldring 4
70569 Stuttgart, Germany
Phone: +49 711 685 63320
Fax: +49 711 685 67681
E-mail: stumpp@iwb.uni-stuttgart.de

8th *fib* International PhD Symposium in Civil Engineering

June 2010, Technical University of Denmark, Kgs. Lyngby, Denmark

order info:
Technical University of Denmark
Department of Civil Engineering, Brovej, Building 118,
DK-2800 Kgs. Lyngby, Denmark
Phone: + 45 45 25 17 00
Fax: + 45 45 88 32 82
E-Mail: byg@byg.dtu.dk

9th *fib* International PhD Symposium in Civil Engineering

July 2012, Karlsruhe Institute of Technology (KIT), Karlsruhe, Germany

Order info:
KIT Scientific Publishing
Straße am Forum 2
D-76131 Karlsruhe, Germany
Phone: + 49 721 608 43104
Fax: + 49 721 608 44886
E-mail: info@ksp.kit.edu
available as download at: http://www.ksp.kit.edu

10th *fib* International PhD Symposium in Civil Engineering

July 2014, Université Laval, Quebec , Canada

Order info:
Research Centre on Concrete Infrastructure (CRIB),
Université Laval,
Quebec (Quebec),
Canada, G1V 0A6
Phone : + 418-656-3303
E-mail : josee.bastien@gci.ulaval.ca
available as download at: https://www.fib-phd.ulaval.ca

15th fib PhD Symposium Hungary 2024

August 28th to 30th 2024
Budapest, Hungary

This is a special invitation for you to participate in the *fib* PhD Symposium 2024 Budapest and to give your presentation as well as to extend your communication with the researchers at this event.

The system of the **PhD Symposium in Civil Engineering** was initiated by the Faculty of Civil Engineering of the Budapest University of Technology and Economics (BME) in 1996. It has been organized every second year at a famous university then.

The reason for initiating such a special Symposium was to provide help to the PhD students to be successful with their PhD research and their PhD defence.

Hope to meet you there,

BUDAPEST UNIVERSITY
OF TECHNOLOGY AND ECONOMICS
Faculty of Civil Engineering - Since 1782

Topics

You are kindly invited to submit your manuscript that is particularly relevant to one or more of the following topics:

Structures

- Structural analysis, modeling and design
- Bridges, dams and tunnels
- Buildings and shells
- Structural reliability and risk analysis

Concretes

- Innovations in concrete and concrete technology
- History of concrete structures and assessment of heritage concrete structures
- 3D concrete printing

Objectives

1. **Only PhD candidates are allowed to give the presentations** and not their supervisors.

2. There is ample time for discussion after each presentation. Discussions are an essential part of the Symposium. Chairmen and chairwomen are encouraged to stimulate discussion.

3. **The Symposium provides good opportunities to meet other researchers** from the same or similar fields of your research fields.

4. **The registration fee must be low** in order not to stop any young colleagues from the participation.

Registration and fees

Registration visiting

https://fibphdsymp2024.bme.hu

The conference fee will be € 250. This covers participation, coffee breaks, lunches, social dinner and the e-proceedings.

Dates and Registration

February 29, 2024	Submission of abstracts
March 31, 2024	Acceptance of abstracts
May 15, 2024	Full paper submission
June 15, 2024	Full paper review
June 30, 2024	Full paper acceptance

Organizing Commitee

György L. Balázs, Sándor Sólyom, András Bíró, Szabolcs Szinvai

Faculty of Civil Engineering

Budapest University of Technology and Economics

Műegyetem rkp 3, 1111, Budapest, Hungary

fibphdsymp2024@emk.bme.hu

Sustainability, durability, service life

- Sustainability of materials and structural systems
- Durability of existing structures and durability for future structures
- Life cycle assessment and design. Rest life

Maintenance, retrofitting, strengthening

- Assessment and structural health monitoring
- Composites for concrete structures
- Maintenance, retrofitting or strengthening of concrete structures

The Symposium

The PhD Symposia started in 1996. The concept was developed by Prof György Balázs. The first edition took place in 1996 in Budapest, Hungary with the support of *fib (International Fedération du Béton)*.

The Symposium provides a **special forum** for PhD students to present and discuss the results of their ongoing research and to gather advice on how to continue the research.

The system of the PhD Symposium is to have oral presentations by the PhD students themselves, then the presentations are immediately discussed, which is an obligatory and outmost important part of the PhD Symposium.

The main results of the study are summarized in the Symposium Proceedings which is openly available for all previous PhD Symposia.

Evaluation and Prizes

All the written and oral presentations are evaluated by the Chairpersons and discussed by the Scientific Committee. Prizes are delivered by the Closing ceremony for the best presentations.

APPRECIATION TO PROF. GYÖRGY L. BALÁZS BY HIS MOST RECENT PHD STUDENT

I am deeply honored to be granted the opportunity to give my greetings ad appreciation on the 65th years birthday celebration of Prof. Dr.-habil Balázs L. György to him, as I was honored the first time when he accepted me to be his PhD student back in 2017. I still remember the first time I met him when he gave me, right after the interview, the 2nd edition of Concrete Technology book written by Neville. Two days later, he asked me if I have finished reading that book of almost 500 pages! I was shocked at the beginning before realizing his strong dedication toward work coupled with the genuine sense of humor. Over the next five years of closely working together, his uplifting and positive encouragement alongside his amusing sense of humor helped me a lot to have a professionally successful and personally happy life during my PhD studies.

Professionally wise, during the period of his supervision, Prof. Balázs taught me all what I need to proceed in my the academic and research field. He used to provide me with valuable lessons in a regular basis, including even how to read a figure, "the good figure is readable and understandable figure in 5 seconds" he said. He taught me how to write technical sentences with the shortest form possible to be simply and understandable for the reader. "Simplicity is the most elegant way of efficiency and effectiveness, and once you will be able to do that, you will enjoy it" he says. Well, I will have to admit now that I enjoy it, and I promise to deliver these precious and beneficial pieces of advice to the next generation. I also remember his endeavors to make Lebanon, Tunisia and UAE joining the *fib* during his remarkably successful Presidency of the International Organization during 2011-2012. One of the lessons I have learned is dedication, when I used to receive his emails at the very early time of the day, as well as I remember him preparing for an opening of the *fib* conference held in Prague, when I saw him reading a full book about Prague to give a short presentation in the city.

Personally wise, my connection with Prof. Balázs goes beyond classes and papers. Our thoughtful discussions about life, personalities, travel, and even politics had a great impression and influence on me. I still remember when I was reading about the group of the Hungarian scientists that immigrated to the USA achieving profound discoveries and achievements, or "The Martians" as they were called in the scientific community. I also still remember when I was trying to write a cover letter for the first time to apply for postdoc positions, when I quoted "my philosophy in life is to love all, trust a few, and do wrong to none", he suggested to change it, "we don't put trust issues or any negative words that could affect the reader". I humorously argued then that this is not my fault, it is Shakespeare's fault. I also cannot forget his great

Photo taken after the PhD defence of Naser Alimrani (left)

generosity by inviting me many times in fancy restaurants in Budapest, including an exceptional invitation one hour before my final defense when we had a delightful conversation about our families.

One of our remarkable discussions was also when he told me about his wallet that has been lost in Spain one time, when a guy found it and brough it to him with no reward or remuneration. Even when he asked the guy to take some money as a reward for his good deed, the guy refused. He always appreciated "niceness and kindness" the most.

Prof. Balázs's fundamental rule in life is to have a trust in people. Trusting people is a worth-living virtue, even for the non-worthy people when you trust them you push them and urge their conscious to the good side. I still remember our different perspectives regarding that point. My argument was to put the trust where it belongs, in which trusting all people expecting that they all will react to your trust with a trust as well, is the same situation that a man would expect a lion does not eat him because he is a vegetarian. However, and after more than 6 years of our first meeting, I confess that the genuine kindness will always prevail.

I will always remember when Assoc. Prof. Katalin Kopecskó, his lovely wife, once called me "his academic son", I could not be prouder then. In the matter fact and interestingly by coincidence, he was born in the same year that my father was born. Finally, these few yet valuable examples show the exceptionally kind, peaceful, and insightful personality that Prof. Balázs has, whom I highly admire and wishing him a long healthy happy life.

Thank you very much indeed.

Dr. Naser S. Alimrani,
most recent PhD student of Prof. Balázs

ON THE EFFECTIVE CONCRETE COMPRESSIVE STRENGTH IN THE THEORY OF PLASTICITY

Andor Windisch

In his fundamental book Nielsen (1984) summarized the basics of application of plastic theories to the design of concrete structures. Since that time extended experimental and theoretical works were carried out. Models based on plastic theories were developed for bending, shear, for beams, plates, etc. The strut-and-tie-, the stress field models and the Modified Compression Field Theory perform further developments of application of the theory of plasticity. Crucial point (the governing material characteristic) of these models is the effective concrete compressive strength. This paper critically reviews its different theoretical origins and despairs of its existence. It reveals that the main source of plastic behavior of structural concrete structures is the reinforcement. In design for shear instead of a preposterous effective concrete strength the effective web thickness and (a maybe slightly reduced) concrete compressive strength should be taken into account. Neither the concrete compressive strength nor any reduced (effective) value of it are applicable as governing material characteristic of any plasticity model for structural concrete structures.

Keywords: *theory of plasticity, effective compressive strength, strut-and-tie-model, stress field model, Modified Compression Field Theory*

1. INTRODUCTION

In the second half of the twentieth century the application of the theory of plasticity in design of r.c. structures was one of the main developments. The fundamental textbook of Nielsen et al. (3rd edition: 2011) summarized the results so far. In the following decades different models based on plastic theories were developed for bending, shear, for beams, plates, etc. The strut-and-tie-, the stress field models and the Modified Compression Field Theory are to be mentioned here. Crucial point (the governing material characteristic) of these models is the effective concrete compressive strength.

One of the basic assumptions of these models is that at application of the plastic theory to concrete the concrete must become plastic and fail in compression. At application of these models to the results of different test series the concrete in compression failed (numerically) far below the strength value determined on the parallel produced cylinders. The nimbus of the effective compressive strength was born. It didn't bother anyone that for each type of structural element, each type of loading action and each model different efficiency factors has been received. Until today it was not possible to find a generally valid efficiency factor.

The reason is very simple: in case of r.c. material to reach the plastic ultimate limit state both materials do not need to be in a plastic state. The one parametric loading procedure of a r.c. member/structure begins at zero. Due to the limited tensile strength of concrete first 'event' fulfilling the lower limit theorem is the cracking of the member. In the cracked cross sections the reinforcement crossing the cracks ensures the tensile forces needed for the equilibrium. Depending on the applied mechanical rate of reinforcement:

a) one or both bands of reinforcement (under-reinforcement) begin to yield along the crack or

b) in case of over-reinforcement, the concrete indeed fails.

At many test series yielding of the reinforcement reduces the stiffness of the member/structure to such an extent that the hydraulic loading system fails to overcome the deformations: the load drops dramatically, the test will be stopped. In case a) the failure load must not be related to the concrete, otherwise crazy effective concrete compressive strength values will be generated.

In this paper the history of the origin of the different effective concrete compressive strength values is elucidated.

2. THE PLASTIC CONCRETE THEORY OF NIELSEN

In their fundamental book of Nielsen et al. (2011) the main target of the chapter dealing with the yield conditions for concrete is to persuade the reader that concrete is a Modified Coulomb Material and mostly fail at relative low ($\sigma < f_c$') strength values. *Fig. 1* taken of Nielsen should prove the existence of the effective compressive strength, i.e. existing cracks reduce the effective compressive strength of the stress field.

The Modified Coulomb material (*Fig. 2*) fails either in uniaxial tension with separation or in (uni- and biaxial) compression undergoing a sliding failure. *Fig. 1 a)* is correct. The specimen (prism or cylinder) fails in the testing machine where the friction along the loading equipment and specimen is eliminated due to longitudinal (tensile) cracks (separation failure). *Fig. 1b)*: inclined cracks never develop in a specimen under pure compression. This crack should have occurred due to another state of stress before this loading producing the compressive principal and tensile stresses to become active. Concrete react to principal stresses only. (This is where the
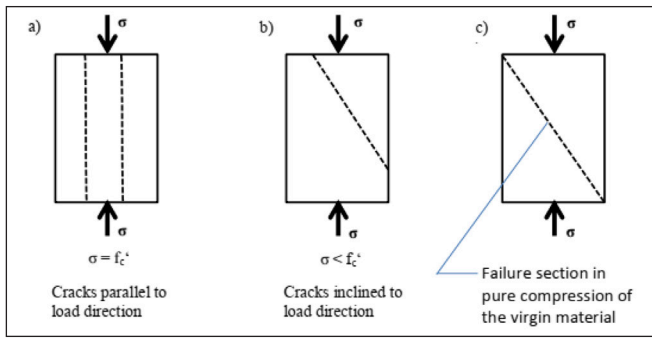
Fig. 1: *Influence of cracks on the compressive strength acc. to Nielsen*

Fig. 2: *Modified Coulomb Failure Criterion*

Fig. 3: *Mohr's circle of uniaxial compression*

distraction of the reader begins!) *Fig. 1c)*: this type of failure never develops. It is in clear contradiction with the correct failure pattern shown in *Figure 1a)*! What should mean the adjective 'virgin'? Important to note: plastic theory is valid in case of one parametric loading only!!! Accordingly the cracks and 'failure sections' due to earlier loading scenarios cannot be considered acc. to the theory of plasticity!!

As a matter of fact from here on, the whole 'theory' of Nielsen is invalid and irrelevant.

Nielsen et al. present the Modified Coulomb Failure Criterion as valid for concrete, see *Fig. 2*. Important characteristics in the σ, τ-coordinate system are the two types of failure: separation and sliding, the τ = c (cohesion) section along the τ-axis and the inclination of the line characterizing the sliding failure, φ. We must note the following:

- the shear stress is a calculation auxiliary quantity only. It 'owes' its existence to the Cartesian global coordinate system. Turning the axis of the coordinate system the stress components (the shear stress, too) continuously change. Not a single stress component can be treated as 'shear strength'.
- The Coulomb Failure Criterion (CFC) is valid in case of already existing sliding surfaces only!! Glue the brick in the well-known brick-on-slope-test to the slope and try to get the brick to slide. You will fail. Q.e.d.

In *Fig. 3* Nielsen shows the Mohr's circle of the uniaxial compression and declares that as the Mohr's circle obviously touches the line of the sliding failure in case of uniaxial loading sliding failure might occur, see *Fig. 4*, where the inclination of the sliding (failure) surfaces are 45° - φ/2 inclined to the loading direction. The following objections must immediately be raised:

- Do not forget that Mohr's circle is a two-dimensional graphical representation of the transformation law for the Cauchy stress tensor, i.e. formulas containing sin², cos² and sin·cos terms.
- All points of the Mohr's circle are equivalent, i.e. the two 'touching points' are not of distinguished rank at all
- As mentioned before, the clear failure pattern of test specimens in pure compression is as shown in *Fig. 1a*. Inclined failure surfaces develop due to not eliminated friction between loading plate and test specimen. Changing the rate of friction the measured strength and the direction of the actual principal stress, i.e. of the actual failure surface, change too.

Fig. 5 shows the failure sections at pure tension acc. to Nielsen. The separation failure is correct. The single raison d'être of the sliding failure pattern at pure tension is that it is possible to draw on a piece of paper a tangent to the Mohr's circle characterizing the pure tension. Under no circumstances can such a fracture pattern occur in the practice at pure tension.
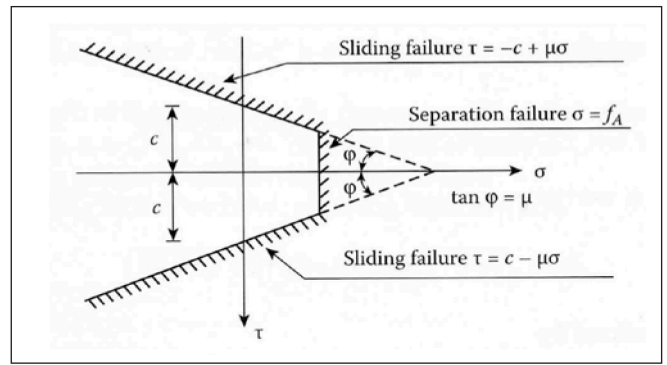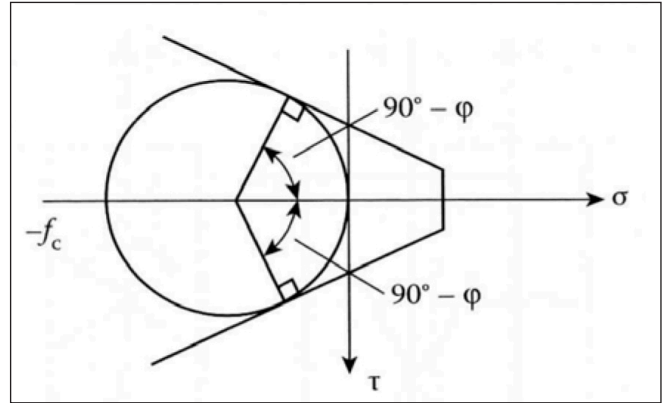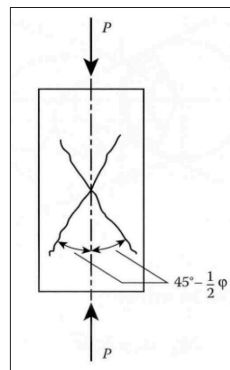
Fig. 4: *Failure sections at pure compression acc. to Nielsen*
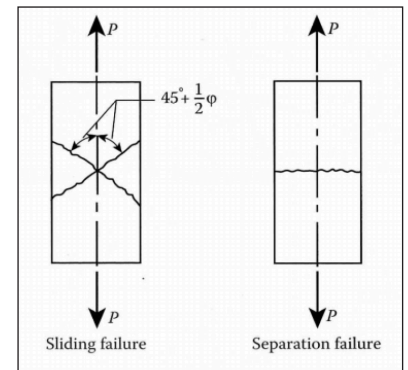
Fig. 5: *Failure sections at pure tension acc. to Nielsen compression*

Pure shear loading results in a principal tension and a principal compression stress of the same size and under 45° directions. As the tensile strength of concrete is very limited the loading procedure finishes with a tensile separation failure.

Let us take a closer look at the Modified Coulomb Failure Criterion: for its definition three data are necessary: c, μ or φ and the tensile strength. In the best case, we only have two material characteristics at our disposal: the compression and the tensile strengths. Even if the Modified Coulomb Failure Criterion would be valid for concrete how could we deduce the necessary coefficients? As mentioned above: pure shear loading results in principle tension. Accordingly the 'cohesion' c must be equal with the concrete tensile strength. Let's calm down. Modified Coulomb Failure Criterion does not apply to concrete at all. Concrete obeys only principal stresses and performs only separation failures.

Thereafter follows the big scientific obfuscation: the gentle reader should distinguish the strength of

- "Cement mortar (isotropic plastic material with the friction angle φ = 0)

- Two-phase material: cement paste and aggregate particles. It is well known that cement paste behaves in a rather brittle way in uniaxial tests. It is explained by the presence of hard unhydrated cement particles. Sliding failure may be prevented by the hard particles leading to the formation of yield lines in front of these particles. … There will also be some resistance from other parts of the yield line, dependent on the amount of microcracking and the amount of load induced cracking. Acc. to the model, the failure in cement paste is always ductile for compression stress fields and the apparent brittleness in cases of small confinement is due to the relatively short lengths of the yield lines formed in front of the hard particles…. You need not try to understand this confusion.
- Structural concrete strength ("Unfortunately, the strength of concrete we observe when testing a structure is usually very different from the strength measured on standard laboratory specimens. The main reason is that the concrete is cracked, and cracking reduces the strength.

The most important consequence of this fact regarding the application of plastic theory is that the strength parameters, which we have to insert into the theoretical solutions, normally are lower than the standard values. We call the strength values to be inserted the effective strength. The effective concrete compressive strength f_{cef} is, defined by

$$f_{cef} = \upsilon\, f'_c$$

where $\upsilon \leq 1$ is called the effectiveness factor for the compressive strength."

That's all.

"The strength reduction due to cracking might be subdivided into (a) strength reduction due to microcracking present even before any load is applied, (b) strength reduction due to load-induced microcracking and finally (c) strength reduction due to macrocracking. While the microcracking present before loading may be assumed to lead to an isotropic material, load-induced microcracking and macrocracking will cause anisotropy, i.e. the strength parameters, for instance the compressive strength, will vary with direction. Strictly speaking, cracked concrete should be treated as an anisotropic material.

However, this cannot be done in a fully rational way… We must content ourselves with a more primitive approach. It consists of either considering cracked concrete to be isotropic with the effective strength parameters or by dealing with the strength parameters only in certain selected direction depending on the crack system."

Not a single word of any scientific justification can be found… First the cement mortar is an isotropic plastic material thereafter rather brittle … You need not understand this confusion.

This order to present a theoretically founded reason of the strength reduction *Fig. 6* is presented: "two parallel macrocracks, which are crossed by a reinforcement bar perpendicular to the cracks, the bar is stressed in tension. Let us assume that some kind of microcracking is spreading out from the macrocracks when the reinforcement stress is increased. The microcracks are shown schematically in the figure. The real microcracking is of course much more complicated." Note: plastic theory is valid in case of one parametric loading only, i.e. the steel stress, the alleged microcracks and the compressive stress between the two macrocracks increase parallel. In addition, the compressive stress prestresses the 'strut', i.e. the impressive and convincing microcracks occur
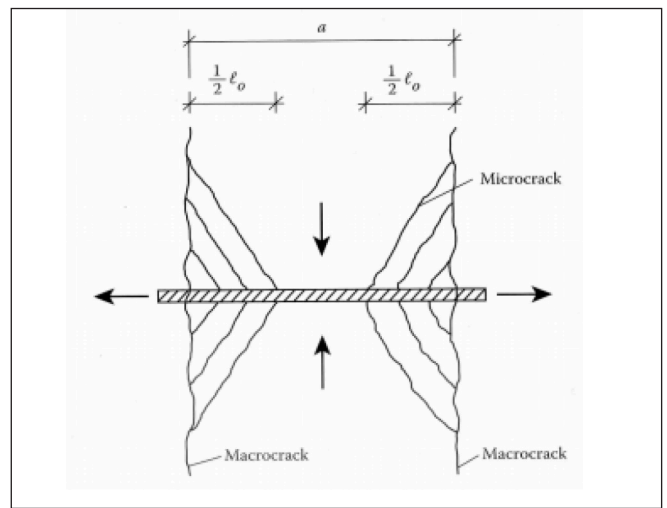
Fig. 6: *'Formation of microcracks between two macrocracks' acc. to Nielsen (1984)*

in a completely different manner, if at all. Do not forget, that microcracking is a natural phenomenon parallel with the compressive loading even during the material testing. The proposed efficiency factor has no theoretical background it is an empirical coefficient which should adjust the shortages of the shear model choosing the direction of the compression field arbitrarily across the shear cracks.

Recent studies revealed that aggregate interlock has negligible contribution to the shear failure load accordingly the inclined compression fields do not cross the shear cracks. Thus, there is no need for the efficiency factor any more.

"We have now finished our review of the rather incomplete knowledge about the effective strength of concrete. It appears that an accurate description of the real behavior of concrete is not possible by simple means. In the main part of this book, we will therefore take an engineering approach to the problem.

The main line will be to develop solutions using plastic theory based on the modified Coulomb failure conditions. These solutions are then modified by the introduction of effective strength parameters determined on basis of the tests available. The physics of the problems may then be well hidden, but it is believed that such an approach will be the most useful for the engineering profession at the present stage of development. By any measure it will be far more useful than a completely empirical approach, which is still dominating many areas of the concrete field."

Heureka.

From now on the applier of the Nielsen-type plastic theory have a multiplier $0 < \nu < 1$, through its application they can adjust their results of calculation to any test results.

3. SHEAR FAILURE OF BEAMS WITHOUT SHEAR REINFORCEMENT

Fig. 7 shows the final crack pattern of a simply supported beam without shear reinforcement loaded with two symmetrical concentrated forces acc. to Nielsen et al. (2011). "The curved cracks in the shear zone are running from the tensile face toward the nearest force when the load is increased. One of these cracks leads to failure because of the low sliding resistance along the crack. The final failure will be a sliding failure along OA and BC and a separation failure along AB,
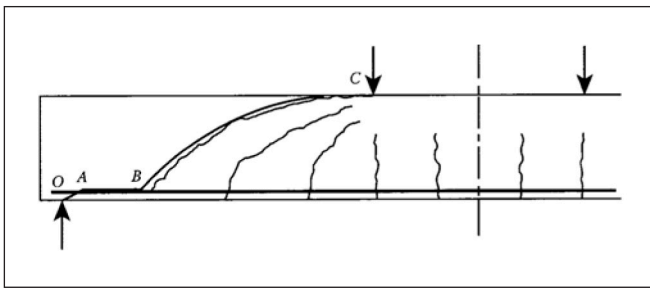
Fig. 7: *Failure of a beam without shear reinforcement*

which is situated just above the longitudinal reinforcement. The yield line along the crack will be more dangerous than a yield line through concrete without microcracks."

This failure pattern needs some comments: The upper part of the flexural-shear crack BC should consist of two parts: section below the neutral axis and along the compression zone, resp. otherwise no flexural equilibrium exist. Moreover, instead of sliding the parts left and right from ABC, resp, rotate relative to each other around the point where the shear crack crosses the neutral axis. Interestingly the compressive forces/stress fields are not mentioned.

Using this unrealistic failure model we arrive at a nonrealistic/not existing material characteristic: the shear strength of concrete.

4. EFFECTIVE COMPRESSIVE STRENGTH OF THIN BEAM WEBS IN SHEAR

Perform the following thought experiment:

Given is a series of simple span beams with four-point loading, their shear slenderness is three. All data are identical (including the diameter, distance and concrete cover of the stirrups), only the web width decreases from beam to beam). The failure in flexure and shear is triggered by yielding of the longitudinal and/or the shear reinforcement. (Often the stirrups spall off the concrete cover nevertheless the stresses in the 'concrete struts' are far from a failure due to compression. The failure occurs when a sliding surface through the compression zone develops and the flexural reinforcement spalls off the concrete cover: a kinematic flexural-shear hinge develops: displacements in the structure progressively increase: failure is attested.) Consider now the development of the inclined compressive stresses: in the beam with rectangular cross section it is small and increases with decreasing web thickness. The stirrups might spall off the concrete cover and at a certain web thickness the 'concrete struts' between the stirrups fail in compression at a compressive stress near to the original compressive strength. Only at this beam occur the shear failure due to both, yielding of steel and exhaustion of load-bearing capacity of concrete. When the advocates of the plastic theory evaluate the results of this last test then the inclined compressive force is related to the whole width of the web, i.e. a pronounced low compressive strength is 'produced numerically', a heavy softening of concrete in compression is attested.

We remind you that in the Codes (e.g. MC2010, 2013, Ch. 7.3.3.3) at calculation of the design shear resistance attributed to the concrete "in case of prestressing tendons in the web with duct diameters $\emptyset_D \geq b_w/8$, the nominal value of the web width

$$b_{w,nom} = b_w - k_D \sum \emptyset_D$$

Values of k_D depend on the material of the duct and whether it is grouted or not. Suggested values for design are:
- grouted steel duct. $k_D = 0.5$
- grouted plastic duct: $k_D = 0.8$
- ungrouted duct: $k_D = 1.2$.

Factor k_D may be reduced in presence of reinforcement transverse to the plane of the web."

As a matter of fact all the rebars in the web: the longitudinal as well as the transverse ones (stirrups) are disturbing elements in the compressive stress field, too. After formation of the flexural-shear cracks the rebars crossing the cracks perform a relative displacement (slip) related to the concrete, i.e. the rebars are in a channel, similar to the ducts, accordingly at the calculation of the nominal value of web width similar reductions should be taken into account. Doing so the fairy tale on the softened concrete strength could be eliminated.

The softened (effective) concrete strength is currently like a dominant religion: researcher who measure contradictory results are ashamed to publish them, they would be considered as heretics.

5. SLIDING FAILURE OF ORTHO-TROPIC PANELS

The panel shown in *Fig. 8* is reinforced with different ratios in perpendicular directions. The initial cracks are formed under 45° with the sections with pure shear and their directions are roughly independent of the reinforcement (so far is Nielsen right)."However, if the reinforcement ratios in the two directions are different, the final crack direction will be different from the initial one. This means that the final compression direction in the concrete might be as shown in *Fig. 8*. It follows that compressive failure may take place by sliding failure along the initial cracks for a very low compressive stress compared to the compressive strength of the virgin material. Such a reduced compressive strength has been measured by Vecchio and Collins and they also measured the strains."

Author's comments (Windisch, 2000):
- Nielsen's statements about the initial cracks are correct. The parts of the concrete panel perform a separation on both sides of the tensile cracks perpendicular to it
- the red rectangle with its axial loading and the 'final crack

Fig. 8: *Orthotropic panel with initial and differing final crack direction (acc.to Nielsen et al. 2011)*
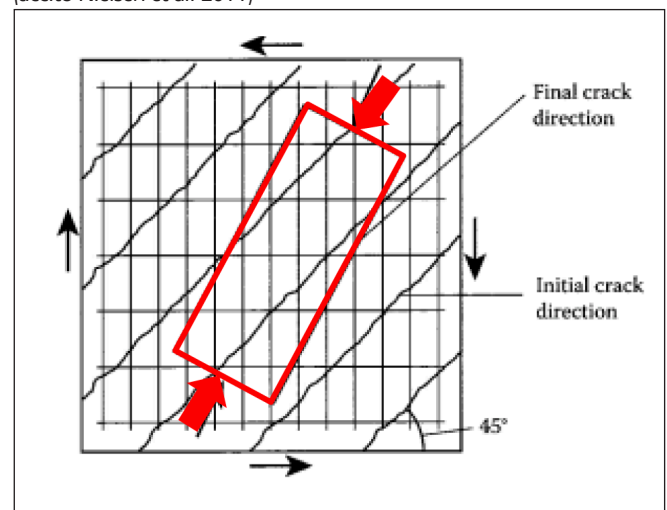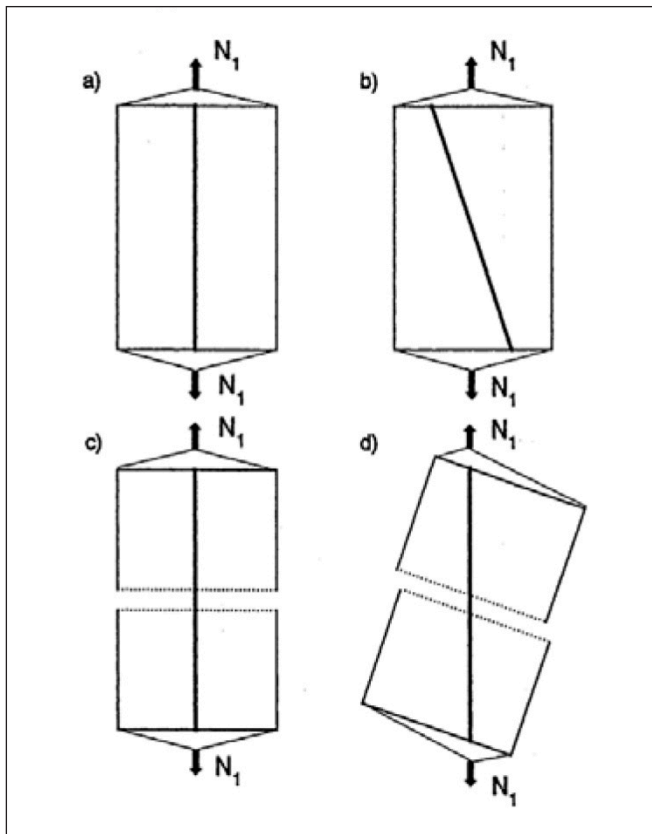
Fig. 9: *Displacements of a membrane element under uniaxial tension*
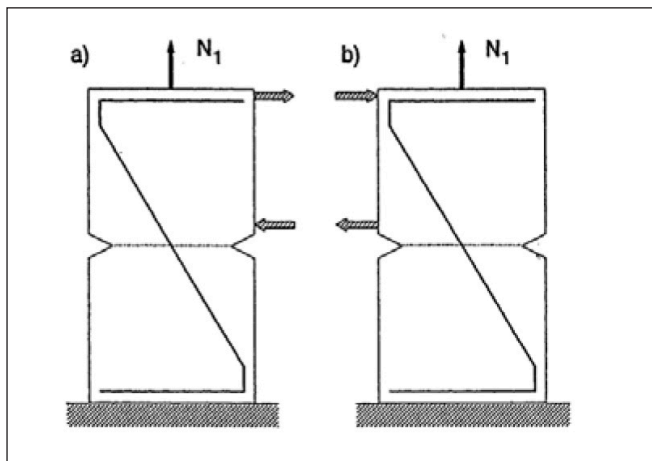
Fig. 10: *Supplementary forces depend on the boundary conditions*

directions' emerge on the drawing board only, never as a consequence of the initial 'pure shear' of a concrete panel

- the panel's behavior after development of the initial cracks cannot be predicted without the knowledge of the boundary conditions.

Fig. 9 shows displacements of two membrane elements under uniaxial tension: the element a) is reinforced in the direction of the tensile force (or with equal rates in two directions symmetrical to the longitudinal axis), the element b) in a different direction (or with equal rates in two directions not symmetrical to the longitudinal axis or with different rates in arbitrary directions). The sketches c) and d) show the corresponding free sliding which are hindered i) by the dowel action of the rebars and ii) through the boundary conditions. Supplementary forces develop, their size and sign (compression or tension) depends on the exact boundary conditions (*Fig. 10*).

In *Fig. 8* the direction of the imagined 'final' compressive force is equated with final (new) cracks. As well known the tensile crack unloads the concrete on its both sides, hence the

cracks cannot rotate neither under the influence of the initial pure shear nor under the unknown supplementary forces. From now on, all further derivations are fiction contrary to the basic properties of reinforced concrete. The resulting discrepancy between the calculation and the experimental results is intended to correct the effective compressive strength of the concrete (also arbitrarily declared). It is interesting to follow what kind of pull-ups are done 'to bring' concrete in 'failure' condition.

Vecchio's and Collins's Modified Compression Field Theory will be discussed in Chapter 7.

6. YIELD CONDITIONS FOR OR-THOGONALLY REINFORCED DISKS

In the following Nielsen's deduction (2011) for the case of pure shear loading is quoted and commented.

"The disk is loaded in pure shear in the x, y-system. For the concrete part of the equilibrating composite material system a concrete stress field characterized by the principal stresses

$$\sigma_{c1} = 0, \sigma_{c2} = -\sigma_c, \tag{1}$$

with the second principal axis forming an angle α to the x-axis are supposed."

Note:

- Pure shear loading τ in the x, y-system means principal stresses $\sigma_1 = \tau$ and $\sigma_2 = -\tau$, the principal axes (we denote them I and II, resp. in order to distinguish them from the 'principal axes' as defined by Nielsen) are inclined at $\pm 45°$ to the x-axis,

- the assumption $\sigma_{c1} = 0$ means that in the direction of the first principal axis the equilibrium is balanced by the tensile forces in the rebars only, i.e. the concrete is cracked along the border of the concrete stress field.

From the compressive stress $-\sigma_c$ in the stress field Nielsen obtains (compressive) stresses

$$\sigma_{cx} = -\sigma_c \cos^2\alpha, \quad \sigma_{cy} = -\sigma_c \sin^2\alpha. \tag{2}$$

Defining

$$A_{sy} / A_{sx} = \mu \tag{3}$$

He gets in the x- and y-direction

$$A_{sx} f_{Yx} = t \sigma_c \cos^2\alpha \quad \text{and} \quad A_{sy} f_{Yy} = t \sigma_c \sin^2\alpha \tag{4}$$

Note: we must fulfil the equilibrium condition in the crack along the border of the concrete stress field as Nielsen simply just doesn't care of it.

$$A_{sx} f_{Yx} \cos^2 45° + A_{sy} f_{Yy} \sin^2 45° = 0.5 (A_{sx} f_{Yx} + A_{sy} f_{Yy}) \tau \tag{5}$$

This means that at design we can choose the amounts and yield strengths of the orthogonal reinforcement nevertheless two points must be considered:

- parallel to the crack components of the tensile forces in the orthogonal reinforcement develop which shift the two parts of the disk separated by the 45° inclined crack. Depending on the support conditions of the disk (of the test specimen) which hinder the shifting, different supplementary forces

(compressive and/or tensile stresses) can develop in the disk.

- it must be emphasized that when the weaker band of reinforcement begins to yield then the deformation of the disk might become partly uncontrolled and it could occur that the loading procedure is finished before the stronger band of reinforcement yields. We recognize that the concrete strength does not influence the behavior of the disk at all, hence the maximum concrete stress achieved during the experiment cannot be attributed to failure of concrete: in any case the concrete did not experience any 'softening'.

"From the two equations (3) and (4) Nielsen compiles a definition for the angle α

$$\tan^2\alpha = \mu, \tag{6}$$

he gets

$$\sigma_c = \Phi_x \left(1 + \mu \right) f_c \tag{7}$$

he pretends that the compressive stress in the stress field is function of the concrete strength nevertheless replacing the definitions of Φ_x and μ we get

$$\sigma_c = (A_{sx} + A_{sy}) f_Y / t \tag{8}$$

i.e. the compression stress in the stress field is completely independent from the concrete class, so far the plastic theory for concrete by Nielsen…

"Having

$$|\tau_{cxy}| = \tfrac{1}{2}\, \sigma_c \sin 2\alpha \tag{9}$$

The shear strength of concrete is

$$f_v = \frac{\sqrt{A_{sx} \cdot A_{sy}}}{t}\, f_Y \tag{10}"$$

Once more there is no sign of dependence on the concrete class.

Note: Eqs. 3, 6, 8 and 10 are valid when the yield strength of A_{sx} and A_{sy} are identical, otherwise f_{sxY} and f_{syY} must be incorporated in the relevant terms.

"This example of using our assumptions clearly shows the importance of the assumption that the tensile strength is zero. We find that in all sections parallel to the η-axis the stress

of the concrete is zero, which can be said to correspond to a continuous distribution of "cracks". In reality, the initial cracks will be in sections under 45° with the coordinate axes x and y. Tensile stresses in these sections would appear before cracking, and the elongations in the x- and y-axes would be zero (i.e., the bars would not come into action). As soon as cracking appears, however, the bars get into action and the uniaxial concrete compression stress rotates to a new direction if $\mu \neq 1$. New cracks may be formed. Thus we may get crack sliding in the initial cracks."

Could somebody explain how and for what reason cracks in new direction could/should appear? Moreover, having continuous (smeared) cracks the reinforcement will never achieve yielding. Nothing is right/correct here!

All stress field models, STM and MCFT are based on this false assumption.

7. MODIFIED COMPRESSION FIELD THEORY

The basic element of the Modified Compression Field Theory is the unidirectional or orthogonal reinforced membrane panel which can model the web of beams or a box formed from four as members loaded in torsion.

Vecchio and Collins (1982, 1986) developed a panel tester where 80cm x 80cm big panels were loaded in pure shear or combined loading. For more details look also to Windisch (2010).

For most specimens, two separate concrete mixes were used. A relative strong concrete was cast in a 100 mm band around the perimeter; a weaker mix was cast in the central regions of the panels": even if the mechanical strain measurements were taken only in the central regions, the stronger boundary concrete unloads the weaker central region thus "pollutes" the results.

The reinforcing meshes in the test panels were constructed of smooth wires welded into an orthogonal grid; typically at 50 mm (2 inches) centres. The smooth bars provide a completely different performance in the concrete panel as deformed rebars, hence the results and conclusions, even if they would be correct, cannot be generalized to panels reinforced with deformed rebars.

MCFT treats "the reinforcement and the cracked concrete separately. The two materials are 'tied together' by the compatibility requirement that the strain in the reinforcement and in the concrete equal those in the panel (*Fig. 11*). It should be noted that the concrete component is not equivalent to an unreinforced concrete element. Rather, it is the concrete in a reinforced concrete element minus the reinforcement."

Fig. 11: *Toronto-testpanel and identical failure patterns of very differently loaded panels*

		PV24	PV25	PV23	PV27	PV28
	f_n/v	-0.83	-0.69	-0.39	0	0.32
	v_u	7.94	9.12	8.87	6.35	5.80

legend: high strength concrete — rebars
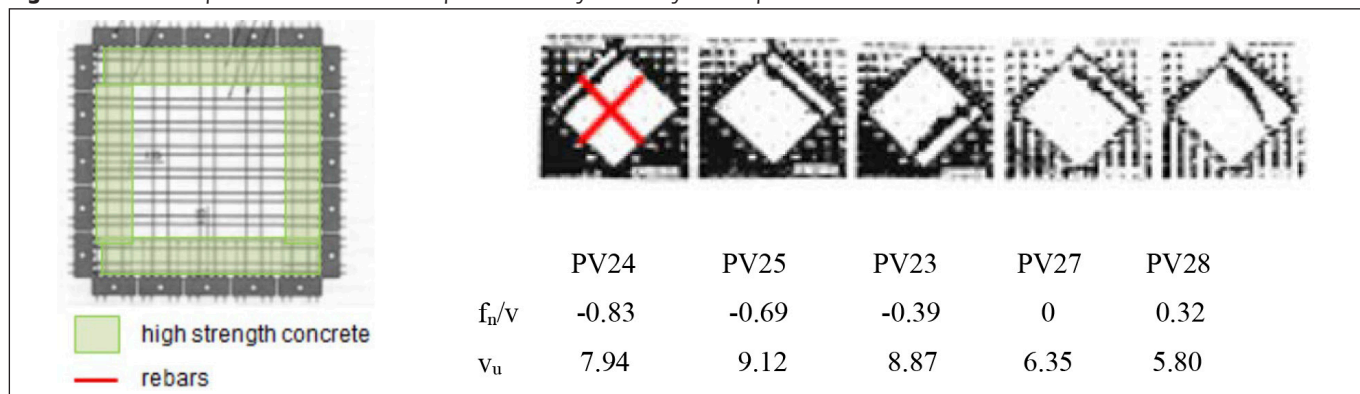
"Constitutive relationships are required to link average stresses to average strains for both the reinforcement and the concrete. These average stress-average strain relations may differ significantly from the usual local stress-local strain relations determined from standard material tests. Furthermore, the average stress-average strain relationships for the reinforcement and for the concrete will not be completely independent of each other, although this will be assumed to maintain the simplicity of the model. The axial stress in the reinforcement will be assumed to depend only on one strain parameter: the axial average strain in the reinforcement. In relation of axial stress to axial strain, the usual bilinear uniaxial stress-strain relationship was adapted."

Vecchio and Collins refer clearly and correctly: "the stress" and strain formulations deal with average values and do not give information regarding local variations. At a crack, the tensile stresses in the reinforcement will be higher than average, while midway between cracks they will be lower than average. The concrete tensile stresses, on the other hand, will be zero at a crack and higher than average midway between cracks. These local variations are important because the ultimate capacity of a biaxially stressed element may be governed by the reinforcement's ability to transmit tension across the cracks."

These local variations are in fact very important, as it will be shown in this paper. It is out of all reason why Vecchio and Collins did not follow this way. During the iteration procedure Vecchio and Collins continuously refer to the necessary control of the steel stress level in the reinforcement, nevertheless, it is not told, what should be done in such cases.

Moreover, at each and every test panel which did not fail at an early stage due to some discrepancies, the failure was always induced by yielding of the weaker i.e. transverse reinforcement: this means that the achieved principal compressive stress depends on the characteristics of the reinforcement which is not reflected in the $\varepsilon_{dt}/\varepsilon_d$ values at all. Further on, if the transverse tensile strain should have a degrading effect then in case of deformed bars this effect must be completely different (even stronger) as deduced in the report.

The principal compressive stresses taken as the basis for the well-known formula:

$$\frac{f_p}{f_c'} = \frac{1}{0.85 + 0.27\,\varepsilon_{dt}/\varepsilon_d} \qquad (11)$$

were derived directly from the average steel stresses (*Fig. 12*). Here ε_d is the principal compressive strain whereas ε_{dt} is the principal tensile strain, both in the diagonally cracked concrete. The additional compressive forces developing due to the fixed links were not considered these are those deviations which gave the impression to Vecchio and Collins of the softening concrete under the influence of $\varepsilon_{dt}/\varepsilon_d$.

It is very important to emphasize that not a single of the panel failure patterns showed a compression character. In *Fig. 11* a series of panels with systematically changing loading (from shear + compression to shear + tension) is shown: the failures occurred systematically at the junction of central panel concrete to the border concrete.

Fig. 13 shows the comparison of calculated vs. measured failure loads of the same panels as in *Figure 12* as calculated by Windisch (2000). The failures were obviously triggered by yielding of the reinforcement.

Fig. 14 reveals that the measured yield loads are between the double yield load of the weaker band of reinforcement
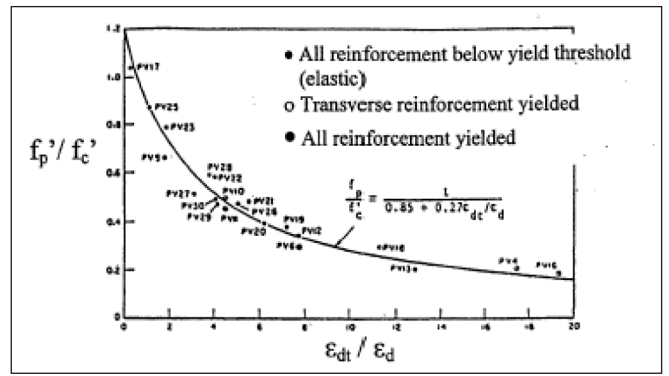
Fig. 12: *Compressive strength softening acc. to Vecchio and Collins (1982)*
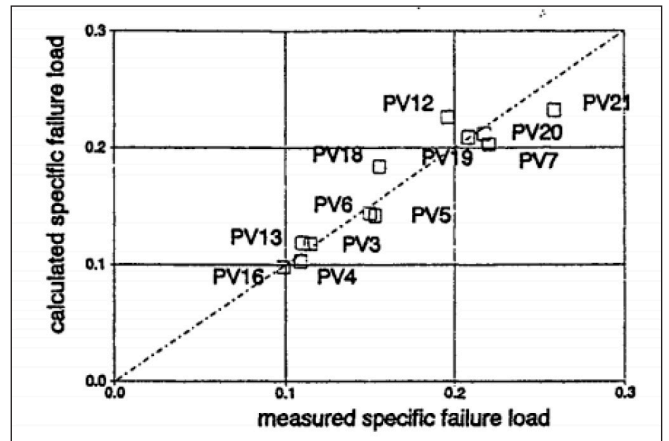
Fig. 13: *Comparison of calculated vs. measured failure loads (Windisch, 2000)*
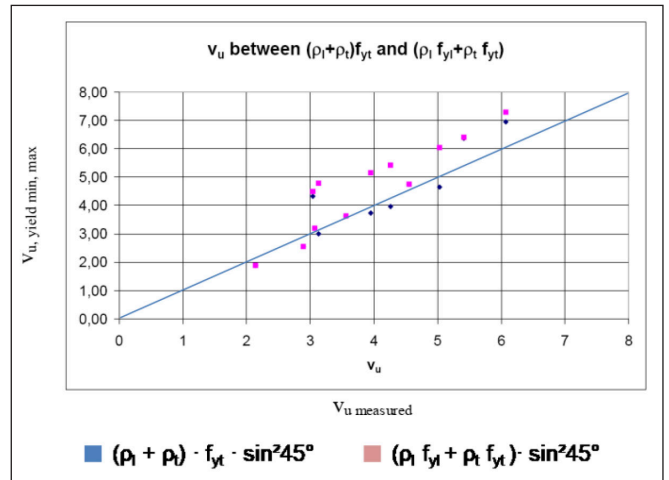
Fig. 14: *Comparison of lower and upper yield loads with the measured yield loads*

and sum of the yield loads of the weaker and stronger reinforcement. The concrete strength has no input at all.

8. STRUT-AND-TIE MODEL

The strut-and-tie model (STM) was proposed by Schlaich et al. (1984, 1987). The basic concept of the generalized truss model states that the flow of the force within a reinforced concrete structure is the same as the flow of the force within a truss. This truss model comprises straight compressive stress fields and straight tension ties. The point at which at least three forces (lines) gather for force equilibrium is called a node. The concrete area at the node position that allows the strut and tie forces to be transmitted through the node is called the nodal zone.

Structural members can be divided into B-regions (Beam or Bernoulli region), where linear strain and beam theory are applied, and D-regions (Disturbed or Discontinuity region) where beam theory is not applied due to applied concentrated loads or discontinuous cross-sections.

Design methods for strut-and-tie models define the nominal compressive strength of a strut as the product of the effective compressive strength of the concrete and the cross-sectional area at one end of the strut. The effective compressive strength is defined e.g. in Section A.3.2 in ACI 318 (2014) as:

$$f_{ce} = 0.85 \, \beta_s \, f_c'$$

where f_c' is the specified compressive strength of the concrete and β_s is a factor "to account for the effect of cracking and confining reinforcement on the effective compressive strength of the concrete in the strut."

A STM has two free parameters in order to adapt the model to the measured load bearing capacity: the inclination of the struts and the effective compressive strength of concrete. In the absence of well-founded theories the researcher tried to find the effective compressive strength of concrete evaluating huge data banks.

The simplest and most often tested structural element is the deep beam. Strut capacity was found to be a function of the effective compressive strength of concrete and is affected by a/d shear slenderness, concrete's strength, load duration effect, transverse tensile strain, and cracking. Normalizing the test results with a/d $\sqrt{f_c'}$ Brown et al. (2008) found efficiency factors, υ between 0.2 and 2.5. The simple reason is that r.c. structures and deep beams, too, don't work like trusses.

Moreover, besides the prismatic strut the bottle-shaped strut was introduced. Drawing the belly stress fields it was inevitable that their curved borderlines crossed cracks. There was great fear and joy that they found a reason for strength reduction that seemed realistic.

Already in 2010 Windisch pointed out that the bottle shape and the related strength reduction contradict the theory of plasticity.

In a test series Pujol et al. (2011) proved the unsustainability of the strength reduction, nevertheless due to collegiality (?) they did not dare to declare that the emperor was naked.

„The reported results show no support for attributing the reduction in the allowable compressive strength at the ends of the „bottle-shaped" strut to the shape of the strut. This does not mean that the limit set by ACI 318-11 for allowable strength of bottle-shaped struts is incorrect. It simply means that the rationalization used for explaining the reduction is incorrect and unnecessary.

In 1932, Hardy Cross wrote, „All analyses are based on some assumptions which are not quite in accordance with the facts. From this, however, it does not follow that the conclusions of the analysis are not very close to the facts."

The fact that the rationale for the strut-and-tie method is incorrect does not necessary mean that the results of the procedure is incorrect. However, it does mean that the method could be explained in a simpler, if arbitrary, fashion. There is little reason for representing the strut-and-tie method in analytical abstractions."

Let's make it clear: at design of deep beams the amount of flexural reinforcement should be properly determined (the inner lever arm cannot be taken freely), the rebars should be properly anchored, the loading- and the support plates properly dimensioned. No υ < 1.0 reduction factors need to be taken into account, moreover the advantages of partial area loading can be considered.

In 1991 Windisch presented the Strut-Crack-and-Tie Model where the material parameter is the effective steel strength, which depends on the angle between the crack and the reinforcing bar crossing this crack. It was shown that the concrete compressive strength is not the governing factor of the load bearing capacity of structural concrete structures determined acc. to the theory of plasticity hence the effective compressive strength cannot be chosen as fundamental material model characteristic.

9. CONLUSIONS

Theory of plasticity is valid in case of one parametric loading only. It is necessary to accept that when applying the theory of plasticity in the case of reinforced concrete structures in ULS, the concrete does not necessarily have to be in a plastic state (satisfying any fracture condition).

The effective concrete compressive strength, $f_{c,ef}$:

$$f_{c,ef} = \nu \, f_c$$

where $\nu \leq 1$ is called effectiveness factor is the result of a theoretically flawed model idea.

The concrete doesnot obey the Modified-Coulomb-Failure Criterion.

The sliding part of the Coulomb-Failure Criterion is valid in case of already existing surfaces only.

Concrete has no shear strength. It fails due to principal stresses only. The failure occurs by separation along planes parallel to the direction of the principal compressive stress.

Yielding of a r.c. panel occurs when one or both bands of the reinforcement reach their yield strength. Depending on the direction and relativ amount of reinforcement at yielding besides crack opening shifting can occur which will be hindered through the boundary conditions supporting the panel. These let develop secondary stresses in the panel which might be tensile or compressive stresses. Anyway thereafter a new chapter of application of theory of plasticity begins, where the precracked r.c. panel has completely different material characteristics compared to the original panel. Note: the boundary conditions are relevant parts of the history. The concrete compressive strength is not the governing factor of the load bearing capacity of structural concrete structures determined acc. to the theory of plasticity, hence the effective compressive strength cannot be chosen as fundamental material model characteristic.

10. REFERENCES

Brown, M. and Bayrak, O. (2008): "Design of Deep Beams Using Strut-and-Tie Models-Part I: Evaluation U.S. Provisions", 105-S37, July-August 2008 *ACI Structural Journal*, 395 p., https://doi.org/10.14359/19853

Brown, M. and Bayrak, O. (2008): "Design of Deep Beams Using Strut-and-Tie Models-Part II: Design Recommendations,," 105-S38, July-August 2008 *ACI Structural Journal*, p.405, https://doi.org/10.14359/19854

fib Model Code for Concrete Structures 2010, October 2013, 432 p., *Ernst & Sohn*, Berlin, ISBN: 978-3-433-03061-5, https://doi.org/10.1002/9783433604090

Nielsen, M.P. (1984): "Limit Analysis and Concrete Plasticity", *Prentice Hall*, Englewood Cliffs, 1984, 261 p

Nielsen, M.P., Hoang, L.C. (2011): "Limit Analysis and Concrete Plasticity". 3rd edition, *Taylor & Frances Group*, CRC Press, 2011, 796 p.

Pujol, S., Rautenberg, J.M., Sozen, M.A. (2011): "Compressive Strength of Concrete in Nonprismatic Elements", *Concrete International* Sept 2011, pp. 42-49

Schlaich, J., Schäfer, K., (1984): „Konstruieren im Stahlbetonbau", in *Beton-Kalender Tome II,*Ernst und Sohn Berlin-München

Schlaich, J., Schäfer, K, Jennewein, M. (1987): "Toward a consistent design of structural concrete", *PCI Journal*, 32 (3) 74-150, https://doi.org/10.15554/pcij.05011987.74.150

Vecchio, F.J., Collins, M.P.(1982): "The Response of Reinforced Concrete to In-Plane Shear and Normal Stresses", *University of Toronto, Department of Civil Engineering*, Publication No. 82-03, Toronto, March 1982, 332 p. , https://doi.org/10.14359/10416

Vecchio, F. J., and Collins, M. P., (1986): "The Modified Compression Field Theory for Reinforced Concrete Elements Subjected to Shear," *ACI JOURNAL, Proceedings* V. 83, No. 2, Mar.-Apr. 1986, pp. 219-231.

Windisch, A. (1991): "Strut-Crack-and-Tie Model in Structural Concrete", *Proceedings of IABSE Colloquium "Structural Concrete"*, Stuttgart, 1991, pp. 539-544

Windisch, A.: On the Design of Two-Way Reinforcements in R/C. Studi e Ricerche – Vol. 21, 2000, Italcementi S.p.A., Bergamo, pp. 283-302.

Windisch, A.: "Design of Deep Beams Using Strut-and-Tie Models-Part I: Evaluation U.S. Provisions". Disc. 105-S37: Paper by Michael D. Brown and Oguzhan Bayrak, May-June 2009 *ACI Structural Journal*, 378 p. https://doi.org/10.14359/19853

Windisch, A. (2009): "Design of Deep Beams Using Strut-and-Tie Models-Part II: Design Recommendations", Disc. 105-S38, Paper by Michael D. Brown and Oguzhan Bayrak, May-June 2009 *ACI Structural Journal*, p. 379, https://doi.org/10.14359/19854

Windisch, A. (2010): "Investigation of Dispersion of Compression in Bottle-Shaped Struts", Paper by Dipak Kumar Sahoo, Bhupinder Singh, and Pradeep Bhargava Disc. 106-S19 Jan-Feb 2010 *ACI Structural Journal*, p. 119-120

Windisch, A. (2010): "Reevaluation of the Toronto Panel Tests and the Modified Compression Field Theory", Manuscript on ResearchGate

Andor Windisch PhD, Prof. h.c. retired as Technical Director of DY-WIDAG-Systems International in Munich, Germany. He made his MSc and PhD at Technical University of Budapest, Hungary, where he served 18 years and is now Honorary Professor. Since 1970 he is member of different commissions of FIP, CEB, *fib* and ACI. He is author of more than 190 technical papers. Andor.Windisch@web.de

GREAT POTENTIAL OF PRECAST CONCRETE STRUCTURES IN CARBON NEUTRALITY

Akio Kasuga

Cement used in structural concrete accounts for 60% of all cement. Thus, the amount of CO_2 emission by cement in structural concrete in a year is about 5% of the amount emitted by mankind. However, the LCA of structural concrete emits CO_2 not only at the product stage but also at the use stage after construction. In other words, LCA of structural concrete should consider not only the materials but also the maintenance phase. Then low-carbon technologies currently in use is introduced. Moreover, the need for multi-cycle structural concrete with a circular economy is presented. The carbon neutrality of precast concrete structure is not a risk but an opportunity for us.

Keywords: *carbon neutrality, precast concrete, LCA, robotics, non-metallic bridge, zero cement concrete*

1. INTRODUCTION

According to European data, 60% of cement is used in structural concrete [1]. Globally, cement emits 2.8 billion tons of CO_2 per year. If the ratio were the same as in Europe, cement in structural concrete would emit 5.2% of the amount of CO_2 emitted by mankind in a year. And a third of these emissions are from precast concrete (Favier, De Wolf, Scrivener, Habert (2018). We cannot just cross our fingers and wait for materials to go zero carbon. The countdown to carbon neutrality has already begun. Therefore, we must start now. Concrete structures have a long-life cycle. And the CO_2 emissions are significant when considering not only the materials, but also the construction, the long period of service afterwards and the demolition. In this paper, CO_2 emissions of precast concrete structures are considered in terms of its entire life cycle, and examples of measures to deal with this are presented.

2. ACCELERATED CONSTRUCTION BY PRECAST

Precast construction methods are suitable for lean construction, where stakeholders are involved from the design phase and aim to improve efficiency by reducing project extra costs, materials, time and labour. And this results in reduced CO_2 emissions. The three examples below are design-build projects by builders. The use of precast construction methods was considered from the design phase, and the result is that projects are being completed faster than ever before. The first example is the precast beams and columns of building. (*Fig. 1*) The joints of the precast members are made by grouting the rebars through voids and filling gaps of a few centimeters with grout. Using this method, a building frame can be constructed in three days per floor. (*Fig. 2*) In Japan, the number of buildings using this construction method has reached 52 since 2003, with a total floor area already exceeding 2 million square meters. The second example is the accelerated construction of a bridge pier. (*Fig. 3*) This pier is the tallest in Japan, at 125m. In order to reduce the weight of the precast members, the outer 14cm thick section from the vertical main reinforcement was precast. Within this 14cm, the horizontal hoop reinforcement is incorporated, so that only the 51mm diameter vertical rebar needs to be assembled on site. (*Fig. 4*) One lot is then completed by pouring concrete into the precast as a substitute for the formwork. The construction

Fig. 1: *Precast beam and column method without cast-in-situ joints (SQRIM method)*

1. Installation of beam precast
2. Installation of column precast
4. Installation of SQRIM-H beam precast
3. Installation of SQRIM-H beam precast
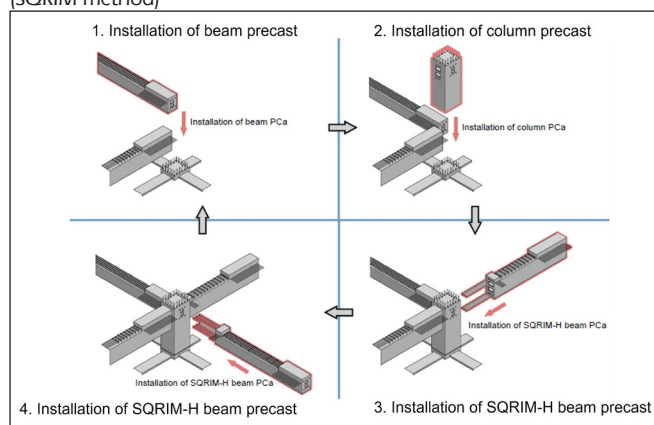
Fig. 2: *Construction of a precast beam*

Fig. 3: The highest bridge pier In Japan

Fig. 4: Partial precast construction method for bridge piers

Fig. 5: Okegawa Viaduct (2015)

Fig. 6: Stock yard of butterfly web panels

speed of this method is 1m per day, which means that it can be constructed in half the construction time compared to the usual cast-in-situ method. The final example is the special precast bridge girders. (*Fig. 5*) Panels called butterfly webs (Kasuga, 2016) are used for the web of the bridge. (*Fig. 6*) And the precast segments, except for the upper slab, (*Fig. 7*) are transported to the bridge site. (*Fig. 8*) The bridge is formed once with the U-shaped cross section beam, and the upper slab is then constructed with cast-in-situ concrete. (*Fig. 9*) In Japan, where transport weight regulations are strict, the number of segments can be reduced by using the U-shape. In addition, the construction of the upper slab can be carried out afterwards and is not critical. This viaduct has a bridge deck area of 35 000 m², but was completed in 18 months, including detail design. Thus, accelerated construction by precast can optimize the project. And, although further research is needed, the impact on surrounding social activities can also be minimized by reduced construction time, with the consequent potential to reduce CO_2 emissions.

3. ROBOTICS FOR PRECAST SEGMENTS IN CONCRETE FACTORIES

Alongside accelerated construction, the introduction of robotics also improves productivity. This section presents an example of the use of robots for the assembly of rebar cage in the precast members of the upper slab of a steel girder bridge. As shown in *Fig. 10*, the robot consists of two arms. It is equipped with a rebar supplier and the arms are fitted with a

Fig. 7: U-shaped precast segment without upper deck

Fig. 8: Construction of U-shaped precast segments

Fig. 9: Construction of cast-in-situ upper deck

Fig. 10: Robotics for rebar cage of the precast bridge deck
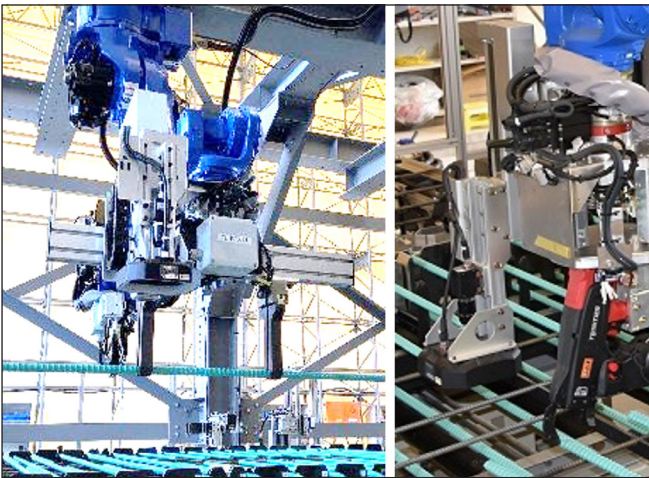
Fig. 11: Rebar holder (left) and rebar binder (right)

Fig. 12: Construction supply chain (EN15978)
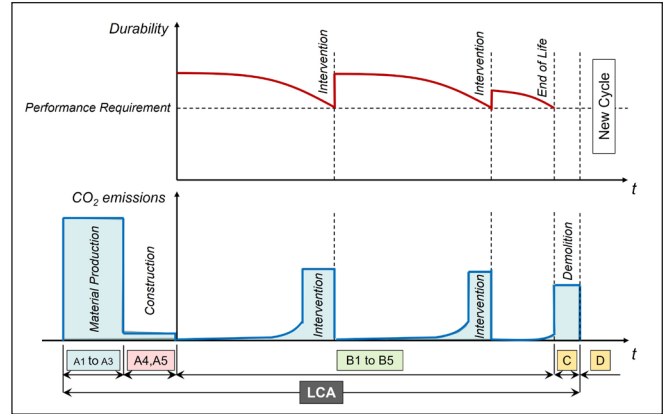
Fig. 13: Conceptual relationship between durability and CO_2 emissions of conventional technologies
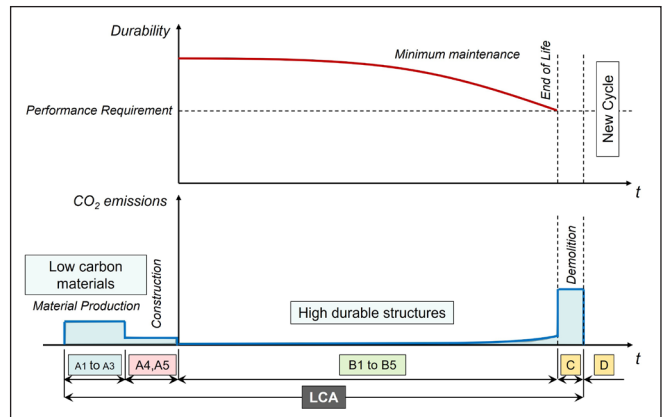
Fig. 14: Conceptual relationship between durability and CO_2 emissions of low carbon technologies

rebar holder and a rebar binder. (*Fig. 11*) The upper slab rebar cage is approximately 10 m wide and 1.75m long and usually takes six workers to assemble two cages a day. However, assembly robots can increase this productivity by three times. In the future, it will be possible to check workability on a computer in advance by linking the robot arm's movements with three-dimensional data.

4. LOW CARBON TECHNOLOGIES FOR CONCRETE STRUCTURES

Fig. 12 shows the construction supply chain according to EN15978. Also shown below is the sorting of each player in the construction supply chain by CDP (Carbon Disclosure

Project) and SBT (Science Based Target). In A1 to A3, steel and cement industries are already taking action with government support to achieve zero carbon emissions. However, we, as users, cannot wait for these carbon neutral achievements. This is because the demand for low carbon from the business sector has already begun. Therefore, we must meet this demand by bringing together low carbon technologies for structural concrete. The conceptual relationship between structural concrete durability and CO_2 emissions is shown in *Fig. 13*. As shown in *Fig. 14*, we must aim to reduce CO_2 emissions at all stages.

4.1 Low Carbon Technology in the Product Stage

The first step is to deal with the product stage. The low carbonization of stages A1 to A3 must be promoted until steel and cement achieve zero carbon. Concrete that replaces cement as a by-product has already been studied and proven in many cases. Of course, it is not possible to substitute all
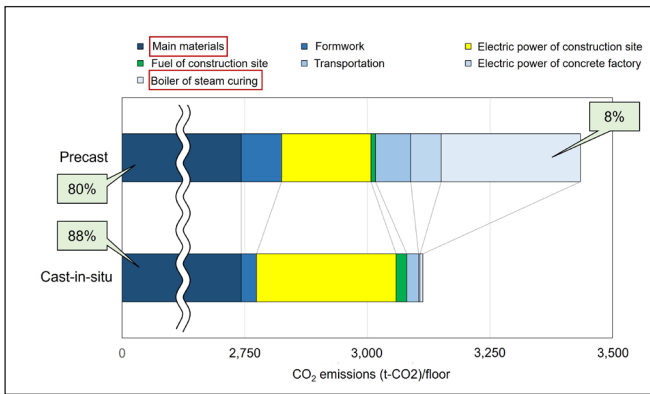
Fig. 15: *CO₂ emissions of precast and cast-in-situ per a typical floor of building*

Fig. 16: *Hydrogen boiler*
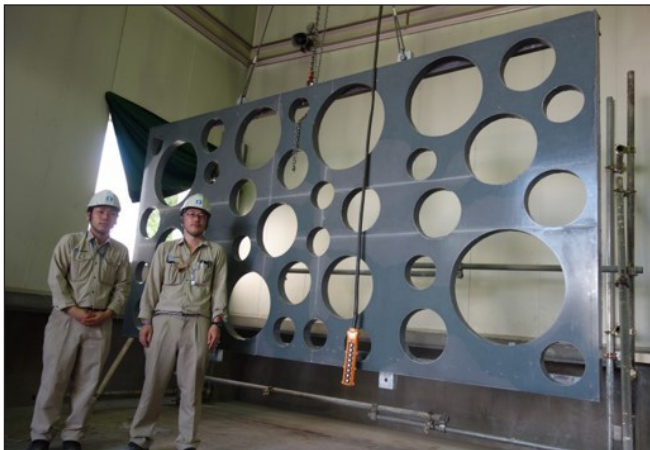
Fig. 17: *Zero cement concrete panel*

current cement with by-products, but it is a transition until zero-carbon cement is achieved. In addition, as low carbon concrete is slow to develop its strength, steam curing is required when used in precast products due to restrictions on the conversion of formwork. However, steam curing using boilers emits as much CO_2 in the exhaust gases as the amount of CO_2 reduced by the concrete itself.

The comparison of CO_2 emissions between cast-in-situ and precast construction is shown in *Fig. 15*. The most of CO_2 emission comes from materials, but 8% comes from curing. Therefore, it is necessary to consider the re-use of CO_2 by means of CCUS (Carbon dioxide Capture Utilization and Storage). One method is hydrogen boilers (*Fig. 16*). Hydrogen is still expensive and supplies of hydrogen, especially green hydrogen, are limited. However, if inexpensive, green hydrogen becomes widespread in the future, it will become an established decarbonisation technology. Alternatively, the use of alkaline solutions from cleaning equipment in large

quantities in precast concrete plants could be considered. For example, CO_2 from boilers is separated by a special membrane and submerged in this alkaline solution to produce calcium carbonate. ($CO_2 + Ca(OH)_2 \rightarrow CaCO_3 + H_2O$) The 8% disadvantage shown in *Fig. 15* can then be solved.

When low carbon concrete is used in structures, a challenge is its strength. There are examples of concrete without cement that has achieved a strength of over 100 MPa, and concrete can reduce CO_2 emissions by about 70% (Matsuda , Mine, Geddes, Walkley, Provis, 2022). (*Fig. 17*) Furthermore, fibre reinforced concrete has also been used in actual bridge components without steel reinforcements (Ashizuka, Miyamoto, Kata, Kasuga, 2012).

4.2 Low Carbon Technology in the Use Stage

At present, there is very little data on the relationship between durability levels and CO_2 emissions in stages B1 to B5. Therefore, information on CO_2 emissions by interventions and maintenance during that time is lacking. And these vary greatly depending on the level of durability decided at the time of design. The biggest challenge in conservation is how to prevent the reinforcing steel from deterioration. The Pantheon in Rome, for example, is an unreinforced structure, so it still functions as a structure after 2000 years. And even if steel and cement achieve zero carbon, durability and CO_2 emissions in the use stage remain issues. Therefore, the high durability of structural concrete is essential to reduce CO_2 emissions at the use stage. Currently available technology, such as stainless steel or aluminium reinforcement and coated steel re-bars, can be used to some extent. Increasingly, FRPs (Fibre Reinforced Plastics) such as carbon, aramid and basalt are being used as reinforcement materials. In 2020, non-metallic bridges with aramid FRP tendons have been constructed as the motorway bridge (Matsuo, Wada, Fujioka, Nagamoto, 2021) (*Figs. 18 &19*). There is also a report of

Fig. 18: *Bessodani Bridge (2020)*

Fig. 19: *Aramid FRP tendons in a butterfly web panel*

Fig. 20: *Girder using zero cement concrete and aramid FRP tendons (2019)*

Fig. 21: *Concept of remanufacturing of concrete structures for multi-cycle use*

a pretention girder combining high-strength zero-cement concrete and aramid FRP tendons (Shinozaki, Matsuda, Kasuga (2022) (*Fig. 20*). This technology has reduced CO_2 emissions by about 80 to 90% compared to conventional technology in the LCA.

4.3 Low Carbon Technology in the End-of-Life Stage and the Next Cycle

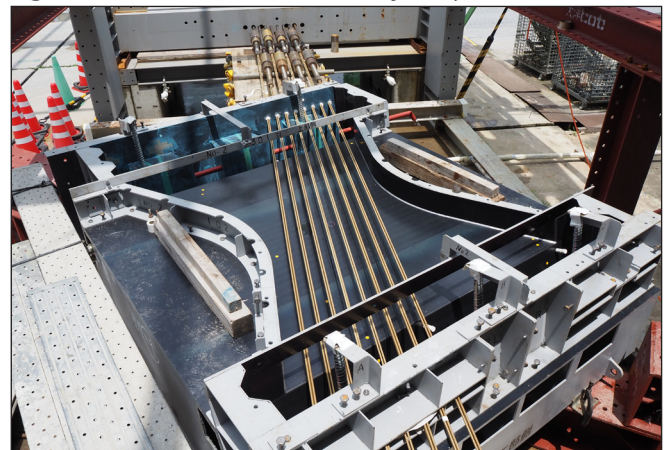The life cycle of concrete structures is long and involves social and environmental changes due to various factors in the use stage. In other words, changes in population, climate and technological paradigm shifts are expected to force changes in the function of the structure. At this time, for example, bridges may be increased or decreased in width, or routes merged or abolished, while buildings may be extended or reduced, demolished and relocated, etc. It is important to design the first cycle with a view to minimizing CO_2 emissions at that time. Concrete structures that are easy to dismantle are required. And as shown in *Fig. 21*, the multi-cycle use of dismantled components by "remanufacturing" (https://www.remanufacturing.eu/about-remanufacturing. php) can bring the CO_2 emissions of A1 to A3 as close to zero as possible. However, various technologies for multi-cycle concrete structures, including standards, are issues that need to be addressed in the near future. New challenges include in-service monitoring, evaluation of components after demolition, techniques to remanufacture them to be equivalent to new ones, and standardization of structures.

5. CONCLUDING REMARKS

It will still take time for reinforcing steel and cement to achieve zero carbon. However, those of us involved in the structural concrete cannot just sit back and wait for that to happen. We are already beginning to be asked for solutions. From now on, we need not local optimization, but global optimization, in other words, "Think globally, build locally". In addition to CO_2 emissions, concrete currently has problems with its materials, water and sand. Drinkable water is used for mixing concrete, but there are more than 2 billion people in the world
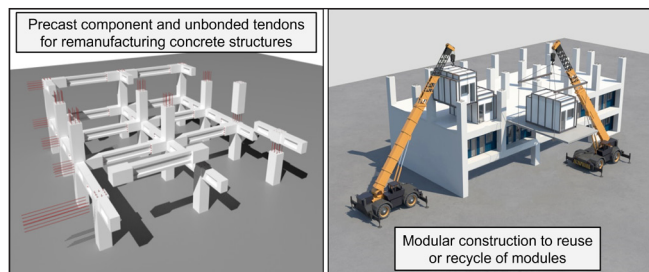
without access to safe water. Furthermore, 7.5 billion tons of sand is used annually, which is equivalent to building a 10m x 10m wall on the equator (40,000 km). Sand is in short supply worldwide. And while countries that import sand make fine concrete structures, countries that export it may risk serious environmental damage. In non-metallic structures using FRP as reinforcement, as discussed above, the concrete can be mixed by seawater, as was the case with Roman concrete, because there is no deterioration factor. Research is also underway to use by-product fine aggregates and desert sand in concrete (Othman, Yehia, Elchalakani, 2022). As described above, precast concrete could be said to have great potential in a world where sustainability is becoming more and more important.

6. ACKNOWLEDGEMENTS

7. REFERENCES

Ashizuka K, Miyamoto K, Kata K, Kasuga A. (2012), "Construction of a butterfly web bridge", *Proceedings fib* Symposium in Stockholm. 2012 Jun.

Favier A, De Wolf C, Scrivener K, Habert G (2018), "A sustainable future for the European cement and concrete industry", ETH, EPFL. 2018.

https://www.remanufacturing.eu/about-remanufacturing.php

Kasuga, A. (2016), "Effects of butterfly web design on bridge construction", *fib Journal Structural Concrete* Vol.18/1. 2016. https://doi.org/10.1002/suco.201600109

Kasuga A. (2023), "Great potential of precast concrete structures for carbon neutrality", CPI – Concrete Plant International, 3 | 2023

Matsuda T, Mine R, Geddes D, Walkley B, Provis J. (2022), "Development of ultra-low shrinkage and high strength concrete without Portland cement with experimental study on its fabrication", *Proceedings*, *fib* Oslo Congress. 2022 Jun.

Matsuo Y, Wada Y, Fujioka T, Nagamoto N. (2021), "Construction of non-metal bridge", *Proceedings fib* Symposium in Lisbon. 2021 Jun.

Othman O, Yehia S, Elchalakani M. (2022), "Development of high strength concrete with fine materials locally available in UAE", *Proceedings fib* Oslo Congress. 2022 Jun.

Shinozaki H, Matsuda T, Kasuga A. (2022), "Construction of non-metallic bridge using zero-cement concrete", *Proceedings fib* Congress 2022 in Oslo. 2022 Jun.

Dr. Akio KASUGA, *fib* Immediate Past President, Sumitomo Mitsui Construction, Japan, akasuga@smcon.co.jp

GREEN CONCRETES – PRINCIPLE DESIGN APPROACHES FOR MATERIALS AND COMPONENTS

Harald S. Müller

This article deals with the evaluation and design of eco-concretes (green concretes) and structural components made from them. Such concretes are characterized by a pronouncedly reduced CO_2 footprint compared to conventional structural concretes made with Portland cement clinker. After an introduction to the sustainability problems of today's structural concretes, the basic approaches to the development of sustainable concretes are presented. The specific parameter Concrete Sustainability Potential is introduced, which combines the main effecting parameters environmental impact, service life (durability) and performance (strength). An overview in possibilities available today for producing green concrete mixtures is given. Certain emphasis is placed on eco-concretes, in which a large proportion of the cement is replaced by rock powders. Further, a new and innovative relationship for sustainability design is introduced. This concept is equally applicable to concrete as a material and to components made from it. The article concludes with considerations on the implementation of this new concept in practice.

Keywords: *green concrete, concrete composition, sustainability, design.*

1. SUSTAINABILITY PROBLEMS ASSOCIATED WITH TODAY'S CONCRETE

Concrete is by far the most important building material of the modern industrial age. It has made possible the economic development of the industrial nations over the last 100 years. With an annual production volume of currently approx. 8 billion m³ of concrete, economic development worldwide would not be possible without it. The decisive advantages of concrete - comparatively high strength and durability combined with high availability in huge quantities and cost-effective production anywhere in the world - are not even remotely matched by any other building material.

However, a very unfavourable factor is the high CO_2 emission associated with concrete production which results mainly from the cement manufacturing. It was not until the turn of the millennium that awareness was raised that the production of cement is one of the most energy-intensive and CO_2-intensive industries in the world, surpassed today only, for example, by energy production through the burning of fossil fuels and the steel production. It is estimated that the cement industry is currently responsible for about 7-8% of the global man-made CO_2 emissions.

These emissions have to be tremendously reduced, as a contribution of the concrete industry, so that the international agreement to limit global warming to a maximum of 1.5 degrees Celsius above pre-industrial levels can be reached. This target was set in the Paris Agreement of 2015 in order to prevent the worst effects of the climate change. It is therefore not surprising that many strategies have been developed, in particularly in the past decade, to significantly reduce the CO_2 footprint associated with concrete construction.

In the subsequent chapters the basic approaches to the development of sustainable CO_2 reduced concretes are presented. As an important tool, the concrete sustainability potential is introduced which combines the governing parameters environmental impact, service life (durability) and performance (strength). Further, an overview on the possibilities available today for producing green concrete mixtures is given. Hereby emphasis is placed on eco-concretes for which a large proportion of the cement is replaced by rock powders. Finally, a new and innovative relationship for sustainability design is introduced. This concept is equally applicable to concrete as a material and to components made from it.

2. APPROACHES TOWARD SUSTAINABLE CONCRETE

In order to meet the requirements of sustainability with regard to concrete as a building material, at first sight the concrete composition must be fundamentally changed. In particular the content of Portland cement clinker, which is associated with extremely high CO_2 emissions, must be reduced or must be substituted as far as possible by more environmentally friendly binders.

However, when evaluating the sustainability of concrete, the reduction of the CO_2 emissions alone cannot be

addressed. For example, if one single high CO_2 emission is associated with a high-quality concrete that may withstand all critical exposures for many decades without repair or replacement, then the initial adverse emission has to be evaluated differently. Moreover, high performance and durability are required from the building material itself in the case of structures, which cannot be guaranteed in principle by ecologically optimized concrete. Therefore, the parameters of performance and service life must be considered equally with the environmental impact in a balance sheet related to sustainability. Taking these considerations into account, the Concrete Sustainability Potential (CSP) was introduced, as defined by equation (1), see (Müller et al 2016 and fib 2023):

$$\text{concrete sustainability potential (CSP)} = \frac{\text{service life } (t_{SL}) \cdot \text{performance } (f_{ck})}{\text{environmental impact (GWP)}} \quad (1)$$

Herein, f_{ck} is the characteristic strength of the concrete in [MPa] representing the possible performance of the material, t_{SL} is the potential service life of the concrete under the specific environmental actions to be expected in the lifetime of the building member in years [a], and GWP is the environmental impact associated with the production of the concrete including all raw materials expressed by the lead parameter Global Warming Potential (GWP) in eq. kg CO_2; for further details see (fib 2023).

Equation (1) represents a simple tool to quantify the advantages and disadvantages of a specific concrete type regarding its potential as a sustainable material. The exploitation of this potential during the design and construction process depends on the designer and user of the building or structure. It should be noted that equation (1) may also be applied for structural components.

According to equation (1), three basic approaches to a sustainable use of concrete exist: The first is the optimization of the composition of the concrete regarding its environmental impact while maintaining an equal or better performance and service life; the second is the improvement of the concrete's performance at equal environmental impact and service life; the third is the optimization of the service life of the building material and the building structure at equal environmental impact and performance. A combination of the above-mentioned approaches appears reasonable. This is also summarized in the subsequent *Fig. 1*. It also indicates some examples, how to maximize service life and performance, and how to minimize the environmental impact.

Related to the environmental impact, i.e. the use of raw materials with reduced eco-impact, e.g. composite cements,

new types of cements (low/no carbon), recycled concrete aggregates and the use/development of concretes with reduced binder and/or cement clinker content, chapter 3 of this paper indicates further details.

As the use of Portland cement is indispensable for producing structural concrete today, the question arises what the most efficient way is when applying this binder in view of minimizing the environmental impact. In this context a concrete data evaluation by Damineli et al (2010) is very revealing. They have defined a so-called binder intensity, and have plotted this binder intensity over the compressive strength (see *Fig. 2*). The decreasing binder intensity with increasing compressive strength indicates that the use of Portland cement is the more efficient (sustainable) the higher the strength is. This is the more pronounced as for higher strength concrete the cross-section of members may be reduced, i.e. a reduction in mass consumption is achieved at a given load-bearing capacity.

Fig. 2 also indicates that for normal and low strength concrete the amount a cement used for these concretes is not necessary for the reason of strength, however, certainly for workability and durability reasons. This means that cement may be saved for these kinds of concrete, if workability and durability are guaranteed by other measures. This would be very efficient in view of sustainability as roughly 90 % of all concretes used in practice have a compressive strength between 20 and 50 MPa.

From *Fig. 2* the general conclusion may be drawn that the reduction of the binder content of ordinary strength concrete and the use of high strength concrete lead to a sustainable use of concrete. The concept of reducing the binder content for ordinary structural concrete while keeping its advantageous technical properties is further analysed in chapter 3 of this paper.

3. GREEN CONCRETE MIXES

3.1 General approaches

In order to meet the requirements of sustainability with regard to concrete as a building material, the currently used concrete compositions must be fundamentally changed. In particular the Portland cement clinker (PC), which is associated with extremely high CO_2 emissions, must be substituted as far as possible by more environmentally friendly binders, for example secondary cementitious materials (SCM) and/or new types of hydraulic binders. Further, substitution with

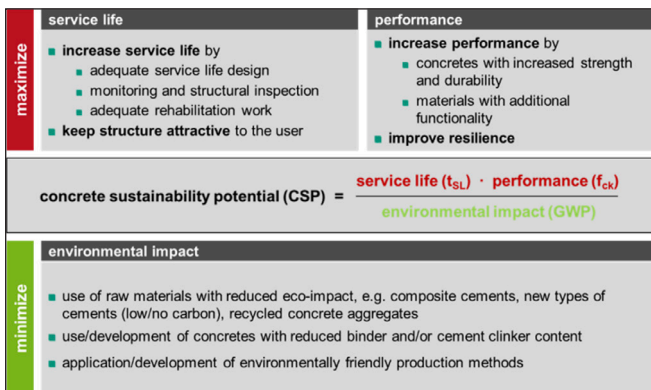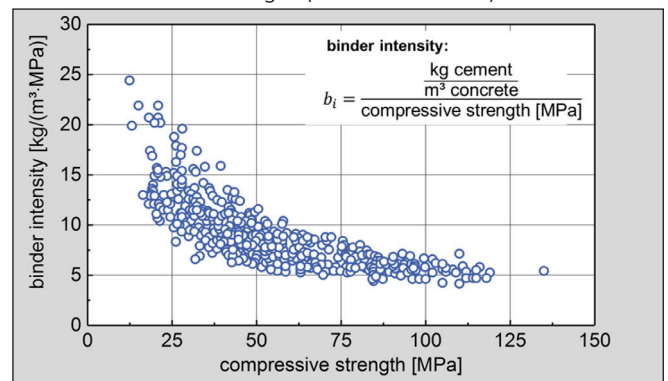**Fig. 1:** *Overview on approaches and tools to develop sustainable concretes*

Fig. 2: *Efficiency of the use of binder depending on the strength of structural concrete according to (Damineli et al 2010)*
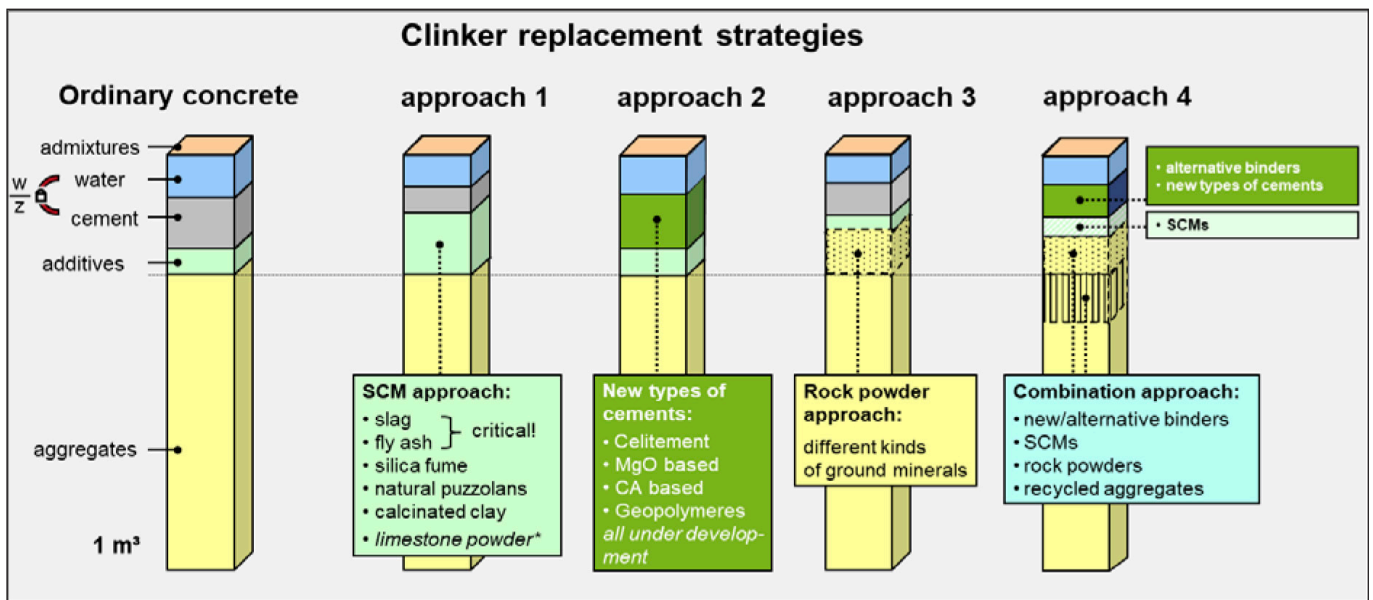
Fig. 3: *Strategies and examples for the reduction or replacement of Portland cement clinker for the production of structural concrete*

inert fines of aggregates is also a very promising approach to significantly reduce the carbon footprint of concrete mixes.

Fig. 3 summarizes the different strategies for clinker replacement by subdividing these strategies into four different kinds of approach. The composition of ordinary structural concrete in volume parts is indicated by the first column (left). Apart from the aggregates which comprise a volume of approx. 70 %, the remaining 30 vol % are filled by water, cement (or substitute products), additives and admixtures.

Approach 1 (see *Fig. 3*) shows a pronounced replacement of the cement by SCM additives. The materials blast furnace slag (BFS) and fly ash (FA) being often used today must be viewed critical. BFS is a by-product of steel production. Therefore, its availability is limited and BFS may never replace PC due to the huge amount of PC which is needed worldwide. FA is a waste-product resulting from coal combustion. However, the energy generation from coal combustion is extremely problematic due to the high associated CO_2 emissions. Therefore, this type of energy is coming to an end in a continuously increasing number of countries. This means that FA will become more and more scarce in the concrete industry and will no longer be available at some point. Silica fume (SF) is also by-product having a very limited availability in the market. The other SCM mentioned in *Fig. 3* (approach 1) can be expected to increasingly enter the market. However, there is still a considerable need for research in the area of calcinated clays.

Approach 2 (see *Fig. 3*) assumes that Portland cement clinker will be completely replaced by new types of cements/ binders. In addition to the product Celitement these are primarily MgO- and CA (= CaAl)-based binders as well as geopolymers. Intensive research is currently being carried out related to these binders. Despite some successes and promising approaches, however, it must also be noted that no binder has yet been developed or is under development which, in terms of its technical properties, is equivalent to the product Portland cement clinker.

Approach 3 (see *Fig. 3*) is characterized by the fact that a large proportion of the cement is replaced by finely ground inert aggregates. The underlying idea is that these aggregates form the necessary fines in the concrete mix to ensure the cohesion and the processing of a concrete mix and also contribute to the concrete strength, which is, however,

mainly provided by the remaining Portland cement clinker. This approach, which dispenses completely with the use of SCM, is further described below.

Approach 4 indicated in *Fig. 3* is a combination of the approaches 1 to 3 with the additional use of recycled aggregates for concrete production.

An alternative to these four approaches is the CO_2 avoidance strategy by carbon capture and storage (CCS) or carbon capture and use (CCU) concepts being under development in some countries. These concepts allow the conventional production of PC as the associated CO_2 emissions are captured by applying available technologies. Although this is a promising approach, it must be noted that there are numerous technical, economic and social problems associated with it. It is very unlikely that a sufficiently large volume of PC may be produced by applying these technologies, in particular not until 2045, when the zero CO_2 emission target should be reached in Europe.

Approach 1 is mainly used by the cement industry to significantly reduce the mass proportion of Portland cement clinker in the binder for concrete. As a result, there is a very wide range of more environmentally friendly, standardized binders/cements for concrete on the market today. Approaches 2 and 3 are in the focus of the current research. This research is entering new areas what is not the case with the cement industry approaches, as it has to stay within the framework of established regulations with its modified binders in order to be able to serve the needs of the market.

3.2 Green concrete by the rock powder approach

As already mentioned above, approach 3 was scientifically investigated in more detail by the author (Müller et al 2016 and 2019). One of the main reasons for this was the positive result of preliminary investigations, which showed that it is possible in principle to reduce the cement content of concrete from over 300 kg/m³ to values of around 100 kg/m³ if the missing cement quantity is replaced by aggregate powders without losing any of the concrete's essential properties. A further positive aspect is that rock powders are available or may be produced anywhere in the world.

However, this change in the composition of concrete, i.e.

Concrete composition				Concrete properties				
component		**ord**	**green**	**parameter**			**ord**	**green**
type of cement	-	42,5 R	52,5 R	compr. strength f_{cm}			38,4	76,9
cement	[kg/m³]	320	113	modulus of elast. E_c	[N/mm²]		33700*	38030
water		192	87	spl. tensile str. $f_{ctm,sp}$			2,9*	2,3
paste content	[Vol.-%]	29	13	flex. strength $f_{ctm,fl}$			4,4*	4,9
w/c ratio (eff.)	[-]	0,60	0,64	inverse carbonation resistance R_{ACC}^{-1}	[(10⁻¹¹ m²/s) /kg/m³]		13,4	18,9
quartz powder 1		-	96	chloride migration coefficient $D_{RCM,0}$	[10⁻¹¹ m²/s]		2,5	2,0
quartz powder 2		-	120	CDF frost spalling	[g/m²]		< 1500	2760
sand 0/2	[kg/m³]	550	955¹⁾	Global Warming Potential	[equ.kg CO_2 /m³]		285	135
gravel 2/8		635	480					
gravel 8/16		640	505					
plasticizer		-	6,5					

* according to *fib* Model Code 2010
¹⁾ splitted in two fractions 0.1/1 and 1/2 mm

Fig. 4: *Comparison of green concrete (cement replacement by rock powder) and ordinary concrete C30/37 – concrete compositions (left) and concrete properties (right)*

the replacement of cement by rock powders is associated with considerable complications. Elaborated particle packing density model approaches must be used to determine the composition of the fines properly. To ensure sufficient workability – the water content of the concrete must be drastically reduced to prevent the water-cement ratio from increasing too much when the cement content reduces – extensive preliminary tests with various superplasticizers proved necessary.

Fig. 4 summarizes important results of the extensive investigations given in (Müller, 2019). It shows the composition (left) of a standard structural concrete and a green concrete produced according to approach 3. The right part of *Fig. 4* shows the concrete properties determined in each case. While the strength parameters and the stiffness of the green concrete are even better compared to ordinary concrete, the lower resistance to carbonation and the insufficient frost resistance in particular are deficits. However, it appears that these disadvantages can also be compensated to a large extent by further developments. On the other hand, such a green concrete could already be used wherever no frost attack is given. Its GWP is reduced to a value of approx. 50 % compared to that of an ordinary concrete (here GWP considers all materials and processes).

A rather particular aspect has to be considered when comparing the composition and the properties of conventional and green concrete produced by the rock powder approach. While the water-cement ratio increases from 0.60 to 0.64, the compressive strength increases from 38.4 to 76.9 MPa as well (see Fig. 4). This is in contrast to Abram's well-established law, which states that with increasing water-cement ratio the compressive strength is decreasing. This means that green rock powder type concretes behave differently than normal concretes, and that well-established relations for normal concretes are not necessarily valid for these types of green concrete.

3.3 General consideration in view of applying green concretes

The positive development of hydraulic binders for concrete with regard to environmental issues due to the increasing substitution of Portland cement clinker is accompanied by a certain disadvantage resulting from the novelty or the lack of experience with these products, respectively. Thus, for classical concrete, whose binder consists essentially of Portland cement clinker and/or granulated blast furnace slag, a very large number of scientific studies are available with

regard to a wide variety of material properties, as well as extensive long-term observations and practical experience. These findings have been reflected in material models and design approaches available to the designing engineer. Since this is not the case for concretes with new binders, the necessary performance tests to ensure safety and durability are of great importance when building with these new types of concretes.

4. DESIGN TOOL FOR CONCRETES AND COMPONENTS

The Concrete Sustainability Potential as defined with equation (1) is a useful tool for making comparative considerations when selecting or specifying a concrete in advance of a construction project. This tool makes it possible to identify a specific concrete with a high sustainability potential that also meets the required technical specifications. However, in order to be able to carry out an engineering design of a concrete for sustainability, equation (1) must be reformulated for various reasons. This also applies for the case that equation (1) is used for the design of components, which is possible in principle as well.

In design, target values have to be related to an upper or a lower limit. Hence, the inverse of the Concrete Sustainability Potential shall be considered. Further, it is very difficult to give limiting values for a property like sustainability, as it is not based on a defined physical dimension like strength or stresses or strains are. Hence, relative values should be determined in which as a consequence the dimensions are cancelled. Further, as the concrete strength is the basis for the design of a member, and is calculated from the requirements regarding the load-bearing capacity, it is kept constant and thus canceled for the design for sustainability.

Taking the afore-mentioned considerations into account, the general format for verification of concrete environmental performance is proposed with equation (2), which defines a limit state, see (fib 2023):

$$ELS_{cal} = \frac{\left[\dfrac{\Sigma EI}{SL}\right]_{eco}}{\left[\dfrac{\Sigma EI}{SL}\right]_{ref}} \leq ELS_{predefined} \leq 1.0 \qquad (2)$$

ELS_{cal} is the calculated concrete environmental performance limit state, $ELS_{predefined}$ is the limit value that defines the ELS criteria, EI is the environmental impact of concrete and concrete production and SL is the service lifetime.

The index *ref* indicates the value calculated for a reference concrete. The index *eco* indicates the value calculated for a concrete for which an optimization has been carried out in such a way that the predefined limit state criteria ($ELS_{predefined}$) is fulfilled.

For practical application, equation (2) can also be simplified, for example by focusing the limit state consideration exclusively on the of CO_2-eq emission. In such case, $\Sigma EI = CO_2$-eq mass per cubic metre [kg/m³] of concrete and SL = 1.0. For more details, see (Haist et al 2022 Oslo, and Haist et al 2022) and (fib 2024 in prep.).

Fig. 5 shows an example of dimensioning according to equation (2). First, different concretes must be compared with each other in terms of their sustainability potential given on the y-axis, see *Fig. 5,* diagram top left. As a result,
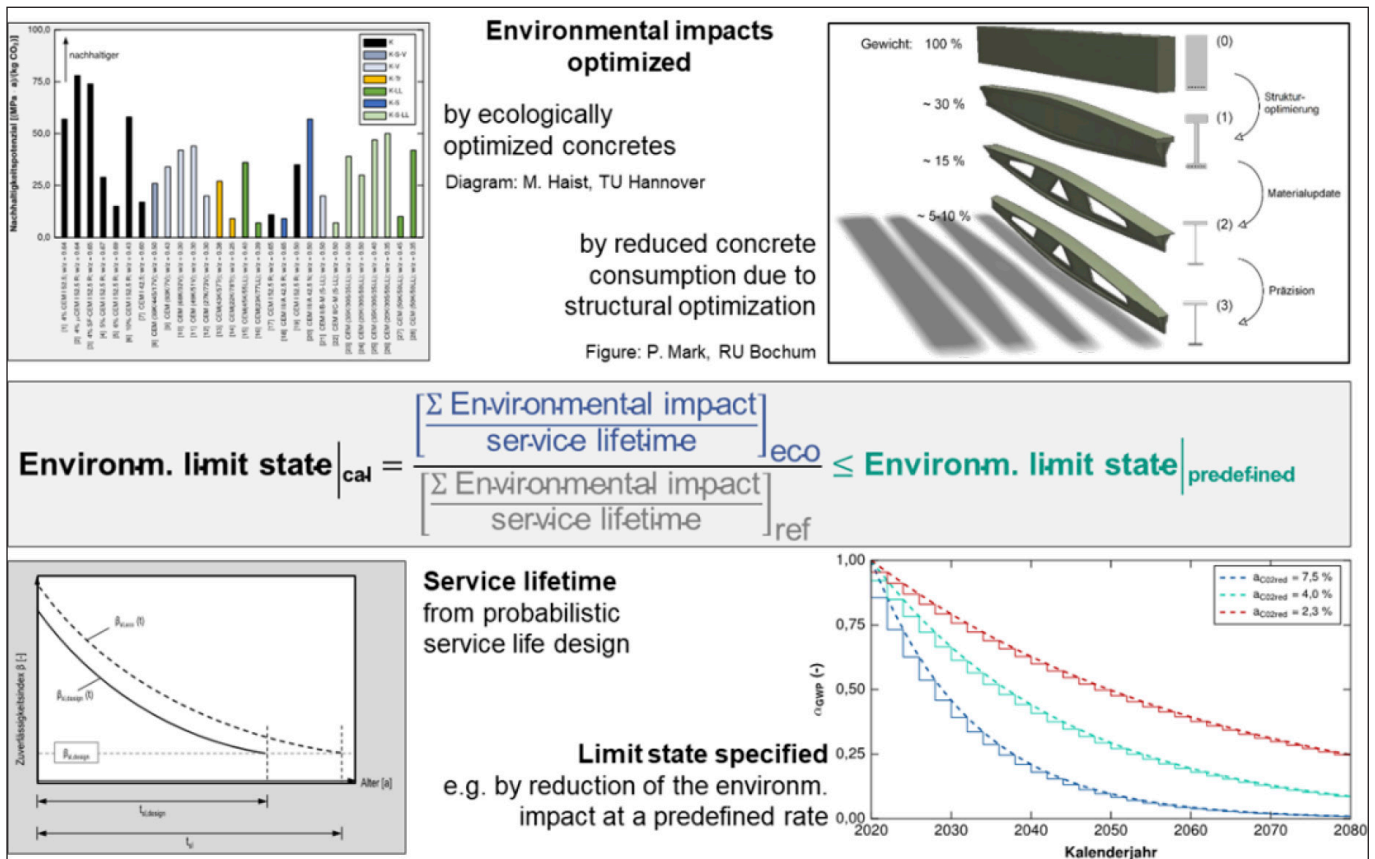
Fig. 5: *Example for design of concrete members by means on the design equation for sustainability as given in (fib 2023)*

a specific ecologically optimized concrete can be selected. A further step is to optimize the structural component in terms of maximizing the load-bearing capacity while minimizing the concrete consumption (see *Fig. 5*, diagram top right). Both considerations and optimizations lead to an optimized environmental impact for the finally used structural component.

The next step in this design approach is to consider the service life (see *Fig. 5*). Ideally, a probabilistic design for service life is carried out. The diagram at the bottom left in *Fig. 5* shows the result of such a design, whereby the reliability index given on the y-axis decreases with increasing time under service. At the end of the defined service life, the given reliability limit state is reached.

In the last step of design, the limit state for sustainability must be defined. Due to the structure of the design equation, this limit state can be expressed by any number between 0 and 1. Since with regard to the reduction of CO_2 emissions, the desirable limit state of zero emissions cannot be achieved immediately but rather through a degressive development over the time, the assessment can be based on corresponding progressions, taking into account the calendar year. The diagram at the bottom right of *Fig. 5* shows the curves for three different annual reduction rates for CO_2 emissions.

This concept for sustainability assessment and design presented here is innovative and new. It can be considered as a basis and framework, and as a starting point for further developments. So far, there is no practical experience in the application of this concept. It is to be expected that the application of this concept in the practice of concrete construction will certainly lead to further improvements in the coming years.

5. CONCLUDING CONSIDERATIONS

The concrete construction industry faces significant challenges, which primarily consist in reducing the CO_2 footprint of concrete construction without negatively influencing the technical performance and the superior durability of the produced structures. Even though environmentally optimized concretes are readily available today and techniques to produce much slimmer and mass reduced structures have been proposed, these techniques are rarely implemented in every day construction as suitable incentives and the necessary knowledge are lacking.

Nevertheless, it is the designer who plays the decisive role on the way to an efficient reduction of the GWP and such the protection of the global climate. The design aids proposed with equation (1) and equation (2) are initial approaches, still to be further developed, for demonstrating the sustainability of materials and components. However, such proofs will only find their way into practice when a core problem that still exists today is overcome. This is that nearly all measures that lead to a significant improvement in sustainability are ultimately still associated with higher costs. As long as this does not change, the cost pressure in the competitive economic environment means that the desired, major progress will fail to materialize.

Ultimately, this deficit can only be eliminated by enforcing sustainable measurement with normative specifications. Since the CO_2 emissions associated with the production of concrete components can be calculated with the tools available today, one concept could be, for example, to price the CO_2 emissions, as is currently already the case with emissions trading. It will be interesting to see what solution politicians come up with in this regard. The necessary tools have already been provided by the research community.

6. REFERENCES

fib International Federation for Structural Concrete (fib) (2023) Final draft of the *fib* Model Code for Concrete Structures 2020. fib Lausanne, Switzerland

fib Bulletin (2024 in prep) Background document to Chapter 14 "Concrete" of the *fib* Model Code 2020. To be published in 2024

Damineli, B.L., Kemeid, F.M., Aguiar, P.S., John, V.M. (2010) Measuring the eco-efficiency of cement use. Cement and Concrete Composites 32, pp. 555-562, https://doi.org/10.1016/j.cemconcomp.2010.07.009

Haist, M., Bergmeister, K., Curbach, M., Mark, P., Müller, C., Müller, H.S. et al. (2022) Climate Limit State (CLS) for Building Structures – a possible companion of ULS and SLS Limit States. Proceedings of the fib International Congress, Oslo, Norway, June 12-16

Haist, M., Bergmeister, K., Curbach, M., Forman, P., Gaganelis, G., Gerlach, J., Mark, P., Moffatt, J., Müller, C., Müller, H.S., Reiners, J., Scope, C., Tietze, M. and Voit, K. (2022) Nachhaltig konstruieren und bauen mit Beton. Beton-Kalender, eds K. Bergmeister, F. Fingerloos and J.-D. Wörner, 421-531, https://doi.org/10.1002/9783433610879.ch7

Müller, H. S., Haist, M., Moffatt, J. S. (2016) Environmental impact, performance and service lifetime – pillars of sustainable concrete construction. Proceedings of the International Conference on Concrete Sustainability (ICCS16), Madrid, Spain, 2016

Müller, H. S., Moffatt, J. S., Vogel, M., Haist, M., (2019) A new generation of sustainable structural concretes – Design approach and material properties. Proceedings of the International Conference Central Europe Towards Sustainable Building (CESB16), Prague, Czech Republic, 2019

Harald S. Müller is professor emeritus of the Karlsruhe Institute of Technology (KIT) in the field of concrete and concrete structures. He serves as senior expert (former CEO) and publicly certified and sworn expert for concrete and masonry constructions at SMP Engineers in Construction Ltd in Germany. Prof. Müller published over 450 papers in his major research fields concrete technology, creep and shrinkage, service life design, sustainability and rehabilitation of concrete structures. He is Honorary President of the *fib*, Honorary Member of the ACI, and he served 2015-2016 as the President of the *fib*. E-mail: h.mueller@smp-ing.de, Prof. Dr.-Ing., SMP Ingenieure im Bauwesen GmbH, Karlsruhe, Germany

NOVEL CONCRETE BRIDGE DESIGN - AS SIMPLE AS POSSIBLE, BUT NOT SIMPLER

Konrad Bergmeister

The paper discusses the need for a simplified and low-maintenance building culture to address global climate change. A transition to a circular economy, giving priority to efficiency rather than quantity is important. Creating structures with minimum material consumption and minimum maintenance with a maximum of recyclability should be our focus. Integral bridges such as the Duke's Bridge in Germany and the Isarsteg-bridge in Munich are innovatively designed while taking into consideration the soil-structure interaction and the temperature induced stresses in structural detailing. The paper also considers additional technical aspects, such as the calculation of the mobilised earth pressure and the relevant deformations. Finally, a holistic approach that aligns with principles of resource efficiency, simplicity, and sustainability is suggested.

Keywords: Integral bridges, resource-efficient, sustainability, soil-structure-interaction, mobilized earth pressure

1. INTRODUCTION – SOME BASIC IDEAS

It is time to adopt a more simple and recyclable building culture to combat climate change, which knows no borders and is a worldwide reality (Glock, Haist, Bergmeister, Voit, Beyer, Heckmann, Hondl, Hron, Schack, 2023). The building industry must undergo a significant transformation, with all materials and resources integrated into a circular economy. Innovations must prioritize efficiency over quantity in the future. This publication focuses on the beauty of simple, but not simpler structures.

The goal should be to build structures that are as simple in terms of material consumption as possible, and as recyclable without waste as possible, as Einstein (1879 – 1955) once said.

The aim of resource-efficient design, dimensioning and construction is to align the load-bearing structure with the load-bearing force flow while taking aesthetics into account. Only as much material should be used as is absolutely necessary!

In current research, load-bearing structures are often designed as bar structures or arches. Optimization methods are also used to take shapes from nature, such as trees, plants and structures, in order to develop a bionic load-bearing structure. However, real construction is more complex! In addition to the primary load transfer, load-bearing elements are also used for installations and extensions. Therefore, newly designed load-bearing structures should be designed both for a long service life and for the most flexible use possible!

In general, we need to focus on resource-efficient and emission-low design developing structural details which require less maintenance as possible and have a predictable life span. Therefore, integral bridges can be for span lengths up to 80 m one piece of the solutions. There is not one solution in order to face climate change, but we have to promote many solutions and we have to change our mindset.

2. LESS IS MORE – BEAUTY REQUIRE AN EFFICIENT CONCEPTUAL DESIGN

Ludwig Mies van der Rohe (1886-1969), the renowned architect, advocated for resource efficiency through the principle of minimalization, famously known as "less is more," which he incorporated into his designs. Simplicity in design does not necessarily mean designing a simple structure, but rather designing a structure that is efficient and uses the minimum amount of materials necessary for its function. This approach can lead to elegant and beautiful designs that are both sustainable and functional. By minimizing the amount of materials used, we can reduce the environmental impact of construction and ensure that resources are used efficiently. Additionally, a focus on simplicity can lead to designs that are easier to construct and maintain, reducing the overall cost of the project.

Plato (428 - 348 BC), the ancient Greek philosopher, is often credited with the quote "Beauty of style and harmony and grace and good rhythm depend on simplicity." This quote reflects the idea that simplicity in design can lead to beauty and harmony in the built environment. In our times, less is more satisfies points like: zero waste (Natanian, 2020), zero energy, zero, emission, less materials, time-save for the realization, easy functionality and less maintenance and finally an authentic and beautiful architecture. Integral bridges satisfy almost every point and they can be built also for an extended life span over 100 years.

3. INTEGRAL BRIDGES

New research on structural details considering the temperature induced stresses are the basis for novel developments of integral bridges (Tue, Della Pietra, Mayer, 2021). The structure-soil interaction play a very important issue and has to be calculated carefully. The choice and application of soil parameters in the design have a major impact on the overall behaviour of a structure. Two philosophies can therefore be pursued in the design:

- Formation of a low degree of restraint in the area of the abutments or supports and low bending stiffness of the foundation. Due to the flexibility, a certain rotational capability of the superstructure can be assumed and the frame corner can be designed relatively simply due to the lower moments. The field moments are similar to those of a conventional supporting structure. This practice is very common in the USA and Canada and is documented in the associated guidelines (e.g. for sheet pile foundations, even for longer supporting structure lengths and temperature gradients)

- High bending stiffness of the abutment or short, solid supports as well as a massively designed foundation lead to a high clamping effect of the superstructure. As a result, lightweight superstructures can be designed because part of the moment is shifted from the field moment to the frame corner. However, the formation of such a frame corner requires more effort for structural detailing. Furthermore, the desired clamping moment must also be realized for the foundation, which inevitably results in high earth resistances and consequently also possibly high undesirable constraints.

The amount of mobilized earth pressure is determined by the size of the abutment wall displacement. This can be determined in different ways, whereby the translational and rotational components must be taken into account in the calculation. Also a simplified earth pressure (e.g. rectangular or triangular (RVS, 2018)) can be used for the design in order to capture the effects of the mobilised earth pressure .

$$e_{mob} = e_0 \cdot [1 + L \cdot (0.06 - 0.005 \cdot H)] \geq e_{0|}$$

e_{mob} = mobilised earth pressure
e_o = earth pressure
H = Height $[m] \leq 10m$
L = Span length $[m] \leq 30m$

The cyclical shift due to the temperature change ΔT results in a pumping movement over the service life of the structure. This leads to an increase in earth pressure when the structure
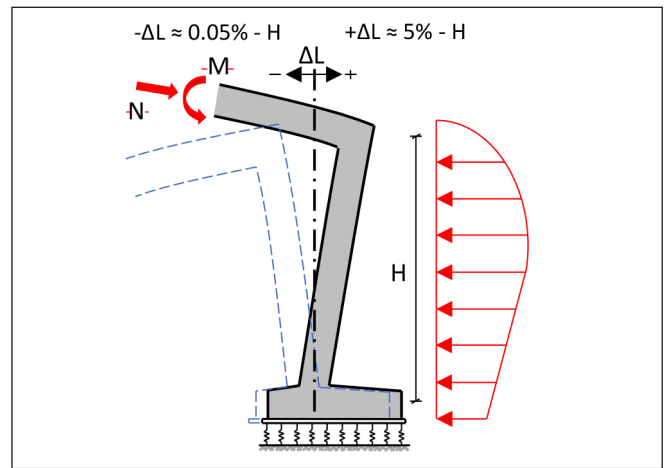
Fig. 1: Schematic force flow of the earth pressure in the abutment zone (taken from Ref. Della Pietra, 2017)

extends (mobilised passive earth pressure) and to a reduction in earth pressure compared to the earth pressure, when the structure is shortened (mobilised active earth pressure). The amount of mobilised earth pressure depends on the size of the abutment wall displacement ΔL. A slight movement away from the soil is sufficient ($-\Delta L \approx 0.05\%$ - H) to mobilise the active earth pressure eactive. On the other hand, large displacements ($+\Delta L \approx 5\%$ - H) are required to fully mobilise the passive earth pressure. However, the necessary large displacements do not occur in the integral bridge construction, resulting in only a partial mobilisation of the passive earth pressure e_{mob} (Della Pietra, 2017).

The following calculation options can in principle be adopted:

- iterative determination of the abutment wall displacement on a model, taking into account a damping factor
- direct determination of the abutment wall deformation on a model, taking into account the existing structural and foundation stiffnesses
- measured values on similar integral bridges.

3.1 An integral concrete bridge

The new Duke's Bridge in Eichstätt - Germany, which was awarded the Bavarian Engineering Award in 2023, is a prime example of beauty, simplicity, and resource efficiency (Bergmeister, Taferner, 2023). The goal was to create a simple monolithic structure with low-maintenance, and without any waterproofing or surfacing layers.

The bridge is a cantilevered integral design with no

Fig. 2: Longitudinal section of the integral Duke's Bridge (www.bergmeister.eu)
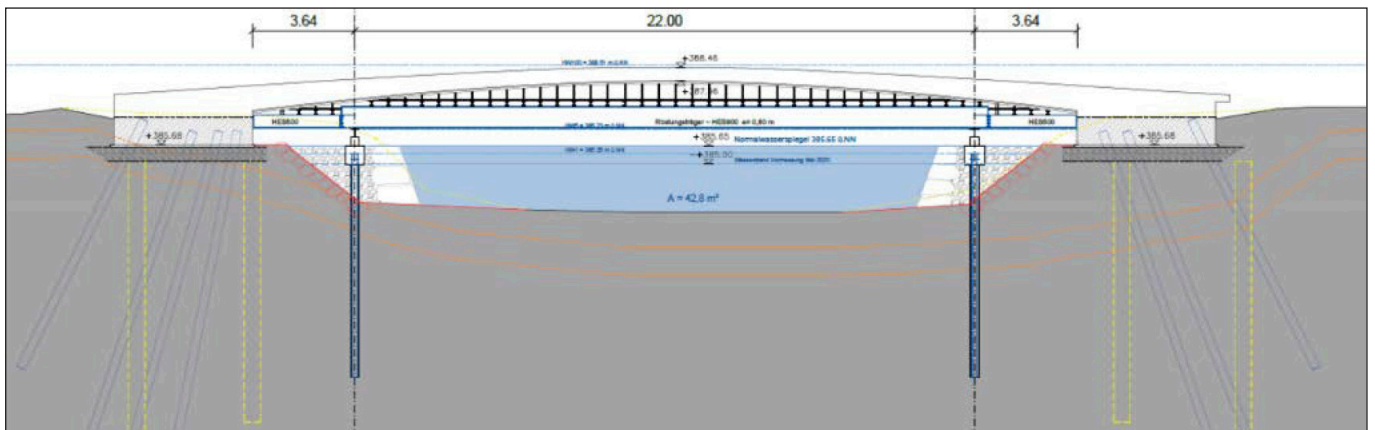
bearings or joints over a length of approximately 30 m. The frame effect is activated by cleverly arranged small bored piles under the strongly designed abutments. The counterweight of the abutments and pairs of forces from the pile foundation transfer the restraining moments. The load-bearing capacity is enhanced by the passive earth pressure. The mobilized earth pressure was determined by wall displacement under summer temperature conditions. In Germany only the summer case is taken into account for the calculation of the mobilised earth pressure, wherever in Switzerland and Austria the total deformation (summer and winter) is used to take. The abutments of the Duke's Bridge are fully integrated into the embankment, and the forces are transferred into deeper load-bearing gravel through small, slightly inclined, grouted bored piles with a diameter of 78 mm.

The integral bridge was designed with an asymmetrical waisted shape. Its structure consists of a flatly curved bending beam made of reinforced concrete that is clamped at the abutments, with a maximum longitudinal inclination of the carriageway of 6%.

The bridge's design widens in a trumpet-like direction, resulting in a width of 5.5 m on one side and 9.8 m on the other. The maximum slab thickness close to the abutment is

Fig. 4: Overview of the integral Duke's Bridge (www.bergmeister.eu)

90 cm, while it is 50 cm at the apex. The cross-section of the bridge is streamlined to the edges, similar to a profile suitable for flood discharge. The rounded underside of the bridge is designed to minimize the surface area for floodwater, flotsam, and debris while offering deflection possibilities in the direction of flow. In the event of a flood, the railing can be easily dismantled by hand within a very short time.

To analyze various deformations, specific 3D calculations were conducted considering shrinkage and long-term creep effects. Additionally, dynamic investigations were carried out to assess possible vibrations, resulting in a first eigenmode in the form of a vertical sinusoidal movement with a natural frequency of 2.57 Hz and a modal mass of approximately 65 tons.

In terms of durability, the carriageway slab was coated with double-deep hydrophobic layers to ensure a minimum lifespan of 100 years even under severe environmental conditions or flooding events. A probabilistic calculation for the durability (*fib* Bulletin 76, 2015) was carried out for a service life of 100 years. An average concrete cover of 42 mm with a standard deviation of 9 mm was selected. The required reliability index β at the end of the estimated service life of 100 years was assumed to be $\beta = 0.5$ for an exposure class XD3. In any case, it was assumed that the bridge is regularly

Fig. 3: Overview of the integral Duke's Bridge (www.bergmeister.eu); completed in 2022; "Prize of Bavarian structural engineering 2022", Architectural Design: J2M Mayr Metz Architekten, Munich; Structural Engineering: Bergmeister Ingenieure GmbH

Fig. 5: Overview of the integral Corten-steel Isarsteg-bridge (www.bergmeister.eu) completed in 2015; "Prize of German steel construction" 2016, Architectural Design: J2M Architekten / Ch. Mayr, Munich; Structural Engineering: Bergmeister GmbH & structures, Photo: O. Jaist

inspected and maintained.

Additionally, specific laboratory tests were conducted on the casted concrete to verify the chloride migration coefficient. The proportion of granulated blast furnace slag in the binder was increased to reduce hydration heat and improve post-hardening and chloride penetration resistance. Stainless steel reinforcement of grade B500B NR/B670B NR "Top12" (material no. 1.4003) was utilized.

3.2 An integral steel bridge

The Isarsteg-bridge in Freising near Munich is an integral steel bridge made of Corten steel. The entire load-bearing structure is composed by the slender superstructure, the stairways and ramps and the soil. All components are connected in a monolithic manner and designed without sliding bearings and joints. The 58 m long river crossing has a triangular, torsional rigid, airtight and watertight welded steel box girder with a variable cross-section.

There are transverse bulkheads every 3 meters inside the box girder. The composite structure consists of the cover plate of the box girder and a 15 cm thick reinforced in-situ concrete slab.

The superstructure from the lower edge of the girder to the upper edge of the pavement, has a constant height of 1.20 meters over the entire length. Its structural height is primarily based on two aspects:

1. The lower edge corresponds to the specified freeboard (distance between the water level and the lower edge of the footbridge), which protects the bridge from damage caused by floating debris in the event of flooding.
2. The walkway level was not allowed to be too high above the embankment paths so that the gradient of the ramps would not be too steep for wheelchair users.

The structurally favorable triangular shape and the ability to respond to different force and moment curves with different sheet thicknesses and cross-sectional shapes also creates a lightweight, robust and economical supporting structure.

The clear lines of the bridge required the cantilevering of the hollow box girder, which deforms by around 72 mm (approx. l/780) under maximum live load (traffic).

The first natural vibration frequency of the structure is 1.33 Hz with a modal mass of 65 tons. A vibration damper in the box girder under the pavement slab ensures user comfort.

The novel design and integrative construction method support the sensitive embedding of the structure in the floodplain landscape, which has been designated as particularly worthy of protection. They also contribute to the fact that the bridge can be described as extremely sustainable without any sliding bearings and expansion joints, which are often made of environmentally harmful materials and are also maintenance-intensive.

Finally, the bridge consists of only two materials:
1. reinforced concrete for the pavement slab and foundations and
2. weldable, weather-resistant structural steel S355 J2G2W (steel in accordance with EN10155 or EN10025-5) for the entire steel structure.

The Corten steel does not require any additional corrosion protection due to its dense oxidized rust coating. In addition, the red-brown color integrates in the landscape as a "branch or tree trunk exposed to the forces of nature". The whole bridge is barely visible from a distance, it emphasizes the lightness and elegance of a bridge structure that sees itself as part of a unique natural landscape.

4. REMARKS ON INTEGRITY AND CONGRATULATIONS TO PROF. GYÖRGY L. BALÁZS

Integral bridges and integral personalities have a lot in common. Integral bridges have a distinguished and humble appearance, are acting together with the soil and require almost no maintenance. György L. Balázs is an example of an integral personality. He always creates an environment of

Fig. 6: *Isarsteg-bridge integrated within the natural landscape (www.bergmeister.eu)*

integrity and humility. As Nelson Mandela said:

„You can never have an impact on society if you have not changed yourself. Great peacemakers are all people of integrity, of honesty, but humility."

Prof. Balázs has a worldwide impact in civil engineering science and on society. I would like to thank him warmly for his outstanding engagement and for our long friendship.

Ad multos annos!

5. REFERENCES

Bergmeister, K., Taferner, J. (2023), „The beauty of simplicity and recyclability", Keynote. Proceedings fib Symposium 2023 Building for the future: Durable, Sustainable, Resilient Istanbul, 05 June 2023, DOI: https://doi.org/10.1007/978-3-031-32519-9_2

Della Pietra, R. (2017), „Integralisierung von Bestandsbrücken", *PhD TU Graz,* DOI: https://doi.org/10.3217/978-3-85125-587-4

Glock, Chr., Haist, M.; Bergmeister, K., Voit, K., Beyer, D., Heckmann, M., Hondl, T., Hron, J., Schack, T. (2023), „Klima- und ressourcenschonendes Bauen mit Beton. Mit Urban Mining zum kreislauffähigen Betonbau", *Betonkalender 2024*, Berlin, Ernst & Sohn (in German)

fib Bulletin No. 76 (2015), "Benchmarking of deemed-to satisfy provisions in standards: Durability of reinforced concrete structures exposed to chlorides", *State-of-the-art report*, Lausanne 2015. DOI: https://doi.org/10.35789/fib.BULL.0076

Natanian, J. (2020), "Beyond zero energy districts: A holistic energy and environmental quality evaluation workflow for dense urban contexts in hot climates", *PhD Thesis*. TU Munich DOI: https://doi.org/10.1016/j.scs.2020.102094

RVS 15.02.12: Bemessung und Ausführung von integralen Brücken. Design and construction of integral bridges – Austrian guide line, Vienna 2018

Tue, N.; Della Pietra, R.; Mayer, M. (2021), „Integralbrücken – Tragverhalten und Anregungen zur Bemessung einschließlich Integralisierung von Bestandsbrücken" *Betonkalender* 2021 Ed. Bergmeister, Fingerloos, Wörner. Ernst & Sohn, Berlin, DOI: https://doi.org/10.1002/9783433610206.ch6

Konrad Bergmeister (born April 19, 1959 in Brixen), is a civil engineer and University Professor at the Institute of Structural Engineering, University of Natural Resources and Life Sciences, Vienna, Austria. From 1988 to 1990, he conducted research at the universities of Leuven, Texas and Stuttgart. In 1990 he founded the engineering company Bergmeister GmbH. In 1998 he was the Technical Director of the Brenner-Highway A 22 in Italy and from 2006 to 2019 CEO of the Brenner Base Tunnel SE. As a project manager he was responsible for more than 800 projects. In 1999 he took over the editorship of the scientific journal Beton- und Stahlbetonbau and in 2003 that of the Beton-Kalender. In 2010, the author of over 700 scientific publications took over the presidency of the Free University of Bozen-Bolzano, which he held until 2018.

Konrad Bergmeister, *Institute of Structural Engineering (IKI), University of Natural Resources and Life Sciences (BOKU), Peter Jordan Straße 82, 1190, Vienna, Austria, e-mail:* konrad.bergmeister@boku.ac.at

(S)FRC IN EC2 AND IN MODEL CODE 2020

Marco di Prisco

The current Eurocodes are under revision and estimated to be available in 2025. For the first time in the European history, Eurocode 2: "Design of concrete structures" will be extended with a European-wide harmonized annex, covering steel fibre reinforced concrete. The work on Annex L – Steel Fibre Reinforced Concrete has already started in 2012 and significantly benefitted from the work carried out for the fib Model Code of Concrete Structures 2010. The use of performance classes of Model Code 2010 as well as parts of the design approach were the basis for the new steel fibre reinforced concrete annex. In addition, the latest state of science has been used to prepare a powerful but, in the same way, easy-to-use design document for structural engineers, covering both ultimate and serviceability limit states for steel fibre reinforced structures, with or without reinforcement. At the same time the new Model Code 2020, mainly concentrated on existing structures and sustainability, extended to all types of fibres as the previous Model Code, has tried to look at FRC as to a generalized concrete, able to exhibit a significant toughness in uniaxial tension, integrating its resistance equations to those of conventional concrete, guaranteeing in many structural cases a sustainable choice for the reinforcement and paying more attention to high- and Ultra-high performance materials and at the same time to hybrid solutions for the reinforcement.

1. INTRODUCTION

Fibre reinforced concrete is introduced in the codes as a composite material. After several decades of research work and some years of pioneer applications, Fibre Reinforced Concrete (FRC) is nowadays a material ready for the construction world community, also considering that design rules are already available in several Countries and fib Model Code 2010 included specific sections for design of FRC elements. FRC can be a suitable solution especially for statically indeterminate structures, where stress redistribution occurs. In addition to the structural bearing capacity, FRC is particularly useful for better controlling crack opening in service conditions, which has a particular influence on structural durability, especially in aggressive environments. Furthermore, structural robustness is nowadays a major concern among structural engineers. Even in this perspective, FRC could improve structural behaviour since it provides structural resistance both in compression and in tension in all the regions of the structural element.

The reasons why FRC is regarded more sustainable than plain concrete can be resumed in the following items: reduction of the global volume of composite and of steel reinforcement, smaller crack widths, stiffer response at SLS, durability increase in relation to fatigue loads, ductility increase, larger specific toughness, robustness increase with reference to unexpected load conditions (resilience increase), lower amount of human workmanship with the only disadvantage of higher costs in recycling if steel has to be separated by concrete.

The performance usually adopted to evaluate a sustainability index is compressive strength for concrete and tensile strength for steel bars, but, as it is well known, the role of fibres in the composite is played mainly on toughness guaranteed by the bond with cementitious matrix, strongly affected by the shape and the material of the fibre itself. So, if we consider in a sustainability index the performance, we have to specify that if we look to uniaxial compressive behaviour, compressive strength f_c weakly improves, but it is not the only interesting parameter to be considered. The post-cracking behaviour can be significantly modified by fibre pull-out and this performance becomes essential all the times we have a failure in compression especially if the failure mechanism is due to cyclic behaviour (as in seismic events) or if the resistant mechanism is conceived in a redundant structure, where the failed mechanism can conserve a certain ductility and the corresponding bearing capacity can be added to the resistance of other mechanisms. Therefore, in uniaxial compression, looking to the performance, we should consider toughness up to a certain strain: with this proposal we could refer to the post-peak branch proposed by Gonzalo Ruiz et al. (2018, 2019). By considering at the denominator of the sustainability index the embodied energy or the energy required to store the CO_2 emitted in the production, subtracting it from the atmosphere, or the addition of both terms, we could obtain a dimensionless term. To consider the dissipated energy means to look at the Ultimate Limit State (ULS), but also the service life could be considered by evaluating the allowable number of cycles between a minimum and a maximum serviceability stress that could be correlated to about 60% of the peak strength f_c; the minimum stress could be set equal to the percentage of the maximum stress related to the dead weight contribution with respect to the total loads acting in rare condition at SLS. The cycle number up to failure could become a significant measure of the service life expectation, giving to the engineer an idea of

Fig. 1: *P.L. Nervi: Pavillon B – Torino. Picture taken in the occasion of the visit organized in the Regenerate workshop carried out in Lecco (2023), in the framework of Recube project financed by EEC*

Fig. 2: *Recube Erasmus Plus project financed by EEC: partners and BME contributions*

damage and irreversible strain evolution in the service life. This measure could be determined on a virgin material from a mechanical point of view or on a material subjected, at least one in his life, to an ULS condition.

An impressive comparison based mainly on the volume reduction was proposed by Voo & Foster (2010) looking to a retaining wall or a simple precast overpass.

P.L. Nervi thinking to ferrocement, but in a certain way anticipating the introduction of FRC, in 1940 wrote: "*We wondered if, increasing significantly the diffusion of the steel and its percentage (i.e. reinforcement ratio), it could not be possible to create a new material characterized by a higher strength and especially a larger elasticity and elongation ...*". The wonderful execution of his light and optimized large-span vaulted ceilings can easily demonstrate the powerful of ferrocement material (*Fig. 1*): in the figure the vault span is equal to 94 m, without any pre-stressing and with 38 mm of thickness of the bottom chords!

For this reason, the research on optimized and challenging solutions to be performed with FRC material has to be inspired by the examples of the great Masters of Engineering as Pier Luigi Nervi. This important cultural European heritage of R/C structures needs to be taken care for and kept integrated in our evolving and changing contemporary life. To this aim, I would like to remember that Prof. Balazs is participating to Recube project (*Fig. 2*), cooperating with other eleven universities, P.L. Nervi foundation and other partners cited in the figure. The purpose of this project is to offer the cultural and technical tools required for a respectful and viable approach to a correct architectural conservation and repurposing of the Modern Heritage and to show it can be structured in an overall European shareable knowledge. Establishing and promoting unified best practices in the field of Modern architectural preservation is one way to strengthen

our common European identity, while opening up new creative possibilities for young designers, builders and city planners.

Looking to design standards, it is worth to note that FRC in Eurocode 2 Annex L is made of steel fibres only, while Model Code 2020 is open also to synthetic fibres. Moreover, even if several countries fought to introduce Annex L as a normative Annex, the majority voted to keep it as an informative one. Several National Standards have been developed in the last 10 years in Europe: a weak form of Annex L could favour the risk to hamper the European market of fibres and diverging criteria in FRC structure design. Only a shared and large scientific community operating in the next years in the fib framework (TG4.1) could prevent this risk.

In the paper the main assumptions introduced in the Eurocode 2 - Annex L and in the Model Code 2020 final drafts are resumed and commented to show the progress and the present research borders at which Prof. Balazs greatly contributed.

2. PERFORMANCE CLASSES

The performance classes introduced in the Model Code 2010 based on the third point loading tests carried out on a notched prismatic specimen, defined in EN 14651, represent the basic identification of the composite to be correctly compared with different solutions offered in the market. It has been conserved both in the Eurocode 2 Annex L and in the Model Code 2020. It should be highlighted that in the Annex L the range accepted is only 1-8 MPa on f_{R1k}, while in Model Code 2020 also classes 10, 12 and 14 MPa are added. This clearly shows the aim in Model Code 2020 to include the mechanical performance of Ultra High Performance FRC. In fact, even

if small cross section specimens made of high performance SFRC can show nominal bending strength values up to 20-30 MPa for a crack opening displacement of 0.5 mm, when testing the material according to EN 14651 standard, the performance class is around 10÷14 b÷c. For common use, it should be underlined that, even if maximum aggregate size, water/cement ratio and compressive strength usually qualify concrete matrixes, often they are not enough for fully qualifying the interaction between fibres and concrete mix. Fibre type, as well as aspect ratio, steel mechanical performance and its shape combined with grading curve, w/c ratio and filler type can significantly contribute to the final SFRC performance. The knowledge on this topic requires further research efforts, because it could allow the producer to dynamically recalibrate the final performance of the composite without facing with a new qualification procedure every time that one of the parameters has to be changed. Several experimental results have confirmed how SFRC performance can be predicted by considering the change of the fibre content (with the same concrete matrix) assuming a linear relationship (between material properties and fibre content) in favour of safety.

It is worth to note that the determination of f_{R1k} and f_{R3k} shall be based on a log-normal distribution according to EN 1990 (5% quantile, 75% confidence level). Unless explicitly agreed otherwise, the coefficient of variation shall be assumed unknown. Only in Annex L a factor $\kappa_{k,max}$ defined in EN 206 shall be taken as 0,6 and the characteristic values f_{Rik} cannot be greater than $\kappa_{k,max} f_{Rim}$. Only in the case the COV on the material extracted by the structure should be also checked, a higher value equal to 0,7 could be used if the COV is lower than 0,15. This condition finds a justification in the difference between the on-site empirical evaluations as compared with the lab-measured strengths.

3. CONSTITUTIVE LAWS

The constitutive law in uniaxial tension introduced in both the standards is rather close to that proposed by Model Code 2010 (*Fig. 3*). Besides the stress-bock models, in the linear models the correlation between the nominal residual strengths f_{Rik} identified in bending by means of EN 14651 and the uniaxial tension strength assumed in the pull-out regime is that proposed by di Prisco et al. (2013). In particular, the f_{Fts} is regarded as a fixed point at a crack width $w_1 = 0.5$ mm, and the two points of the linear pull-out branch are referred to as follows:

$$f_{Ft1} = 0.37\ f_{R1k} = f_{Fts} \tag{1}$$

$$f_{Ft3} = 0.57\ f_{R3k} - 0.26\ f_{R1k} \tag{2}$$

with:

$$\varepsilon_{Ftu} = 2.5mm/l_{cs}\ ;\ l_{cs} = \min\{h;\ s_{rm}\} \tag{3a,b}$$

where l_{cs} is the structural characteristic length and depends on the kinematic model. If a plane-section model is assumed, it can be defined by Eq. (3); s_{rm} represents in this case the minimum crack distance. In case a F.E. approach is used, l_{cs} is correlated to the element size and needs a careful calibration. The dashed linear piecewise branches are introduced to favour localization in case of F.E. use. If plane-section model is adopted, the pull-out branch can intersect directly the initial elastic branch, without any peak, because the
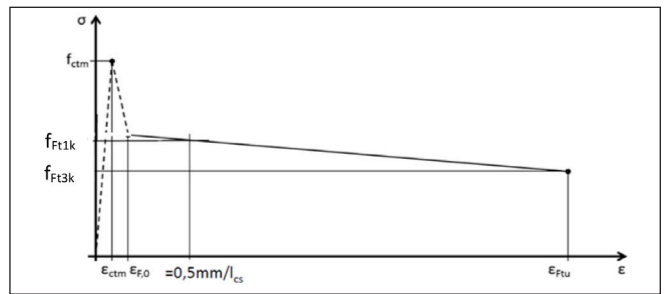
Fig. 3: Constitutive law in uniaxial tension according to Annex L

peak contribution is negligible and is not considered in R/C structures.

The Model Code 2020 introduces the same softening related to fibre pull-out in terms of σ−w and transforms it in σ−ε by using the same l_{cs}, but in case of design suggests a model that is elasto-softening or rigid-softening. When the model is used to check a serviceability condition of an uncracked element, the pre-peak is two-piecewise and the first post-peak softening branch is the same suggested for plain concrete.

It is worth to note that in Model Code 2020 also specialized models valid for high performance concrete are suggested, like those indicated in *Fig. 4*, which are able to appreciate the

Fig. 4: Constitutive laws in uniaxial tension for high performance materials, not fully hardening: (a) quasi-plastic materials ($f_{Fts} > 0.8\ f_{ctm}$); (b) hardening materials ($f_{Ft} > f_{FTS}$) with peak strain (ε_p) < 0.01.

(a)

(b)

$$\varepsilon_{c1}(\%o) = 0.7 f_{cm}^{1/3}(1+0.03 f_{R,1k})$$

and, for $\varepsilon_{c1} \le \varepsilon \le \varepsilon_{cu1}$:

$$k = 1+\frac{20}{\sqrt{82-2,2 f_{R1,k}}}$$

and $\varepsilon_{cu1}=k\, \varepsilon_{c1}$
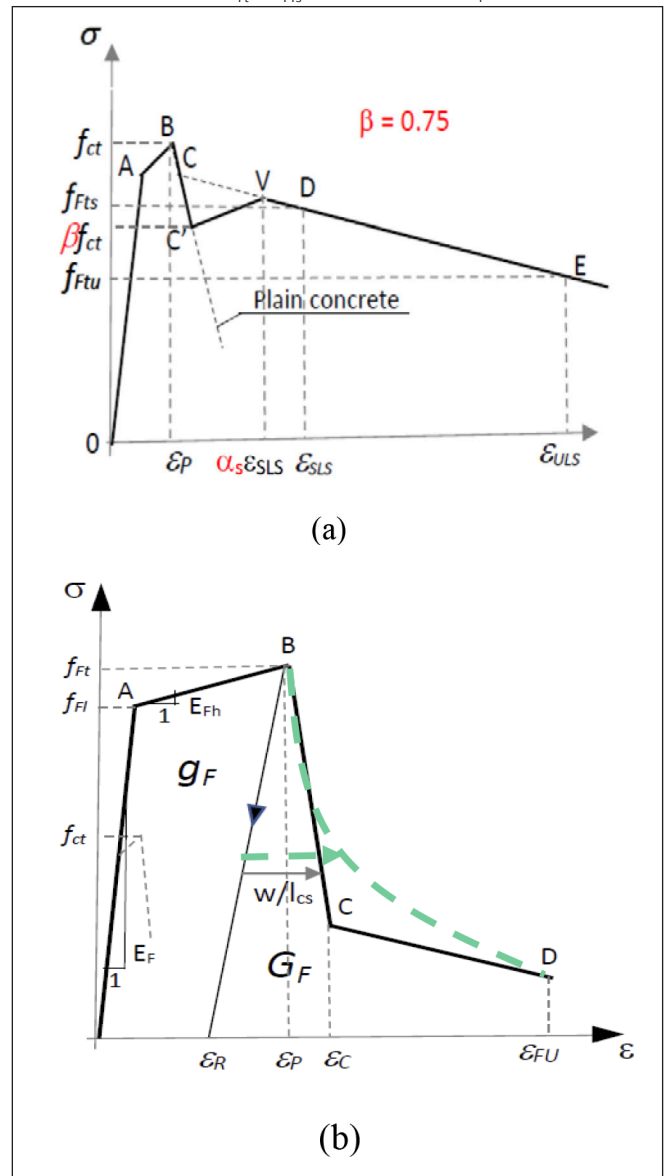
Fig. 5: *Constitutive law in uniaxial compression for FRCs*

stabilizing contribution of fibres to the pre-peak behaviour, associated to the stable crack propagation occurring with the multi-cracking, before localization.

More details on the last model *(Fig.4b)* can be searched in Zani and di Prisco (2023). Of course, the constitutive law in uniaxial tension can be identified also via uniaxial tension test.

Finally, in both the codes, Annex L and Model Code 2020, a novel uniaxial compression law affected by f_{R1k} is also introduced (*Fig. 5*; Gonzalo Ruiz et al., 2018, 2019).

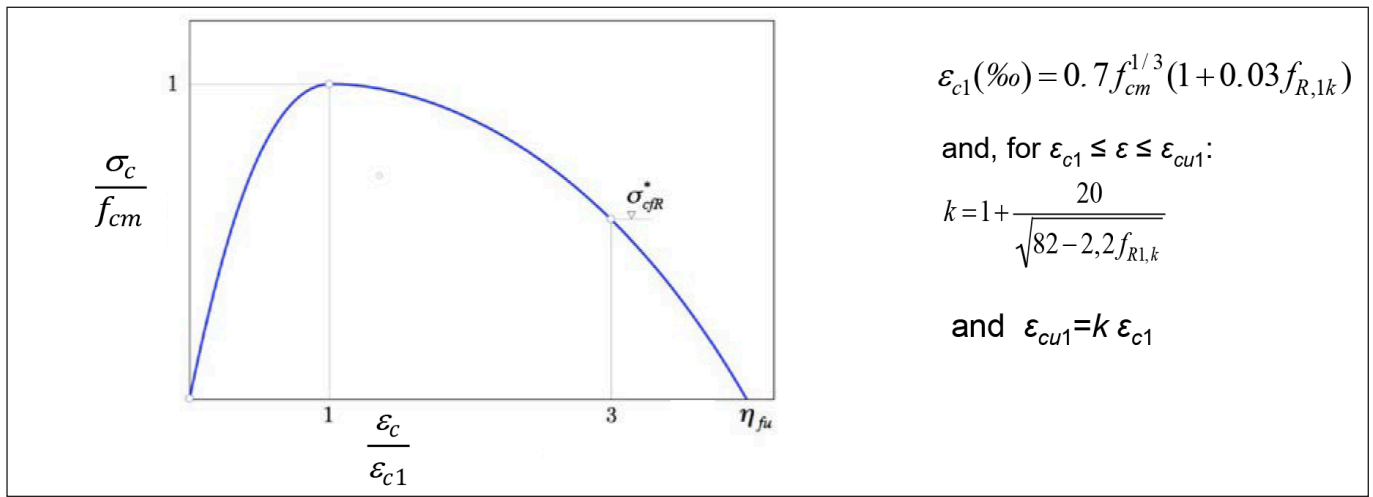The proposed model becomes very significant every time failure is caused by the reaching of the ultimate strain in compression: fibre reinforcement guarantees a passive confinement to the loaded volume, amplifying the stable crack propagation, accompanied by a weak increase of the compressive strength, and favouring the dissipation in the unstable crack propagation.

4. EFFECTIVE STRENGTHS: ORIENTATION AND SIZE EFFECT COEFFICIENTS

Random distribution of fibres can be regarded as a strength as well as a weakness. It is a strength because the single fibre randomly oriented can work for a very wide range of directions.

In fact, if we consider scantly effective the fibre contribution out of a double cone characterized by an angle $\alpha = 30°$ astride its axis, the solid angle covered by a single fibre corresponds to a solid angle $\omega = 3.86\pi$. This peculiarity is also a weakness, because the designer cannot know precisely its distribution and orientation that is affected by casting procedure and its boundary conditions.

Fibre distribution is assumed usually homogeneous in the cast, even if this property has to be checked in the real conditions; on the contrary orientation factor can be significantly affected by cast direction, flowability of the mix, boundary conditions imposed by the formwork and its filling strategy. In both the codes a coefficient κ_0 is introduced ranging between 0.5 and 1.7. It expresses the ratio between the orientation factor of the cast in a specific location and that computable for the EN14651 specimen, equal to about 0.54÷0.58 according to Dupont and Vandewalle (2005) depending on the fibre length. It may be helpful to remember that a value of 0.5 corresponds to a perfect 3D random orientation, while the unity corresponds to the perfect

alignment at right angle with the cracked plane. This value can be predicted by means of suitable numerical models (Ferrara et al., 2017) or can be measured on-site in case of a real construction by means of a magnetic device applied to a cylindrical specimen cored in the specific point of interest, or testing the same cylinder by means of Double Edge Wedge Splitting test (Martinelli et al., 2021; Laranjeira et al., 2011).

To simplify the computation of the bearing resistance of a hybrid structure, where conventional reinforcement is coupled to FRC, the effective strength in uniaxial tension considers a second coefficient, taking into account the reduction of the standard deviation identified by means of bending tests (EN14651; *Fig. 6a*) with the size of the volume involved in the failure process and the increase of redistribution capacity of the structure (Fig.4b; di Prisco et al., 2016; Pourzarabi et al., 2018, Colombo et al., 2017). This coefficient denominated k_G corresponds conceptually to the coefficient K_{Rd} already introduced in the Model Code 2010.

The coefficient κ_G is evaluated in the Annex L according to a simplified expression firstly introduced in the Austrian guidelines:

$$\kappa_G = 1.0+0.5 \times A_{ct} \le 1.5 \tag{4}$$

where A_{ct} is the area of the tension zone (in m²) of the cross section involved in the failure of an equilibrated system. In the Model Code 2020 the same expression is suggested, but also a more complex and precise evaluation is indicated.

By introducing the safety coefficient $\gamma_F = 1.5$, as in the previous Model Code 2010, the uniaxial tension design strength becomes:

$$f_{Ft1d} = \kappa_O \cdot k_G\ f_{Ft1}/\gamma_F \tag{5a}$$

$$f_{Ft3d} = \kappa_O \cdot k_G \cdot f_{Ft3}/\gamma_F \tag{5b}$$

A similar approach has to be followed also for stress-block constitutive models or any kind of law deduced according to a more complex identification procedure or directly by a uniaxial tension test.

To complete the identification of the σ−ε law, the computation of the crack distance s_{rm} has to be computed by adopting the equation based on the equilibrium of a tie portion as described in *Fig. 7*.

$$s_{rm} = \left(k_c c + k_{\phi/\rho} k_{fl} k_b \frac{(f_{ctm}-f_{Fts,ef})\phi}{\tau_{bms}\rho_{s,ef}}\right) \tag{6}$$
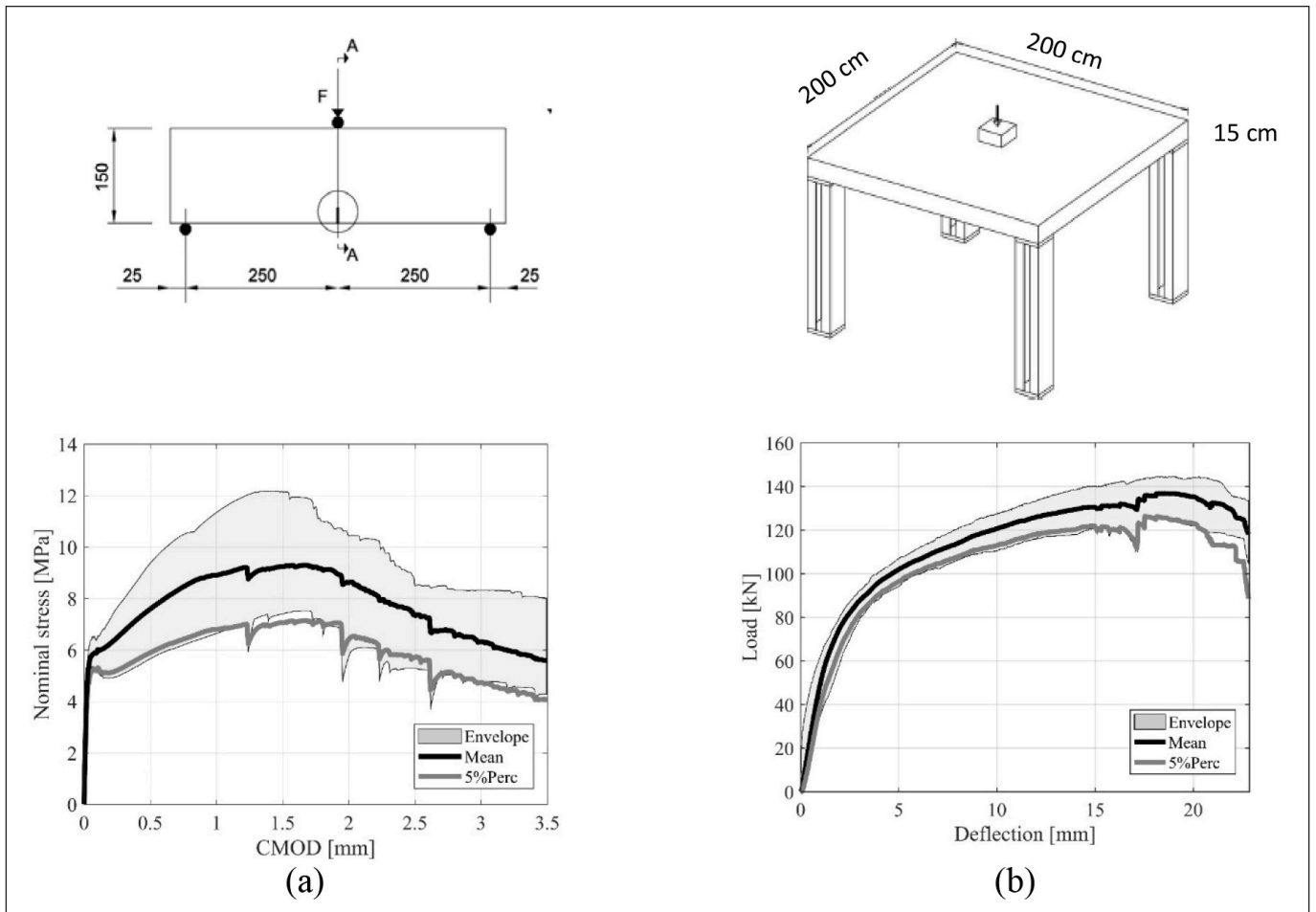
Fig. 6: *Reduction of standard deviation passing from the test specimen (a) and the structural response of a plate supported in the corners (b) made of the same FRC*
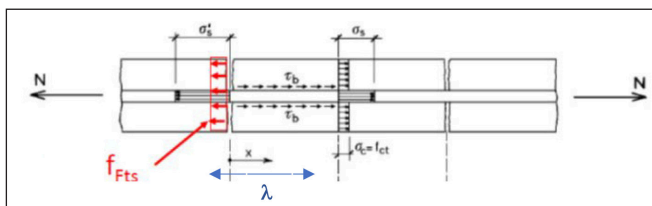

Fig. 7: *Equilibrium of a tie portion to compute the distance between a crack and a cross section where the concrete stresses are at the onset of cracking.*

where k_c is a coefficient to account the effect of the cover, often simplified with the value 1.5, c is the cover, ϕ is the bar diameter, $\rho_{(s,ef)}$ is the reinforcement ratio, $k_{\phi/\rho}$ is a coefficient that accounts for the bond τ_{bms} (if the bond τ_{bms} is constant $k_{\phi/\rho}$=0.25), k_{fl} is a factor to account the stress distribution before cracking and finally k_b is a factor to accounts the casting position ranging between 0.9 and 1.2 and $f_{Fts,ef} = \kappa_O f_{Fts}$. The term $f_{Fts,ef}$ represents the stresses applied on the cracked plane which are usually considered negligible in case of plain concrete. It is worth to note that in the equation no increase of τ_{bms} is suggested, even if several experimental tests have proven a growth of τ_{bms} strength with fibre contribution (Tiberti et al, 2015). The crack opening is therefore reduced by the decrease of crack spacing, but also by the reduction of the steel stress due to contribution of fibre in tension.

It is also interesting to observe that in some structural situations we can define several l_{cs} depending on the bending we are examining even if the material is only one FRC. In fib bull. 105 the case of a U channel made of FRC and reinforced with few bars located just in the corners is shown and commented (*Fig. 8*). The longitudinal bending of the whole
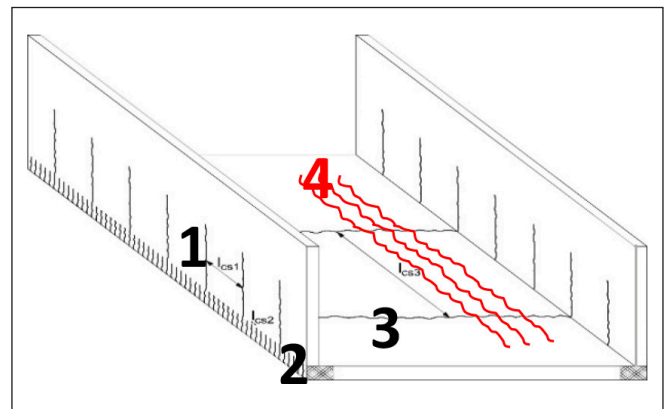
Fig. 8: *The case of U channel, where 4 characteristic structural lengths can be defined.*

profile can show 3 different structural characteristic length: one associated to the reinforced bottom chord, one associated to the two webs and one associated to the bottom slab that is subjected mainly to uniaxial tension, but is reinforced only at the two side borders. The fourth structural characteristic length is that correlated to the crack distance introduced by the transversal bending of the profile.

5. STRUCTURAL DUCTILITY

The topic that adsorbed the largest effort in the debate of TG2 committee devoted to the preparation of Annex L was the evaluation of the structural ductility. Dancygier and Karinsky (2019) have highlighted as R/C beams characterized by a minimal reinforcement showing a ductile

behaviour can become brittle if concrete is substituted by a FRC. The physical reason is associated to the degree of heterogeneity introduced by fibre distribution. If the amount of reinforcement associated to the level of hardening of steel is able to prevent localization, ductility is preserved and brittleness does not appear (Gebreyesus et al. 2023). This experimental observation pushed the committee to exclude the possibility to use hybrid solution to obtain a minimum reinforcement: minimum reinforcement in longitudinal bending of beams cannot be reduced by fibre addition. Looking to the elevated plates, they can be helped by internal structural redundancy, but they cannot be advantaged by soil interaction as ground slabs: for these elements it is important to understand if they can be computed by means of yield lines, that implies to respect the assumptions of limit analysis, even if in some points the specific bending behaviour could be softening. By testing a series of elevated plates in two laboratories at Politecnico di Milano and at the University of Brescia, (di Prisco et al., 2019; Colombo et al., 2023), it has been shown that the limit analysis can be always adopted and the design rules indicated in the two codes implies a design value of the bearing capacity which remains always on the safe side. At the same time hybrid solution appears as the most effective solution both in terms of serviceability behaviour and ultimate bearing capacity.

6. CONCLUDING REMARKS

The results obtained in many experimental campaigns have confirmed the effectiveness of fibre reinforced concrete as a construction material. It allows a significant increase of durability, an optimization of the construction process both in terms of economics and in terms of building speed.

Even if some topics like multi-axial behaviour, fatigue, shear, punching, torsion, structural creep, fire resistance and high-strain rate behaviour require further research efforts, the applications carried out all over the world justify its powerful growth in the market and the introduction in the future Eurocode 2 will promote it furthermore in the civil engineering application fields. At the same time the future work that will start next year in the *fib* TG4.1 will try to collect the novelties on the knowledge border, trying to clarify the aspects that are not yet fully understood.

7. ACKNOWLEDGMENTS

8. REFERENCES

fib (2013) Model Code for Concrete Structures 2010. Ed, *fib* – International Federation for Structural Concrete, Ernst & Sohn, Berlin, https://doi.org/10.1002/9783433604090

fib Bulletin 105 (2022). Fibre Reinforced Concrete, ISBN 978-2-88394-161-8, pp.1-446.

Colombo, M., Martinelli, P., di Prisco, M. (2017). On the evaluation of the structural redistribution factor in FRC design: a yield line approach. *Materials and Structures*, 50:100. https://doi.org/10.1617/s11527-016-0969-3

Colombo, M., Conforti, A., di Prisco, M., Leporace-Guimil, B., Plizzari, G., Zani, G. (2023). The basis for ductility evaluation in SFRC structures

in MC2020: An investigation on slabs and shallow beams, *Structural Concrete*, 24 (4), pp. 4406-4423. https://doi.org/10.1002/suco.202300114

di Prisco, M., Colombo, M., Dozio, D. (2013), Fibre-reinforced concrete in fib Model Code 2010: Principles, models and test validation, *Structural Concrete*, 14 (4), pp. 342-361. https://doi.org/10.1002/suco.201300021

Dancygier, A. N., Karinski, Y. S. (2019). Effect of cracking localization on the structural ductility of normal strength and high strength reinforced concrete beams with steel fibers," *Int. J. Prot. Struct.*, vol. 10, no. 4, pp. 457–469, https://doi.org/10.1177/2041419618824609

di Prisco, Marco, Paolo Martinelli, and Daniele Dozio. 2016."The structural redistribution coefficient K_{Rd}: a numerical approach to its evaluation." *Structural Concrete* 17: 390-407. https://doi.org/10.1002/suco.201500118

di Prisco, M., Colombo, M., Pourzarabi, A. (2019). Biaxial bending of SFRC slabs: Is conventional reinforcement necessary? *Materials and Structures*, 52 (1), art. no. 1, https://doi.org/10.1617/s11527-018-1302-0

Dupont, D., Vandewalle, L. (2005), Distribution of steel fibres in rectangular sections, *Cement and Concrete Composites*, 27 (3), pp. 391-398. https://doi.org/10.1016/j.cemconcomp.2004.03.005

EN 14651 (2004) Test method for metallic fibered concrete – Measuring the flexural tensile strength (limit of proportionality (LOP), residual). Brussels

Ferrara, L., Cremonesi, M., Faifer, M., Toscni, S., Sorelli, L., Baril, A., Réthoré, J., Baby, F., Toutlemond, F., Bernardi, S. (2017), Structural elements made with highly flowable UHPFRC: Correlating computational fluid dynamics (CFD) predictions and non-destructive survey of fiber dispersion with failure modes, *Engineering Structures*, 133, pp. 151-171. https://doi.org/10.1016/j.engstruct.2016.12.026

Facconi, L., Plizzari, G., Minelli, F. (2019) "Elevated slabs made of hybrid reinforced concrete: proposal of a new design approach in flexure". *Structural concrete*, 20(1), pp. 52-67. https://doi.org/10.1002/suco.201700278

Gebreyesus, Y.Y., Karinski, Y.S., Dancygier, A.N., di Prisco, M. (2023). Experimental investigation of cracking localization in RC beams with steel fibers, *Structural Concrete*, 24 (1), pp. 1386-1401. https://doi.org/10.1002/suco.202200095

Laranjeira F, Grünewald S, Walraven J, et al (2011) Characterization of the orientation profile of steel fiber reinforced concrete. *Mater Struct Constr* 44:1093–1111. https://doi.org/10.1617/s11527-010-9686-5

Martinelli P, Colombo M, Pujadas P, de la Fuente A, Cavalaro S, di Prisco M. (2021). Characterization tests for SFRC elevated slabs: identification of fibre distribution and orientation effects. Mater Struct.;54(3). https://doi.org/10.1617/s11527-020-01593-7

Pourzarabi, A., Colombo, M., di Prisco, M. (2018). On the mechanical response of a fibre reinforced concrete redundant structure; the redistribution factor, *Proc. of the 12th fib International PhD Symposium in Civil Engineering*, pp. 625-632.

Ruiz, G. De La Rosa, Á. , Poveda, E. (2019). Relationship between residual flexural strength and compression strength in steel fiber reinforced concrete within the new Eurocode 2 regulatory framework. *Theoretical and Applied Fracture Mechanics* 103. https://doi.org/10.1016/j.tafmec.2019.102310

Ruiz, G. De La Rosa, Á. Wolf, S., Poveda, E. (2018). Model for the compressive stress–strain relationship of steel fiber–reinforced concrete for non–linear structural analysis. *Hormigón y Acero* 69 Suppl. 1, 75–80. https://doi.org/10.1016/j.hya.2018.10.001

Tiberti G., Minelli F., Plizzari G.A. (2015). Cracking behavior in reinforced concrete members with steel fibers: A comprehensive experimental study. *Cement and Concrete Research*, vol. 68, p. 24-34. https://doi.org/10.1016/j.cemconres.2014.10.011

Voo, Y.L., Foster, S.J. (2010), Characteristics of ultra-high performance 'ductile' concrete and its impact on sustainable construction, *IES Journal Part A: Civil and Structural Engineering*, 3, pp. 168-187. https://doi.org/10.1080/19373260.2010.492588

Zani, G., di Prisco, M. (2023), Identification of Uniaxial Tensile Laws for UHPFRC Modelling, FRC2023: Fiber Reinforced Concrete: from Design to Structural Applications, Joint ACI-fib-RILEM International Workshop, Phoenix

Marco di Prisco

Marco di Prisco is Presidium member of *fib*, fellow of *fib* and rilem, Series Editor of *Lecture Notes* and *Tracts in Civil Engineering* for Springer-Nature, expert in advanced cement-based materials, reinforcement-concrete interaction mechanisms, concrete structures, exceptional loads, tunnel and bridge safety, R/C heritage. Since 2018 he is Technical Director of DSC-Erba Company.

Marco di Prisco is Professor of Structural Design, Politecnico di Milano, Department of Civil and Environmental Engineering, Italy, marco.diprisco@polimi.it

UHPC IN CZECHIA – RESEARCH AND APPLICATIONS

Jan L. Vítek

Ultra-high-performance concrete (UHPC) is in this paper always considered as a cement composite material made of local constituents and reinforced with high strength steel fibres. Extensive research was carried out in order to understand its behaviour under different loading conditions. Successful tests enabled its application in various structures. Footbridges are structures where UHPC can be successfully applied. The next step of research works was focused on rehabilitation of existing concrete structures. Promising research results led to rehabilitation of a large bridge in Prague using UHPC. The Technical specifications prepared by the Czech Concrete Society will be soon approved by the Ministry of Transport. Then the new applications for Highway and Railway administrations are expected.

1. INTRODUCTION

UHPC (ultra-high-performance concrete) is an excellent material which was developed in 90th of the last century. Its extraordinary properties like high compression and tensile strengths and resistance to environmental impact are now well known and provide field for its application in new structures as well as in rehabilitation of existing structures. In this paper, the term UHPC is used exclusively for material which is made of concrete matrix and high strength fibres (although some authors call this material UHPFRC – Ultra-High-Performance Fibre Reinforced Concrete).

The development of UHPC in Czechia started about 2010. At that time, precasting plant of the company Skanska started to produce small slabs applicable as a lost formwork for bridge decks. At the ready-mixed concrete producer TBG Metrostav, s.r.o., the extensive research was begun with the aim to produce UHPC from local materials applicable not only for precast elements but also for cast in situ structures. First the composition of the mortar was developed, further experiments were focused on concrete composition. Beside classical material tests (like compression strength, flexural strength, elastic modulus), additional properties were investigated. Early shrinkage development (autogenous shrinkage in particular) is very important for production of elements and their demoulding. The mould often prevents free deformation of elements. The restrained deformation in early stages can be a reason for initial cracking of structural elements. Attention was paid also to the bond between UHPC and mild and prestressed reinforcement. Further research was focused performance of structural details like joints and composite steel concrete elements (Vitek, Citek, 2016), (Vitek, Citek, 2017).

During the time the research results appeared as promising and possible applications were found. The paper will illustrate some experiments in the laboratory, and on sites, and finally, some applications in structures are described. Initially the compression strength of 150 MPa and higher was considered as a minimum for UHPC. During last years, it was concluded that the compression strength is not the most important parameter. The tensile strength, ductility and preferably the durability was considered as more important in dependence on the applications. Now a suitable material with the compression strength 110 MPa and higher can be considered as UHPC, if its properties satisfy specific conditions. In Czechia, the Technical specifications of UHPC were developed in the Czech Concrete Society. They will be soon approved by the Ministry of Transport, which will provide a possibility for application of UHPC in structures of the transport infrastructure.

2. EXAMPLES OF LABORATORY AND SITE EXPERIMENTS

2.1 Bond of reinforcing steel and UHPC

Bond of reinforcing steel and UHPC is very important. It was expected that the bond could be rather good. However, a verification and quantification were necessary. The bond was tested using a simple pull-out test. The mean bond stress τ_m was calculated from the loading force very simply using Eq.1

$$\tau_m = \frac{P_m}{a\,o} \qquad (1)$$

where P_m is the pulling force, a is the anchorage length and o is the perimeter of the reinforcing bar. In the first series of tests, different diameters of reinforcing bars were used, while the anchorage length remained constant (5 diameters of the bars). The bars were embedded in UHPC and in ordinary concrete of the class C30/37. The tests of specimens made of ordinary concrete finished by failure of bond, while the tests of specimens made of UHPC finished by failure of steel. The bond of steel and UHPC was higher than the strength of the bars (*Fig. 1*). The second series used only one diameter
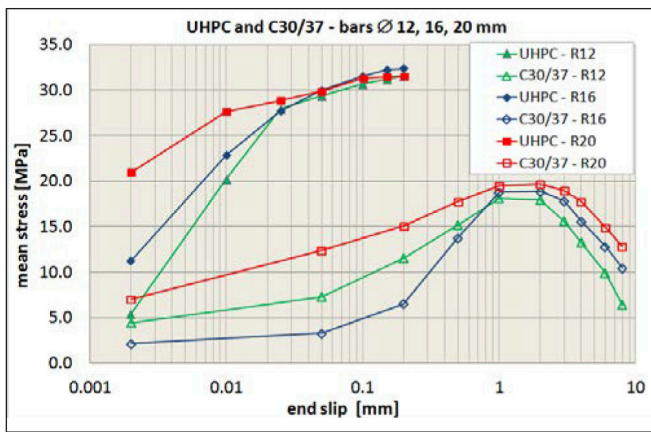
Fig. 1: Pull-out tests. Mean bond stress – comparison of specimens made of UHPC and C30/37
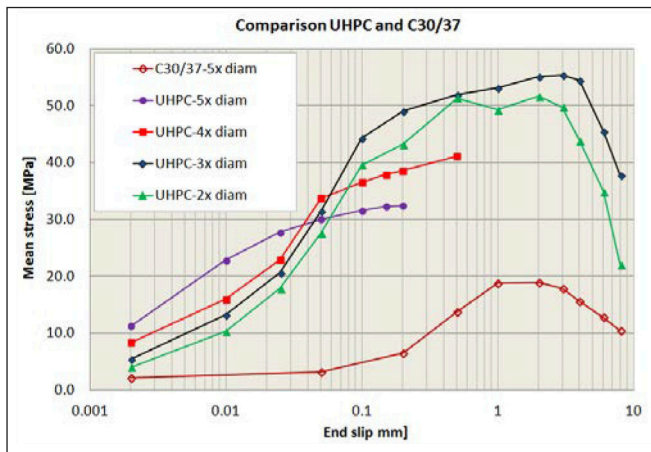

Fig. 2: Pull out tests. Mean bond stress – comparison of different anchorage lengths

of the steel bar and the anchorage lengths varied from 2 to 5 diameters of the bar. The results are plotted in *Fig. 2*. The anchorage lengths 5 and 4 diameters were sufficient and the failure was in steel bar. The anchorage lengths 2 and 3 diameters resulted in failure of bond. The extensive experimental study on bond resulted in recommendation that the minimum anchorage length in UHPC is 10 diameters and for dynamically loaded elements it should be increased to 15 diameters.

2.2 Joints of precast elements

UHPC is an expensive material. It should be used for those parts of structures, where its properties are really needed. The joints of precast elements can be one of the areas of its application. Precast elements are usually members exhibiting very good quality. On site they are connected into the final structure. The joints used to be the weakest points of a precast structure. Application of UHPC can be a possibility of improvements of the joints. First, the quality of UHPC is superior, it is a suitable material for joints, second, a small anchorage length of reinforcing bars makes it possible to reduce the dimensions of joints in comparison with a classical solution where the joints are filled with ordinary concrete.

The slabs with joints were tested. The two joint reinforcements were tested in slabs of the span of 2.5 m. Type R (*Fig. 3*) had a simple overlap of the bars in the joint. The anchorage length of bars was 170 mm, overlap length 140 mm (=10 profile of the bar). Type S (*Fig. 3*) had bent bars in the joint. The bents from each side were overlapped. The slabs were subjected to 3-point bending test. The results were compared with those measured on reference slabs without
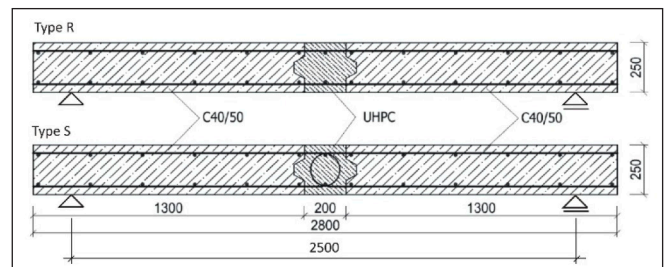

Fig. 3: Longitudinal sections of the slabs with joints

any joint. The results were almost identical, no difference in load carrying capacity was observed. All slabs cracked; no cracks were observed in the joint. The cracks were either on the contact of UHPC and ordinary concrete or in ordinary concrete. The slabs with the type R reinforcement had slightly higher load carrying capacity than those with reinforcement of the type S. It was possible to conclude that the joint made with UHPC has no effect on load carrying capacity of the slab. The long-term tests even with shorter overlap lengths confirmed the same results. However, overlap length of 12 profiles for elements with static loading and 18 profiles for elements with dynamic loading were recommended as a conservative measure.

2.3 Joints of precast elements in steel-concrete composite slab

Steel-concrete composite slabs are often used in bridges as well as in buildings. It is convenient to use precast slabs and which can be connected using UHPC over the steel beams. The most unfavourable situation can be close to the support, where the joint is subjected to tension in the longitudinal and also in the transversal directions. The models were produced in the laboratory and tested. The 2 models were produced – without the joint and with the joint. In the longitudinal section the cantilever was loaded with 2 point loads acting on the edges of the slab. The length of the cantilever was 2.2 m. The standard rolled steel IPE beam of the depth 400 mm was connected to the slab 800 mm wide and 150 mm thick. The cross-sections of the reference beam and of the beam with the UHPC joint are plotted in *Fig. 4*.

The arrangement of the test is illustrated in *Fig. 5*. The results showed that the behaviour of the beams with the UHPC joint were slightly stiffer than that of reference beams at larger load levels. The failure load was rather similar. The tests proved that the joint has no effect on reduction of the load carrying capacity or stiffness and it can be used in bridges and buildings as a reasonable method for connecting precast elements.

2.3 Tests on structural elements

Many tests were executed on elements which were parts of actual structures (Vitek, Coufal 2013). The deck of the
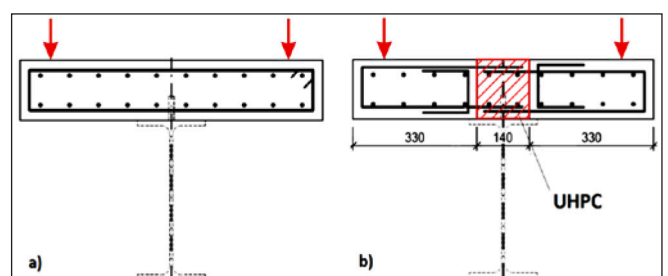
Fig. 4: Cross-section of the reference beam (a) and of the beam with the joint (b)

Fig. 5: *Steel concrete composite beam with the UHPC joint of the precast slab – scheme of the test*

Fig. 6: *Model of the footbridge segment loaded by 2 point loads representing an axle load of the light vehicle*

Fig. 8: *Punching test of the slab of the segment – test arrangement*

Fig. 9: *Punching test of the slab of the segment – failure cone*

footbridge had a slab only 60 mm thick without any bar reinforcement, only with fibres. The safety verification involved also testing of the slab in transversal bending and in punching. The cross-section of the footbridge had two edge beams *(see Fig. 12)* connected with a 60 mm thick slab and transversal ribs. The ribs were reinforced with 2 bars 16 mm in diameter and they were 160 mm deep at the ends.

The footbridge was designed primarily for pedestrians and cyclist. The vehicle of the rescue system also were able to drive along the footbridge. It represented the highest local load acting on the bridge deck. The weight of this small

vehicle was 3.5 t. The back axle was loaded by 25 kN. A model of the footbridge segment in the scale 1:1 was cast. Its length was only 1.5 m, while the width of the model was 3.5 m. The model was initially loaded by 2 point loads, each of 12.5 kN, which represented the axle load (*Fig. 6*).

When the total load reached about 80 kN and no cracks appeared, the loading scheme was changed to 1 point load in the middle of the width of the segment. The model failed in transversal direction (the transversal ribs failed in bending) at the loading level of 110 kN (*Fig. 7*), which is more than 3 times the total weight of the vehicle. The slab of the segment remained without significant damage, with exception of few cracks.

The load carrying capacity of the slab in punching was tested on the entire footbridge segment (3.5 m wide and 5.6 m long). The segment was loaded by a single point load in different positions The point load was acting on the circular area of 200 mm in diameter. The test arrangement is illustrated in *Fig. 8*. The load was slowly increased and the

Fig. 7: *Failure of the model in transversal bending*
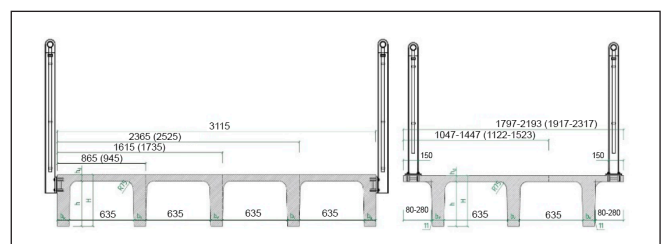
Fig. 10: *Cross-sections of small footbridges made of UHPC*

Fig. 11: *Loading test of a pretensioned beam*

failure load in punching was in the range of 320 to 370 kN, in dependence on its position, which is about 10 times the weight of the vehicle. The flat failure cone is shown in *Fig. 9*.

The load carrying capacity of the slab in punching is very large. However, in spite of this result, it was not recommended for future structures to reduce the thickness of load carrying slabs without bar reinforcement. The load carrying capacity significantly drops down if the thickness is reduced. Additionally, it is strongly dependent on the distribution and orientation of fibres. If the thickness is reduced, a thorough testing is recommended.

Light footbridges with small spans can be made of UHPC. The entire footbridge can be cast as one element in a precasting plant. A pretensioning technology is suitable, UHPC provides excellent protection of prestressed strands and no ducts and grouting are necessary. The weight of footbridges is small, the transport and the assembly with the crane are rather easy. Typical cross-sections of footbridges applicable for the span length up to 12 m are shown in *Fig. 10*.

Before the production of the footbridges started, the model was tested. *Fig. 11* shows a very large deflection of a pretensioned beam. The crack width remained moderate, because of fibres in UHPC and because of the bonded pretensioned reinforcement.

3. STRUCTURES MADE OF UHPC

UHPC was used preferably for smaller precast elements and for footbridges. A number of footbridges were already built, some representatives will be mentioned in this chapter.

3.1 Footbridge in Celakovice

Footbridge is Celakovice crossing the Labe River is located about 30 km east of Prague (Vitek, Kalny 2015). It was the first large footbridge with the deck made of UHPC in
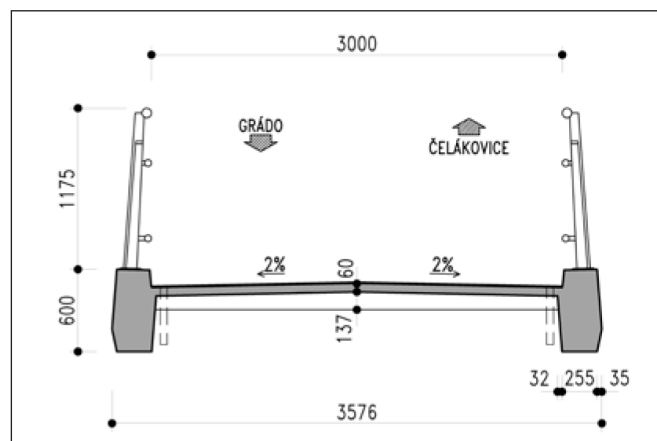
Fig. 12: *Cross-section of the footbridge in Celakovice*
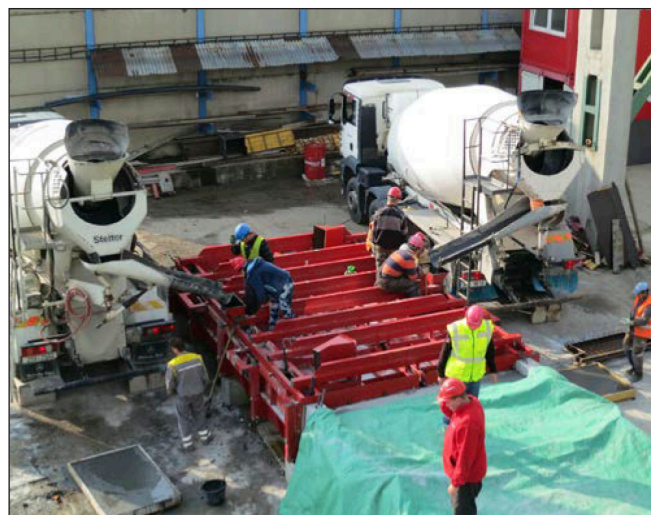
Fig. 13: *Filling of the mould by UHPC from 2 truckmixers*

Czechia, completed in 2014. The footbridge for pedestrians, cyclists is a three-span cable stayed bridge. The main span is 156 m long, the side spans have the length of 43 m. The bridge deck is made of precast segments made of UHPC and the 2 pylons (37 m high) are made of steel. The free width of the footbridge between railings is 3.0 m.

The cross-section of the bridge deck is plotted in *Fig. 12*. The two edge beams are 0.6 m deep and 0.3 m wide. The slab is only 60 mm thick, and it is reinforced only by fibres. There is no bar reinforcement in the slab. The slab is stiffened by transversal ribs 160 mm deep located in spacing of 1.0 m. The ribs are reinforced by 2 bars 16 mm in diameter. The edge longitudinal beams are reinforced by small longitudinal bars and stirrups. Two prestressing bars and one prestressing cable composed of 15 strands 15.7 mm in diameter are located in each of the edge beams. The bars were prestressed during construction of the bridge deck and the cables were prestressed after its completion.

The bridge deck is assembled from precast segments. This structure was the first large application of UHPC in Czechia, therefore, because of the lack of experience, a great attention was paid to casting segments. Many tests were carried out to develop a suitable technology of casting to keep the fibres uniformly distributed in segments. Because of the inclined and uneven top surface of the segment, the top cover of the formwork had to be used. Each segment of the bridge deck was 11.3 m long. In order to make the casting feasible and reliable, only a half of the segment was cast in one step (5.65 m). The steel mould was smaller and reinforcing bars were used to bridge the working joint between the two halves of the segment. The mould was filled by UHPC from two truck mixers by simple flowing of UHPC into the mould (*Fig. 13*).

After filling the mould, the mould was heated to accelerate hardening of UHPC. After about 9 hours after pouring of UHPC, the segment could be demoulded.

The segments were produced in a precasting plant close to the river, where only the space for production of segments was rented. Then most of the segments were transported by pontoons to the site. The UHPC was not produced in that precasting plant, it was transported from Prague (about 25 km). The production also verified, that the transport of UHPC in truck mixers is possible. Now the progress in concrete technology allows for the transport of distances more than 100 km long. The segments were match-cast. During the assembly of the deck, the joints were glued by

Fig. 14: Assembly of the segments in the main span

Fig. 15: Completed footbridge in Celakovice (2014)

epoxy resin and prestressed with 2 prestressing bars in each edge beam. The assembly is illustrated in *Fig. 14*.

A special gantry for assembly of the segments was developed. Because of lifting the segments from pontoons, the gantry was located above the bridge deck.

After assembly of all segments the two cables were prestressed and all ducts were grouted. All prestressed units are bonded and protected by grouting using a cement grout. Additional protection against water is a sprayed waterproofing which is continuous along the entire length of the footbridge. A completed footbridge can be seen in *Fig. 15*.

3.2   Footbridge in Luzec

A similar cable stayed footbridge was built some years later in Luzec crossing the Vltava River north of Prague (Tej, Vrablik 2022a). The footbridge is slightly smaller. The footbridge has two spans and only 1 pylon. The main span crossing the

Fig. 16: Cross-section of the footbridge in Luzec

Fig. 17: Assembly of segments of the footbridge in Luzec

river is 99 m long, and the side span is 32 m long. The pylon is almost 40 m high. The bridge deck is made of segments produced of UHPC and the pylon is made of steel.

The contractor simplified the production of segments significantly. The cross-section of segments is plotted in Fig. 16. The top surface is flat which made it possible to use a simple mould without a top cover. The transversal slope is achieved by slight inclination of the entire segment. The joints of segments were not match-cast but cast in situ. So called wet joints were used. The joints of the thickness of about 25 mm were filled with a special high strength mortar. The surface is not protected by additional layer, it is directly exposed to the traffic.

The segments 4 m long were assembled by a large crane. The crane put the segments on the gantry which was located under the bridge deck (*Fig. 17*). The two segments were assembled, the joints were filled and after hardening of the joints, the two bars were prestressed. After completion of the deck, two external cables composed of 19 strands 15.7 mm in diameter were prestressed. The cables are protected against corrosion using the HDPE duct grouted by cement mortar. The cables are not hidden inside the deck, regular inspections are possible. A completed footbridge is shown in *Fig. 18*.

Fig. 18: Completed footbridge in Luzec (2020)

3.3   Comparison of the two cable stayed footbridges

Both footbridges are cable stayed and both have a bridge deck made of UHPC and pylons made of steel. The difference is mainly in joints and in prestressing. The match cast segments of the footbridge in Celakovice are connected using dry joints glued with epoxy resin. The joints of the footbridge

in Luzec are wet joints. Prestressing of the Celakovice footbridge is bonded inside the cross-section. Prestressing of the footbridge in Luzec is external outside the cross-section. The protection of prestressing steel against corrosion is in both cases satisfactory and complying with the requirements on the long-term durability. The footbridges show that both alternatives of joints and prestressing are applicable. The construction of the Luzec footbridge was slightly simpler. The Luzec footbridge was completed in 2020 and it was possible to observe, that the experience from earlier built UHPC structures was used.

3.4   Footbridge in Pribor

Footbridge in Pribor (northern Moravia) is a simply supported beam made of UHPC (Tej, Vrablik, 2022b). It is a post-tensioned structure assembled of 5 segments of the length 7.2 m. The span of the beam is 35 m and the width is only 2.5 m. The cross-section is a rectangular box girder with 3 webs (*Fig. 19*). The depth of the cross-section is very low – only 0.8 m.
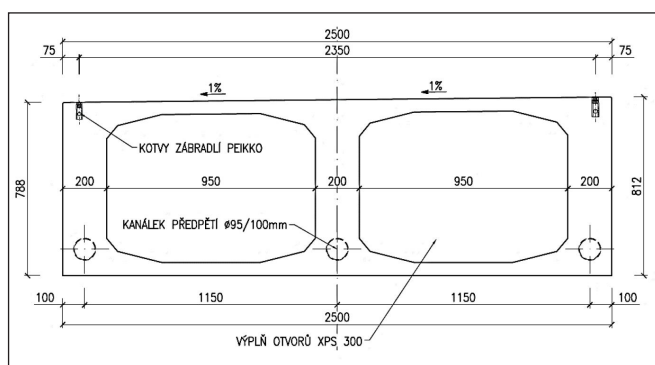
Fig. 19: Cross-section of the footbridge in Pribor

The longitudinal prestressing is composed of 3 cables 17 ∅15.7 mm. In order to guarantee the long-term durability, the monostrands were used, which are additionally grouted in ducts. In the joints, special connectors of ducts are used, which improve their tightness.

The segments were cast in a steel mould. Although the segments were not match-cast, the dry joints glued by epoxy resin were used. The segments were assembled on the fixed scaffolding, the joints were glued and the footbridge was prestressed.

The surface is directly exposed to traffic and no protection of the top surface used. A completed footbridge is shown in *Fig. 20*.

Fig. 20: Completed footbridge in Pribor (2019)
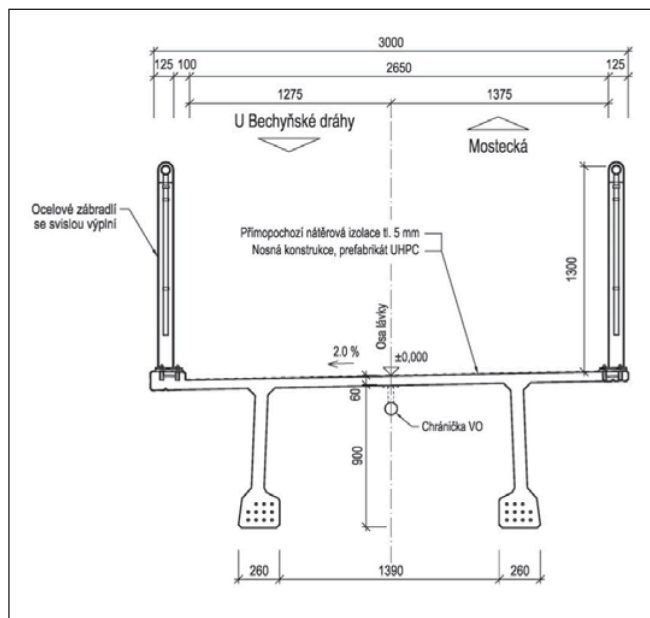
Fig. 21: Cross-section of the footbridge in Tabor

Fig. 22: Completed footbridge in Tabor (2018)

3.5   Footbridge in Tabor

Tabor is a regional city about 90 km south of Prague. The footbridge is a simply supported beam made of UHPC (Komanec, Kalny, 2022). The span of the 3 m wide footbridge is 27 m long. The beam is pre-tensioned. It was cast in a precasting plant in one step without any working joints. The cross-section is plotted in *Fig. 21*.

The cross-section of the double T shape is prestressed by 11 strands (profile 15.7 mm) in each web. The thickness of the top slab is only 60 mm and the depth of the cross-section is 960 mm.

The footbridge was transported to the site and assembled using two cranes within 2 hours. No temporary structures were used for assembly. The top surface is protected by sprayed waterproofing which also provides anti-sliding surface. A completed footbridge is illustrated in *Fig. 22*.

3.6   Comparison of the two simply supported footbridges

The footbridge in Pribor and the footbridge in Tabor have similar spans (35 and 27 m). The Tabor footbridge is shorter but wider. Their areas are not too different (Pribor 90 m² and Tabor 82.5 m²). When looking at the cross-sections *(Figs. 19 and 21)*, a significant difference can be seen. The footbridge in Pribor has the very thick cross-section (3 webs, each 200 mm thick – *Fig. 19*), while the cross-section of the footbridge in Tabor is rather thin-walled (*Fig. 21*). A material consumption shows even more different figures. Consumption of UHPC and of prestressing steel: Pribor 0.39 m³/m² and 24 kg/m², Tabor 0.14 m³/m² and 8,65 kg/m². The

durability of the footbridge in Pribor required application of monostrands grouted in ducts with special sealing elements in joints. This is rather expensive solution which still has a risk of incorrect function. The pretensioning, which is used at the footbridge in Tabor is a cheapest possible solution without any difficulties and easy to execute. The UHPC provides very good protection of strands because of fibres and practically total elimination of cracks.

A construction process also exhibits significant differences. While the footbridge in Pribor required a fixed scaffolding, assembly of segments with adjustments, gluing of joints and finally post-tensioning and grouting, the assembly of the footbridge in Tabor was easy, made in two hours using standard cranes.

It is necessary to learn from such experience. It is important to decide already in the initial stage of the design on the structural system and on the materials taking the construction process into consideration. The section of the Pribor footbridge could have been designed from any concrete, no UHPC was necessary. Only by this change a significant savings could have been achieved. The footbridge in Pribor could have been made also as a pretensioned lightweight structures without joints. The span of 35 m would allow for the assembly of one beam. On the other hand, the footbridge in Tabor is a nice example of a structure, where the design, material choice and construction are in mutual balance resulting in efficient and also sustainable structure.

3.7   Footbridge in Hradec Kralove

Hradec Kralove is a city about 100 km east of Prague. The footbridge is crossing the Labe River close to the city centre. An original design of the suspension footbridge combines steel structure with a concrete deck. The deck is made of segments made of UHPC. The footbridge has 2 spans 69 and 33 m long. They are supported by 2 suspension ropes which support the bridge deck by means of slender steel frames (*Fig. 23*).

Although the structural system is rather complex and the construction of the footbridge was not easy, this example shows a suitable application of UHPC. A thin bridge deck is light and it is directly exposed to traffic. The quality of UHPC can guarantee a long-term durability of the bridge deck.

Fig. 23: Completed footbridge in Hradec Kralove (2022)

3.5   Footbridge in Prague

This year (2023), a new footbridge made of UHPC was opened in Prague. It connects two parts of the city and the island Stvanice in the Vltava River. It is a rather long continuous parapet girder made of white UHPC. The longest spans are 55 m long. A white colour was required by the architect. In the Czech conditions, there is only one white cement available. Rapid hardening and high heat of hydration of the cement are the properties, which made the execution difficult. The footbridge is made of large U – shape segments (*Fig. 24*). They are typically 5 m wide and 5.5 – 6.0 m long. The depth of the parapets is 1.85 m.

Segments were produced in the precasting plant in the

Fig. 24: *Typical segment of the footbridge in Prague (2023)*

Fig. 25: *A completed footbridge in Prague (2023)*

opposite position. After demoulding, they were turned to the definitive position and transported to the site. On the site, the segments were put on the fixed scaffolding, the joints were glued and the bonded prestressing cables were prestressed. Some joints were wider (cast on the site) which allowed for adjustments of the footbridge geometry.

A completed footbridge is shown in *Fig. 25*. The footbridge was rather expensive. Many questions could be posed, e.g., if the design is so excellent that it is worth to invest high costs, or whether it was really necessary to use UHPC for this design. If the bridge was made of a good quality ordinary concrete, would it be so different? etc.

4.   UHPC IN RECONSTRUCTIONS

4.1   Experience from research

UHPC is a material with excellent properties, which makes it suitable also for applications in repair and in rehabilitation of existing structures. Extensive research was carried out in Czechia (Vitek, Bohacek, 2022). Usually, added thin layer of UHPC cast on top of the existing structural element can significantly improve its load carrying capacity or even its stiffness. The amount of added material is low, additional weight represents only a small increase of loading of existing structure and it makes the strengthening efficient.

The old concrete elements were tested in different loading situations. Experimental works showed that the interaction of added layers of UHPC with existing concrete belongs to crucial factors influencing the behaviour of the rehabilitated structure. If concrete of the existing structure is good, in most cases no connectors between existing concrete and UHPC are necessary. The bond between UHPC and concrete could be sufficient for reliable connection of individual materials. However, if the quality of existing concrete is not very good, it is highly recommended to think about the application of UHPC, if it is really the optimal way of repair, or at least

to apply the connectors. In loading situations with prevailing shear loading, like punching of slabs, it is recommended to use shear connectors also if existing concrete is of a good quality.

The different approach for strengthening must be selected in buildings and in bridges. In buildings, often the floors are strengthened. The floors are usually horizontal and they are not exposed to environmental impacts. The self-compacting UHPC can be used for additional layer. In usual floors, some parts of the additional layer are subjected to compression and some to tension (assuming continuous slabs). The reinforcement of the UHPC in areas subjected to tension improves the ductility and increases the load carrying capacity. In areas close to columns, where punching is expected, the shear connectors should be installed.

In bridges, the surfaces of bridge decks are usually in slope. Special composition of UHPC is then required, so that the additional layer could be cast and flowing away was avoided. In bridges the added layer of UHPC can work also as a waterproofing. Then it is necessary to avoid cracking. High fibre content is therefore necessary. The working joints have to be executed as watertight. Additional layer of UHPC can help to increase significantly the load carrying capacity as well as the durability of the existing structure. The service life of the UHPC layer is much higher than that of any classical waterproofing layer.

4.2 Strengthening of the bridge

The Barrandov bridge in Prague is a heavily loaded bridge. Daily, more than 140 thousands vehicles drive along the bridge. The bridge has two independent superstructures completed in 1983 and in 1988. Each superstructure carries 4 lanes of traffic. Now after almost 40 years, a corrosion of prestressing cables was observed, waterproofing required repair and general maintenance of the bridge is necessary.

The bridge is about 350 m long, it has 6 spans, the length of the main span is 72 m (*Fig. 26*). The cross-section of individual bridges is composed of 3 boxes. Original prestressing is located in webs of the cross-section. The main parts of the rehabilitation cover installation of additional unbonded cables, which increase the prestressing force in the entire bridge and complete replacement of layers on the top of the bridge deck. The rehabilitation is planned to 4 seasons. Because of the heavy traffic, only 2 lanes from 8 can be temporarily closed. The works started in 2022 and continued in 2023 on the south bridge, where the works are now completed. In the next 2 years the works will continue on the northern bridge. In 2022 it was decided that UHPC could be a good alternative for strengthening of the south bridge (Vitek, Bohacek, 2023). However, there was no earlier experience with this technology. The client agreed to use the UHPC as a strengthening layer but he did not accept the risk of leakage if
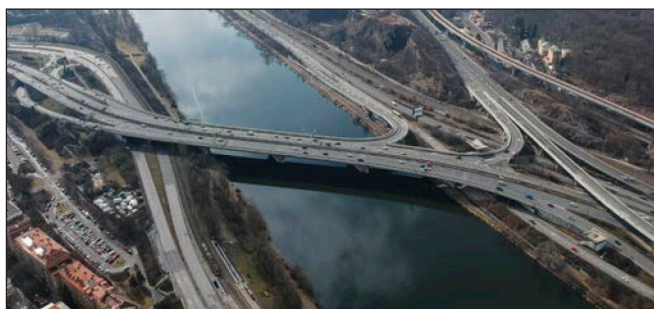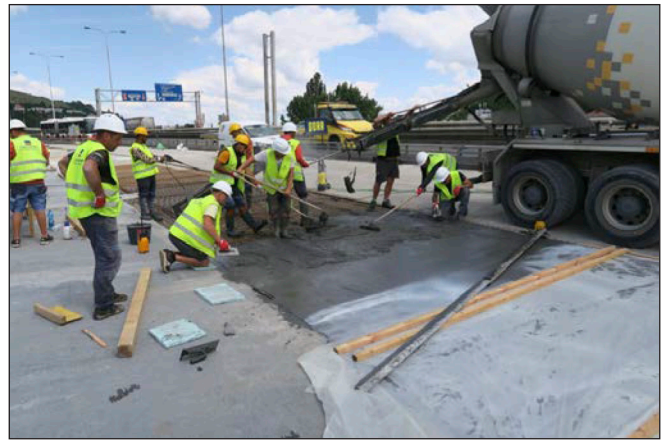
Fig. 27: Pouring of UHPC on the bridge deck and immediate curing

the UHPC was used also as a waterproofing. It was a correct decision, since no tests for waterproofing were executed in Czechia before. Now the tests are prepared and if they are successful, the UHPC could be used also as waterproofing on the northern bridge in 2024 and 2025.

The UHPC for the strengthening of the bridge deck was developed on the basis of the results of the research project. The mix has a maximum aggregate size 4 mm and fibre contents of 3% of high strength fibres. The flexural strength measured on beams with the notch exceeds 20 MPa. The UHPC was transported by truck mixers to the site. During the day, the amount of $30 - 40$ m³ was delivered.

The quality of surface of the bridge deck was rather variable. The tear off tests exhibited a large scatter. The surface was treated by water jet blasting using a pressure from 2000 to 2500 bars. In some parts a combination of milling and water jet blasting was used.

The reinforcement of the additional UHPC layer was used if its thickness exceeded 40 mm. All the works were executed in summer time, when the traffic is lower due to the holiday season. High temperatures resulted in rapid drying of concrete. In the first stage of repair, the edges of the cast segments of UHPC delaminated due to drying shrinkage. In the second stage, the anchors were used at the edges (along the working joints, which resulted in avoiding the delamination.

The UHPC was poured from the truck mixer and distributed manually (*Fig. 27*). The use of finisher will require additional research and more experience.

Immediately after finishing, the surface was protected against drying by using a spray against evaporation of water and it was covered by a PE foil.

The experience for the first stage of repair in 2022 led to some improvements realized in the second stage (2023). The technology of strengthening with UHPC was successful and now preparation works are made for the 3rd stage which will be started in summer 2024.

5. CONCLUSIONS

Almost 15 years of development of UHPC in Czechia brought some promising results. Successful new footbridges were built and the works on reconstructions show a slow progress too. Czech Concrete Society produced guidelines for production, design and execution of structures made of UHPC with an annex describing principles of application of UHPC in reconstructions. The guidelines became a basis for Technical specifications of Ministry of transport on using of UHPC. It is expected that this document will open the

Fig. 26: View on the Barrandov bridge in Prague before reconstruction

door for application of UHPC also in large structures of the transport infrastructure.

On the other hand, UHPC is still a new material and the knowledge on its behaviour is limited. New research results are very welcome. The structures where application of UHPC is expected must be designed by experienced engineers so that the favourable properties of expensive UHPC could be used. A single wrong application of UHPC which would result in some difficulties can be a reason for stopping or slowing down of future applications for years.

UHPC is a specific material. It is expensive and it is also demanding in terms of the ecological reasons. High amount of cement means also high CO_2 emissions and apparently a material which is not very suitable for sustainable structures. However, sustainability must be evaluated on the entire structure and not only on the material which is applied. Some examples illustrated here show that the consumption of UHPC can be very small and although the cement consumption is high in the material, the cement consumption in the structure can be reasonably small and consequently such structure can be more sustainable than that made of ordinary concrete (especially if durability is considered).

UHPC is considered as an advanced material. Many unexperienced designers try to apply it under any circumstances. Incorrect use of UHPC results in structures which are expensive and finally need not be durable. The durability of the structure is given by the element with the lowest durability. In case of a bridge, the details which are sources of cracking, working joints which leak, corrosion of steel etc., can be sources of difficulties and of reduction of the durability or even the load carrying capacity, although UHPC is used.

Design of structures (or rehabilitation works) requires experienced designer who is able to evaluate all influencing factors which are in favour or against application of UHPC and who decides on optimal choice of the material. The structural design and the design of construction process are mutually interrelated with material. Only the right way of application of UHPC, where its properties are actually used can lead to future successful structures.

6. ACKNOWLEDGMENTS

7. REFERENCES

Komanec, J., Kalny, M., et al. (2022), Precast footbridges made of UHPC, *fib* Czech national report, *fib* Congress in Oslo 2022. pp. 70-75

Tej, P., Vrablik, L, et al. (2022a), Footbridge over the Vltava River in Luzec nad Vltavou, Czechia, *fib* Czech national report, *fib* Congress in Oslo 2022. pp. 62-69

Tej, P., Vrablik, L. et. al. (2022b), Design ans manufacture of segment prestressed footbridge from UHPFRC in Pribor, Moravia. *fib* Czech national report, *fib* Congress in Oslo 2022. pp. 76-81

Vitek, J. L., Coufal, R., et.al., (2013), UHPC - Development and testing on structural elements. Concrete and Concrete Structures 2013, University of Žilina, pp. 218-223 https://doi.org/10.1016/j.proeng.2013.09.033

Vitek, J.L., Kalny, M. (2015), Cable stayed footbridge with deck made of UHPC. Proc. of the conference Multi-Span Large Bridges, Pacheo and Magalhaes (Eds.), Taylor and Francis Group, pp. 993-999

Vitek, J. L., Citek, D., et.al., (2016), Application of UHPC in Bridge Construction – Experimental testing. HiPerMat 2016, 4th Internatinal symposium on UHPC and high performance materials, Kassel, March 9-11, 2016

Vitek, J. L. Citek, D., Coufal, R., (2017), Precast structural elements made of UHPC. Proc. of the AFGC-ACI-fib-RILEM Int. Symposium on Ultra-high-Performance Fibre-Reinforced Concrete UHPFRC 2017, Oct. 2-4, 2017, Montpellier, France, pp. 115-124

Vitek, J.L., Bohacek, L., Coufal, R. (2022), UHPC – Efficient method for strengthening of concrete structures. Proc. of the Central European Congress on Concrete Engineering, Zakopane, Poland, Sept. 2022, 379-391

Vitek, J. L., Bohacek, L, Coufal, R., Vrablik, L. (2023), UHPC in existing structures. Proc. of the fib symposium 2023, LNCE 349, pp. 1866-1874, 2023, https://doi.org/10.1007/978-3-031-32519-9_187

Jan L. Vitek is professor for concrete structures at the Faculty of Civil Engineering, Czech Technical Univeristy (CTU) in Prague. He works also in Metrostav a.s., major contracting company in Czechia as expert on structures. He served as a president of the Czech Concrete Society, he represents Czechia in *fib* (International federation for structural concrete) where he is a convener of technical groups. He is a member of the Czech Engineering Academy, member of the Scientific board of the Faculty of Civil Engineering, CTU in Prague, and honorary member of *fib*.
E-mail: vitek@fsv.cvut.cz, jan.vitek@metrostav.cz

VARIABILITY OF LIGHTWEIGHT AGGREGATE SOURCE: EFFECT ON THE DEVELOPMENT OF HIGH STRENGTH LIGHTWEIGHT SCC MATRIX BLENDED WITH NORMAL WEIGHT AGGREGATE
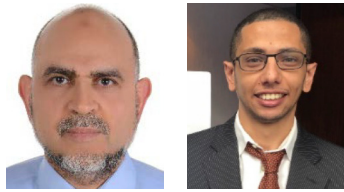
Sherif Yehia   -   Sharef Farrag

Structural lightweight concrete is a valuable alternative to normal weight concrete. Concrete prepared with coarse lightweight aggregate provides reduction of a structure self-weight and better structural performance in regions prone to seismic activities. However, variability of the coarse lightweight aggregate affects production and properties of the concrete. In addition, availability of the aggregate influences the long-term use and stability in the construction industry. Lightweight aggregate is imported from Iran, Turkey, Saudi Arabia, UK, and Greece to the United Arab Emirates (UAE) and has been used in structural and non-structural applications.

This paper presents the development of a self-consolidating high strength lightweight concrete (SCHSL-WC) matrix with available materials in UAE. Specific gravity, unit weight, gradation, particles' shape and absorption were used during the development and selection of aggregates source. In addition, percentage of normal weight aggregate that could be used to improve the matrix was optimized. Results of the experimental investigation showed that self-consolidating concrete mixes with more than 50 MPa cube compressive strength could be produced with aggregates having specific gravity factors in the range of 1.15 to 1.4. Additionally, up to 12% per volume of the coarse lightweight aggregate could be replaced by normal weight coarse aggregate while maintaining a unit weight less than 2000 kg/m³.

Keywords: self-consolidating concrete, SCC, Lightweight aggregate, Aggregate source

1. INTRODUCTION

Durability and strength requirements are equally important for normal and lightweight concrete mix development/ proportioning. Exposure conditions influence the short and long-term structural performance; on the other hand, strength is essential for the structural design. Durability requirements are achieved by controlling the water-to-cementitious ratio (*w/cm*); reduction of cement content and addition of other cementitious materials (slag, silica fume, fly ash and natural pozzolans) based on exposure conditions. Generally, aggregate strength and cementitious materials paste affect concrete strength; however, in the case of lightweight concrete, interfacial transition zone (ITZ) contribute to the overall strength. Therefore, aggregate strength, specific gravity, unit weight, and absorption capacity are the most important parameters which should be considered during any lightweight concrete mixture development. These parameters are related to aggregate type and production method.

Several sources of lightweight aggregates are available in the United Arab Emirates (UAE); however, the variability of the aggregate source; often times the variability within the same source, affects the fresh and hardened concrete properties. Therefore, the objective of this research is to develop a self-consolidating high strength lightweight concrete (SCHSLWC) mixture utilizing lightweight aggregate from a single source that is available in UAE.

In addition, lightweight aggregate from four other sources available in UAE, were used to evaluate the variability of the aggregate source on the developed mixture. The evaluation criteria during this stage of the project were fresh properties, unit weight, and compressive strength.

2. BACKGROUND

Many research efforts were devoted lately to the development and evaluation of lightweight aggregate concrete. These efforts could be classified under three categories; aggregate production/properties, mix proportioning, and durability/ strength evaluation. These efforts are briefly discussed in the following subsections. In addition, several guidelines for the development of Self-Consolidated Concrete (SCC), High-Strength Concrete (HSC), High-Strength Lightweight Concrete (HSLWC), and Self-Consolidated High Strength Lightweight Concrete (SCHSLWC) found in the literature were summarized and presented.

2.1 Lightweight Aggregate Production/ Properties

Utilizing lightweight aggregate in concrete mixtures help reduce structures' dead load, in addition, it provides other desired qualities for concrete such as, thermal and acoustic insulation, and fire resistance (Banawair et. al. 2019, Nadesan

and Dinakar 2017, Cerny 2016, Barbosa et al., 2012; Jo et al., 2007). However, performance of lightweight aggregate concrete is controlled by the physical and mechanical properties of the lightweight aggregate used in the mixture. These properties include specific gravity factor, water absorption, aggregate size and shape, porosity, gradation and aggregate strength (Chi et al., 2003; Lo & Cui, 2004; Lo et al., 2007; Lo et al., 2008; Bentz, 2009; Silva et al., 2010; Kockal & Ozturan, 2010, Yang et. al 2014, Nadesan and Dinakar 2017). Absorption and aggregate's strength greatly influence concrete production and mechanical properties of lightweight concrete. Total pore volume accessible to water determines the absorption of the lightweight aggregate. Generally, absorption is in the range of 5 to 20 % by mass of the dry lightweight aggregate and may reach up to 30% in certain types of lightweight aggregate (LWA) (Chi et al., 2003). This high absorption imposes difficulty in determining the *w/cm* needed for the mix (ACI 318-19). Moreover, the ACI213R-14 emphasizes on the importance of pre-wetting because of the absorptive nature of lightweight aggregates. In addition, slump or self-consolidation levels will be difficult to achieve without a pre-wetting process (ACI 213R-14; Kabay & Aköz, 2012). It is also, expected that a longer mixing duration will be required when mixing lightweight concrete to achieve homogeneity (Barbosa et al., 2012).

The cellular structure of the LWA affects aggregate strength and consequently affects the concrete strength. LWA has a high crushing value which is an indication of low strength, typically, is in the range of 22- 40% (Haque et al., 2004). Several research efforts were devoted to improve both properties by using different binders, special heat treatment or by adding polymers to enhance the durability and strength of the lightweight concrete (Wasserman & Bentur, 1996; Kockal & Ozturan, 2011, Nadesan and Dinakar 2017, Yang et. al. 2014). However, the commonly used lightweight aggregates for structural applications are Pumice, Foamed Slag, Expanded Clays and Shales, and Sintered Pulverized–fuel ash aggregate (ASTM 2014; Chandra, Berntsson, & Knovel (Firm), 2002; Neville, 1995). The specific gravity factors of the lightweight aggregate for structural applications is typically in the range of 1.2 to 1.5 for coarse aggregate and the bulk density of the aggregate is in the range of 300 – 900 kg/m^3 based on the production process (Chandra et al., 2002; Neville, 1995). Furthermore, the ASTM C330 specifies (880 kg/m^3) as the maximum dry loose bulk density of lightweight aggregates for structural concrete coarse aggregate. This means in some cases, the aggregate will have a lower density than that of the mortar paste (typically 2100-2200 kg/m^3), compromising stability of the mix and segregation becomes a concern especially in the case of self-consolidation or if vibration is required et al., 2005). Moreover, whether the aggregate will float or not depends not only on the density difference, but also viscosity of the mix will play a role in determining the resultant driving force.

2.2 Mix Development

Mix proportioning to achieve self-consolidating, high strength lightweight concrete should consider guidelines/ recommendations specified for each characteristic. The following subsections summarize different approaches for mix proportioning, sample of mixes found in the literature and general guidelines for producing SCC, HSC, HSLWC, and SCHSLWC.

2.2.1 Mix proportioning - Available approaches from literature

The microstructure of the lightweight aggregate usually leads to high absorption, which imposes difficulties in determining the mixing water and the amount that will be absorbed by the aggregate. Therefore, different approaches could be followed to proportion and determine the weight of each ingredient. ACI PRC-211.1-22 methods (weight method and volumetric method) and Densified Mixture Design Algorithm (DMDA) (Hwang & Hung, 2005) are examples of these approaches. However, these methods require adjustment; therefore, trial batches should be prepared to adjust mixing water, target slump, and unit weight of fresh concrete.

2.2.2 Lightweight Concrete Mixtures from literature

Several lightweight, self-consolidating, high strength and self-consolidating high strength lightweight concrete mixtures found in literature were summarized as shown in Figure 1. These mixtures were classified based on the ACI 213R-14 strength requirement (40 MPa) and on concrete workability. Taking into consideration, variability of the lightweight aggregate (properties, particle size, gradation, etc.), variability of the local materials (including admixtures) and variability of the volumetric ratios for each ingredient, these mixtures were compared with respect to unit weight, structure efficiency (strength/unit weight), strength, and percentage of coarse aggregate, as shown in Figure 1. The comparison showed that the volumetric ratio of the coarse lightweight aggregate should be in the range of 30 to 45% of the total mix. In addition, high strength could be achieved by w/cm in the range of 0.32 to 0.42 and by utilizing supplementary cementitious materials, which will help in producing a dense Interfacial Transition Zone (ITZ), hence, improving concrete strength (Kockal & Ozturan, 2010). General guidelines collected from the literature to produce SCC and HSC with normal weight aggregate and lightweight are summarized in Table 1. These guidelines provide a volumetric range of each ingredient and recommendations about materials' specifications.

The minimum durability and strength requirements in ACI 318 building code are based on the exposure categories and classes. Development of sustainable, dense, and impermeable concrete could be achieved by the use of supplementary cementitious material and by controlling w/cm ratio (Chen & Liu, 2008). In addition, dense mixes will help achieve high strength; however, strength of lightweight concrete (LWC) depends also on the interfacial zone (ITZ). The ITZ is affected by aggregate absorption, porosity of the interface which in turn is affected by the use of supplementary materials and fine sand (Liu et al., 2011). However, higher percentage of fines influences the time-dependent properties (shrinkage and creep) and impact concrete durability. Therefore, careful mix proportioning is necessary to control factors that affect shrinkage and creep (ACI 213R-14).

In this paper, an experimental investigation to develop a SCHSLWC utilizing local material available in the UAE is presented. Lightweight coarse aggregate and normal weight fine aggregate were used during the investigation.
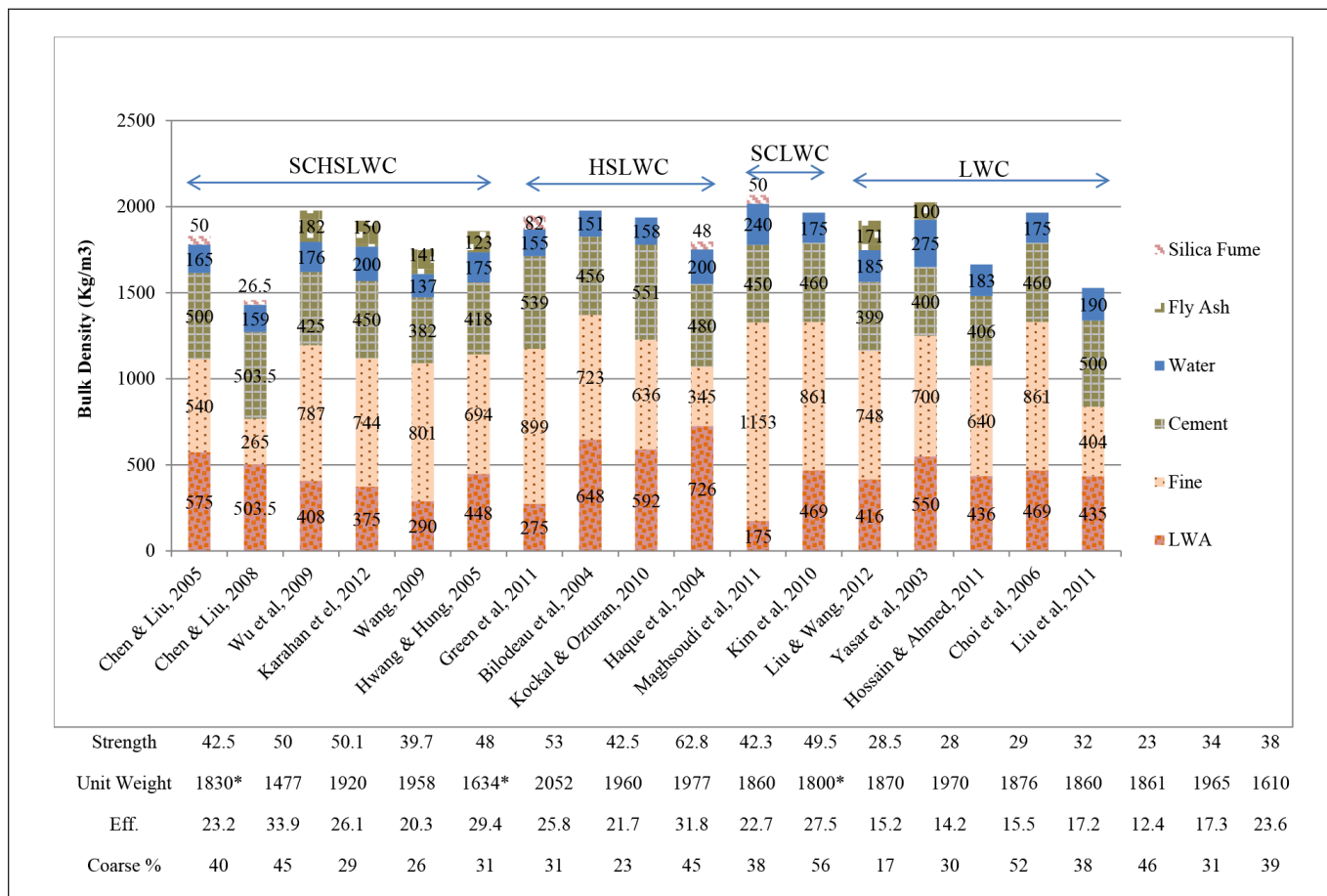
Fig. 1: Sample of SCHSLWC, HS LWC, SCLWC and LWC mixtures found in the literature

Table 1: Guidelines for materials' proportioning SCC, HSC, HSLWT and SCHSLWC (ACI, 2003, 2004, 2007, 2010, 2011b; 2014, 2022, Bilodeau et al., 2004; Chen & Liu, 2005, 2008; Choi et al., 2006; Green et al., 2011; Haque et al., 2004; Hossain & Ahmed, 2011; Hwang & Hung, 2005; Karahan et al., 2012; Kim et al. , 2012; Kimet al., 2010; Kockal & Ozturan, 2010; Liu et al., 2011; Liu & Wang, 2012; Maghsoudi et al., 2011; Wang, 2009; Wet al., 2009; Yasar et al., 2003)

	SCC	HSC	HSLWT	SCHSLWC
Water Cement Ratio	Based on strength requirements, refer to w/cm ratio and strength relation	Typically w/c >0.4	Based on strength requirements, refer to w/c ratio and strength relation	To achieve high strength with self-consolidation, typically w/c falls within 0.32-0.42.
Water Content	Refer to ACI 318-11, Table 4.4.1	100- 140 kg/m³, depends on the use of Super plasticizers and mineral admixtures	Not specific content because of the higher absorption capacity and difficulty in determining the free water in the mix.	Not specific content because of the higher absorption capacity and difficulty in determining the free water in the mix. Typically 140-200 kg/m³ (15-25% of total volume).
Cementitious Material Content	18% per volume or maximum 200 kg/m³ (12.48 lb. /ft³). Typically silica fume can replace up to 5% of cement to enhance strength gain and viscosity, and fly ash up to 10% to enhance strength and flowability	350 – 400 kg/m³, typically silica fume can replace up to 5% of cement to enhance strength gain and viscosity, and fly ash up to 10% to enhance strength and flowablity	420-500 kg/m³ (25.9 – 31.11 lb./ ft³) for 40 MPa concrete strength – 630 kg/m³ (38.89 lb./ft³) for 70 MPa concrete strength	380-520 kg/m³ (10-20% of total volume). Typically silica fume can replace up to 5% of cement to enhance strength gain and viscosity when avoiding for avoiding viscosity modifying admixtures, and fly ash up to 10% to enhance strength and flowablity
Fine normal weight aggregate	350-450 kg/m³ (21.9 – 28.09 lb./ft³) – Max fly ash 25% by weight	Fine aggregate with fineness modulus (F.M.) > 2.9 due to high cement content	Can replace light weight fine aggregate to improve placing and compaction – increase in concrete density is expected	Can replace light weight fine aggregate to improve placing and compaction to improve placing and compaction – increase in concrete density is expected. Typically 270-860 kg/m³ (10-40% of total volume)

Fine lightweight Aggregate	N/A	N/A	Fines passing #4 sieves (4.75 mm) are expected to greatly affect strength, for they lower crushing strength. Thus inclusion will unlikely provide more than 40 MPa f'c.	Fines passing #4 sieve (4.75 mm) are expected to greatly affect viscosity and stability of flowable concrete, for finer particles will not blend properly in the matrix, causing segregation
Coarse Aggregate	Should be in the range of 0.48-0.54 – 1/2 in. nominal aggregate size	Smaller maximum size of aggregate to improve strength; typically maximum size of 10 mm.	Smaller maximum size of aggregate to improve strength, typically 10 or 5 mm.	Smaller maximum size of aggregate to improve strength, mainly maximum size of 4.75 mm (#4 sieves). Typically 300-580 kg/m^3. (20-50% of total volume)
Chemical Admixtures	Should follow the manufacturer recommended dose	Should follow the manufacturer recommended dose	Should follow the manufacturer recommended dose	Should follow the manufacturer recommended dose. Super plasticizer dose is 1-2% of total volume.

3. EXPERIMENTAL PROGRAM

The main objective of the experimental program was to develop a self-consolidating high strength lightweight concrete (SCHSLWC) for structural applications meeting the target strength [40 MPa (6000 psi)] and unit weight less than 2000 kg/m^3 (120 lb/ft^3) as defined by ACI 213R-14. This objective could be achieved by using 100% coarse lightweight aggregate or by partial replacement of normal weight coarse aggregate in addition to normal weight fine. Therefore, optimization of the percentage of normal weight coarse aggregate that could be used while maintaining the unit weight requirement was investigated. In addition, effect of aggregate source variability on the properties of developed mixes was evaluated by monitoring the variation in concrete properties. Therefore, the experimental program consisted of two phases: Phase I focuses on the development of the mix and phase II concentrates on the evaluation of aggregate source variability on the developed mix at the fresh and hardened stages.

3.1 Methodology

The following highlights the main steps of the mix development:

1- SCHSLWC mix is developed to achieve higher compressive strength with one source of LWA in the UAE, utilizing 100% coarse LWA and normal weight sand in all mixes. Then, adjust the mixture to meet characteristics of SCC.
2- Partial replacement of normal weight coarse aggregate is introduced to achieve dense mix, hence, improve concrete strength.
3- Mixes are evaluated and adjusted for workability and compressive strength.
4- In the optimized mix, lightweight aggregates (specific gravity, particle size and shape, gradation) from another source is used to evaluate the effect on workability, unit weight and strength.

3.2 Phase I – Development of SCHSLWC mix

Material properties
Lightweight Aggregate – Source #1
Lightweight aggregate from one source in UAE was used during this phase of the investigation. Figure 2 shows a sample of the aggregate (Pumice) which is labeled "Source #1" in the discussion.

The aggregate gradation is shown in Table 2. The sieve analysis of the samples as received indicated that about 55% of source #1 had size less than 4.75mm (Sieve No. 4); however, 45 % of this source had sizes between 9.5 and 4.75mm.

Other Materials
Concrete mixes in this study, in addition to the lightweight coarse aggregate, utilized an ordinary Portland cement Type-I (SG 3.14), fly ash class F (SG 2.1), silica fume (SG 2.22), normal weight coarse aggregate (SG 2.58) with 10 mm nominal maximum aggregate size (for partial replacement), normal weight dune sand (particle size 100% passing 0.6 mm, SG 2.60), and coarse sand (maximum particle size 4.75 mm, SG 2.60).

Mix Proportioning
The mix proportion of the SCHSLWC mix was similar to that of a self-consolidating high strength normal weight (SCHSNW) mix developed by (Yehia et. al. 2009). The

Figure 2. Pumice – Sample of Source 1

Table 2: Gradation of aggregate used in the investigation

	Sieve Size (mm)								
	19	12.5	9.5	4.75	2.36	1.18	0.3	0.15	0.075
	ASTM C 330M-2009 Limits (Coarse 9.5-2.36 mm)								
	As Received (%Passing)								
Grading requirement / Aggregate source	-	100	100-80	40-5	20-0	10-0	-	-	10-0
Source #1	0	100 (Y)	100 (Y)	55 (N)	30 (N)				
Source #2	0	100 (Y)	99.3 (N)	70.5 (N)	42 (N)	25.1 (N)	8.8	3.3	0.3 (Y)
Source #3	0	100 (Y)	71.1(N)	39.8 (Y)	19.1 (Y)	5.3 (Y)	0.34	0.13	0.13 (Y)
Source #4	0	100 (Y)	66.1 (N)	8.9 (Y)	3.5 (Y)	2.9 (Y)	0.3	0	0 (Y)
Source #5	0	100 (Y)	19.9 (N)	6.5 (Y)	4.6 (Y)	4.1 (Y)	3.3	1.5	0 (Y)
	ASTM C 330M-2009 Limits (Combined fine and aggregate, 9.5-0 mm)								
	Combined with fine 100% (%Passing)								
Grading requirement / Aggregate source	-	100	100-90	90-65	65-35	-	25-10	15-5	10-0
Source #2	100	100 (Y)	99.2 (Y)	60.6 (N)	57.1 (Y)	49.2	34.5 (N)	16.1 (N)	2.3 (Y)
Source #3	100	100 (Y)	100 (Y)	60.1 (N)	55.2 (Y)	45.6	29.7 (N)	10.1 (Y)	1.2 (Y)
Source #4	100	100 (Y)	100 (Y)	80.9 (Y)	55.8 (Y)	47.4	28.9 (N)	8.4 (Y)	2.1 (Y)
Source #5	100	100 (Y)	100 (Y)	59.7 (N)	56.1 (N)	47.9	33.1 (N)	12.5 (Y)	1.4 (Y)
	ASTM C 330M-2009 Limits (Combined fine and aggregate,12.5-0 mm)								
	Combined with fine 88-12% (%Passing)								
Grading requirement / Aggregate source	100	100-95	-	80-50	-	-	20-5	15-2	10-0
Source #2	100(Y)	100(Y)	97.5	55.6 (Y)	51.5	43.4	28.9 (N)	8.6 (Y)	0.9 (Y)
Source #3	100(Y)	100(Y)	97.5	57.9 (Y)	53.4	46.7	33.5 (N)	16.8 (N)	2.5 (Y)
Source #4	100(Y)	100(Y)	98.4	73.8 (Y)	66.6	44.4	31.1 (N)	11.6 (Y)	1.2 (Y)
Source #5	100(Y)	100(Y)	98.3	55.5 (Y)	51.4	42.6	30.0(N)	7.42 (Y)	0.5 (Y)

Source #2 Light expanded clay	Source #3 Pumice	Source #4 Pumice	Source# 5 Sintered pulverized–fuel ash aggregate

*Shaded cells do not meet ASTM gradation requirement

volumetric ratios of the SCHSNW mix based on the absolute volume method were 19.5 % cement and mineral admixtures (fly ash and silica fume) and 63% aggregate (31% coarse and 32% fine aggregate). These volumetric ratios are comparable and are within the ranges of that reported in the literature, Table 1. Therefore, the same volumetric ratio of the normal weight aggregate (NWA) was replaced by source #1 LWA; however, minor adjustments were required to determine weight of the lightweight aggregate and w/cm needed for the mix. In addition, normal weight coarse and dune sand were used in all mixes.

Mixing

Several mixes were prepared with the full gradation of source #1; however, difficulties were encountered due to the high percentage of fine lightweight blended with the

coarse aggregate (about 60% of the particle had size less than 4.75 mm). Therefore, particle size of the LWA smaller than 4.75 mm was excluded from all mixes after the initial trials. In addition, optimization was conducted to determine percentage of NWA that could be used maintaining the target unit weight and compressive strength. Workability, unit weight, and compressive strength were the evaluating criteria at this stage.

3.2.1 Results and discussion - Phase I - Development

The experimental investigation included several mixes with 100 % normal weight aggregate (control mix), 100% lightweight aggregate and partial replacement of lightweight aggregate with normal weight aggregate. Two ratios 25% (75LWA-25NW) and 50% (50LWA-50NW) of the volumetric ratio of the LWA were substituted with NWA. Results of the evaluation criteria during this stage is discussed in the next subsections.

Workability and surface finish

Slump flow test was used to evaluate flowability and visual stability of the mixes. All mixes [control (100% SCHSLWC) and LWA with partial replacement of NWA] had acceptable flow with a diameter in the range of 550 to 600 mm in less than a minute with no sign of segregation. In addition, there was no aggregate floating at the surface and there was no difficulties finishing the surface, as shown in Figure 3 (source #1).

Optimization to introduce coarse NWA – partial replacement of coarse LWA

Average cube compressive strength of the control mix and 100% LWC source #1 was 65 MPa and 48 MPa, respectively. Results of the 50LWA-50NW showed that the dry unit weight is higher than 2000 kg/m³; therefore, higher percentages of NWA were not included in the optimization. Figure 4 shows the results of the optimization with respect to the unit weight. A target unit weight (1850 kg/m³) was selected from the optimization chart and corresponding percentage of NWA which could be used, was determined to be 12%. The 88LW-12NW mix was prepared and evaluated. The average cube compressive strength was 63 MPa and the dry unit weight was 1843 kg/m³. These results showed that the mix 88LWA-12 NWA met the unit weight and compressive strength requirements for structural applications. Figure 5 provides a comparison between average compressive strength and unit weight of all mixes in phase I. The results showed that the 12% NWA replacement would help improve the compressive strength while maintaining the unit weight less than 2000 kg/m³. However, this percentage depends on gradation, particle shape and specific gravity factor of the LWA used in the investigation.

3.3 Phase II – Evaluation of Different Sources of LWA

The main objective of this phase is to investigate impact of aggregate source variability on the concrete properties. Four physical properties (specific gravity factor, bulk density, gradation, and absorption) are believed to have influence on the lightweight concrete production ((Banawair et. al. 2017, Nadesan and Dinakar 2017, Cerny 2016, Kockal & Ozturan, 2010; Lo et al., 2008; Lo et al., 2007). Therefore,
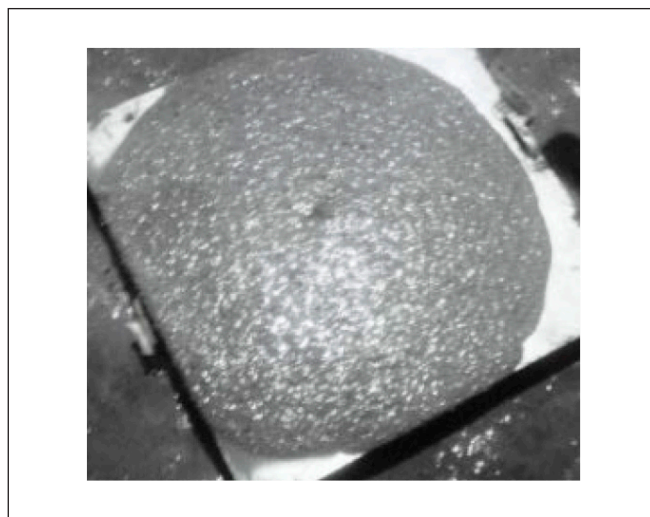
Fig. 3: Slump flow test – Source 1
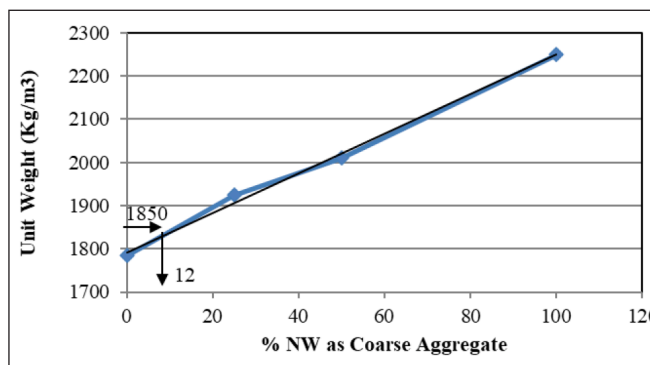
Fig. 4: Unit Weight vs. percentage of NWA used in the optimization
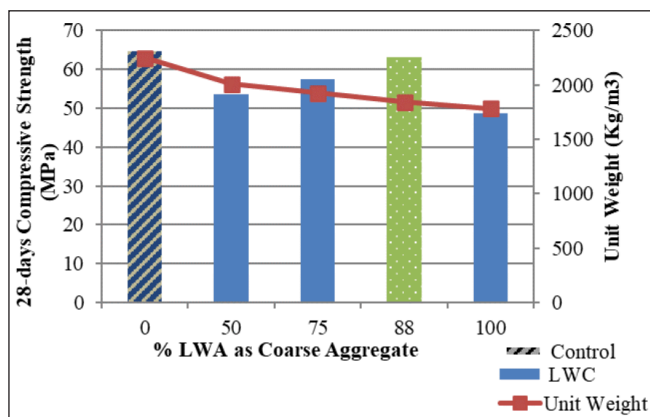
Fig. 5: Summary of the optimization results

these properties were considered in the evaluation. The mix developed in phase I, 88LWA-12NWA, was taken as a control mix in this phase.

Material properties - Lightweight Aggregate

Light expanded clay (source #2), pumice lightweight aggregate from different sources (source #3, source #4) and sintered pulverized–fuel ash aggregate (source # 5) were used in this investigation, samples are shown in Table 2. Sources #2 and #5 particles had spherical shape, while sources # 3 and # 4 particles had angular shape (crushed with rough surface). Sieve analysis was conducted for all samples as received and compared to the grading requirements by ASTM C330/ C330M, as shown in Table 2. The Sieve analysis indicated that source #2, source #3, and source # 4 had about 50%, 70%, and 50% passing from 4.75mm (Sieve No. 4), respectively. On the other hand, about 1% of source #2 had sizes between 12.5

Table 3: *Properties of the lightweight aggregate and concrete produced with respective sources*

Property	Source #1	Source #2	Source #3	Source #4	Source #5
Specific gravity	1.3	0.7	0.7	1.35-1.40	1.15-1.25
Bulk density (kg/m³)	560-660	380 - 480	490 - 575	750 - 800	700-800
Particle shape	Angular	Spherical	Angular	Angular	Spherical
Microstructure (Absorption as indicator)	11	20	36	18	28
Cube concrete strength produced with the source (MPa)	63.1	26	10	57.7	52.2
Dry unit weight at 28-days (kg/m³)	1843	1946	1776	2060	1954

and 9.5mm, whereas sources #3 and #4 have no aggregate size greater than 9.5 mm. Therefore, lightweight coarse aggregate (aggregate retained on Sieve No. 4 and above) was only considered in this study, as the case of source #1. In addition, sieve analysis was conducted for the following samples (i) coarse LWA (particles more than 4.75mm) and fine normal weight and (ii) coarse LWA, fine normal weight and coarse normal weight. Results showed that inclusion of normal weight aggregate (12%) with a size larger than 9.5 mm (12.5 mm) enhanced the aggregate gradation, although particle sizes (4.75 mm, 0.30 mm and 0.15 mm) for one or more sources did not meet the ASTM C330/C330M due to the replacement of the lightweight fine aggregate by normal weight dune and coarse sand. However, the authors decided to include these sources to evaluate the effect of particle size and specific gravity factor on the strength and unit weight of the developed mix. Bulk dry density and specific gravity factors (SGF) of all sources are summarized in Table 3. Specific gravity factors less than "1" was determined by trial and error in separate batches by evaluating the yield and unit weight of wet concrete.

3.3.1 Results – Phase II

Fresh stage evaluation

The 88LWA–12NWA developed in phase I was used as a control mix for comparison and to investigate impact of variation of aggregate properties (source variability) on the fresh and hardened properties. Variation of the specific gravity factors and absorption among the four sources and their impact were taken into consideration during the mix proportioning. However, cementitious materials and w/cm were kept the same for all mixes. Table 4 provides a comparison of the fresh stage (workability and surface finish) properties evaluated in the study.

Mixing

Specific gravity factor of sources #2 and #3 were less than 1; consequently, the aggregate was floating to the surface during mixing, as shown in the pictures, Table 4.

Workability

The slump flow test showed that all mixtures met the ACI 237-07 SCC characteristics (500 mm spread) without segregation for sources #4 and #5; however, sources #2 and #3 a small percentage of the lightweight aggregate was piled in the center of the spread as indicated by circle in the pictures correspond to these sources in Table 4. This could be explained by the low specific gravity of sources #2 and #3 that caused floating of the particles and segregation to occur.

Surface Finish

Lightweight aggregate sources #2 and #3 were floating due to their low specific gravity; as a result, volume instability was exhibited and difficulties were encountered during the surface finish of the samples, as shown in Table 4.

Hardened stage evaluation

Cube compressive strength and dry unit weight were the evalaution ceriteria at this stage of the investigation. Compressive strength and dry unit weight of source #1 were the base of comparison while using the same volumetric ratio of light to normal weight coarse aggregte. Table 3 summarizes the results of the 28-day testing. In addition, monitoring of the strength development was also conducted for all concrete mixtures.

Compressive strength

Cube compressive strength for sources #4 and #5 achieved more than 50 MPa which is less than that for source #1. This could be attributed to the difference in particle size and distribution. In addition, source# 4 achieved higher compressive strength than that for source #5, this was believed to be due to the particles' shape since all other parameters (specific gravity and bulk density) are within the same range. The above findings are acceptable for the specific gravity factor in the range of 1.15 to 1.4 and bulk density between 500 to 800 kg/m³ (Chen & Liu, 2008).

On the other hand, sources #2 and #3 had compressive strength less than 40 MPa which is the value defined by ACI 213R-14 as high strength lightweight concrete for structural applications. Low specific gravity factor (less than 1), higher percentage of smaller size aggregate (4.75 mm) and high absorption are the reasons for not achieving dense mixes and high compressive strength (Lo et al., 2007). Particle shape in both sources was not the determining factor of the performance; however, performance of source #2 was better than that of source #3, this might be contributed to the spherical shape particles (Cui et al., 2012). Close inspection for several cross-sections of the mixtures revealed that sources #2 and #3 had high percentage of internal voids and voids between aggregate particles, as shown in the pictures, Table 5. The presence of these voids is expected to lead to high shrinkage and creep strains in addition to low compressive strength (Neville, 1995).

Failure patterns

Pictures in Table 5 show typical failure patterns of cylindrical specimens during the compressive strength testing. Specimens from sources #1, #4, and #5 showed vertical splitting which is commonly observed in high-

Table 4: *Fresh stage properties phase II*
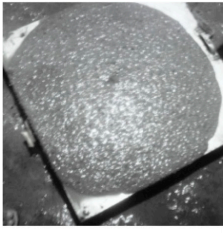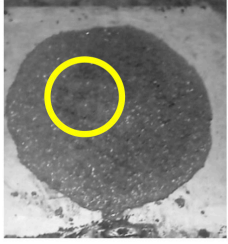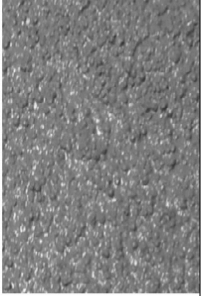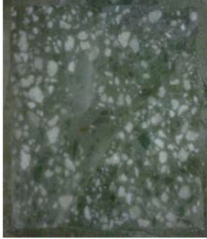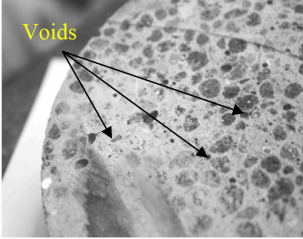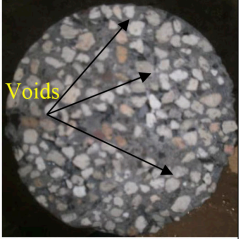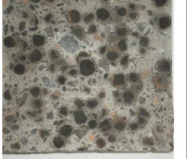
Source Property	Source #1	Source #2	Source #3	Source #4	Source #5
Workability					
Surface finish					

Table 5: *Hardened stage properties*

Source	Source #1	Source #2	Source #3	Source #4	Source #5
Typical Failure Mode					
Cross section		Voids	Voids		

strength concrete specimens. However, failure patterns from sources #2 and #3 specimens' indicated weak bond between the lightweight aggregate and the cementitious materials, in addition to weakness due to high porosity of the aggregate. This also could be explained by the weak interfacial transition zone (ITZ) as discussed by (Lo & Cui, 2004; Bentz, 2009).

Unit weight

Dry unit weight was determined for samples from all sources and summarized in Table 3. Sources #1 and 4 #5 had slightly higher unit weight than that recommended by ACI 213R-14; however, higher compressive strength was achieved by these sources. The other two sources met the recommended unit weight; however, both had low compressive strength for the reasons discussed before in previous section.

Static stability

Specimens from all sources were examined to ensure that the proposed SCHSLWC mixes maintain adequate resistance to segregation and settlement. Specimens (100mm x 200mm cylinders) were cut to four sections each 50mm and labeled as top (a), middle1 (top (b) and bottom(c)), middle 2 (top (d) and bottom (e)), and bottom (f), as shown in Table 6. The cross sections of source #1, source # 4 and source # 5 specimens showed good distribution of the lightweight aggregate and no sign of segregation was found. However, sources # 2 and # 3 showed a clear segregation, which was identified by the low concentration of the lightweight aggregate within the bottom 100 mm of the cylinders, as shown in "e and f" source #2 and #3, Table 6. This could be explained by the low specific gravity factors of these two sources, which led to floating of the aggregate in the flowable SCC mix.

Table 6: Cross section evaluation for static stability
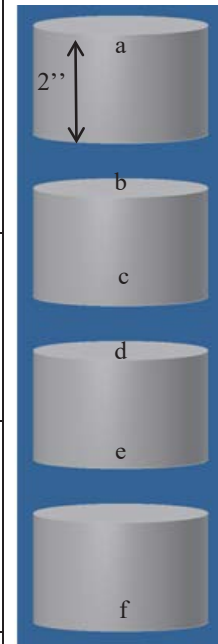
3.3.2 Discussion

Effect of aggregate properties on concrete properties

Specific gravity factor and aggregate bulk density are the most important properties that should be considered when selecting lightweight aggregate for structural applications. Higher specific gravity factor and bulk density will help achieve durable and high strength concrete. This also influences the microstructure of the coarse aggregate (porosity), which in turn, affects the absorption. On the other hand, aggregate gradation (particle size and distribution) affects the compacted density and the ability to achieve high strength. In addition, smaller size in the range of 4.75 mm to 12.5 mm of coarse aggregate will help minimize the effect of aggregate weak strength and will not affect the self-consolidation. It is also important to note that in case of different aggregate with comparable properties (specific gravity factor, bulk density, particle size and gradation); particle shape plays a role in achieving better bond with the paste and overall higher strength.

Structural efficiency factor (SEF)

The structural efficiency factor (strength/unit weight) for the concrete produced with the lightweight aggregate from the five sources was compared as shown in Figure 6. Concrete produced with aggregates from sources #1, #4 and #5 has SEF 34, 28 and 27; respectively. The high compressive

Fig. 6: Structure efficiency factor for mix 88LW-12NW- all aggregates source
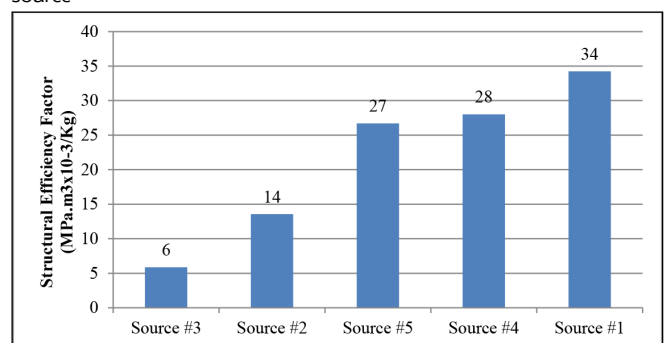
strength and low unit weight helped achieving high SEF values. On the other hand, concrete produced by aggregates from sources #2 and #3 has lower unit weight, however, compressive strength was low and consequently, SEF values were small. This is another reflection of aggregate properties on the concrete quality.

4. CONCLUSIONS

The current study focused on the development of a SCHSLWC mix utilizing local available materials in the UAE. SCHSLWC concrete was produced utilizing coarse lightweight aggregate from 5 different sources. The main objective of the experimental program is to evaluate the impact on the fresh and hardened properties of concrete due to variability of the aggregate source. Mixes with 100% LWT coarse aggregate and normal weight coarse and fine sand were evaluated. In addition, volume fraction of normal weight coarse aggregate was introduced to the mixture while maintaining the target unit weight (2000 kg/m^3) and achieving high compressive strength (40 MPa or higher). Results from both phases showed the following:

- Specific gravity and unit weight are important properties of the lightweight coarse aggregate for structural applications. For comparable properties from different sources, particle shape will considerably impact concrete quality
- Self-consolidating, high strength lightweight concrete with cube compressive strength up to 60 MPa could be produced with aggregates having specific gravity factors in the range of 1.15 to 1.4 and aggregate unit weight in the range of 500-800 kg/m^3
- Up to 12% of the coarse lightweight aggregate could be replaced by normal weight coarse aggregate while maintaining a unit weight less than 2000 kg/m^3
- Structural efficiency factor in the range of 27- 34 could be achieved by lightweight coarse aggregate available in UAE

Other mechanical properties of the 88LW-12NW mix needs to be evaluated to ensure adequacy for structural applications. In addition, durability of concrete produced by the lightweight aggregate from available sources should be investigated.

5. REFERENCES

ACI. (2022). Selecting Proportions for Normal-Density and High -Density Concrete — Guide. Farmington Hills, Mich: American Concrete Institute.

ACI. (2014). Guide for Structural Lightweight Concrete. Farmington Hills, Mich.: American Concrete Institute.

ACI. (2004). Standard Practice for Selecting Proportions for Structural Lightweight Concrete. Farmington Hills, Mich: American Concrete Institute.

ACI. (2019). Self-Consolidating Concrete *ACI 237*. Farmington Hills, Mich: American Concrete Institute.

ACI. (2010). Report on High-Strength Concrete (ACI-363R). Farmington Hills, Mich.: American Concrete Institute.

ACI. (2011a). Building code requirements for structural concrete (ACI 318M-11) and commentary / reported by ACI Committee 318.

ACI. (2011b). Building Code Requirements for Structural Concrete and Commentary (ACI 318-11). Farmington Hills, Mich.: American Concrete Institute.

ASTM. (2023). Standard Specification for Lightweight Aggregates for Structural Concrete *C330/C330M*. West Conshohocken, PA: ASTM International.

ASTM. (2019). Standard Test Method for Determining Density of Structural Lightweight Concrete *C567 / C567M* West Conshohocken, PA: ASTM International.

ASTM. (2012). Standard Test Method for Density, Relative Density (Specific Gravity), and Absorption of Coarse Aggregate *ASTM C127 - 12*. West Conshohocken, PA: ASTM International.

Banawair , A.S., Qaidb , G.M., Adilc , Z.M., Nasird, N.A.M, (2019) "The strength of lightweight aggregate in concrete – A Review," Earth and Environmental Science 357 012017 Publishing doi:10.1088/1755-1315/357/1/012017

Barbosa, F. S., Farage, M. C. R., Beaucour, A.-L., & Ortola, S. (2012). Evaluation of aggregate gradation in lightweight concrete via image processing. *29*, 7–11. doi: 10.1016/j.conbuildmat.2011.08.081

Bentz, D. P. (2009). Influence of internal curing using lightweight aggregates on interfacial transition zone percolation and chloride ingress in mortars. *31*(5), 285–289. doi: 10.1016/j.cemconcomp.2009.03.001

Bilodeau, A., Kodur, V. K. R., & Hoff, G. C. (2004). Optimization of the type and amount of polypropylene fibres for preventing the spalling of lightweight concrete subjected to hydrocarbon fire. *26*(2), 163–174. doi: 10.1016/S0958-9465(03)00085-4

BSI. (2012). Testing hardened concrete. Shape, dimensions and other requirements for specimens and moulds (British Standard) *BS EN 12390-1:2012*. London, UK: British Standards Institute.

Vit Cerny, V., Kocianovaa, M., Drochytka, R., (2017) "Possibilities of lightweight high strength concrete production from sintered fly ash aggregate," Procedia Engineering 195, 9 – 16 https://doi.org/10.1016/j.proeng.2017.04.517.

Chandra, S., Berntsson, L., & Knovel (Firm). (2002). *Lightweight aggregate concrete science, technology, and applications Knovel civil engineering & construction materials* (pp. xx, 430 p.) https://doi.org/10.1016/B978-081551486-2.50009-2.

Chen, B., & Liu, J. (2005). Contribution of hybrid fibers on the properties of the high-strength lightweight concrete having good workability. *35*(5), 913–917, https://doi.org/10.1016/j.cemconres.2004.07.035.

Chen, B., & Liu, J. (2008). Experimental application of mineral admixtures in lightweight concrete with high strength and workability. *22*(6), 1108–1113. doi: 10.1016/j.conbuildmat.2007.03.001

Chi, J. M., Huang, R., Yang, C. C., & Chang, J. J. (2003). Effect of aggregate properties on the strength and stiffness of lightweight concrete. *25*(2), 197–205. doi: 10.1016/S0958-9465(02)00020-3

Choi, Y. W., Kim, Y. J., Shin, H. C., & Moon, H. Y. (2006). An experimental research on the fluidity and mechanical properties of high-strength lightweight self-compacting concrete. *36*(9), 1595–1602. doi: 10.1016/j.cemconres.2004.11.003

Cui, H. Z., Lo, T. Y., Memon, S. A., & Xu, W. (2012). Effect of lightweight aggregates on the mechanical properties and brittleness of lightweight aggregate concrete. *35*, 149–158. doi: 10.1016/j.conbuildmat.2012.02.053

Green, S. M. F., Brooke, N. J., McSaveney, L. G., & Ingham, J. M. (2011). Mixture design development and performance verification of structural lightweight pumice aggregate concrete.(Author abstract). *Journal of materials in civil engineering, 23*(8), 1211, https://doi.org/10.1061/(ASCE)MT.1943-5533.0000280.

Haque, M. N., Al-Khaiat, H., & Kayali, O. (2004). Strength and durability of lightweight concrete. *26*(4), 307–314. doi: 10.1016/S0958-9465(02)00141-5

Hossain, K. M. A., & Ahmed, S. (2011). Lightweight concrete incorporating volcanic ash-based blended cement and pumice aggregate.(Technical Note)(Author abstract). *Journal of materials in civil engineering, 23*(4), 493, https://doi.org/10.1061/(ASCE)MT.1943-5533.0000180.

Hwang, C.-L., & Hung, M.-F. (2005). Durability design and performance of self-consolidating lightweight concrete. *19*(8), 619–626. doi: 10.1016/j.conbuildmat.2005.01.003

Jo, B.-w., Park, S.-k., & Park, J.-b. (2007). Properties of concrete made with alkali-activated fly ash lightweight aggregate (AFLA). *29*(2), 128–135. doi: 10.1016/j.cemconcomp.2006.09.004

Kabay, N., & Aköz, F. (2012). Effect of prewetting methods on some fresh and hardened properties of concrete with pumice aggregate. *34*(4), 503–507. doi: 10.1016/j.cemconcomp.2011.11.022

Karahan, O., Hossain, K. M. A., Ozbay, E., Lachemi, M., & Sancak, E. (2012). Effect of metakaolin content on the properties self-consolidating lightweight concrete. *31*, 320–325, https://doi.org/10.1016/j.conbuildmat.2011.12.112.

Kim, H. K., Jeon, J. H., & Lee, H. K. (2012). Workability, and mechanical, acoustic and thermal properties of lightweight aggregate concrete with a high volume of entrained air. *Construction and Building Materials, 29*(0), 193-200. doi: http://dx.doi.org/10.1016/j.conbuildmat.2011.08.067

Kim, Y. J., Choi, Y. W., & Lachemi, M. (2010). Characteristics of self-consolidating concrete using two types of lightweight coarse aggregates. *24*(1), 11–16. doi: 10.1016/j.conbuildmat.2009.08.004

Kockal, N. U., & Ozturan, T. (2010). Effects of lightweight fly ash aggregate properties on the behavior of lightweight concretes. *179*(Issues 1–3), 954–965. doi: 10.1016/j.jhazmat.2010.03.098

Kockal, N. U., & Ozturan, T. (2011). Durability of lightweight concretes with lightweight fly ash aggregates. *25*(3), 1430–1438. doi: 10.1016/j.conbuildmat.2010.09.022

Kok-Seng, C., Chen-Chung, K., & Min-Hong, Z. (2005). Stability of Fresh Lightweight Aggregate Concrete under Vibration. *ACI Materials Journal, 102*(5), 347-347, https://doi.org/10.14359/14714.

Liu, Chia, K. S., & Zhang, M.-H. (2011). Water absorption, permeability, and resistance to chloride-ion penetration of lightweight aggregate concrete. *25*(1), 335–343. https://doi.org/10.1016/j.conbuildmat.2010.06.020

Liu, X., Chia, K. S., & Zhang, M.-H. (2011). Water absorption, permeability, and resistance to chloride-ion penetration of lightweight aggregate concrete. *25*(1), 335–343. doi: 10.1016/j.conbuildmat.2010.06.020

Liu, X. J., & Wang, Y. M. (2012). Mix Proportion Design and Basic Mechanical Properties Experiment of Self-Compacting Lightweight Concrete. *Advanced Materials Research, 450-451*, 329-333, https://doi.org/10.4028/www.scientific.net/AMR.450-451.329.

Lo, T. Y., & Cui, H. Z. (2004). Effect of porous lightweight aggregate on strength of concrete. *58*(6), 916–919. doi: 10.1016/j.matlet.2003.07.036

Lo, T. Y., Cui, H. Z., Tang, W. C., & Leung, W. M. (2008). The effect of aggregate absorption on pore area at interfacial zone of lightweight concrete. *22*(4), 623–628. doi: 10.1016/j.conbuildmat.2006.10.011

Lo, T. Y., Tang, W. C., & Cui, H. Z. (2007). The effects of aggregate properties on lightweight concrete. *42*(8), 3025–3029. doi: 10.1016/j.buildenv.2005.06.031

Maghsoudi, A. A., Mohamadpour, S., & Maghsoudi, M. (2011). Mix design and mechanical properties of self compacting lightweight concrete. *International Journal of Civil Engineering, Vol. 9*(3).

Nadesan, M. S., Dinakar, P., (2017) "Structural concrete using sintered fly ash lightweight aggregate: A review," Construction and Building Materials 154, 928–944, https://doi.org/10.1016/j.conbuildmat.2017.08.005.

Neville, A. M. (1995). *Properties of concrete* (4th and final ed.). Harlow: Longman Group.

Silva, L. M., Ribeiro, R. A., Labrincha, J. A., & Ferreira, V. M. (2010). Role of lightweight fillers on the properties of a mixed-binder mortar. *32*(1), 19–24. doi: 10.1016/j.cemconcomp.2009.07.003

Wang, H.-Y. (2009). Durability of self-consolidating lightweight aggregate concrete using dredged silt. *23*(6), 2332–2337. doi: 10.1016/j.conbuildmat.2008.11.006

Wasserman, R., & Bentur, A. (1996). Interfacial interactions in lightweight aggregate concretes and their influence on the concrete strength. *18*(1), 67–76. doi: 10.1016/0958-9465(96)00002-9

Wu, Z., Zhang, Y., Zheng, J., & Ding, Y. (2009). An experimental study on the workability of self-compacting lightweight concrete. *23*(5), 2087–2092. doi: 10.1016/j.conbuildmat.2008.08.023

Yang, K., Kim, G., Choi Y., (2014) "An initial trial mixture proportioning procedure for structural lightweight aggregate concrete," Construction and Building Materials 55, 431–439, https://doi.org/10.1016/j.conbuildmat.2013.11.108

Yasar, E., Atis, C. D., Kilic, A., & Gulsen, H. (2003). Strength properties of lightweight concrete made with basaltic pumice and fly ash. *57*(15), 2267–2270. doi: 10.1016/S0167-577X(03)00146-0

Yehia, S., Abudayyeh, O., Bhusan, B., Maurovich, M., & Zalt, A. (2009). Self-Consolidating Concrete Mixture with Local Materials: Proportioning and Evaluation. *Materials Science Research Journal, Volume 3*(Issue 1/2).

Prof. Sherif Yehia is a Professor of Civil Engineering and Co-developer of the newly conductive concrete application for deicing operations. His research interests include behavior of reinforced and prestressed concrete, sustainability, smart structures, composite structures, special concrete, infrastructure management systems and engineering database management and information technology. He has authored or co-authored more than 200 articles and technical reports published in internationally recognized journals / conference proceedings and holds 2 US patents.
Professor, Department of Civil Engineering, American University of Sharjah, P.O. Box 26666, Sharjah, United Arab Emirates, E-mail: syehia@aus.edu, Corresponding author

Sharef Farrag is a Postdoctoral Associate at Rutgers University. He obtained his Ph.D. in Civil and Environmental Engineering from Rutgers University in 2023. His research interests cover experimental and numerical evaluation of bridges. Specific areas of interest in his work include large-scale testing, accelerated structural testing, dynamic soil-structure interaction, finite element modeling, nondestructive evaluation, and development of sustainable concrete.
Postdoctoral Associate, Center for Advanced Infrastructure and Transportation (CAIT), Rutgers University, Piscataway, NJ, 08854 E-mail: sharef.farrag@rutgers.edu

RESEARCH RESULTS ON STRUCTURAL STRENGTHENING WITH FRP COMPOSITES – STATE OF THE ART FROM TIMIŞOARA

Tamás Nagy-György

Twenty-five years ago, no one could have expected that the use of Fiber Reinforced Polymer (FRP) composites in construction would be so widespread and so successful. It needed dedicated people like Prof. György L. Balázs, who saw the potential in this material, clearly understood the limits of these solutions, and devoted a lot of time to popularizing, improving, and implementing standards for secure applications. When we are discussing research related to the use of FRP in construction performed in Timişoara, two important personalities must be mentioned. The first is Prof. Balázs, who, starting from 1998, supported the development of FRP research in Timişoara with his advice and active participation by guiding the first BSc and MSc thesis and then taking part as an opponent in the first PhD defended in this field. The second person is Prof. Stoian Valeriu, a dedicated professor and excellent structural engineer who recognized the opportunities of the FRPs and trusted in this research direction. In the last 25 years, he has brought up a generation, conducting nine successfully defended PhD theses and several MSc theses in this domain. Congratulations to both! This paper briefly tries to summarize the main research results obtained in the field of structural application of FRP materials realized in the past two decades at the Politehnica University of Timişoara, Faculty of Civil Engineering.

Keywords: *strengthening, FRP composites, EBR, NSM, masonry, RC walls, slabs, dapped-end beam*

1. INTRODUCTION

The efficiency of FRP composites for structural applications has been proven and validated over the last two decades through several applications and research performed. This paper tries to review the research performed in this period at the Faculty of Civil Engineering, Politehnica University Timişoara, Romania.

The first documented application of FRP composites for structural strengthening in Romania was in 1978, after the major earthquake of 1977, for retrofitting reinforced concrete (RC) beams and walls with glass FRP (GFRP) fabrics (*Fig. 1*) (Balan et al., 1982).

In Timişoara, research in the field of structural use of different FRP systems was documented in 1983 as a part of the PhD thesis defended by Liana Bob in 1999, consisting of the use of GFRP materials in the form of externally bonded reinforcement (EBR) fabrics as well as near surface mounted (NSM) rebars for glulam beams (*Fig. 2*) (Bob, 1999).

After these studies, there was a longer break in this field until two theoretical studies were published in the frame of a Scientific Student Conferences (Nagy-György, 1999; Nagy-György, 2000), followed by a BSc thesis (Nagy-György, 1999) and then an MSc thesis (Nagy-György, 2001). All four of these last works were supervised and coordinated by Prof. Balázs and Prof. Stoian.

Beginning with 2002, a new era started regarding research in structural strengthening and retrofitting using FRP

Fig. 1: Post-earthquake retrofitting of RC beams and walls with GFRP fabrics - field application in 1978 (Balan et al., 1982)
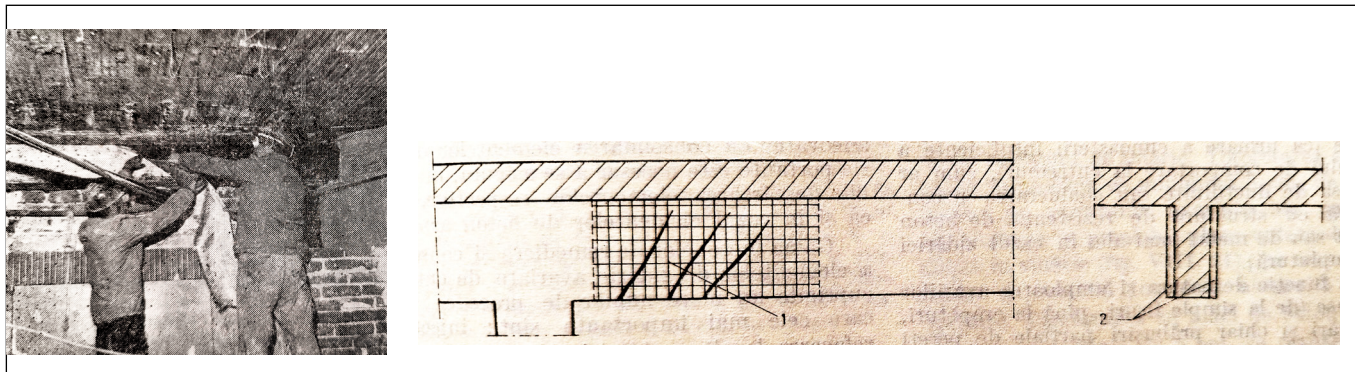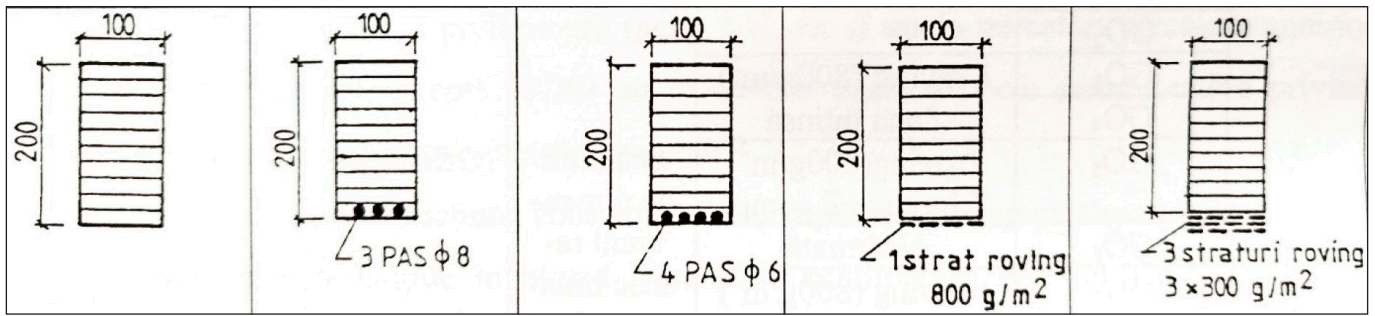
Fig. 2: *Strengthening of glulam timber beams with GFRP bars using NSM and EBR techniques (Bob, 1999)*

composites. In the following, the most important results will be presented.

2. SHEAR STRENGTHENING OF MASONRY WALLS

The objective of these studies (2000–2007) was to investigate the behaviour of the unreinforced clay brick masonry walls subjected to in-plane shear loads strengthened with different techniques (Nagy-György et al., 2010).

The considered retrofitting systems were different fibre reinforced polymer (FRP) composites, classical reinforced mortar jacketing (RMJ), and bidirectional steel wire meshes (SWM) applied with resins using the EBR technique. Based on the nonlinear numerical analysis results, an experimental program was conceived by realizing more than 20 specimens with 150 x 150 x 25 cm dimensions, tested in the setup presented in *Fig. 3*. The specimens were tested in as-built condition up to failure and then retrofitted and retested. The walls were subjected to a constant vertical force (V) and a monotonic increasing horizontal force (H), applied by an increment of 5 kN up to failure. The recorded data were the horizontal load, the horizontal and vertical displacement, the strain in the retrofitting systems, and the specimens' failure modes.

The correction and the injection mortars played an important role in restoring the load bearing capacity. The width of the initial crack is decisive in the evolution of the final capacity of the strengthened wall: when tight, the capacity increased significantly over the reference value; when wide, the ultimate load capacity was approximately equal or lower compared to the baseline values.

A considerable capacity increase was observed for the pre-cracked shear walls retrofitted with all systems (practically, the load bearing capacity of the cracked walls was negligible). The failure of the retrofitted walls was different in function of the system used.

In the case of FRP strengthened walls, the failure was caused by the extensive opening of the principal crack followed by FRP debonding and not due to tensile or shear failure of the FRP. It is necessary to mention that the vertically applied composites debonded just in the vicinity of the major crack, while those applied horizontally debonded in large areas, in the middle part, and even on the entire wall width. In this case, the use of anchorages could substantially increase the final capacity of the retrofitted wall.

In the case of RMJ strengthened walls, the failure was caused by cracking of the jacketing in tension, followed by debonding of the mortar jacket in the compressed corners, and finally through tensional failure of some horizontal steel bars of the mesh.
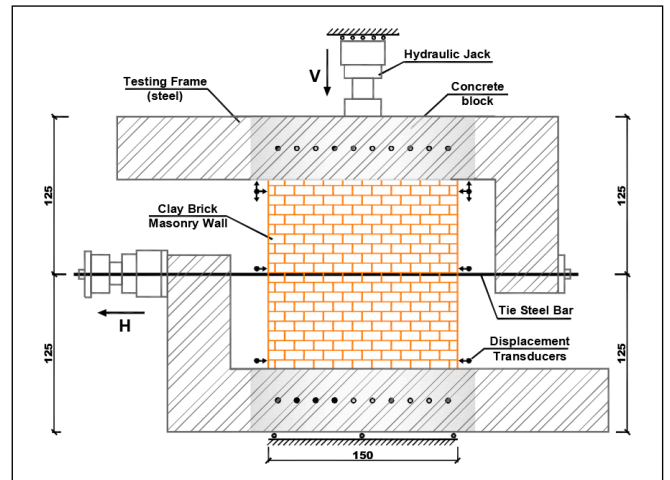
Fig. 3: *Setup for in-plane testing of masonry specimens (Nagy-György, 2004).*

In the case of SWM strengthened elements, the failure was produced by yielding and then by rupture of the horizontal and vertical wires along the diagonal principal crack, with small debonding near the crack.

The maximum horizontal displacements increased at least twice compared with the displacements of the reference specimens, which demonstrated an increase in the ductility and energy absorbing capacity of the retrofitted walls (*Fig. 4*).

The most advantageous strengthening system with respect to increasing load bearing capacity proved to be the SWM system, while the FRP system with the dry fiber application process proved to be the fastest application method. The cheapest system, considering the material and application costs, and at the same time the most efficient system, calculated from the ratio of the execution costs and the reached maximum loads, proved to be the RMJ system.

2. SHEAR STRENGTHENING OF RC WALLS WITH OPENINGS

2.1 RC walss with staggered openings

The objectives of this study were the experimental investigation of RC shear walls with staggered openings (Moșoarcă, 2004) as well as to assess the CFRP composites efficiency for seismic retrofit of these walls. There have been studied the behaviour of the strengthened elements, a specific anchorage detail, the strengthening system layout, the stiffness and ductility modifications, and the failure mechanism (Nagy-György et al., 2007).

There were tested five 1:4 scale cantilever type shear walls with staggered door openings, which were subjected to a constant vertical load V = 50 kN, while the horizontal load
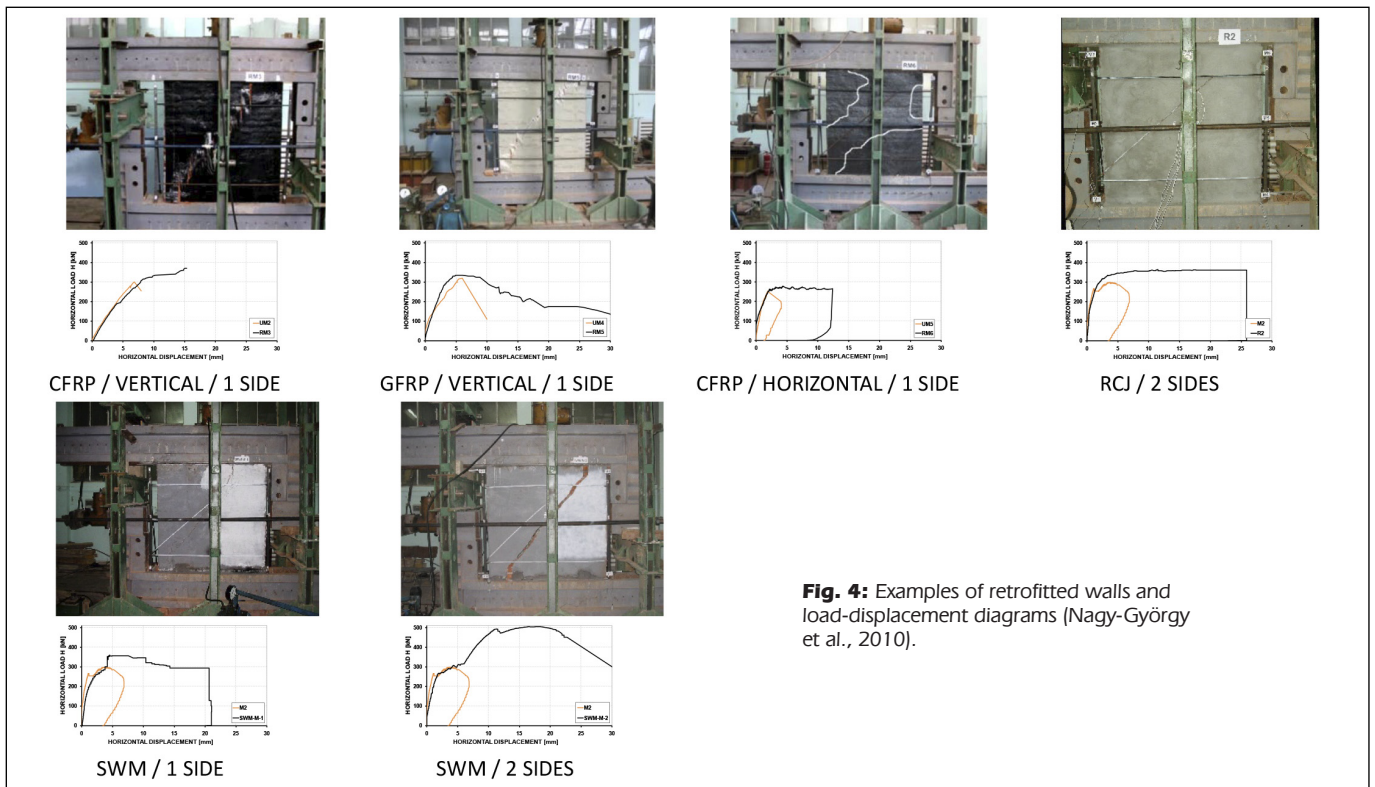
Fig. 4: Examples of retrofitted walls and load-displacement diagrams (Nagy-György et al., 2010).

(H) was applied monotonically for the wall without openings and cyclically for the rest of the elements in a displacement-controlled mode (*Fig. 5*). The top displacements were increased with an average drift.

In the next phase, the walls were retrofitted. The damaged or crushed parts of the elements were replaced with an epoxy-based repairing mortar, and the existing cracks were filled with an epoxy resin. All the walls have been strengthened with unidirectional CFRP composite fabric on one side using the EBR technique. There was developed an anchorage zone, which was proven to be very efficient, as later mentioned in fib Bulletin 90.

As conclusions, it was observed that the elastic limit of the walls increased on average by 47%, the failure load increased on average by 45%, the stiffness of the elements decreased on average by 53%, and the ductility of the elements decreased on average by 60%. The failure mode of all the specimens was similar: FRP debonding in compression (fiber buckling), followed by excessive crack openings and tensile or compression failure of FRPs.

2.2 RC walls with cut-out openinigs

The conceptual outline of the research was to investigate the seismic performance of the precast RC walls, considering the outrigger effect of adjacent structural members, assess the weakening effects caused by doorway cut-outs, and reveal the effects of the seismic retrofit by CFRP-EBR. It is important that the foregoing analysis can be achieved at three structural levels of complexity, namely for a structural element, a building system, or the entire building structure. The test program was structured at three levels. The first level is represented by a bare solid wall, which was the reference specimen. The second level included two bare walls with cut-out openings, which were identical in all aspects to the solid reference except for the presence of the cut-outs. The difference between the elements of this level was the width of the door opening. The third level is composed of two pairs of strengthened specimens, which corresponded in all regards to the second level walls and were additionally retrofitted. Besides the opening size, the difference between

Fig. 5: Test setup, crack pattern and retrofitting schemes of the specimens. Anchorage detail (Nagy-György et al., 2007).
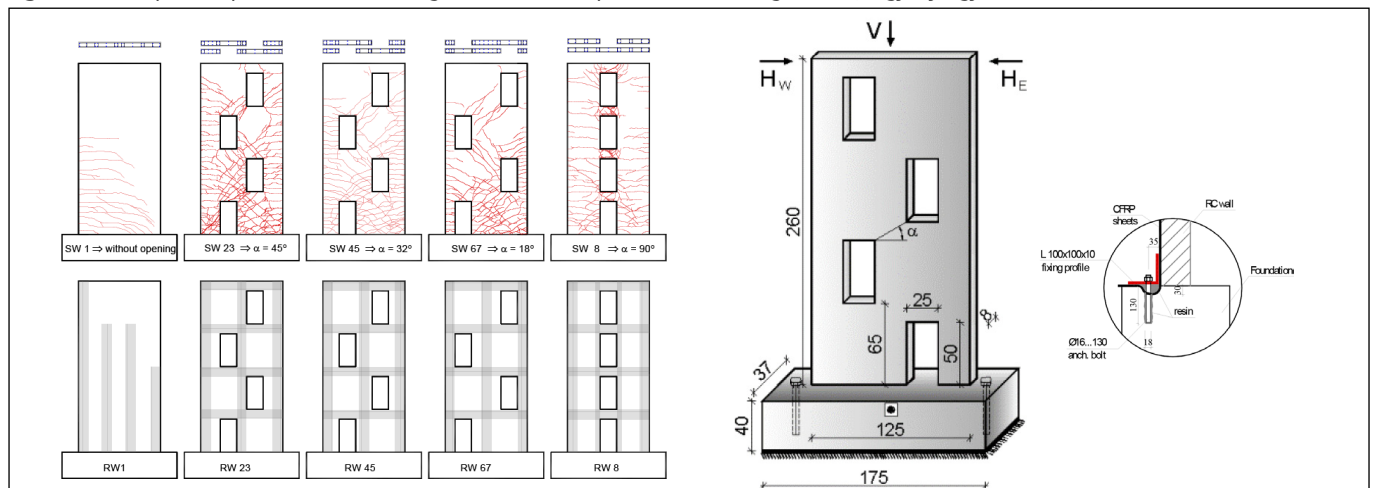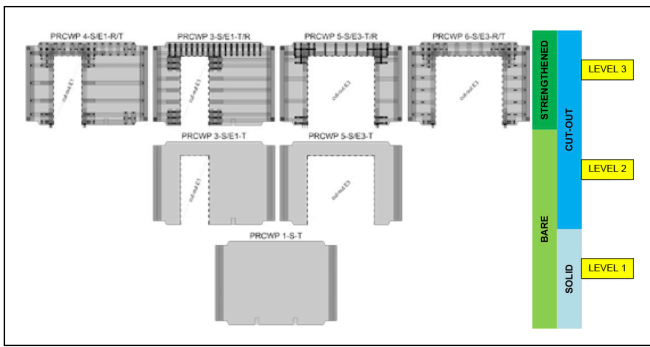
Fig. 6.a: *Variables of the experimental program (Demeter, 2011)*
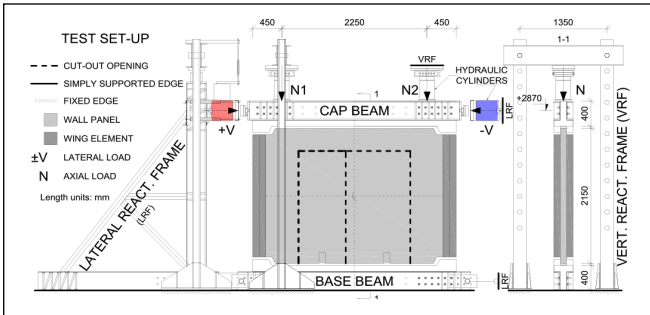
Fig. 6.b: *Test setup of the experimental program (Demeter, 2011)*

the specimens of the third level consisted of the state of the walls at the time of retrofitting: after sustaining a number of damaging load reversals, the specimens of the second level were upgraded to the third one by repair and post-damage strengthening, whereas their counterparts were prior-to-damage strengthened (Demeter, 2011).

In conclusion of the study, it was shown that in the given circumstances, the response of the RC wall panels is characterized by very high shear resistance and about a 10% energy dissipation ratio. The weakening effect of the cut-out opening was found to be in agreement with the predictions provided in the literature. Regarding the CFRP-EBR strengthening, the experimental results indicated that the energy dissipation capacity of the walls retrofitted by this
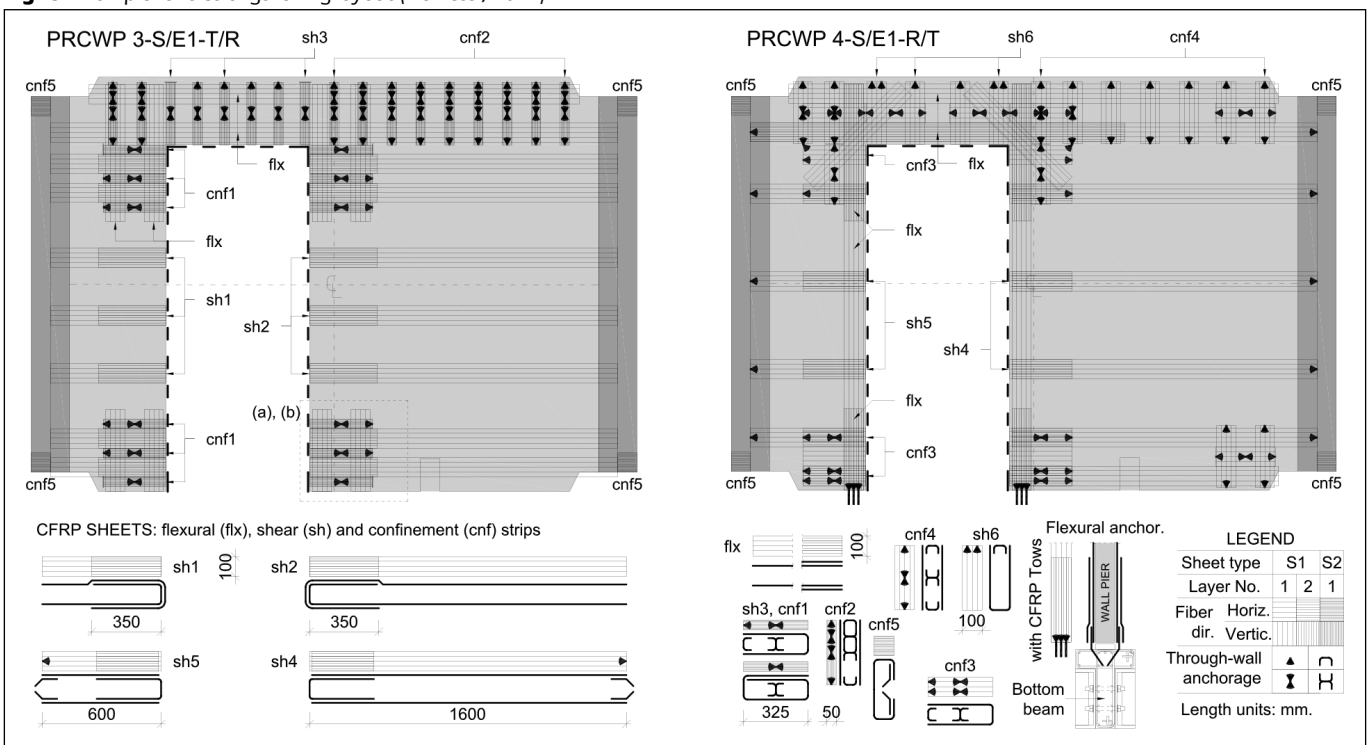
technique increased significantly, whereas the other response characteristics were influenced to a smaller degree. This improvement in seismic performance should be attributed primarily to the confinement and shear components of the strengthening system (*Fig. 6*). The flexural FRPs were found to be susceptible to premature failure; however, it is not clear whether this type of failure is triggered by concrete substrate deterioration, i.e. local spalling and crushing, or directly by the adverse loading conditions (tension-compression reversals).

3. PRECAST RC SLABS WITH CUT-OUT OPENINGS

The goal of the theoretical and experimental program was to assess the behaviour of RC slabs weakened by cut-out openings retrofitted with CFRP composites (*Fig. 7*). The experimental program consisted of tests on full scale two-way RC slabs. Two full slabs served as control specimens, while within the other four, various configurations of cut-outs were sawn in at a corner or along an edge. All specimens were tested in two stages, as follows: initially in as-built condition up to a level that would imply the need for retrofitting, and then a full failure test conducted after applying the strengthening solution. The applied strengthening technique was a mixed one, associating the use of both NSMR-FRP and EBR-FRP. By performing twelve tests, the effectiveness of the proposed technique was assessed. The results clearly prove that the proposed technique is viable, as the specimens' capacity can be very easily regained or increased by applying the specific strengthening or retrofitting system. The crack patterns of all tested elements show a greater concentration of cracks for the retrofitted elements in comparison with the reference bare elements, suggesting a more favorable behavior in terms of cracking and crack width opening. The proposed simplified analytical calculation approach was verified and was recommended to be applied as a fast design solution for this type of element (Floruț, 2011).

Fig. 6: *Example for a strengthening layout (Demeter, 2011)*
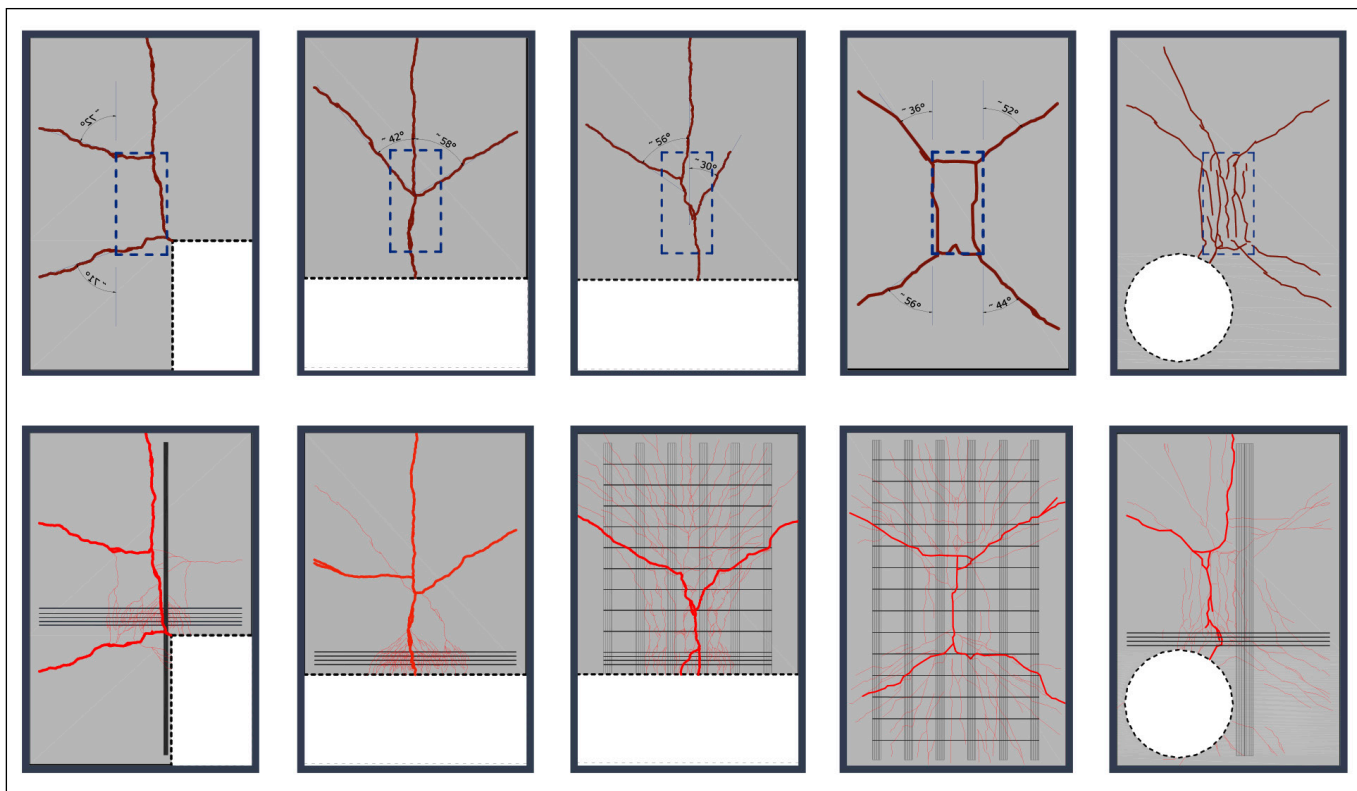
Fig. 7: *Crack patterns for un-strengthened and strengthened slabs (Florut, 2011)*

4. DAPPED-END BEAMS

In the first phase of this study, an experimental and numerical assessment of the effectiveness of strengthening dapped-end RC beams using EBR CFRPs was performed (*Figs. 8 and 9*). The research was based on a real application in which the dapped-ends of several precast prestressed beams developed diagonal cracks due to errors during assembly. Hence, the dapped-ends were strengthened on-site using CFRP plates to limit further crack opening. In the empirical phase of the study, four similar specimens were tested: one unstrengthened reference specimen, two strengthened with high-strength CFRP plates, and one with high-modulus CFRP sheets. The specimens strengthened with plates had slightly higher load carrying capacity than the reference element but failed by debonding, while the specimens strengthened with sheets showed no increase of capacity and failed by the fibers rupturing. Nonlinear finite element analysis of the specimens under the test conditions indicated that: (a) debonding is more likely to occur at the inner end of dapped-ends and (b) the capacity could have been increased by up to 20% if the plates had been mechanically anchored (Nagy-György et al., 2012).

In the second phase, a parametric investigation based on non-linear finite element modeling was performed to identify the most effective configuration of CFRP strengthening for dapped-end beams. There were 24 EBR and NSM configurations compared, assessing the yield strain in steel and the capacity and failure mode of dapped-end beams. The investigated parameters were the mechanical properties of the CFRP, the strengthening procedure, and the inclination of the fibers with respect to the longitudinal axis. Two failure scenarios were considered: rupture and debonding of the FRP. The results indicate that high-strength NSM FRPs can considerably increase the capacity of dapped-end beams, and the yielding strains in reinforcement can be substantially reduced by using high modulus fibers (Sas et al., 2014).

5. CONCLUSIONS

The research results listed above clearly indicate how much potential there is in the use of FRP composite materials for structural strengthening and retrofitting of RC and masonry elements. All the presented solutions demonstrated their effectiveness, and they were applied in real case studies. Due to space limitations, it is not possible to discuss other research program results, such as the superstition effect of NSM steel rebars with EBR-FRP confinement, several anchorage systems developed for EBR-FRPs, and the efficiency of EBR-FRP systems for strengthening precast and hollow core slabs. But it must be noted that all these studies are the results of the support of Prof. Balázs in the initial stages of the research, as well as of Prof. Stoian's continued and selfless dedication (*Figs.10 and 11*).

6. REFERENCES

Balan St., Cristescu V. and Cornea I., (coordinators), The 1977 March 4 Earthquake in Romania (in Romanian), Editura Academiei, Bucharest, 1982.

Bob L., Contributions regarding the use of composite elements for the realization of structures, PhD thesis, 1999.

Demeter I., Seismic retrofit of precast RC walls by externally bonded CFRP composites, PhD Thesis, Politehnica Publishing House, Timișoara, Romania (2011)

Floruț C., Nagy-György T., Stoian V., Tests on reinforced concrete slabs with openings retrofitted using carbon fibre reinforced polymers, FRPRCS-12 & APFIS-2015 Joint Conference, 14-16 December 2015, Nanjing, China, ISBN xxx, pg x

Floruț S. C., Performance study of elements strengthened with FRP composite materials subjected to flexure, PhD Thesis, Ed. Politehnica, Timisoara 2011.

Moșoarcă M. (2004), Contributions in design and detailing of reinforced concrete structural walls, Ph.D. Thesis, Politehnica University of Timișoara, Romania, 2004

Nagy-György T., Structural retrofitting an existing precast RC slab usinf CFRP composites, Scientific Student Conference – Timișoara, May, 1999

Nagy-György T., Attic construction using different structural materials by retrofitting the existing structure, BSc thesis, Politehnica Univeristy Timișoara, June, 1999
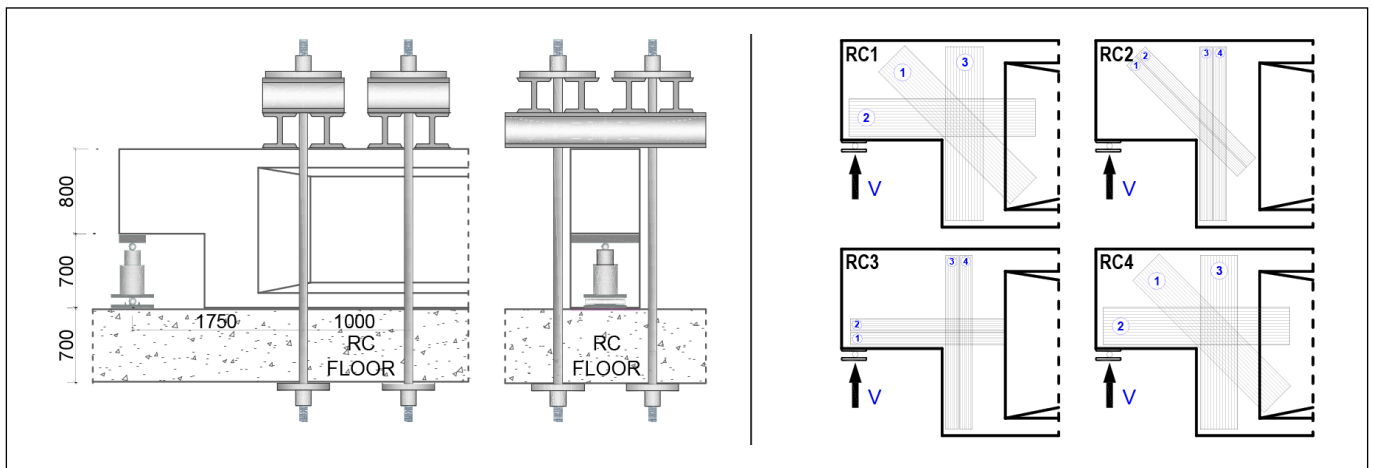
Fig. 8: *Test setup and the experimentally tested strengthening systems (Nagy-György et al., 2012).*
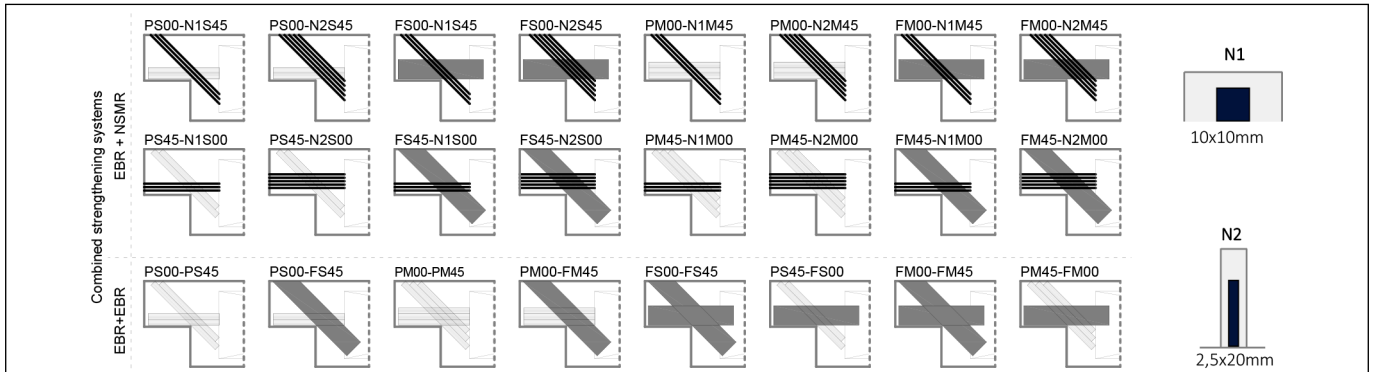
Fig. 9: *Schematic presentation of the combined strengthening solutions from the numerical optimization (S – high strength, M – high modulus, 00 – 45 angles, N1, N2 – NSMR types) (Sas et al., 2014)*

Fig. 10: *Snapshot after the author´s PhD defense in 2004 (from left to right: Assoc. Prof. János Gergely - UNC Charlotte, the author, Prof. Valeriu Stoian– Politehnica University Timișoara, Prof. Radu Pascu – Technical University of Civil Engineering Bucharest, Prof. Corneliu Bob - Politehnica University Timișoara, Prof. György L. Balázs - Budapest University of Technology and Economics)*

Fig. 11: *Prof. Balázs in Timisoara in 2016, after the habilitation thesis defense of the author (in front of the largest span bridge in the world in 1909 with RC beams, designed by Prof. Mihailich Győző)*

Nagy-György T., Strengthening RC structural element using FRP composites, Scientific Student Conference – Timișoara, May, 2000

Nagy-György T., Strengthening RC Beams for Bending and Shear Using FRP Composite Materials, MSc thesis, Politehnica Univeristy Timișoara, June, 2001

Nagy-György T., Using FRP Composite Materials for Strengthening Brick Masonry and Reinforced Concrete Elements, Ph.D. Thesis, Politehnica University of Timișoara, Romania, 2004

Nagy-György T., Stoian V., Dan D., Dăescu C., Diaconu D., Sas G., Moşoarcă M., Research Results on RC Walls and Dapped Beam Ends Strengthened with FRP Composites, FRPRCS-8, Patras, Greece, July 16-18, 2007, ISBN 978-960-89691-0-0, pp.320-322 (+8pg)

Nagy-György T., Stoian V., Dan D., Strength and Economic Assessment of Different Retrofitting Methods for Shear Deficient Masonry Walls of Heritage Structures, Third International Workshop on Civil Structural Health Monitoring (CSHM-3), Ottawa, Canada, 2010, ISBN 978-0-88865-883-8, pp 161-172

Nagy-György T., Sas G., Dăescu C., Barros J.A.O., Stoian V., Experimental and numerical assessment of the effectiveness of FRP-based strengthening configurations for dapped-end RC beams, Engineering Structures 44 (2012) 291-303, ISSN: 0141-0296. https://doi.org/10.1016/j.engstruct.2012.06.006

Nagy-György T., Demeter I., Dan D., Retrofitting Strategies of RC Wall Panels with Cut-Out Openings Using CFRP Composites, 12th International Conference on Steel, Space and Composite Structures, 28-30 May 2014, Prague, Czech Republic, ISBN 978-981090077-9, pp 267-273

Sas G., Dăescu C., Popescu C., Nagy-György T., Numerical optimization of strengthening disturbed regions of dapped-end beams using NSM and EBR CFRP, Composites Part B: Engineering 67 (2014), 381-390, ISSN: 1359-8368. https://doi.org/10.1016/j.compositesb.2014.07.013

Tamás Nagy-György (1976), Civil Engineer, PhD, habil., Professor at the Department of Civile Engineering of Politehnica University Timișoara, Romania. His main fields of activities are the theoretical and experimental investigation of RC structures, design and strengthening of structures using advanced materials and techniques. Member of *fib* and ACI. E-mail: tamas.nagygyorgy@ct.upt.ro

NATIONAL EXPOSURE CLASSES OF CONCRETE IN HUNGARY

Tibor Kausay

Sufficient durability of concrete and reinforced concrete structures is always required, mainly if it is exposed to extraordinary (severe) environmental attack - much over the well-known classes in European Standard for Concrete EN 206. In this case, appropriate concrete composition (e.g. special binders, etc.), strength, low porosity and sufficient concrete cover are required to withstand these special environmental exposures. The present paper deals with the additional exposure classes for these severe cases added to the Hungarian Standard MSZ 4798, which is the national version of EN 206. Maybe CEN could also use and add some of these "X-new" classes in the following version of the standard EN 206.

Keywords: chemical attack, abrasion, water head, concrete corrosion, concrete exposure class

1. INTRODUCTION

Hungary has been a full member of CEN (Comité Européen de Normalisation) since 1 January 2003 and has to introduce the European standards EN (Normes Européennes) with unchanged content within six months of publication. (The MSZ designation is derived from the "Hungarian Standard" initials.) For example, the Hungarian version of the European concrete standard EN 206 is marked MSZ EN 206, and the Hungarian national application document (NAD) of the standard MSZ EN 206 is marked MSZ 4798.

In the Hungarian standard MSZ 4798, the exposure classes of concrete are given special attention. N*ew Hungarian exposure classes* have been introduced, which represent the extension and supplementation of the exposure classes of EN 206. The sign for the new Hungarian exposure classes contains in parenthesis the internationally approved country sign (H) of Hungary, for example:

- sign of the Hungarian exposure class of concrete with a subordinate role: XN(H);
- sign of the Hungarian exposure class of concrete not exposed to harmful environmental effects: N0b(H);
- the symbol of the Hungarian exposure class X0v(H) means a slightly reinforced concrete that will not be exposed to any adverse environmental effects other than carbonation;
- sign of the Hungarian exposure class of concrete exposed to freeze-thaw: XF2(H) – XF4(H) *without entrained air* ("air bubbles);
- sign of the Hungarian exposure class of concrete exposed to chemical corrosion by aggressive rainwater, wastewater, liquids, condensation water and vapours: XA4(H) – XA6(H);
- sign of the Hungarian exposure subclass of concrete in the ground, in wet environments but not exposed to water pressure: XV1(H)/V0;
- sign of the Hungarian exposure class of concrete exposed to water pressure: XV1(H) – XV3(H);
- sign of the Hungarian exposure class of concrete exposed to abrasion (wear): XK1(H) – XK4(H).

Annex F of the standard MSZ 4798 (similar to EN 206) containing the limit values of concrete compositions belonging to the exposure classes (together with the amendments, e.g.: MSZ 4798:2016/2M:2018 and MSZ 4798:2016/4M:2023) are requirements, which must be complied with.

2. HUNGARIAN EXPOSURE CLASSES FOR NO RISK OF CORROSION OR ATTACK

If the concrete of subordinate strength, such as a base concrete, concrete base layer, cement stabilisation, etc., is not exposed to an adverse environmental impact, the concrete shall be classified in exposure class XN(H).

Concrete of higher strength, such as base concrete, backing and backing concrete, hand-held masonry concrete units, etc., which are not adversely affected by the environment, are classified in exposure class X0b(H).

Concrete of slightly reinforced concrete structures, such as demarcated concrete, etc., may be classified in exposure class X0v(H) if the concrete is not exposed to any adverse environmental effects other than carbonation. A slightly reinforced concrete structure shall be considered as one in which the total cross-sectional area of the steel - that can be taken into account in verifying compliance with the load-bearing requirements - is less than the minimum required for the dimensioning and/or construction of load-bearing reinforced concrete structures.

Concrete classified in exposure classes XN(H), X0b(H) and X0v(H) shall have a composition in accordance with *Table 1*.

3. HUNGARIAN SUPPLEMENT TO THE EXPOSURE CLASSES FOR RISK OF CORROSION INDUCED BY CHLORIDES

Concrete of reinforced concrete or prestressed concrete structures in contact with aggressive water (groundwater, other natural water, sewage or other aggressive liquids) shall

Table 1: *Limits for concrete composition in case of no risk or effect of corrosion*

Requirements	Hungarian exposure classes		
	XN(H)	X0b(H)	X0v(H)
Maximum water/cement ratio	0.90	0.75	0.70
Minimum strength class	C8/10	C12/15	C16/20
Minimum cement content, kg/m³	165	230	250
Planned air content of fresh concrete	*See Table 6*		

be classified as exposure class XD2 only if the chloride ion content (Cl⁻) of the aggressive water is more than 500 mg/litre.

Concrete exposed to both frost and deicing agents shall be classified in one of the exposure classes XF2, XF2(H), XF4 or XF4(H) instead of the exposure class XD.

4. HUNGARIAN EXPOSURE CLASSES FOR RISK OF FREEZE/THAW ATTACK

According to Table F.1 of European Standard EN 206, concrete of exposure classes XF2, XF3 and XF4 exposed to freezing shall be made of fresh concrete with an air content of at least 4.0% by volume, which means that concrete of exposure classes XF2, XF3 and XF4 shall be made of air-entrained concrete with an air-entraining admixture ("air bubbles").

In Hungary, concrete exposed to frost and a deicing agent is allowed to be made *without air-entraining* admixture if it is *not made for road or airport pavement*. Such concrete without artificial air bubbles shall be classified in accordance with standard MSZ 4798 as XF2(H), XF3(H) and XF4(H).

In exposure class XF2(H) (characterised by moderate water saturation, with a deicing agent), infrastructural constructions (e.g. bridges, roads), other monolithic structures and precast concrete products with a vertical or steeper surface than 5%, made *without air entraining agent*, are classified as XF2(H), if they are exposed to frost and saltwater spray.

In exposure class XF3(H) (characterised by high water saturation, without deicing agent), infrastructural constructions (e.g. bridges, roads), other monolithic structures and precast concrete products with a horizontal or a maximum slope of 5%, made *without air entraining agent*, are classified as XF3(H) if they are exposed to frost and water.

In exposure class XF4(H) (characterised by high water saturation, with deicing agent), infrastructural constructions

(e.g. bridges, roads), other monolithic structures and precast concrete products with a horizontal or a maximum slope of 5%, made *without air entraining agent*, are classified as XF4(H) if they are exposed to frost, precipitation and salt.

The inclination angle of the 5% elevation or inclination surface is arctg (0.05) ~ 2.86°.

The composition requirements for concrete classified in exposure classes XF2(H), XF3(H) and XF4(H) are *given in Table 2*.

Concrete with a horizontal slope and not more than 10 metres from the traffic surface or with a slope of not more than 5%, exposed to water splashing from a traffic surface or to water spray from the traffic surface, shall be classified in exposure class XF3 or XF3(H).

If the water or the water spray contains salt, the concrete with a horizontal surface or a slope of not more than 5% and not farer than 10 m from the traffic surface is classified in exposure class XF4 or XF4(H).

Concrete of exposure classes XF2, XF3 and XF4 may be made with silica fume only if the water/binder ratio is less than or equal to 0.37 and the set of such concrete is not delayed by a two-effect admixture.

The frost resistance and the frost and melting salt resistance of all XF and XF(H) exposure classes of concrete shall be carried out by slab test method (reference method) or with cube test method or CD/CDF test method in accordance with CEN/TS 12390-9 technical specification. The test procedures are given in *Table 3,* and the specifications for the permissible amount of scaled-down material are given in *Table 4*.

The Hungarian requirements for the air-bubble structure of hardened frost- and deicing agent resistant concrete made with air entraining admixture are *given in Table 5*.

Table 2: *Limits for the composition of frost resistant and frost – and salt resistant concrete made without air entraining agent*

Requirements	Hungarian exposure classes		
	XF2(H)	XF3(H)	XF4(H)
Maximum water/cement ratio	0.50	0.45	0.40
Minimum strength class	C35/45	C40/50	C40/50
Minimum cement content, kg/m³	320	340	360
Planned air content of fresh concrete	*See Table 6*		
Other requirements	The use of these exposure classes is prohibited for road and airport pavements. The aggregate for concrete shall be frost- and melting salt-resistant.		

Table 3: *Conditions for the performance of the concrete CEN/TS 12390-9 Technical Specification frost resistance and frost and deicing salt resistance test applied in Hungary*

Frost resistance test
XF1 exposure class concrete
The frost resistance test may be omitted upon agreement if the concrete composition meets the requirements of exposure class XF1.
XF3 exposure class concrete
The concrete shall comply with the freeze resistance requirement for concrete of exposure class XF3 according to one of the test methods in *Table 4*. The frost resistance test may be omitted upon agreement if the hardened concrete air bubble structure meets the requirements of *Table 5*.
XF3 exposure class concrete
The concrete shall comply with the freeze resistance requirement for concrete of exposure class XF3 according to one of the test methods in *Table 4*.
Resistance to freezing and deicing salt test
XF2 exposure class concrete
The concrete shall comply with the freeze and deicing agent resistance requirements for exposure class XF2 according to one of the test methods in *Table 4*. The frost and melting salt resistance test may be omitted upon agreement if the hardened concrete air bubble structure meets the requirements of *Table 5*.
XF2(H) exposure class concrete
The concrete shall comply with the freeze and deicing agent resistance requirement for concrete of exposure class XF2(H) according to one of the test methods in *Table 4*.
XF4 exposure class concrete
The concrete shall comply with the freeze and deicing agent resistance requirement for concrete of exposure class XF4 according to one of the test methods in *Table 4*. Upon agreement, the frost and deicing salt resistance test can be omitted if the air void indices (bubble) structure of the hardened concrete meets the requirements of *Table 5*.
XF4(H) exposure class concrete
The concrete shall comply with the freeze and deicing agent resistance requirement for concrete of exposure class XF2(H) according to one of the test methods in *Table 4*. The water tightness of hardened concrete shall also be checked in accordance with EN 12390-8, and the maximum individual water penetration value shall not exceed 20 mm as determined from at least 3 test specimens.

5. HUNGARIAN ADDITIONS TO THE REQUIREMENTS FOR THE FRESH CONCRETE AIR CONTENT AND THE AIR VOID (BUBBLE) STRUCTURE OF THE HARDENED CONCRETE

In Table F.1 of European Standard EN 206, a minimum air content of 4.0% by volume for concrete of environmental classes XF2, XF3 and XF4 is demanded, though it is not cleared up in the standard, whether the sum of the air-pore (entrapped air) content and the air-bubble (entrained air) content of fresh concrete is given. The latter is measured by the compression method. These figures may be very small in some cases, but in the absence of other more accurate data, it is suitable for use in the first approximation to design the approximate composition of frost and deicing agent resistant fresh concrete with the above ones.

In Hungary, the composers of the standard MSZ 4798 clarified the air content of fresh concrete made *without air entraining agent* (*Table 6*) and *the total air content* of fresh concrete made *with air entraining agent* (*Table 7*).

6. HUNGARIAN EXPOSURE CLASSES IN RISK OF CHEMICAL ATTACK

In Table 1 and Table F.1 of European Standard EN 206, concrete is supposed to be exposed only to chemical corrosion by soil and natural groundwater and is classified for these hazards in environmental classes XA1, XA2 and XA3. In the Hungarian standard MSZ 4798, the conditions for the classification of concrete in contact with aggressive rainwater, municipal water, industrial and agricultural wastewater, condensation water and other aggressive liquids, gases, vapours, sprays and fermentation materials are defined as XA4(H), XA5(H) and XA6(H).

CLASSIFIED IN EXPOSURE CLASS **XA4(H)**:
a) concretes in contact with *slightly* aggressive liquids, which can be discharged into the public sewer,

Table 4: *Requirements for the concrete CEN/TS 12390-9 technical specification frost resistance and frost and melting salt resistance test applied in Hungary.*

	Frost resistance test	Resistance to freezing and melting salt test
Slab test method		
Freezing liquid	3 mm deep deionised water	3 mm deep 3% NaCl solution
Maximum permissible mass of exfoliated material, g/m²	XF1 class	XF2 and XF2(H) class
	average: 1500, single value: 2000	
	XF3 and XF3(H) class	XF4 and XF4(H) class
	average: 1000, single value: 1350	
Cube test method		
Freezing liquid	Deionised water covering the test specimen at a height of 25 ± 5 mm	3% NaCl solution covering the test specimen at a height of 25 ± 5 mm
Maximum permissible mass of exfoliated material, % w/w	XF1 class	XF2 and XF2(H) class
	average: 6.5, single value: 7.5	
	XF3 and XF3(H) class	XF4 and XF4(H) class
	average: 4.0, single value: 5.0	
CD/CDF test method		
Freezing liquid	10 mm deep deionised water	10 mm deep 3% NaCl solution
Maximum permissible mass of scaled down material, g/m²	XF1 class	XF2 and XF2(H) class
	average: 1500, single value: 2000	
	XF3 and XF3(H) class	XF4 and XF4(H) class
	average: 1000, single value: 1350	

Table 5: *Requirements for the air bubble structure of hardened, frost and deicing agent resistant concrete made with air-entraining admixture in Hungary*

Exposure class	XF2 and XF3	XF4
Spacing factor, max. mm,	0.22	0.18
Amount of air bubbles (effective) with nominal diameter less than 0.3 mm, min. V%	1.2	2.2
Note: The spacing factor of hardened concrete with air bubbles and the amount of effective air bubble volume shall be measured in accordance with EN 480-11.		

Table 6: *Planned air content of fresh concrete to be made without air entraining agent in Hungary*

Consistency	Slump classes	—	S1	S2, S3	S4, S5
	Compaction classes	C1	C2	C3	C4
	Flow classes	F1	F2	F3	F4, F5, F6
Compressive strength class		Planned fresh concrete air content, up to, % V/V			
C8/10		5.0	4.0	3.0	2.0
C12/15		4.0	3.0	2.0	1.5
C16/20		3.5	2.5	1.5	1.0
C20/25		3.0	2.0	1.0	1.0
C25/30		2.0	1.5	1.0	1.0
C30/37		1.5	1.0	1.0	1.0
C35/45 – C100/115		1.0	1.0	1.0	1.0

In the case of prestressed concrete, the air content of fresh concrete should be 20% lower than the above volumetric values if the volume is ≥ 1.5 V%.

In the case of concrete with crushed stone aggregate, the fresh concrete may have an air content 25V% higher than the above-listed values - excluding the exposure classes XK2(H), XK3(H) and XK4(H), planned for abrasion-resistant concretes.

Table 7: *Planned total air (air-pore + air-bubble) content of fresh concrete in Hungary made with air-entraining agent*

Exposure class	XF2 and XF3	XF4
Maximum size of the aggregate, mm	Total fresh concrete air (air-pore content + air-bubble content), % Vol	
8 and 12	4.0 – 6.0	6.0 – 10.0
16	3.0 – 5.0	4.5 – 8.5
24 and 32	2.5 – 5.0	4.0 – 8.0
63	2.0 – 4.0	3.0 – 7.0
In the case of prestressed concrete, the air content of fresh concrete should be 20% lower than the above values if its volume is ≥ 1.5 V%.		
In the case of concrete with crushed stone aggregate, the fresh concrete may have an air content 25% higher than the above values, excluding the exposure classes XK2(H), XK3(H) and XK4(H), planned for abrasion-resistant concretes.		

- such concrete is, e.g. that of the tertiary (physicochemical) treatment structures of the *newly established* wastewater treatment plants, regardless of the chemical characteristics, according to *Table 8*.
- if the *existing structure is in contact with slightly aggressive* liquids and *renovated or enlarged*, the new concrete shall be classified in the environmental class according to *Table 8*.

b) and concretes near *slightly* aggressive waters and liquids, gases, vapours, sprays, and fermenting substances. Concrete of rainwater storage structures, etc. - in contact with slightly aggressive chemicals - shall be classified in the environmental class according to *Table 8*.

Acid rains act intermittently, it is generally sufficient to classify the concrete as XA4(H).

CLASSIFIED IN EXPOSURE CLASS **XA5(H)**:

a) concretes in contact *with moderately* aggressive liquids, which can be discharged into the public sewer,
- Such are the *newly established* sewers, shafts, public area pumping stations and primary (mechanical and secondary, biological treatment structures of the wastewater treatment plant, as well as the concrete of the wastewater sludge treatment structures, regardless of the chemical characteristics according to *Table 8*.
- If the *existing structure in contact with moderately aggressive* liquids is renovated or enlarged, the new concrete shall be classified in the environmental class according to *Table 8*.

b) and concretes in the vicinity of *moderately aggressive* waters and liquids, gases, vapours, sprays, and fermenting substances. Concrete of other concretes, slurry storage and treatment pools, stall floors, leachate storage pools, crops storage facilities, chimney wreaths, etc., in contact with moderately aggressive chemicals shall be classified in the environmental class according to *Table 8*.

CLASSIFIED IN EXPOSURE CLASS **XA6(H)**:

a) concretes in contact with *highly aggressive* liquids which *cannot* be discharged into the public sewer,
- Such are the *newly established sewers,* shafts, pumping stations and wastewater treatment plant structures, regardless of the chemical characteristics, according to *Table 8*.
- If the *existing structure in contact with highly aggressive* liquids is renovated or expanded, the new concrete shall be classified in the environmental class according to *Table 8*.

b) and concretes in the vicinity of *highly aggressive* waters

and liquids, gases, vapours, sprays, and fermenting substances. Concrete of other concretes, cooling towers with or without flue gas discharge, animal feeding troughs, feed silos, agricultural fermentation silos, wood drying halls, railway car wash facilities, hazardous waste storage facilities, etc., in contact with highly aggressive chemicals shall be classified in the environmental class, according to *Table 8*.

The limit values for the chemical characteristics of the exposure classes XA4(H), XA5(H) and XA6(H) are *given in Table 8*.

The composition requirements for XA4(H), XA5(H) and XA6(H) exposure classes are *given in Table 9*.

7. DETERMINATION OF SULPHATE CONTENT

The sulphate ion (SO_4^{2-})-content of soil and groundwater for the classification of concrete as XA1, XA2 and XA3 and of the wastewater and other aggressive waters and liquids for the classification of concrete as XA4(H), XA5(H) and XA6(H) shall be determined by the test method in accordance with EN 206 and MSZ 4798, respectively, in accordance with the test method in accordance with EN 196-2.

In our case, the sulphate content is determined not on cement but on concrete corrosive materials. Some steps of the test method according to EN 196-2 cement test standard should be regulated accordingly.

7.1. Determination of sulphate content of soils

7.1.1 Determination of sulphate content of soils by hydrochloric acid process

For the classification of concrete in environmental classes XA1, XA2 and XA3, the soil sample of at least 2 kg taken from the soil to be tested shall be reduced to 250 g by quartering step by step. This part shall be dried at a temperature of 110 ± 5 °C and then chopped to a grain size of less than 0,5 mm. For the test, 50 g of dried, shredded soil sample is used, which is allowed to stand for 24 hours when poured with 150 ml of distilled water. The next day, the soil sample poured over with distilled water shall be shaken for 1 hour on a shaker, filtered into a 250 ml volumetric flask and washed with additional distilled water until a volume of 250 ml has been reached. If the filtrate is cloudy, it should be settled by centrifugation, and a clear portion of the solution should be used for further testing.

Table 8: *Limits for exposure classes for chemical corrosion by waste waters and other aggressive waters, liquids, gases, vapours, sprays and fermenting substances*

Chemical Characteristic	Test method	Hungarian exposure classes		
		XA4(H)	XA5(H)	XA6(H)
pH Value. Acid attack corrosion. In the case of sulfuric acid corrosion, additional sulphate attack corrosion, too	EN ISO 10523 (Reference method) EN 15933 MSZ 260-4 MSZ 1484-22	≤ 6.5 and ≥ 5.0	< 5.0 and ≥ 4.0	< 4.0 and ≥ 3.5
Water hardness. Acid attack corrosion	MSZ 448-21	≥ 3 and ≤ 7 °dh or ≥ 0.54 and ≤ 1.25 mmol/litre of soft water	< 3 °dh or < 0.54 mmol/litre of very soft water	
Aggressive carbon dioxide (CO_2) dissolved in water, mg/litre. Acid attack corrosion	EN 13577 (Reference method) MSZ 448-23	≥ 15 and ≤ 40	> 40 and ≤ 100	> 100
Magnesium ion (Mg^{2+}), mg/litre. Acid attack corrosion	EN ISO 7980 (Reference method) EN ISO 14911 MSZ 260-52 MSZ 1484-3	≥ 100 and ≤ 1000	> 1000 and ≤ 2500	> 2500
Ammonium ion (NH_4^+), mg/litre. Acid attack corrosion	ISO 7150-1 (Reference method) EN ISO 14911 MSZ 260-9	≥ 15 and ≤ 30	> 30 and ≤60 / In the case of sewage: / > 30 and ≤ 100	>60 / / > 100
SO_4^{2-}content, mg/litre. Sulphate attack corrosion	EN 196-2	≥ 200 and ≤ 600	> 600 and ≤ 1500	> 1500
***Additional requirements for new concrete for existing structures**, for structures to be renovated or enlarged, exposed to aggressive liquids causing chemical corrosion*				
The ratio of dichroic chemical oxygen demand (DCOD) and 5-day biochemical oxygen demand (BOD5), DCOD/BOD5. Acid attack corrosion	DCOD, for mg/litre: ISO 6060 BOD5, for mg/litre: EN ISO 5815-1, EN 1899-2	≥ 4	< 4.0 and ≥ 2.5	< 2.5
Oxidation-reduction potential (ORP), mV. Acid attack corrosion	ASTM D1498-14	≤ -50 and ≥ -100	< -100 and ≥ -150	< -150

Table 9: *Limits for the composition of concretes exposed to corrosion by waste waters and other aggressive waters, liquids, gases, vapours, sprays and fermenting substances*

Requirements for the addition of a type II supplement	Hungarian exposure classes		
	XA4(H)	XA5(H)	XA6(H)
Maximum water/(effective binder) ratio	0.45	0.43	0.40
Minimum strength class	C30/37	C30/37	C35/45
Cement content, kg/m³	320-365	330-380	345-395
Planned air content of fresh concrete	*See Table 6*		
Maximum depth of water penetration tested in accordance with EN 12390-8, mm	average: 20, single value: 22		

For the gravimetric determination of sulphate ions according to EN 196-2 paragraph 4.4.2.2, 100 ml of this filtrate shall be measured, the hydrogen ion concentration of which shall be adjusted to pH = 1.0-1.5 with 1+11 dilution hydrochloric acid (HCl). The sulphate ions produced when the sample is excavated with hydrochloric acid are separated with barium chloride ($BaCl_2$-) solution at pH 1.0-1.5, as described in EN 196-2. Wash the separated and fine pore-

filtered solution with boiling water to a chloride-free state and heat to constant weight at 950 ± 25 ºC. The mass of the barium sulphate thus obtained ($m_{\text{bariumsulphate}}$) multiplied by 0.343 is the mass of SO_3 (sulphur trioxide), from which the *sulphite* content of the soil, expressed as SO_3, is calculated as a percentage by the following equation:

$$SO_3^{[\%]} = \frac{m_{\text{bariumsulphate}} \times 0.343046 \times 100}{m_{\text{soil sample}}} = 34.30 \times \frac{m_{\text{bariumsulphate}}}{m_{\text{soil sample}}} = \frac{SO_3^{[\text{mg/kg}]}}{10000}$$

The conversion factor of 0.343 in the formula is the ratio of the relative molecular weight of the *sulphite* ion (SO_3) and the barium sulphate ($BaSO_4$): $80.06/233.38 = 0.343046$.

For the classification of concrete in the environmental class in Table 2 of EN 206, the limit values for the sulphate content of the soil are not given in SO_3 [%] (sulphite), but SO_4 [mg/kg] (sulphate); therefore, the percentage *sulphite* ion content in EN 196-2 shall be converted to the sulphate ion content expressed in mg/kg. The conversion formula is $SO_4^{[\text{mg/kg}]} = 1.2 \times SO_3^{[\text{mg/kg}]} = 1.2 \times 10^4 \times SO_3^{[\%]}$ because the relative molecular weight of the sulphate ion (SO_4^{2-}) is 96.06, the relative molecular weight of the sulphite (SO_3^{2-}) is 80.06, and their ratio is 1.2.

The sulphate ion content of the soils, expressed in mg/kg, required for the classification of the concrete in environmental class XA1, XA2 or XA3 according to EN 206 shall be obtained by multiplying the percentage test result expressed as $SO_3^{\%}$ in accordance with EN 196-2 by 1.2×10^4:

$$SO_4^{\left[\frac{\text{mg}}{\text{kg}}\right]} = 1.2 \times 10^4 \times SO_3^{[\%]} = 411655 \times \frac{m_{\text{bariumsulphate}}}{m_{\text{soil sample}}}$$

If the sulphate ion content in the 50:250 = 1:5 soil sample extract test is more than 6000 mg/kg, the test shall be repeated with a 1:10 soil sample extract test.

7.1.2 Determination of sulphate content of soils by aqueous process

According to Table 2 of EN 206, the sulphate content of soils may be determined by the aqueous process instead of the hydrochloric acid process if there is experience.

In this case, the determination is carried out with a sample prepared in accordance with EN 1744-1. The soil sample of at least 2 kg shall be reduced to 250 g by quartering step by step. This part shall be dried at a temperature of 110 ± 5 °C and then chopped to a grain size of less than 0.125 mm until at least 20 g of soil sample has fallen through a sieve with a mesh size of 0.125 mm.

The test is then carried out according to EN 196-2 paragraph 4.4.2.2 by weighing $2.00 + 0.05$ g of powdered sample. The test result:

$$SO_4^{\left[\frac{\text{mg}}{\text{kg}}\right]} = 411655 \times \frac{m_{\text{bariumsulphate}}}{m_{\text{soil sample}}}$$

7.2. Determination of sulphate content of groundwater, wastewater and other aggressive liquids

Concrete in contact with sulphate-containing groundwater is classified in exposure class XA1, XA2 or XA3 and concrete in contact with sulphate-containing sewage or other aggressive liquids is classified in exposure class XA4(H), XA5(H) or XA6(H).

For the classification of concrete as XA1, XA2, XA3, XA4(H), XA5(H) or XA6(H), the sulphate content of the groundwater, rainwater, wastewater or other aggressive liquids, etc., surrounding the concrete shall be determined by the method in accordance with the EN 196-2 cement test standard and expressed in mg/litre.

When determining the sulphate content of groundwater, rainwater, wastewater or other aggressive liquids, etc., the procedure according to paragraph 4.4.2.2 of EN 196-2 cement test standard is modified by using 250 ml of filtered groundwater, wastewater or other aggressive liquids, etc., instead of cement pulp, whose pH value is adjusted to 1.0-1.5 with 1+11 dilution hydrochloric acid. This solution shall be used for the gravimetric determination of sulphate ions, hereinafter referred to as 'Bring to the boil and boil for 5 minutes', according to EN 196-2 paragraph 4.4.2.2. beginning with the fourth paragraph.

The test result in this case:

$$SO_4^{\left[\frac{\text{mg}}{\text{kg}}\right]} = 411655 \times \frac{m_{\text{bariumsulphate}}}{m_{\text{soil sample}}}$$

8. WATERTIGHT CONCRETE AND CONCRETE EXPOSED TO WATER ABSORPTION, HUNGARIAN EXPOSURE CLASSES

According to the standard MSZ 4798, concrete shall be classified in
- exposure class XV1(H), if the *water column* pressure is > 100 mm and < 2000 mm;
- exposure class XV2(H), if the *water column* pressure is > 2000 mm and < 10000 mm;
- exposure class XV3(H), if the *water column* pressure is > 10000 mm.

The concrete is categorised as exposure class XV1(H) if the hydrostatical head is less than 2 m (e.g. cellar walls, rainwater drainages, cisterns, water culverts, gutters, downpour reservoirs, rainwater collector shafts, etc.).

The concrete is categorised as exposure class XV2(H) if the hydrostatical head is between 2 m and 10 m (e.g. channels, dams, river walls, outer boundary structures of underground garages and subways, hydraulic engineering structures, etc.).

The concrete is categorised as exposure class XV3(H) if the hydrostatical head is more than 10 m (e.g. outer boundary structures of underground parking garages and tunnels, hydraulic engineering structures, etc.).

According to the standard EN 12390-8, the highest allowed individual depth values of water penetration (measured on three different specimens) into the concrete of exposure classes XV1(H), XV2(H) and XV3(H), respectively, are summarised in Table 10.

Water is considered to be not under pressure if the water head is ≤ 100 mm. For example, concrete embedded in a wet medium is exposed to water without pressure. Furthermore, concrete surrounded with soil moisture basements above the groundwater level is classified into exposure subclass XV1(H)/V0 according to MSZ 4798 upon their water absorption. Such are, e.g. basements or cellar walls above groundwater level that are exposed to soil moisture or vapours

Table 10: Limits for the composition of watertight concrete and concretes exposed to water absorption

Requirements	Hungarian exposure classes			
	Impact: water absorption	Impact: water pressure		
	XV1(H)/V0	XV1(H)	XV2(H)	XV3(H)
Maximum water/cement ratio	0.55	0.55	0.50	0.45
Minimum strength class	C25/30	C25/30	C30/37	C30/37
Minimum cement content, kg/m³	300	300	300	300
Planned air content of fresh concrete	*See Table 6*			
Other requirements	The coefficient of water absorption of concrete (determined according to the standard EN ISO 15148) should be $W_{wt} \leq 2,0$ kg/(m²·h^½).*	Maximum individual water penetration depth tested on min. 3 specimens in accordance with EN 12390-8, mm		
		50	35	20

* Remind: for the internal plaster hindering the wettening, see the text above Table 10.

or concretes in the vicinity of underground parking garages, where the water pressure has been permanently eliminated, e.g. by groundwater level lowering. The environmental subclass XV1(H)/V0 may also be suitable for limiting the water absorption of other structures, such as concrete block walls, that come into contact with the ground on one side, generally together with other exposure classes.

XV1(H)/V0 exposure subclass concrete shall not be considered watertight concrete.

The concrete of a structural element exposed to environmental moisture but not to water pressure can be categorised as exposure subclass XV1(H)/V0 if its water absorption coefficient – determined according to the standard EN ISO 15148 – is: $W_{wt} \leq 2,0$ kg/(m²·h^½).

The concrete categorised as exposure subclass XV1(H)/V0 *is not watertight*, therefore – depending on the thickness of the structural element and Darcy's water permeability coefficient (according to standard EN ISO 17892-11) and its temporal change. (e.g., change in the surrounding soil, embedding layer, excavation pit filling, and any unexpected water level rise – it may get wet). The recommended thickness of the wall structural element and base plate should be at least 200 mm and 150 mm, respectively, and the *k*, i.e. Darcy's water permeability coefficient (according to standard EN ISO 17892-11) of the surrounding soil, embedding layer, or excavation pit filling should be minimum $k = 5 \cdot 10^{-5}$ m/s, i.e. the material surrounding the concrete should be water permeable to avoid water stagnation.

Furthermore, the author means that the owner may prevent the risk of any possible wetting or soaking by applying (at their own charge) an internal (i.e. the side of the interior area) water-repellent plasterwork. For example:

- if the value of the concrete's water absorption coefficient (capillary water absorption number) is $W_{wt} \leq 0,5$ kg/(m²·h^½), then it is *recommended* to apply an appropriate layer of water-repellent coating on the internal surface (interior side) of the concrete;
- if the value of the concrete's water absorption coefficient (capillary water absorption number) is $0,5 < W_{wt} \leq 2,0$ kg/(m²·h^½), then it is *highly recommended* to apply an appropriate layer of water-repellent coating on the internal surface (interior side) of the concrete;

The composition requirements for concrete classified in exposure subclasses XV1(H)/V0, XV1(H), XV2(H) and XV3(H) are *given in Table 10.*

9. HUNGARIAN EXPOSURE CLASS OF CONCRETE EXPOSED TO ABRASION

According to standard MSZ 4798, if the concrete is exposed to abrasion by abrasive, sliding, rolling, frictional, impact or water flow driven rolling stock, the concrete shall be classified into environmental class XK1(H), XK2(H), XK3(H) or XK4(H).

If the loss in *volume ΔV* of concrete at 28 days age, determined by the *Böhme method* according to method B. of standard EN 14157 (using 71 ± 1.5 mm test cubes) shall not exceed:

- in the case of dry abrasion, 14000, 12000, 10000, 8000 mm³, respectively;
- in the case of abrasion of water-saturated test, 21000, 18000, 16000, and 14000 mm³, respectively.

Concrete is classified in the XK1(H) class if it is exposed to abrasion of light granular materials, pedestrian traffic, and blown tyre vehicles. Examples are silos, bunkers, tanks for storing lightweight aggregates, agricultural crops, etc., and concrete for sidewalks, stairs, garage floors, etc.

Concrete is classified in the XK2(H) class if it is exposed to rolling loads caused by heavy loads and to the abrasion of solid-wheeled vehicles. Examples are concrete tracks for concrete roads, forklifts, structures in contact with rolled sediment, etc.

Concrete is classified in the XK3(H) class if it is exposed to sliding-rolling loads caused by very heavy loads and to the abrasion of steel-wheeled forklifts. Examples are concrete for landing and take-off tracks and taxiways at airports, as well as floor coverings for container loading stations and heavy industry assembly halls, etc.

Concrete is classified in the XK4(H) class if it is exposed to abrasion of sliding-rolling loads caused by extremely heavy loads or if high surface accuracy and dust-freeness are required. Examples are concrete for halls, warehouses and pavements exposed to extremely heavy loads and traffic of caterpillar vehicles, hard surface dust-free industrial floor coverings without wear layer or bark reinforcement, etc.

The composition requirements for concrete classified in exposure classes XK1(H), XK2(H), XK3(H) and XK4(H) are *given in Table 11.*

Table 11: *Limits for the composition of wear/abrasion-resistant concretes*

Requirements	Hungarian exposure classes			
	XK1(H)	XK2(H)	XK3(H)	XK4(H)
Maximum water/cement ratio	0.50	0.45	0.40	0.38
Minimum strength class	C30/37	C35/45	C40/50	C45/55
Minimum cement content, kg/m³	310	330	350	370
Planned air content of fresh concrete	*See Table 6*			

10. CONCLUSIONS

To ensure the durability of concrete, reinforced concrete and prestressed reinforced concrete structures, the concrete must be classified into exposure classes according to the standards EN 1992-1-1, MSZ EN 206, MSZ 4798, and the concrete composition must be designed to comply with the requirements *of the concrete* belonging to one or the other given exposure classes.

The exposure class is not a property of the concrete but that of the environment surrounding the concrete. The term "concrete complying with a given exposure class" means a concrete that meets all the requirements of class X, which is ordered to (Annex F).

The exposure classes in the European standard EN 206 are X0; XC1 – XC4; XS1 – XS3; XD1 – SD3; XF1 – XF4; XA1 – XA3.

These classes have been extended in the Hungarian national standard MSZ 4798 with the following ones: XN(H), X0b(H), X0v(H), XF2(H), XF3(H), XF4(H), XA4(H), XA5(H), XA6(H), XV1(H)/V0, XV1(H), XV2(H), XV3(H), XK1(H), XK2(H), XK3(H), XK4(H) – where those signed with A(H) are taking into account more severe chemical exposure.

In the standard MSZ 4798 and its amendments (for example: MSZ 4798:2016/2M:2018 and MSZ 4798:2016/4M:2023), the criteria for exposure classification are based on environmental effects that may cause concrete or steel reinforcement corrosion, - such as moisture and its forms (e.g. water, ice, steam), the *chemical composition* of air or other gases or water or other liquids, the water pressure and the degree of abrasion (wear), etc.

The requirements of the Hungarian exposure classes relate, *on the one hand, to the concrete composition parameters*, namely the maximum permissible water-cement (*w/c*) or water-efficient binder ratio (*w/b*), the minimum and maximum permissible cement or effective binder content in the case of a risk of concrete corrosion due to a solution, the air content, sometimes the properties of the concrete components; - *and on the other hand, the hardened concrete properties*, such as compressive strength class, the permissible chloride content or sometimes the frost resistance or frost and melting salt resistance, the air bubble system, water absorption, water tightness and abrasion resistance.

11. ACKNOWLEDGEMENTS

12. REFERENCED STANDARDS

ASTM D1498-14	Standard test method for oxidation-reduction potential of water
EN 196-2	Methods of testing cement. Part 2: Chemical analysis of cement
EN 206	Concrete. Specification, performance, production and conformity
EN 480-11	Admixtures for concrete, mortar and grout. Test methods. Part 11: Determination of air void characteristics in hardened concrete
EN 1744-1	Tests for chemical properties of aggregates. Part 1: Chemical analysis
EN 1899-2	Water quality. Determination of biochemical oxygen demand after n days (BOD_n). Part 2: Method for undiluted samples
EN 1917	Concrete manholes and inspection chambers, unreinforced, steel fibre and reinforced
EN 1992-1-1	Eurocode 2: Design of concrete structures. Part 1-1: General rules and rules for buildings
EN 12390-8	Testing hardened concrete. Part 8: Depth of penetration of water under pressure
EN 13577	Chemical attack on concrete. Determination of aggressive carbon dioxide content in water
EN 13755	Natural stone test methods. Determination of water absorption at atmospheric pressure
EN 14157	Natural stone test methods. Determination of the abrasion resistance
EN 15933	Sludge, treated biowaste and soil. Determination of pH
EN ISO 5815-1	Water quality. Determination of biochemical oxygen demand after n days (BOD_n). Part 1: Dilution and seeding method with allylthiourea addition
EN ISO 7980	Water quality. Determination of calcium and magnesium. Atomic absorption spectrometric method
EN ISO 10523	Water quality. Determination of pH
EN ISO 14911	Water quality. Determination of dissolved Li^+, Na^+, NH_4^+, K^+, Mn^{2+}, Ca^{2+}, Mg^{2+}, Sr^{2+} and Ba^{2+} using ion chromatography. Method for water and wastewater
EN ISO 15148	Hygrothermal performance of building materials and products. Determination of water absorption coefficient by partial immersion

EN ISO 17892-11	Geotechnical investigation and testing. Laboratory testing of soil. Part 11: Permeability tests
ISO 6060	Water quality. Determination of the chemical oxygen demand
ISO 7150-1	Water quality. Determination of ammonium. Part 1: Manual spectrometric method
MSZ EN 206	Concrete. Specification, performance, production and conformity (In Hungarian)
MSZ 260-4	Wastewater analysis. Determination of hydrogen ion concentration (pH value). Withdrawn standard (In Hungarian)
MSZ 260-9	Wastewater analysis. Determination of ammonium ion content. Withdrawn standard (In Hungarian)
MSZ 260-52	Wastewater analysis. Determination of calcium and magnesium content by complexometric method (In Hungarian)
MSZ 448-21	Drinking water analysis. Determination of total hardness, arithmetic of carbonate hardness and non-carbonate hardness (In Hungarian)
MSZ 448-23	Drinking water analysis. Determination of active, fixed, poise and aggressive for lime carbon dioxide (In Hungarian)
MSZ 1484-3	Testing of water. Determination of dissolved, suspended and total metals in water by AAS and ICP-OES (In Hungarian)
MSZ 1484-22	Water quality. Part 22: Determination of pH and pH in equilibrium state (In Hungarian)
MSZ 4798	Concrete. Specification, performance, production and conformity, and rules of application of EN 206 in Hungary (In Hungarian)
MSZ 4798:2016/2M:2018	Concrete. Specification, performance, production and conformity, and rules of application of EN 206 in Hungary. Amendment No. 2. (In Hungarian)
MSZ 4798:2016/4M:2023	Concrete. Specification, performance, production and conformity, and rules of application of EN 206 in Hungary. Amendment No. 4. (In Hungarian)

Hon. Prof. Dr. Eng. Tibor KAUSAY (1934), MSc in civil engineering (1961), reinforced concrete engineer (1967), candidate of Technical Sciences (1978), Ph.D. (1997), associate professor (1985), honorary professor at the Budapest University of Technology Department of Civil Engineering (2003), member of the Hungarian Section of the *fib* (2000), commemorative medal of Count Menyhért Lónyay of the Hungarian Academy of Sciences (2003), holder of the László Palotás Prize (Hungarian Section of the *fib*, 2015). His activities cover research, development, expertise, education and standardisation in the concrete technology and stone and gravel industries. The number of his publications is about 220. e-mail: betonopu@t-online.hu

THE AESTHETICS OF CONCRETE

Paládi-Kovács Ádám

We cover the external facades of our buildings with different materials, which significantly determine the appearance, and aesthetics of the building while meeting many requirements. The article covers the number of ways and how facades created with concrete elements, concrete cladding or exposed concrete can be shaped, and how they react to external influences and conditions.

The article examines how today's modern concrete facades, in addition to providing the necessary technical function, can give an aesthetic façade appearance or even how the façade can even represent the spirit of the building.

In addition to the already established concrete façade technologies, what new procedures are there in the construction industry and what additional possibilities are there in this material during façade use.

Keywords: concrete surface, decoration, relief, colored concrete, folded concrete, photogravure, concrete printing

1. THE POSSIBILITIES HIDDEN IN CONCRETE FACADES

The appearance of a building in space is created through the combination and interaction of various materials. The look, processing, and malleability of materials are crucial for the overall impression. When we talk about concrete or concrete structures, we primarily think of load-bearing elements and less of the beauty inherent in the material or the aesthetic possibilities. However, the architect must keep the final overall picture in mind and select the necessary materials even before the actual physical appearance of the building.

Every material has a certain visual language that the designer must utilize. The form of concrete or artificial stone is determined by the formwork. Ductile concrete can take on virtually any shape until it solidifies. Working with concrete requires great expertise and imagination from the architect, but at the same time, it also demands self-restraint, as the versatile possibilities of this material are practically limitless.

Designing a concrete facade surface means that the designer must not only consider the structural properties but also make use of the material's shaping possibilities. Surface appearances shiny-matte, smooth-rough, coarse-fine, to name just a few from the infinite variations are all dependent on the material.

Fig. 1: *Concrete Slit House, designed by Atelier Zhanglei (Ghile, 2013)*
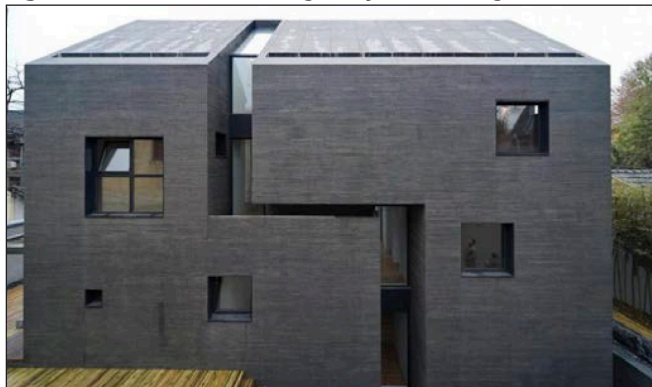
These forms develop from the interaction of different materials, or they reveal certain components of a particular material.

These solutions can either strengthen or weaken the architectural language of the building but undoubtedly influence each other. They determine the optical impression, which can be further defined with the use of different colors. The *relief-like shaping* of the surface adds interesting light and shadow effects to the facades.

Surface structures can also be created through the special shaping of certain architectural details (e.g., joints, patterns). The selected appearance of the components must always be in harmony with the immediate surroundings of the building, and more importantly, with the overall urban context. Designing the facades of buildings should be considered a public matter, not just meeting the expectations of the client but also keeping in mind a more complex system of relationships in urban planning.

2. CONCRETE SURFACES AND FORMWORK STRUCTURE

Concrete consists of components such as cement, aggregates, additives, and water. After solidification, it takes on the properties, appearance, and form of rocks. Fresh concrete is poured into a formwork and allowed to set there. The imprint of the formwork appears on the hardened concrete surface, which can be either rough or smooth in structure. Various optical effects can be achieved based on the pattern of the formwork or the imprint left on the concrete. A well-known

Fig. 2: *The impression of the formwork structure on the surface of the concrete (Doka, 2009)*

optical effect is that by structuring with dense, vertical lines, we perceive the facade as taller and narrower.

On the other hand, a wide spacing between horizontal lines reduces the perceived height and makes the building appear broader. Irregularly oriented structures provide a flat, wallpaper-like pattern, and material structures can evoke various material associations (e.g., wood grain pattern). Some line patterns can create a perspective representation of a surface, or by varying the density of lines, a flat surface may appear either convex or concave.

3. DECORATION AND RELIEF

In addition to material-dependent surface structures, visible surfaces can also be adorned, achieving significant architectural (aesthetic) impact. Decorative forms, utilizing the third dimension, become reliefs. To create reliefs, a negative element containing the desired forms must be inserted into the formwork, defining the future pattern. Decoration provides the architect with an opportunity to break up the surface and dissolve the solid form of the building's facade and material. Reliefs can articulate, enliven, and give the building a distinctive, unique exterior. The patterns on the facade, as imprints of the negative plastic form placed in the formwork during prefabrication, endure on the concrete elements. These embellishments can appear not only on the exteriors of buildings but also as interior design motifs within internal spaces.

Thanks to the latest developments, these reliefs can now be produced through 3D concrete printing. A notable example is the ribbed concrete ceiling created by researchers at ETH Zurich. The project involved experts from the Swiss university's Digital Building Technologies (DBT), Block Research Group (BRG), and Architecture and Buildings Systems (A/S) departments. The prototype of the structure, named HiRes Concrete Slab, was installed in one of the university's offices used by robotics researchers. According to their claims, beyond its relatively thin and uniquely beautiful, meandering patterned aesthetics, the ceiling is also energyefficient.

The true purpose behind developing the HiRes Concrete Slab was to explore and showcase the advantages of 3D printing. During the printing of the prototype, concrete was

Fig. 3: *HiRes Concrete Slab (Aouf, 2022)*

Fig. 4: *Concrete slab (Aouf, 2022)*

poured into 43 forms, each 50 mm thick, using 3D technology. The thickest parts of the ceiling, reaching a maximum of 300 millimeters, are at the intersections of the modules. The forms were supported by a laser-cut wooden formwork during the process.

The technology's energy efficiency is attributed to reduced material requirements and the integration of various building services during the production of the Concrete Slab, such as ceiling heating-cooling or ventilation. Developers from the Architecture and Buildings Systems department integrated four custom polymer ventilation channels into the prototype structure using 3D printing before pouring the concrete.

The shape of the tubes was designed for optimal airflow properties and minimized energy indices. Truth be told, thanks to their aerodynamic characteristics, the 3D printed ducts are much more efficient than other previous systems," explained Andrei Jipa, a doctoral student at DBT. The A/S team determined the printed patterns based on the hydraulic circuits of the cooling-heating pipes, using precise computational calculations. The result is an extremely efficient radiant surface with better thermal performance than traditional flat ceilings.

The form and size of the formwork were designed to fit into the compartment of the 3D printer and to be easily removable from the final cast. The slightly vaulted design of the modules takes advantage of the high compressive strength of concrete, and it requires less material than traditional methods. Horizontal forces are absorbed by four tensioning structures placed at each corner of the module. Additionally, the ribbed design provides natural sound diffusion/damping properties, which are essential in today's communal, open-plan offices, or conference rooms.

4. COLORED CONCRETE AND COLORED COATING

Interesting shape-forming effects can be achieved with the application of colored concrete elements. In such cases, colored pigment is added to the concrete mix. For red, yellow, brown, and black tones, mainly iron oxide pigment is used, while for green shades, chrome oxide and chrome oxide hydrate pigments are employed. Blue tones, on the other hand, may utilize a mixture crystal-based pigment such as cobalt-aluminum-chrome oxide. Concrete coloring is durable and weather-resistant. When using gray cement, the color

Fig. 5: *Mahadeva Prayer Space, Designer: Karan Darda Architects (Szilvási, 2019)*

Fig. 6: *The white chapel forms a perfect unity with the landscape (Szilvási, 2019)*

Fig. 7: *Teotitlan del Valle Community Cultural Center building (Szilvási, 2019)*

tone is darker, whereas with white cement, it is lighter and cleaner. Fine surface detailing further enhances the color. To highlight larger surfaces on a building, similar surface sections or individual building elements can be colored. However, the used paint must always be in harmony with the properties of concrete. Increasingly, visually appealing concrete surfaces with colored materials are appearing on the facades of buildings, emphasizing the aesthetic value of concrete. In the previous part of our article, we presented the use of white concrete; today, we focus on red concrete.

The prayer space was designed by the Indian firm Karan Darda Architects using locally producible materials. Local architects constructed the temple of Mahadeva (Shiva), the most important Hindu deity, using red concrete. The modern reinterpretation of the red concrete prayer space reflects the traditional rural Indian temple architecture. In this environment, the rough finish of the surface, the occasional irregularities in joints, and the color variations in the concrete do not adversely

affect the appearance of the structure. The prayer space is placed on a yellow-gray concrete slab, separating it from its surroundings. The differing color palettes of the building and the base plate harmonize with the environment, where the red concrete also serves as the focal point of depth.

The architecture of Lima has exceptionally expanded with a beautiful university campus. The university building was recognized with an international RIBA award in 2016. The building's perforated concrete block, with its silky white appearance, connects Lima to the sea like a modern Machu Picchu. The design of the building was conceived by Iwan Baan, a designer at the Grafton Architects studio. Concrete appears on the facade and in the interior, becoming part of the interior design. The flawless joints of the large-panel formwork and the imprints of spacers stand out on the facades, and their regular layout is an integral part of the architectural spectacle. The concrete surfaces are homogeneous whites, free from bleedings and irregularities, providing a true visual concrete experience. The outer edge of the building rises like a rock above the cut with its height and articulation. The inner part is built down in terraces to the ground floor.

The architectural firm Productora designed the Community Cultural Center building in Teotitlan del Valle, Mexico. The concrete of the building carries the colors of the rocky desert environment, where the local rock aggregate added to the mix gives the concrete a yellowish hue. The texture of the formwork wood also appears on the surface.

Another option is to paint the finished concrete surface in the desired color. Paint can be applied directly to the facade concrete surfaces. The paints that can be applied to concrete surfaces must meet the following requirements:
- resistance to alkaline effects coming from the concrete
- good adhesion to the concrete
- good bonding within the coating system
- repaintability with the same paint
- weather resistance
- resistance to industrial environments and/or water-soluble substances
- light and UV resistance
- low susceptibility to pollution
- satisfactory vapor permeability
- resistance to flowing water
- resistance to washing or scrubbing.

Among the paints, primarily mineral and silicate paints

that cure in the air or hydraulically, as well as plastic-based dispersion or polymerized resin-based paints, can be considered. When selecting the paint, it is important to consider that repainting may be required periodically. Colors cannot replace deficient architectural design, but they can be well-utilized as aids and supplements. The method of coloring can be material-dependent or independent. The goal may be to achieve an effect related to semantics or integration into a larger context. The design of the facade color scheme should be an essential component of every construction and permit plan.

5. STONE-CARVING-LIKE AND OTHER PROCESSING OPTIONS

In stone-carving-like processing methods (such as bush-hammering, grooving, and sandblasting), the top layer of cement is removed from the concrete. This results in a rough surface that reveals partially fractured additives. The use of white cement, colored additives, or colored paint can achieve special effects, enhanced by light and shadow effects.

Another method of processing concrete surfaces is scraping, sandblasting, and flame treatment. In these methods, the top layer of cement and the additive, serving as a shaping element, are removed. In scraping, individual additive particles are exposed and cleaned. Sandblasting creates a rough surface, while in flame treatment, the heat causes the top additive particles to burst, resulting in a jagged surface. The additive structure becomes visible through grinding and polishing of the concrete surface. Concrete stones processed in this way can be versatilely used, for example, in facades, walls, and even window sills.

6. WASHED CONCRETE AND EXPOSED AGGREGATE CONCRETE SURFACES

The most commonly used technique for surface treatment is washing away the top cement layer, a process in which the cement mortar is removed from the top layer of concrete using

Fig. 8: Stone-carved-like facade concrete, Grand Tokaj Winery (Kis, 2016)

Fig. 9: The concrete facade of Grand Tokaj Winery, Designer: Péter Kis (Kis, 2016)
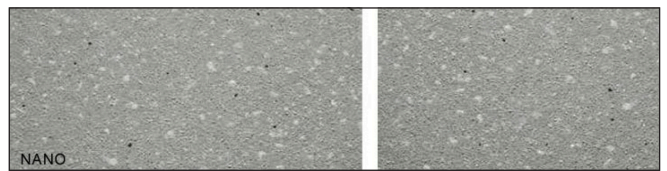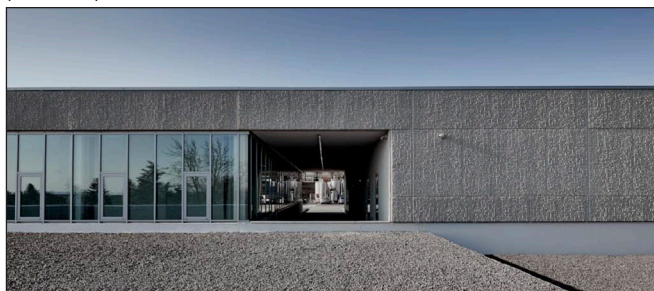
Fig. 10: Nano-particle surface appearance (Reckli, 2021)
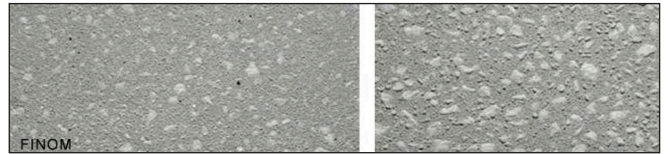
Fig. 11: Fine-washed concrete surfaces (Reckli, 2021)
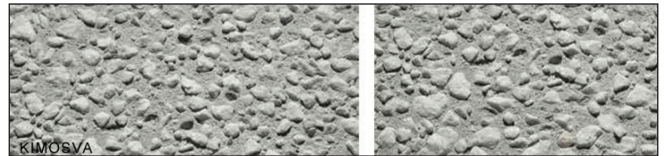
Fig. 12: Coarse-washed weathering on the surface (Reckli, 2021)

high-pressure water or wire brushing. This reveals the stone aggregate used in the concrete mix.

The procedure allows achieving various washing depths, resulting in surfaces with increasingly distinctive appearances. Another option is to achieve different effects by using various additives with different properties and colors. The appearance of the concrete is always different depending on whether angular or rounded, light or dark, monochromatic or colored stones are mixed with the additives.

Another method involves applying surface retarders to the inner side of the formwork. This allows only the top millimeters of the surface to be washed out, a technique known as exposed aggregate finish. This gives the concrete a very interesting sandstone-like appearance, which can be further colored with appropriate additives and pigments.

7. FOLDED CONCRETE BUILDING

In the design of large-scale concrete facades, not only the imprint of patterns but also the shape of the elements can have a powerful visual impact, as seen in the manufacturing and office building of the Textilmacher company in the industrial quarter of northern Munich.

Its iconic appearance is attributed to the geometrically precise folded facade. A fascinating aspect is that, with the changing periods of the day, the interplay of light and shadows gives the building varying aesthetics. The anthracite gray matte concrete surface harmonizes with its surroundings. Besides the

Fig. 13: Large-panel concrete facade, Designer: Tillicharchitektur (Compensis, 2013)

advantage of prefabrication, the large-scale facade cladding offers a short construction period and cost effective conditions. The elements were transported to the site after production and intricately fitted together like a puzzle.

8. EMERGENCE OF NEW TECHNOLOGIES

8.1 Photogravure concrete surfaces

A new technology for displaying custom photos on concrete surfaces is called "photoengraving." The process involves scanning the photograph(s), increasing their resolution, digitizing them with software, and then carving the pattern into so-called "master plates."

Using the master pattern created in this way, a formwork for photoengraving with a flexible pattern is produced. The completed formwork can then be used either at the precast concrete plant or on-site during concrete pouring. After removing the formwork pattern, the photograph appears on the cast facade concrete surface.

8.2 Striped, printed concrete surfaces

By utilizing the latest technologies, new textures are emerging, such as a residential house created with a 3D printer that aims to exploit the malleability of concrete. Thus, in the suburbs of Eindhoven, the Project Milestone, a complex of five buildings constructed using 3D printing, has been established, considered Europe's first 3D-printed residential complex where people actually live. The project involves printing a complex of five buildings.

The city decided back in 2017 to build with 3D technology and subsequently lease houses that meet all comfort requirements. The buildings, designed in a wooded park environment, are sustainable, energy-efficient, comfortable, lightweight, and quiet. In 2017, they already constructed a pre-stressed concrete bridge for cyclists, printing it from 800 layers. The bridge was printed at the Eindhoven University of Technology, which is at the forefront of concrete printing research and played a role in implementing the Milestone project.

The first building will be a 95 sqm, single-story house with three rooms, and they aim to complete it in the first half

Fig. 15: *Photogravure image on concrete surface, Quebec, Canada (Építési Megoldások, 2023)*

Fig. 16: *Project Milestone visual plan. Designer: Witteveen+Bos (Dery, 2018)*

Fig. 17: *Project Milestone: the first completed house. Designer: Witteveen+Bos (Sebes, 2021)*

of 2019. The other four buildings will be multi-story houses. The elements of the initial buildings will be created with the university's 3D concrete printer (3DCP), while for the last house, they plan to use an on-site printer. The development and implementation of this on-site printer can be a crucial step for

Fig. 14: *Photogravure facade concrete surface (Építési Megoldások, 2023)*

Fig. 18: *Concrete elements 3D printing (3DCP) at Eindhoven University of Technology (Project Milestone, 2019)*

Fig. 19: *Facade of the Vienna University of Economics and Business Library (Hadid, 2013)*

the technology's future widespread adoption. One advantage of 3D-printed buildings, as seen in the renderings, is that the designers have planned futuristic, free-form structures that fully utilize the possibilities offered by 3D printing. These unique free-forms are challenging and expensive to achieve with traditional technologies. Another significant advantage is the reduced need for concrete with this technology. In traditional concrete pouring, the concrete completely fills the formwork, while here, concrete is printed only where needed. This translates to less cement usage, potentially reducing overall construction costs and contributing to lower carbon dioxide emissions, as cement production is associated with high CO_2 emissions.

The structure's additional advantage is that its operation requires only a few people, and the printer head and printing results are monitored by a camera. Thus, a double-layered wall of 1 m^2 can be completed in 5 minutes. The technology provides great freedom for design, as, unlike traditional methods, the 3D printer does not pose technological challenges even for organic curved forms.

Since the beginning of the project, the same technology has been used to create Europe's largest residential building in Wallenhausen, and the first such residential building in Tempe, Arizona, in the United States.

9. RESISTANCE OF CONCRETE FACADES TO DIRT AND WEATHER

When creating a durable and aesthetically pleasing building facade, it is important to consider the inevitable accumulation of pollutants over time and ensure proper drainage of rainwater on the facade. Concrete elements used to cover facade surfaces are grateful structures in this regard.

The direction and strength of the wind determine how much water can accumulate in certain areas and where dirt deposits may form. The flow pattern of water is crucial, as it allows pollutants to be washed out of the facade surface, and under certain conditions, some of them may redeposit elsewhere.

The slope or inclination of the concrete surface is equally important. Vertical surfaces receive relatively little water and are easily cleaned. The amount of rain falling on surfaces leaning backward is much greater. However, their cleaning ability is somewhat lower, and pollutants often accumulate on the lower edges. Forward-leaning surfaces generally remain dry and are the least prone to contamination. The upper part

must be designed so that water cannot flow onto the surface, as otherwise, the flow pattern becomes evident very suddenly and can compromise the appearance of the facade. Taking these conditions into account is an essential basis for shaping facades with concrete. Properly designed elements can effectively prevent the facade from getting dirty over time.

A facade of the Library and Learning Center of the Vienna University of Economics and Business is made with FibreC concrete cladding – glass fiber-reinforced concrete elements dominate the appearance of the building designed by Zaha Hadid. The two interconnected main parts of the building are made unmistakable by their appearance: black for the public space and white for the private space. The architect chose glass fiber-reinforced concrete elements as the distinctive material for the facade.

In any case, as seen from the examples mentioned, concrete facades do not lag behind more traditional brick, stone, or other claddings in terms of appearance, durability, weather resistance, and cost-effectiveness. They provide an aesthetic appearance for almost any type of building.

10. CONCLUSIONS

Concrete is becoming increasingly popular and diverse in appearance on facades and interiors alike, allowing for the creation of durable, simple, yet elegant and striking surfaces. It is even capable of initiating trends. Thanks to the latest technologies, it is now easy to retroactively create exposed concrete surfaces.

The examples presented highlight the many ways in which we can shape the facades of our buildings to adequately represent the spirit and appearance of the structure. These external concrete facade surfaces represent great flexibility in formability during production, solidifying to provide proper protection for internal spaces.

They do not only meet technical necessities such as weather resistance, heat effects, sunlight, precipitation, wind effects, moisture effects, protection against contaminants and chemical effects, mechanical protection, frost resistance, shape and size durability, fire safety, color retention, durability, easy maintenance, and space separation, but also serve aesthetic, interesting, attention-catching, and unique representation of the building's external appearance, reflecting the internal function.

With the emergence of new innovative technologies, such as concrete printing, cost savings, and reduced carbon dioxide emissions can be achieved compared to traditional concrete

walls, moderating the eco-footprint of such buildings.

The wide variety of ways in which concrete facades can be shaped demonstrates the potential hidden in concrete, which, in my opinion, has not been fully exploited. Significant reserves lie in the facade usability of this material.

11. REFERENCES

ArchDaily (2023), Textilmacher / tillicharchitektur, industrial architecture, office buildings, showroom, https://www.archdaily.com/536964/textilmacher-tillicharchitektur

ArchDaily (2021), The Future Is Now: 3D Printed Houses Start To Be Inhabited in the Netherlands, Published on May 11, 2021. https://www.archdaily.com/961135/the-future-is-now-3d-printed-houses-start-to-be-inhabited-in-the-netherlands

ArchDaily (2018), Tejorling Radiance Temple / Karan Darda Architects, Temple, Pune, India, https://www.archdaily.com/896923/tejorling-radiance-temple-karan-darda-architects

Archiproducts, Reckli photo-engraving by coplan, Matrix for fair faced concrete wall, https://www.archiproducts.com/en/products/coplan/matrix-for-fair-faced-concrete-wall-reckli-photo-engraving_2792

Aouf, R. S. (2022), ETH Zurich creates dramatically contoured concrete slab ceiling, dezeen (2022.) https://www.dezeen.com/2022/07/08/eth-zurich-contoured-concrete-slab-ceiling-architecture/

Barker, N. (2022), Ten houses made from colourful concrete, de Zeen Arhitecture, https://www.dezeen.com/2022/02/11/colourful-concrete-houses-roundups/

Cherdo, L. (2023), The 13 best construction 3D printers In 2023 , Aniwaa Updated on Mar. 29, https://www.aniwaa.com/buyers-guide/3d-printers/house-3d-printer-construction/

Deco Magazin, (2020) A beton térhódítása: Kevés anyag képes így megújulni, fejlődni és alkalmazkodni. OCTOGON Architecture & Design, 2020/2 lapszám, felelős kiadó: Vertigo Publishing Kft. Bucsay Orsolya lapigazgató ISSN 1418-5229, https://www.octogon.hu/deco/a-beton-terhoditasa

DOKA (2009), Látszóbeton zsaluzása gyakorlati információk, DOKA GMBH

Építési megoldások (2014) „Összhangban a modern betonnal" – Várkert Bazár, 2014. december 04. kiadó: Artifex Kiadó Kft. szerkesztő: Bethlenfalvy Gábor NAIH-80970/2014. https://www.epitesimegoldasok.hu/osszhangban-a-modern-betonnal-varkert-bazar.html

Építési megoldások (2009), Előregyártott látszóbeton kéregelemek, október 15. kiadó: Artifex Kiadó Kft. szerkesztő: Bethlenfalvy Gábor NAIH-80970/2014. https://www.epitesimegoldasok.hu/20091015eloregyartott_latszobeton_keregelemek.html

Építési Megoldások (2023), Egyedi látszóbeton felületek kialakítása rugalmas sablonokkal január 19. kiadó: Artifex Kiadó Kft. szerkesztő: Bethlenfalvy Gábor NAIH-80970/2014. https://www.epitesimegoldasok.hu/egyedi-latszobeton-feluletek-kialakitasa-rugalmas-sablonokkal.html

Fürdős Zs. (2018), Üveg Beton és Vas hármasa. Karakteres, funkcionális és jövő orientált az EGM Architects tervezte holland irodaház, amely egy hajóépítőállomáson épült fel. OCTOGON Architecture & Design, 2018/12/04, felelős kiadó: Vertigo Publishing Kft. Bucsay Orsolya lapigazgató, ISSN 1418-5229 https://www.octogon.hu/epiteszet/uveg-beton-es-vas-harmasa/

Ghile G. (2013), Concrete Slit House – betonba metszett forma, Kortárs kínai: finom vasbeton héj és karakteres sliccek jellemzik ezt a nanjing-i családi házat. TERVLAP, | 2013.03.08. https://tervlap.hu/cikk-nezet/concrete-slit-house-betonba-metszett-forma

Kis P. (2016), Tolcsva borászat, palackozó üzem PLANT http://www.plant.co.hu/cards/view/141

Kreativlakás, Előre gyártott betonelemes homlokzati burkolás, Épületek külső burkolatai / Előre gyártott betonelemes homlokzati burkolás, https://kreativlakas.com/kulso-burkolat/elore-gyartott-betonelemes-homlokzati-burkolas/

MAGYAR ÉPÍTŐFÓRUM, (2020) 3D nyomtatott ház és a betonnyomtatás – amit tudni érdemes, 2020. október 16. Kiadja a Brand Content Kft. főszerkesztő: Kövesdy Gábor, https://www.maeponline.hu/kisokos/3d-nyomtatott-haz-betonnyomtatas/#legujabbszambol

Dery, M. (2018), 3D printing houses can cut construction time, cost and waste, July 3, 2018 CREATE engineering ideas into reality, https://createdigital.org.au/3d-printing-house-cut-time-cost-waste/

Móré L. (2019) Nyomtassunk házakat! ÉPÍTÉSZFÓRUM Technológia 2019.03.19. https://epiteszforum.hu/nyomtassunk-hazakat1

NEWS (2021), Netherlands unveils home 3D printed with concrete, and it wants to use the technology to house its growing population at 6:46amSaturday 1 May 2021 at 6:46am, updated Sun 2 May 2021 at 3:41am, https://www.abc.net.au/news/2021-05-01/3d-printed-home-in-dutch-city/100109484

Neira, J. (2022), Japanese company serendix is 3D-printing houses in less than 24 hours, DESIGNBOOM, https://www.designboom.com/technology/serendix-3d-printed-house-24-hours-03-14-2022/

Octogon, Deco Magazin, (2020), A ház, ahol még a kerítés is beton. A letisztult, elegáns betonház lakótér és kerámia stúdió is egyben. OCTOGON Architecture & Design 2020/6 lapszám, felelős kiadó: Vertigo Publishing Kft. Bucsay Orsolya lapigazgató, ISSN 1418-5229 https://www.octogon.hu/epiteszet/a-haz-ahol-meg-a-kerites-is-beton/

Octogon, (2019) Ipari negyed, Ipari negyed ipari épülete is lehet nagyon vonzó, Különleges geometriájú épülete kapott egy müncheni textilgyártó vállalat. OCTOGON Architecture & Design, 2019/07/02, felelős kiadó: Vertigo Publishing Kft. Bucsay Orsolya lapigazgató ISSN 1418-5229 https://www.octogon.hu/epiteszet/ipari-negyed-ipari-epulete-is-lehet-nagyon-vonzo/

Pásztor M. (2021), Elkészült az első 3D-technológiával nyomtatott bérlakás, EURONEWS https://hu.euronews.com/2021/05/12/elkeszult-az-elso-3d-technologiaval-nyomtatott-berlakas

Project Milestone (2019), 3D Printedhouse 2019. https://www.3dprintedhouse.nl/en/

RECKLI, (2021) Design your concrete, Mosott beton előállítása keményedés késleltető segítségével

Sebes P. (2021), Elkészült az első európai 3D nyomtatott családi ház, TERVLAP, | 2021.05.07, https://tervlap.hu/cikk-nezet/az-elso-europai-3d-nyomtatott-csaladi-haz

Souza, E. (2021), The Possibilities of Pigmented Concrete: 20 Buildings Infused With Color, ArchDaily, Published on February 22, 2021 https://www.archdaily.com/910825/the-possibilities-of-pigmented-concrete-18-buildings-infused-with-color

Stinson, L. (2020), This pink concrete home is an affordable housing prototype, The design is part of a larger exploration of attractive homes for middle- and low-income families

Szarka Sz. (2016), SWALL homlokzati elemek a tolcsvai borászati központban BETON szakmai lap 2016. december XXIV. évfolyam VIII. szám. https://www.betonujsag.hu/lapszamok/cikk/1914/swall-homlokzati-elemek-a-tolcsvai-boraszati-koezpontban

Szilvási A. (2018), Színes betonépületek 1. rész. BETON szakmai lap 2018. december XXVI évfolyam VI. szám, https://www.betonujsag.hu/lapszamok/cikk/2119/szines-betonepueletek-1-resz

Szilvási A. (2019), Színes betonépületek 2. rész. BETON szakmai lap 2019. február XXVII évfolyam I. szám, https://www.betonujsag.hu/lapszamok/cikk/2132/szines-betonepueletek-2-resz

Vörös K. (2018), Látványos betonfelületek családi házon, HOME Info, Üzemeltető és tulajdonos: Develon Hungary Szolgáltató kft. nyilvántartási sz: 5729/2017/B. https://www.homeinfo.hu/epitkezes-felujitas/szerkezet/2571-latvanyos-betonfeluletek-csaladi-hazon

Zaha Hadid Architects, (2013) Library and Learning Centre, ARCHELLO https://archello.com/project/library-and-learning-centre

Dr. Ádám Paládi-Kovács DLA, h. associate professor, architectural engineer, civil engineer, architect senior designer. From 1994, at the invitation of Professor Sándor Karácsony, he was a teaching assistant and then assistant professor at the BME Department of Civil Engineering until 2002. In Germany he worked like the designer of the FLL Architekt office. He's coming home he worked with his master, Henrik Hőnich, on several successful design projects and design competitions. 2014-2017. student at the Breuer Marcell Doctoral School. In addition to the authorship of numerous technical articles and publications, quite a few completed buildings are linked to his name. Member of the Hungarian Association of Architects (MÉSZ) and the public body of the Hungarian Academy of Arts (MMA). 1996. Commemorative Plaque for Hungarian Technical Progress, 2013. Hall Grand Prize for Quality Hall Construction, 2014. Design Award, 2020 Office of the Year Award, 2021. Budapest Capital Level Award, Commendation, 2022. Construction Industry Level Award, Certificate of Commendation 2022. FIABCI XXIV. Hungarian Prix d' Excellence, received a special award. He is currently a teacher at the Department of Construction Materials and Technologies at the Budapest University of Technology and Economics. E-mail: paladi-kovacs.adam@emk.bme.hu

WHAT A SPATIAL GRAPHICS - THE M44 TISZA BRIDGE

Zoltán Teiter

In this paper the design and the construction of a unique bridge are presented, and the history of the basic idea is described as well. The bridge spanning over the second largest river is innovative in many ways in Hungary, such as the first bridge with non-prestressed reinforced concrete pylons (allowing tension), the first cable-stayed bridge applying cable saddles, the first cable bridge with composite stiffening girder, etc. These facts and the immaturity of the preliminary designs repeatedly raised problems to which unique answers had to be found in the detailed design phase.

To bring them into their exact final position, the erection control of the pylon and the composite stiffening girder had to be designed and carried out, which required extremely precise calculation and construction. The building of the half ellipse pylon, which also proved to be a serious challenge to the contractors is also discussed.

Keywords: *arched pylon, concrete pylon, cable-stay, composite stiffening girder*

1. INTRODUCTION

The history of the bridge started in 2005 with an invitation-only design competition announced by the Town of Esztergom for a study titled "New Danube Bridge between Esztergom and Štúrovo." The idea occurred that the bridge was so wide (two lanes of traffic, sidewalks, and a bike lane on both sides) that only a smaller bridge could cross it. An arch would be suitable for this, and the roadway would just need to be ‹attached› to it. Using 3D software, a rudimentary model was built, and the result was remarkable. To everyone's surprise, this version was finally awarded, and the Uvaterv Bridge Department placed second.

The competition itself was exemplary, offering a rare opportunity for bridge designers to a brainstorm without constraints or obligations. Until that time and since then, no such opportunity has arisen. After the award ceremony, the group of designers gathered spontaneously in a local

Fig. 1: *Main properties of the bridge*
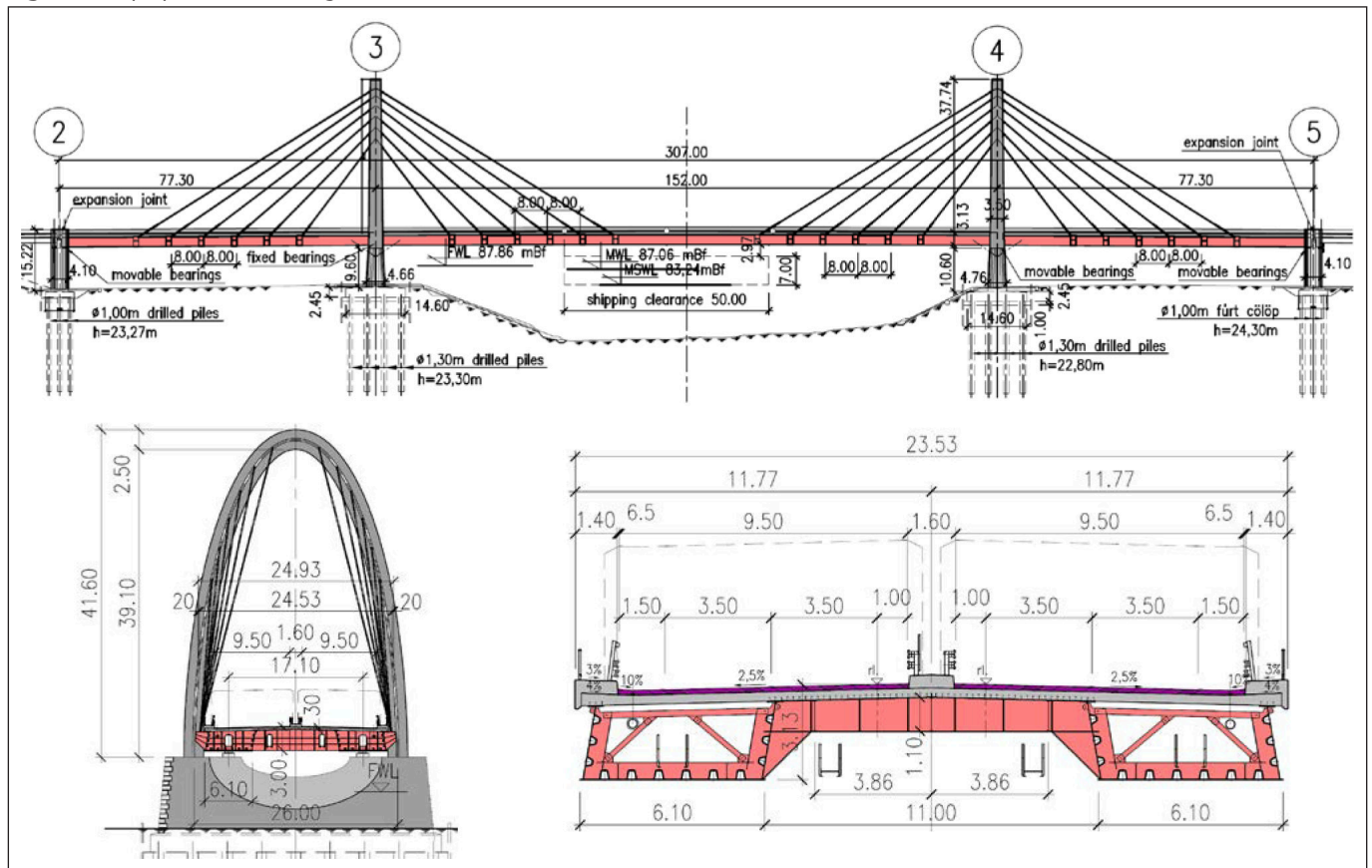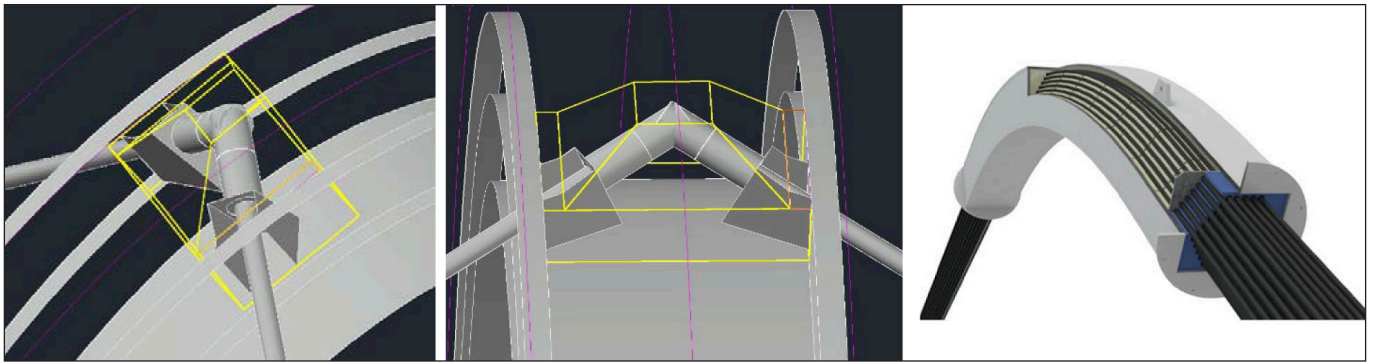
Fig. 2: *Earlier and final version for the pylon-cable joint*

restaurant, where they praised each other›s work while also criticizing it. It was there that the opinion was first expressed that the shape was interesting, but in such a scale, it was impossible to implement.

2. PRELIMINARY DESIGN PHASE

Fortunately, encouraged by the success, the Bridge Department did not let the project sink into oblivion. As much as possible, it was continuously included in multiple study plans as a potential design option. Finally, in 2015, a study plan was created for the Tisza Bridge, as a part of the M44 expressway, with several variations. The cable-stayed bridge with an arched pylon and composite stiffening girder proved to be economically competitive and enjoyed the support of the client.

In 2016, the designs for approval could be prepared for this favourite idea. During the planning process, the specific proportions and dimensions, including the pylon height-span ratio, the quantity of cables, and their connection points (both at the pylon and the superstructure) were roughly estimated for the first, and essentially for the last time. The height and elliptical shape of the pylon were also determined. The cross-section of the stiffening girder was designed by considering and coordinating as many aspects as possible (*Fig. 1*).

The steel section of the stiffening girder was a beam grillage consisting of two box-girder longitudinal beams and the cross beams between them, which would later be covered with reinforced concrete. The final width of the box-girder was intended to be optimized in later stages of the design, reducing it as much as possible within the limits of the calculations. A composite stiffening girder was chosen because, unlike the original Esztergom Bridge, the span to be bridged was at the lower end of the economic range for cable-stayed bridges, and the heavier reinforced concrete deck could increase the weight and stiffness of the structure. I presented this design phase at the CCC2017 international conference, where the "impossible" opinion was heard for the second time (Teiter, 2017).

3. CONSTRUCTION DESIGN PHASE

Designing continued in 2018 when Duna Aszfalt Co. Ltd. won the tender for both the construction and the right to have a 3rd party to design the bridge for construction. The basis of the public procurement procedure was the approval design for the bridge, which meant that the tender design phase was skipped. As a result, the existing plans, although not mandatory in terms of details according to professional requirements, were legally "frozen" due to the tender process.

There was no longer any possibility to change the drawn - at that time still approximate - dimensions, cable layouts, and main details of the approved version, so the narrowing of the above-mentioned steel box couldn't be carried out.

According to the tender specifications, the contractor had 38 months to complete the project, during which time they had to have us prepare construction and fabrication designs from the approval designs. Typically, only this design phase would take 1.5-2 years in such cases.

When selecting the appropriate one from the initial study designs - which were essentially visual designs - and had us design the final approval version, our primary task was to pour the form into drawings and (according to the requirements) ensure the adequacy and feasibility of the main dimensions. The initial approximate designs that became mandatory were therefore not well thought out in many aspects (Teiter and Bedics, 2022)..

According to more experienced colleagues, the above-mentioned "impossible" level has become even more difficult. The main challenges were as follows:
- driven by the aesthetics, the usual backstay cable of cable-stayed bridges was not used, which made it difficult to stabilize the pylons;
- the cable anchoring cantilevers of the stiffening girder were located outside the cross-section, causing problems in taking up the horizontal components of the cable forces (it is not without reason that pedestrians usually walk outside the cable line);
- the introduction of the forces of these cantilevers into the steel-reinforced concrete composite stiffening girder had to be done by the steel structure only, which meant that the steel structure had to transfer unusual additional forces to the concrete deck slab;
- the aesthetic solution of the pylon-cable joint could only be achieved by anchoring the cables in the pylon or passing the cables through the pylon by a cable saddle (*Fig. 2*). The former was not possible due to space constraints, so the saddle had to be chosen, but then there could be no significant difference in the forces in the cables at the two sides, so complicated construction phases had to be incorporated in order to keep the proportions under control;
- by determining not only the amount of steel but also the camber of the steel structure due to the necessity of production at the beginning of the design, this already meant a constraint and a given for the further design period. As the different construction phases approached in time, they became more precise, additional demands and changes arose from the contractor, which also affected the cambering. Since we had already specified it earlier, production continued, we could "play" only with the remaining free parameters - primarily the magnitude and

Fig. 3: *Cable anchoring cantilever of the stiffening girder*

sequence of the stressing forces - to keep the cambered shape of the steel structure still appropriate.

- however, the variation with the stressing forces was restricted by keeping the displacements of the pylons within limits (see later in the construction technology) and by the ratio of the cable forces on both sides due to application of saddles in the pylon;
- the final cable stress was intended to be helped by the weight of the reinforced concrete deck slab, so the first stressing happened against only the relatively lighter steel structural part. In order to do this, at the specified stages of construction, we had to use such anchoring elements at the temporary lifting points next to the vertical bearings situated at the pylons that could be removed later;
- Sűsimilarly, for the reasons mentioned above, it was problematic that the inclined cables in the transverse direction applied a pulling effect on the outer upper flange of the steel main girder that was not stiffened. Thus, a stiffening system had to be found that prevented the upper flange from horizontal curving while only minimally increasing the amount of steel.

During the design period, we continuously sorted out the above and always focused on the most important ones and looked for the solution. Of these, the unique design of the cable connection cantilever of the stiffening girder is unique in our opinion. It is unusual, simple, yet rigid, and the result of our thorough research (*Fig. 3*).

Despite the constraints of the construction design phase, the engineering consulting firm, Speciálterv Ltd., which carried out the independent structural analysis of the bridge, examined various parabolic pylon shapes, most of which would have been structurally more favourable. However, for aesthetic reasons, we decided to insist on the half-ellipse form. Subsequently, Király's Scientific Student Research Project at the Department of Bridges and Structures at BME dealt with the shape of the pylon, revealing numerous advantages of curved pylons over shapes such as Λ, Π, etc (Király, 2021).

4. CONSTRUCTION

The pylon was made of solid reinforced concrete and was built by the subcontractor (A-HÍD Co. Ltd.) using a climbing

formwork, which was re-adjusted for each concrete placement phase. The ellipse started from two independent "legs", then at 3/4 of the total height, the legs were temporarily braced together to finish the peak (*Fig. 4*).

The placement of the saddles required exceptional precision in both during calculation and construction phases. When specifying their coordinates, it was necessary to take into account all the later displacements of the pylon legs until the finished state, and we had to ensure that their exit direction would point towards the cantilevers of the stiffening girder in the final state.

In order to protect the surrounding areas and to enable the parallel work necessary due to time constraints, the subcontractors (Hódút Kft., Steel-Millennium Kft.)

Fig. 4: *Pylon under construction*
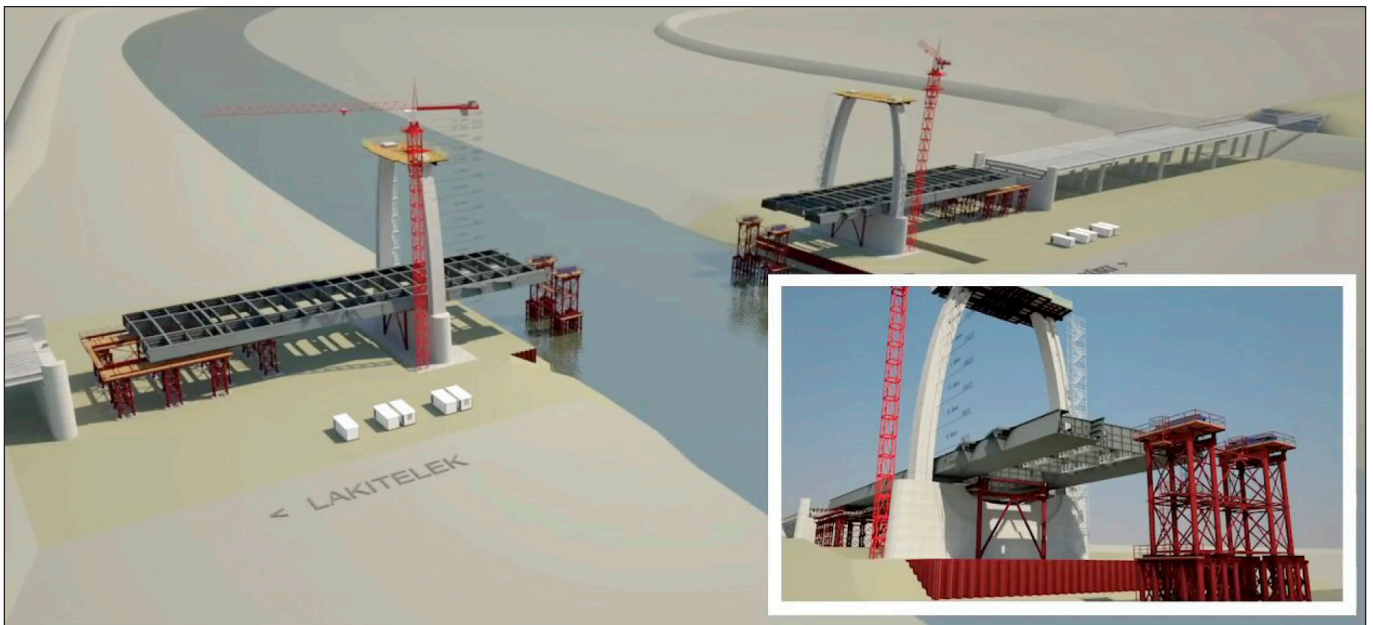
Fig. 5: *Parallel construction from four places*
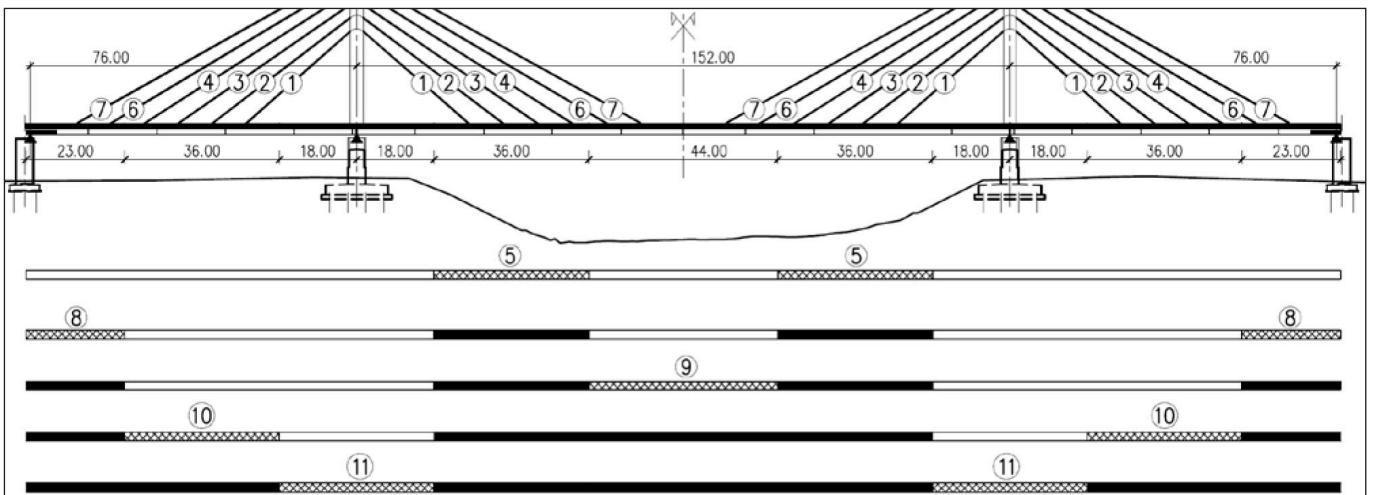
Fig. 6: *Construction stages: order of prestressing and concreting*

constructed the steel part of the bridge's stiffener girder at the same time by incremental launching from behind the pylons (*Fig. 5*). To help the launching, temporary supports were used in the first quarters of the bed width. When the steel structure met at mid-span, the connections were completed, and the final steel segment was built between the assembly-launching platform and the abutment in the outer spans.

Also, due to the need for parallel construction, it was required that the construction of the reinforced concrete pylon and the installation of the steel structure should not interfere with each other so that construction could proceed at four locations simultaneously, at the two pylons and from the launching platforms of the two sides.

After these, the cables were tensioned and the deck was concreted, both in multiple stages and partly overlapping each other for static reasons (*Fig. 6*). The effect of concreting of a composite superstructure in several stages was already well known (Teiter, 2008).

5. COMPLETED BRIDGE

The completed bridge shows a different image from every point due to the twisting cable surface in space. Travelers on the river see a cable-stayed bridge, while those driving on the

road see two arches whose cables embrace vehicles and lure them to pass under the pylon (*Fig. 7*). Eleonóra Balogh, a Hungarian award-winning glass artist and restorer, expressed it in a professional way: *"What a 'space graphics'... When the function and the structure draw the form in an authentic way, building from itself! ... The well-considered, self-building structure cannot make a formal mistake... such as nature...".*

6. CONCLUSIONS

In addition to its form (*Fig. 8*), the third cable-stayed river bridge in Hungary's bridge-building history displays many professional innovations. The concrete structure of the pylon is unique in our country. For the first time in Hungary, a larger bridge pylon was constructed with reinforced concrete without any tensioning elements. At the joining of the pylon and cables, a simple and clean appearance was maintained by implementing cable saddles, which otherwise caused many technical difficulties, and which was also unprecedented in the case of a Hungarian cable-stayed bridge.

The biggest professional challenge was the completion of the stiffening girder supporting the roadway. In Hungary, there has never been a cable bridge (be it an arch or a pylon structure) where such a stiffening girder was composite

Fig. 7: *View of the pylons from the bridge*

Fig. 8: *The bridge from the air after its opening*

(combining reinforced concrete slab and steel main girder). In addition to the construction difficulties, this structure - due to the concrete part - has time-dependent stiffness, and thus its deflection also constantly changes. Accordingly, the shape (vertical position) of the stiffening girder must be designed by taking into account the timing of the main construction phases, and its characteristics during its service life. Although this type of structure is cheaper, due to its complexity, riskiness, and a previous bad domestic example, most engineers are cautious about designing larger composite structures. This bridge is an example of how such a bridge can be built well. The bridge's stiffening girder and thus the vertical alignment of the road passing over it were realized with an accuracy of 1 cm.

7. ACKNOWLEDGMENT

Only a brief overview of the project could be provided here, which is obviously result of a teamwork. Information about the participants and many other details can be found on the *m44tiszahid.hu* website (articles, pictures, videos, reports, publications, etc., Teiter, 2021).

8. REFERENCES

Király, N. (2021), "Examination of cable-stayed bridges built with arched pylons", Students Scientific Paper, Budapest University of Technology, Budapest, 51 p. (in Hungarian)

Teiter, Z. (2021), https:\\m44tiszahid.hu (in Hungarian)

Teiter, Z., Bedics, A. (2022), "Design of a composite stiffening girdered cable-stayed bridge with arched reinforced concrete pylons", Proceedings of "Hidász Napok 2021" conference, Lánchíd füzetek 29., Debrecen, pp. 139-162. (in Hungarian)

Teiter, Z. (2017), "Spectacular Structure in an Economical Way", Proceedings of the 12th Central European Congress on Concrete Engineering, Budapest, pp. 493-500

Teiter, Z. (2008), "Hints for Designing Composite Beam Bridges - Summary and Conclusions of Composite Bridge Designs in Hungary", Proceedings of Eurosteel 2008: 5th European Conference on Steel and Composite Structures, Graz, pp. 1239-1244

Zoltán Teiter: Civil engineer, PhD, Honorary Associate Professor, Head of the Bridge Department of Uvaterv Co. Ltd. He has been working at the consulting firm Uvaterv for almost 30 years making renovations, studies, designs, inspections, and expertise of many bridges. He was an active participant in the Hungarian composite bridge construction renewal around the millennium. The pinnacle of his bridge design work was the subject of this article being awarded several prizes. From 2012 to 2023, he was responsible for and an instructor of bridge-related courses at the Department of Structural Engineering and Geotechnics at the Széchenyi István University in Győr. In 2017, he obtained his PhD with his thesis on "The Effect of Construction Technology on the Behavior of Composite Beam Bridges." He participates in the maintenance of domestic bridge regulations and is a member of the Hungarian National Group of *fib*. E-mail: teiter@uvaterv.hu

SIMULATING THE FLEXURAL PERFORMANCE OF ONE-WAY REINFORCED CONCRETE SLABS WITH OPENINGS STRENGTHENED BY THE USE OF CARBON FIBER REINFORCED POLYMER (CFRP)
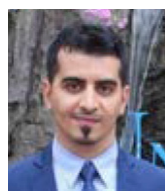
Wael S. Hameedi - István K. Völgyi – Waleed S. Hameedi

Over the past decade, the use of fiber-reinforced polymers (FRPs) as bonding agents to enhance and rehabilitate concrete structures has become widespread. Despite the demonstrated effectiveness of this approach in numerous experimental studies, there are still concerns about the time and expense required for these investigations. To address this issue, The objective of this study was to investigate how the carbon fiber-reinforced polymer (CFRP) reinforcement affects the bending performance of one-way reinforced concrete slabs using advanced finite element software (ABAQUS). To investigate the impact of various factors on slab performance, two models of one-way RC slabs were developed, taking into account concrete grade, number of CFRP layers, and opening size (600x600mm). By comparing the results obtained in this study with existing experimental data, the findings indicated that the approach adopted in this research could offer a cost-effective and efficient way to evaluate the performance of FRP-strengthened concrete structures.

Keywords: *Carbon fiber reinforced polymer (CFRP); Strengthening; Finite element analysis (FEA); one-way RC slab*

1. INTRODUCTION

FRP's (Fiber Reinforced Polymers) have been widely employed in recent times for the purpose of strengthening or reinforcing structural components, whether by externally wrapping them with sheets or using them as internal reinforcement. Additionally, the methods that use externally bonded FRP materials are the most commonly used techniques for upgrading and reinforcing existing structures that have been damaged (Al-Amery and Al-Mahaidi 2006). This is because they possess a high ratio of strength to weight, are highly rigid, can be easily installed, and maintain a stable shape throughout their operational lifespan (Costa and Barros 2010), (Rafi et al. 2008), (Benjeddou et al. 2007).

Many studies (Kim and Shin 2011), (Toutanji et al. 2006), (Anania et al. 2005), (Li et al. 2008), (Gao et al. 2005), (Ceroni 2010), (Rafi et al. 2008), (Benjeddou et al. 2007) have been conducted on reinforced concrete (RC) beams that were reinforced using FRP sheets in order to enhance their flexural strength. This was achieved through experimental, finite element, and analytical methods. The findings of these studies indicate that the use of FRP to reinforce beams in flexural strengthening can prevent debonding failure if a properly designed anchorage is implemented (Kim and Shin 2011), (Rafi et al. 2008), (Ceroni 2010), (Esfahani et al. 2007), (Chajes et al. 1994), (Wenwei and Guo 2006). This provides a favorable level of both strength and ductility when subjected to flexural stress. Concrete slabs, on the other hand, are a common building element used in various construction projects, ranging from residential buildings to commercial facilities. These slabs can sometimes have openings or penetrations, such as for ducts, pipes, or other services.

However, these openings can weaken the overall structural integrity of the slab and compromise its load-carrying and energy dissipation capabilities, stiffness, and ductility of the slabs (Anil et al. 2013). To ensure the strength and stability of the slab with openings, various repair and strengthening techniques are employed. One effective method for strengthening concrete slabs with openings is the use of Carbon Fiber Reinforced Polymer (CFRP) sheets. CFRP sheets are made of high-strength carbon fibers embedded in a polymer matrix, which provides exceptional tensile strength, stiffness, and durability. The use of CFRP sheets for concrete slab strengthening has gained significant attention in recent years due to their high strength-to-weight ratio, ease of installation, and durability. By applying CFRP sheets to concrete slabs with openings, their load-carrying capacity and overall performance can be significantly improved, ensuring the structural integrity of the slab and extending its lifespan. Despite the many benefits of using CFRP to strengthen one-way RC slabs, most research in this area is based on experimental studies and numerical modeling has been limited. Civil engineering departments at universities could greatly benefit from further research into the use of CFRP, exploring its advantages and disadvantages and the impact on the flexure and shear capacity of structural members. Additionally, further research could lead to reduced cost, time, and work required for experimental studies.

One of the first studies that focused on concrete slab strengthening was Ebead and Marzouk (2004), which investigated nine square slabs with dimensions of 1.90 m and thickness of 0.15 m. The slabs had different amounts of reinforcement and were simply supported along the edges with free corners. They were loaded through the column stub

at the center. The authors found that failure mode depended on the reinforcement ratio, with slabs having less than or equal to 0.5% reinforcement failing in flexure and those with 1.0% or more failing due to punching shear. The lowest first crack loads were observed for slabs with a reinforcement ratio of 0.35%, while the use of CFRP and GFRP slightly increased the equivalent reinforcement ratio. As the reinforcement ratio increased, deflection values decreased, with a decrease from 42 to 24 mm for ratios of 0.35% to 1.0%. The load-deflection curve for flexural strengthening specimens had a higher slope than that of the reference specimens, and their average deflection at ultimate load was approximately 0.6 that of the reference specimens. Flexural strengthening specimens also experienced less deformation due to the effect of the FRP materials on the overall behavior of the slabs in relation to punching-shear strengthening. Furthermore, a study was conducted by Smith and Kim (2009), which comprehensively explored the use of (FRP) composites in strengthening one-way reinforced concrete slabs with central holes. The study involved testing four wide slabs with cut-outs and two narrow slabs without cut-outs to evaluate the impact of different load application positions on the performance of the slab. The results of the study were impressive, with all of the FRP-strengthened slabs exhibiting a higher load-carrying capacity compared to their unstrengthened counterparts. However, the failure mode in all cases was debonding at intermediate cracks, which were found to be diagonal and originating from the corners of the cut-outs of the slabs. This study did not only assess the load-carrying capacity of the FRP-strengthened slabs but also examined how this strengthening method could distribute stresses around the holes in RC structures, the failure mechanisms, and the pre and post-debonding behavior of the strengthened structures. To achieve this, the researchers recorded strains on the FRP, concrete, and internal steel reinforcement, as well as deflections at different positions on the slab surfaces. Overall, this study provided valuable insights into the effectiveness of FRP composites in strengthening concrete slabs with central holes and highlighted the importance of considering failure modes in the design process. in addition to their experimental work a finite element model was created to predict the ultimate moment of resistance around crucial crack lines, and it was discovered that the model's predictions closely aligned with the experimental outcomes. The model successfully accounted for the varied bending behaviors of the slabs and the debonding failure of the reinforced slabs, indicating its suitability for application in future strengthening initiatives.

Last but not least Anil et al. (2013) conducted research on the flexural Performance of one-way RC slabs that were strengthened using CFRP strips. The study focused on the impact of the size and location of openings in the slab on its behaviour. Three square openings with side lengths of 300 mm, 400 mm, and 500 mm were examined and placed in either the bending or shear zone. 13 slabs were examined, with one serving as a reference, six without CFRP strengthening, and six with CFRP reinforcement around the opening. The study found that the use of CFRP strips greatly increased the load-carrying capacity and stiffness of the specimens, and the technique could be quickly and cost-effectively applied during construction or while the structure was in use, without disturbing occupants. Nevertheless, there has been no numerical analysis conducted on this research in order to investigate additional parameters, while minimizing the need for expensive and time-consuming experimental work.

2. METHODOLOGY

Structural engineering often utilizes finite element analysis to gather valuable information on structure stress and strain distribution. This information is not readily available through experimental means, and numerical investigation can provide complementary data for better understanding. Additionally, finite element models can be subjected to parametric studies to optimize a structural design. Advances in FE formulation have resulted in sophisticated algorithms capable of handling complex geometries, contact interactions, plasticity, and large deformations (Starossek et al. 2010). In this chapter, three-dimensional finite element simulations with nonlinear characteristics were produced employing the commercially available ABAQUS/Standard 6.13 program.

In this study, two models of one-way reinforced concrete slabs were analyzed. The first model, referred to as Slab1, was a control slab with a 500×500 mm opening located at the region with maximum moment. The second model, Slab2, was identical to the first but was strengthened by adding CFRP strips. Both slabs were simply supported with dimensions of 3000×1000×150 mm in length, width, and depth respectively.

Anil et al. (2013) conducted an experiment aimed at investigating the flexural behavior of one-way reinforced concrete slabs that contained structural holes, and to assess the impact of (CFRP) strengthening on this behavior. The experimental setup involved the use of eleven steel rebars of Ø10 for main reinforcement, and transverse reinforcement was provided with Ø10 steel rebars that were spaced at 250 mm. To simulate a real-world scenario, the reinforcement around the opening was removed. The slab specimens underwent a four-point loading examination where the ratio between the shear span and the effective depth was 7. The load on the separator beam›s center was evenly divided and applied as two concentrated loads, allowing for the assessment of the slab›s flexural strength and behavior under load. The experimental results were analyzed to evaluate the effectiveness of the CFRP stips strengthening in improving the flexural behavior of the slabs, and to identify any potential issues that may arise when using such reinforcement in practice. *Figs. 1 and 2* show the arrangement of loading, reinforcement specifications, and dimensions of the specimens.

CFRP strengthening scheme of specimen Slab2 is shown in *Fig. 3*.

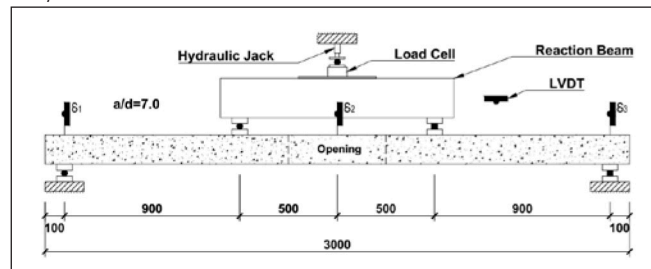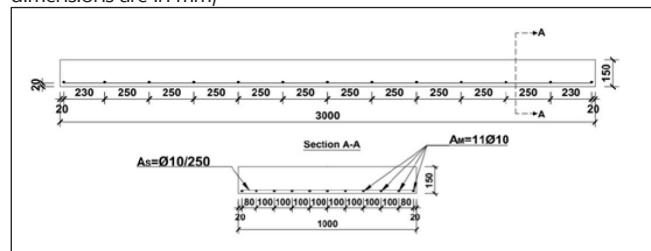**Fig. 1:** *Load configuration for all slab samples (all dimensions are in mm)*

Fig. 2: *Reinforcement details and dimensions of the specimen (all dimensions are in mm)*
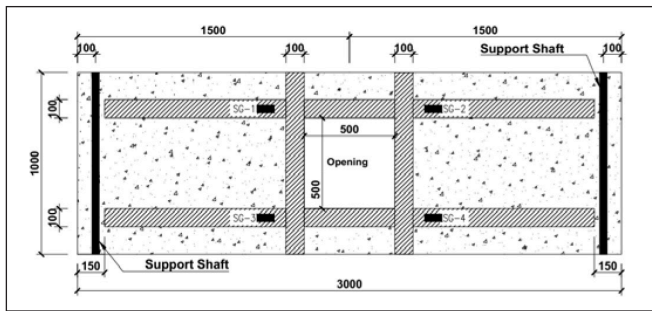
Fig. 3: CFRP Strengthening scheme of Slab2 (all dimensions are in mm)

2.1 Finite Element Analysis

Because of the simplicity of the examined specimen, it was possible to model it as a full-scale slab without being segmented for its symmetry. However, some measurements of the loading rods, support rods, loading plate, and reaction beam were missing from the experimental details. To overcome this challenge, these unknown measurements were estimated systematically to produce results that were as close as possible to the experimental results. The estimated dimensions can be seen in *Fig. 4*. Concrete, loading rods, support rods, loading plate, and reaction beam were modeled using the three-dimensional eight-node element (C3D8), reinforcement was modeled using the three-dimensional two-node truss element (T3D2), and the CFRP strips were modeled using a 4-node shell element (S4R).

A convergence study was conducted on the full-scale slab model to determine the optimal mesh density. This is accomplished by decreasing the mesh size and observing the resulting changes in the ultimate load. The RC slab was modeled with mesh sizes 120, 100, 60, 40, and 30 mm, *Fig. 5* shows that the difference in the ultimate load was negligible when the mesh size was reduced from 40 mm to 30 mm. As a result, the 40 mm model was selected for all slabs, as depicted in *Fig. 6*.

Fig. 4: Estimated dimensions in mm
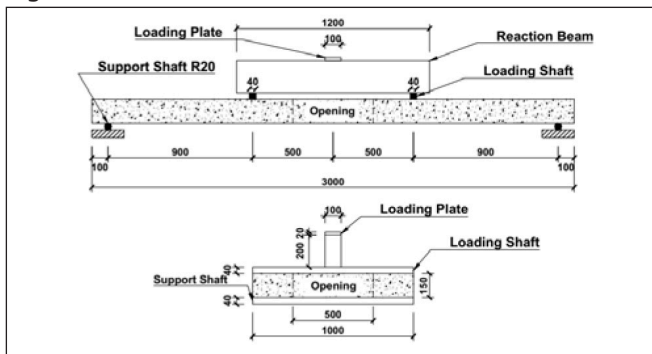
Fig. 5: Convergence study results
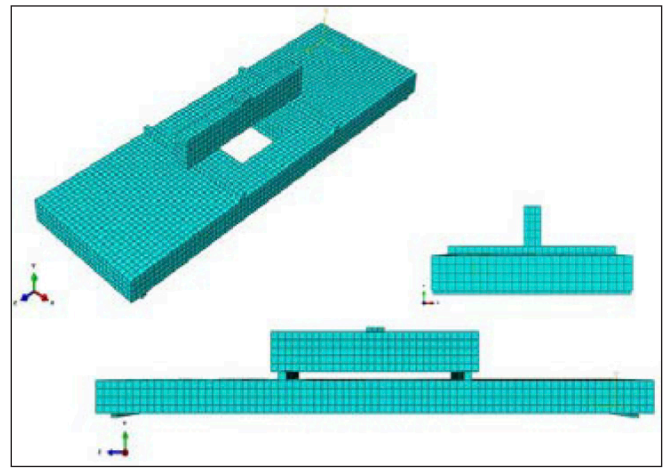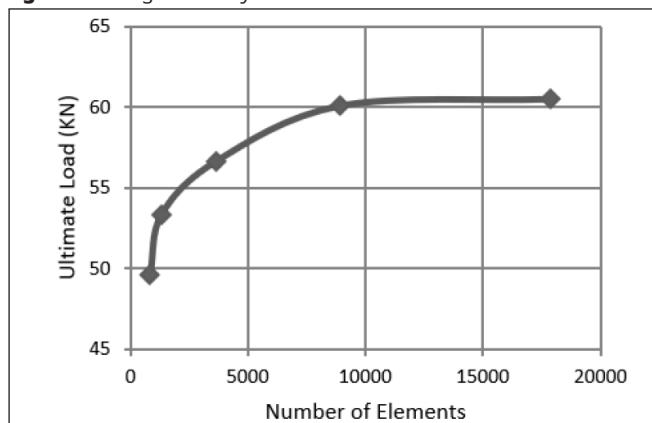
Fig. 6: Finite element mesh

2.2. Loading and boundary conditions

In the numerical analysis, a uniform load was applied to the loading plate, which transferred the load to the reaction beam. The reaction beam then divided the load into two equal parts that acted on the loading shafts. The load was ultimately transferred to the top surface of the simply supported slab. To model the interaction between the loading plate, reaction beam, loading shafts, and concrete, a surface-to-surface contact was used.

It is important to note that the bond between the CFRP strips and the concrete slab was perfect, and the adhesive layer was not considered in the numerical analysis . This was because the primary failure mechanism observed in the strengthened slabs, as detailed in the investigations by Anil et al. (2013), was the failure of the CFRP material itself (as depicted in *Fig. 7*); so, there is no need to model the bonding material between CFRP and RC slab surfaces. To accurately simulate the system, the supporting rods were fixed at their lower surface, preventing any movement in any direction, while the upper surface of the loading plate was fixed in all directions except for vertical displacement. The lateral faces along the length of the slab were restricted horizontally from movement in the X-direction and from rotating in the Y and Z-directions.

2.3 Characteristics of Materials and Assumed Parameters

In this paper, two specimens from the experimental test with the same opening size have been used: the first is without CFRP strengthening and compared with FEM model Slab1, and the second is with CFRP strengthening and compared with FEM model Slab2. The material properties used in the analysis of the slabs are listed in *Tables 1 and 2*, which detail the properties of the concrete, reinforcement, and CFRP fabric. However, certain properties, like steel's Young's Modulus, had to be estimated and were assumed to fall within the range of 200 to 210 GPa, as their exact values were deemed to have an insignificant impact on the result of the study.

3. ANALYSIS RESULTS

Finite element analysis is a powerful tool in the field of structural engineering that can provide valuable insights into the stress and strain distributions within structures. Unlike experimentation, numerical simulations can capture a range

of detailed information, which can serve as complementary data to enhance understanding. Moreover, the use of finite element models allows for the exploration of a variety of model parameters through parametric studies, thus improving the design process. In this chapter, we employ ABAQUS, a commercially available simulation software, to develop 3D, materially nonlinear finite element models. These models are designed to accurately capture the sophisticated behaviors of the structures under study and provide an effective means of predicting their performance.

Table 1: Concrete characteristics

Slab1		
Modulus of elasticity (MPa)*	E_c	19661
Compressive strength (MPa)	f'_c	17.5
Tensile strength (MPa)**	f_t	1.38
Poisson's ratio***	v_c	0.2
Slab2		
Modulus of elasticity (MPa)*	E_c	21071
Compressive strength (MPa)	f'_c	20.1
Tensile strength (MPa)**	f_t	1.48
Poisson's ratio***	v_c	0.2

* $E_c = 4700\sqrt{f'_c}$ ** $f_t = 0.33\sqrt{f'_c}$ *** Assumed value

Table 2: Main, transverse reinforcement bars and CFRP fabric characteristics

Main and distribution reinforcement bars		
Modulus of elasticity (GPa)*	E_s	200
Steel yield strength (MPa)	f_y	480
Ultimate tensile strength (MPa)	f_{pu}	627
Poisson's ratio*	v_s	0.3
Bar cross-sectional area (mm²)	A_s	78.5
CFRP sheet		
Thickness (mm)	t	0.12
Poisson's ratio*	v_f	0.3
Young's modulus (GPa)	E_f	231
Tensile strength (MPa)	f_y	4100

* Assumed value

3.1   Analysis results of RC Slab1

Fig. 8 compares the load-deflection curves obtained from the experimental test and the finite element analysis for RC Slab1. The results from the numerical simulation are in close alignment with the experimental findings throughout the entire loading process. However, a slightly stronger numerical response can be observed near the maximum load. The predicted maximum load of 61.6 kN is slightly higher than the experimental value of 60 kN, with a difference of 2.66%. The calculated maximum deflection of 98.9 mm is also slightly higher than the experimental value of 98.7 mm, with a difference of 0.19%. *Fig. 9* shows the distribution of the plastic strain of Slab1 at the maximum load. The figure suggests that the areas with the highest plastic strain are the zones most impacted by the loading and that cracks are likely to form in these areas.

Fig. 7: Example pictures for CFRP failures
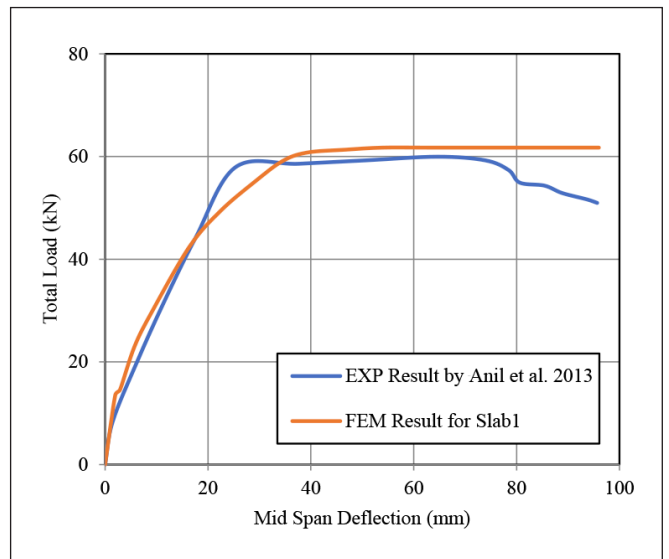
Fig. 8: Exp. and num. load-displacement curve of Slab1 without CFRP strengthening

3.2   Analysis results of RC Slab2

The load-deflection behavior of RC slab2 reinforced with CFRP strips is depicted in *Fig. 10*. The experimental and analytical results show good agreement throughout the loading range, with a slightly stiffer response observed in the experimental data at stages close to ultimate load. The experimental ultimate load was found to be 93.8 kN, while the numerical result was 88.7 kN, resulting in a difference of 5.58% between predicted and actual values. Additionally, the experimental ultimate deflection of 93.2 mm was marginally higher than the numerical result of 92.9 mm, with a difference percentage of 0.32%. *Fig. 11* presents the magnitude of the plastic strain of Slab2 at the ultimate load, indicating that areas with the highest plastic strain are susceptible to cracking and are the most influenced zones.

4.   PARAMETRIC STUDY

The objective of this study is to investigate the effect of various parameters on the flexural behavior of reinforced concrete (RC) slabs that are reinforced with (CFRP) strips. To achieve this, a thorough parametric analysis was conducted to assess the influence of three key parameters: the number of CFRP strip layers, concrete compressive strength, and different size of the opening (600×600 mm).

Each parameter was examined in isolation, with all other
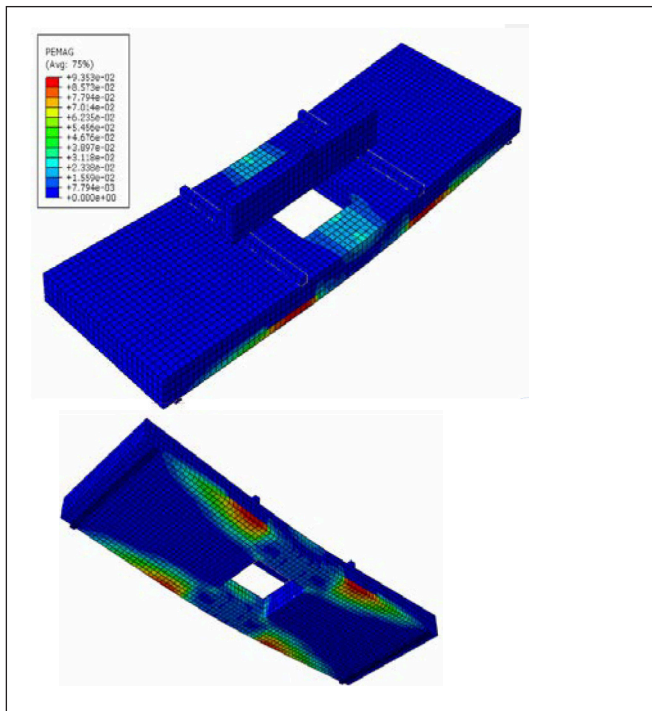
Fig. 9: *Plastic strain magnitude of Slab1 at ultimate load*
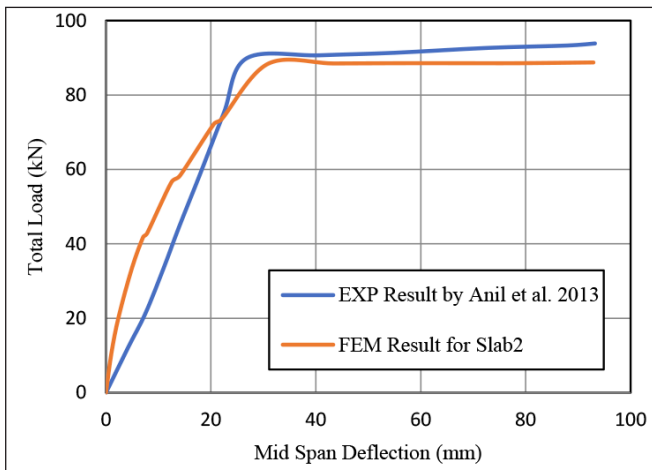
Fig. 10: *Exp. and num. load-displacement curve of Slab2 with CFRP strengthening*
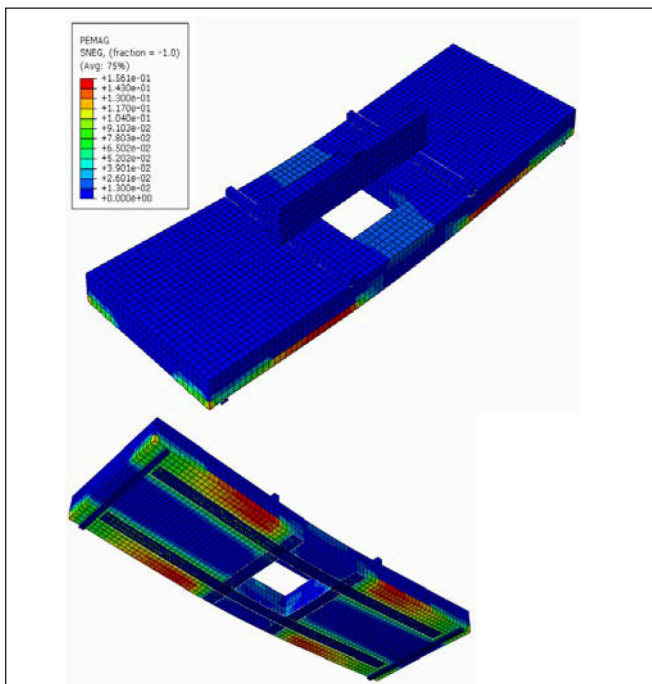
Fig. 11: *Magnitude of plastic strain for the specimen Slab2 at maximum load*

variables held constant to accurately evaluate the impact of the specific parameter on the behavior of the slab. The numerical tests were designed to comprehensively analyze the flexural behavior of the RC slabs reinforced with CFRP and to gain a deeper understanding of the underlying mechanics of the system. The results of this study will provide valuable insights for the design and construction of reinforced concrete structures that utilize CFRP reinforcement, and will aid in the development of more efficient and reliable structural systems.

4.1 Influence of adding additional layers of CFRP strips

During the actual experimental test, a single layer of CFRP strips was utilized for Slab2. In order to investigate the impact of adding more layers of the CFRP strips on the behavior of Slab2, it was modeled by adding a second CFRP sheet on top of the existing sheet in the finite element analysis, and identified as Slab3. The results obtained from the numerical simulation are presented through the load-deflection curves depicted in *Fig. 12*. These findings provide valuable insights into the effectiveness of using double layers of CFRP and can assist in optimizing the design of reinforced concrete structures with openings.

Alternatively, numerical results demonstrate a clear relationship between the number of CFRP layers and the ultimate load capacity of Slab2. Specifically, as the number of CFRP layers increases from 1 to 2, there is a noticeable increase in the ultimate load capacity. In fact, the increment in ultimate load capacity is approximately 10%, indicating a significant improvement in structural performance. These findings highlight the importance of considering the number of CFRP layers when designing and assessing the load-bearing capacity of reinforced concrete structures.
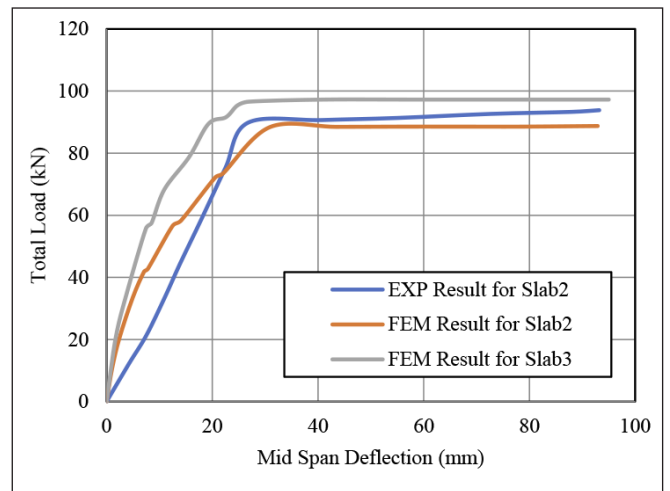
Fig. 12: *Load-deflection diagram based on FEM analysis for Slab2 with single CFRP layer compared to Slab3 with double CFRP layers*

4.2 Influence of different concrete compressive strength

A parametric study was conducted to investigate the effects of concrete grade on Slab2 performance. The purpose of this study is to assess the precision of the finite element analysis, and it's not intended to reflect realistic conditions, since the compressive strength of the tested slab can not be changed. *Fig. 13* sheds light on how different concrete grades affect the load-deflection response of Slab2. Our study evaluated the
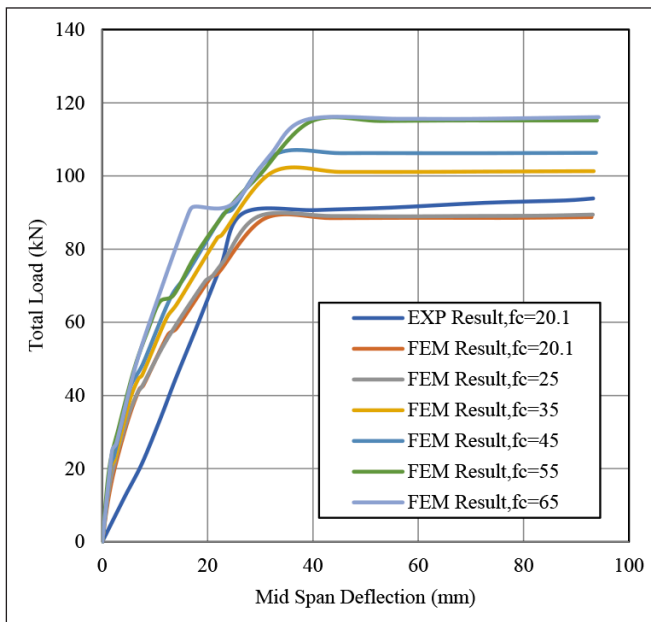
Fig. 13: *Influence of concrete compressive strength on the load-displacement curve of the Slab2*

Fig. 14: *Load-deflection diagram based on FEM analysis for Slab2, Slab4 and Slab5*

impact of five concrete compressive strengths, ranging from 25 to 65 MPa, on the slab's performance. It was observed that as the compressive strength of the concrete increased, so did its ultimate load-bearing capacity as expected.

Compressive strength is the most important parameter of the concrete material, influencing its various other properties, including tensile strength, bending strength, shear resistance, and bond with reinforcement bars. The higher the compressive strength, the better the concrete performs, resulting in up to 30% higher failure loads.

In conclusion, the results of our study highlights the importance of using higher-grade concrete in construction projects, as it leads to improved load-deflection response and general performance of Slab2. Further enhancements are required in the finite element model to accurately capture the debonding failure between the RC slab and the CFRP sheets. Additionally, incorporating the debonding behavior especially into this parametric investigation will yield distinct and more accurate outcomes.

4.3 Influence of different hole sizes

This study analyzed the impact of a larger opening size on the performance of a reinforced concrete slab using FEM modeling. A 600×600 mm opening has been made at the maximum moment region in the model referred to as Slab4 without externally strengthening the opening's edges by CFRP strips, while strengthened one referred to as Slab5, bothspecimens subjected to the same loading conditions, material properties, reinforcement specifications, boundary conditions, mesh density, and CFRP strip thickness as the previously analyzed Slab2.

This section aimed to numerically evaluate the effectiveness of using CFRP strips to strengthen a one-way reinforced concrete slab with a larger opening. Cutting a 600×600 mm hole at the maximum moment region of the reference slab, which was examined in previous experimental work (Anil et al. 2013), will reduce its load-bearing capacity by 44%, i.e., the opening will result in less main reinforcement, so the last will yield at a lower load level. Although applying CFRP strips using the same scheme applied to Slab2, as shown in Fig. 3, on the edges of the opening as a strengthening technic will increase the slab carrying capacity by 25%. It should be
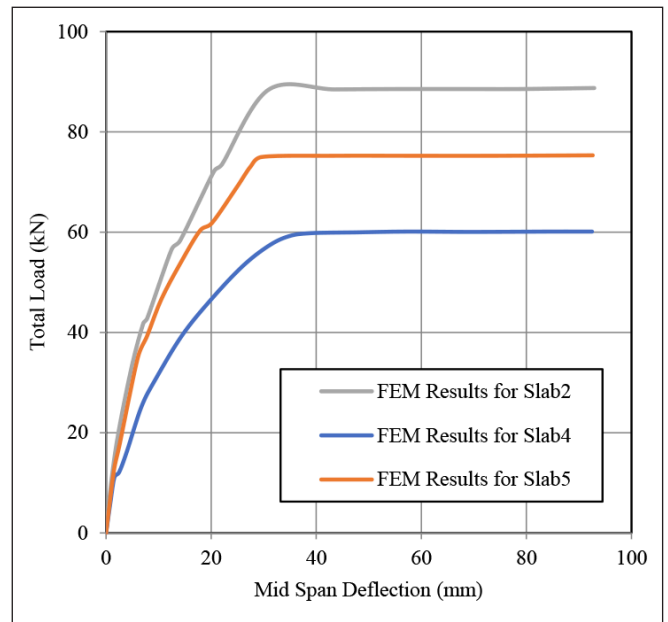
pointed out that this strengthening method can restore about one-third (33%) of the original strength of the reference slab that was compromised due to the hole. Moreover, a comparison of the load-deflection curves between Slab2 and Slab4 with different opening sizes, as shown in *Fig. 14,* Indicates that increasing the size of the opening to 600×600mm would result in a reduction of the load-bearing capacity by 15%. These results highlight the importance of proper strengthening techniques in RC slabs with larger openings.

5. CONCLUSIONS

This study aims to investigate the impact of using Carbon Fiber Reinforced Polymer (CFRP) strips on the flexure behavior of Reinforced Concrete (RC) slabs. Utilizing the ABAQUS 6.13 software, numerical simulations were carried out to predict the overall flexural Performance of the strengthened slabs. The use of CFRP on the external surface of RC slabs has been acknowledged as an effective method of enhancing the behavior and strength of these structures. In general:

1. The load-midspan displacement curves from the simulation results match the experimental data for all specimens analyzed in this paper. The ultimate loads obtained through numerical analysis varied from the experimental ultimate loads by 1% to 6%, in other words, this high percentage indicates that the finite element model is sufficiently accurate to produce outcomes that are very similar to those obtained through experimental work.

2. The ultimate load capacity of Slab2 can be affected by the compressive strength of the concrete, as suggested by the numerical simulations. The results demonstrate that a higher concrete compressive strength, such as 65 MPa compared to 25 MPa, can result in a 30% increment in the ultimate load capacity of the slab.

3. The numerical analysis results indicated that adding an extra layer of CFRP strips to Slab2 led to a 10% increase in the ultimate load capacity.

4. The study revealed that when removing a 600×600 mm hole from the middle of the monolithic slab that was previously tested, its load-bearing capacity will decrease

by 44%. This occurs because the hole reduces the amount of tension reinforcement, causing it to fail at a lower load level. However, strengthening the opening edges with CFRP strips will increase the slab›s load-carrying capacity by 25%. Additional research is necessary to determine the precise quantity of CFRP strips needed to completely restore the flexural capacity of slabs with openings to their initial states prior to the removal of the hole.

6. REFERENCES

Al-Amery R, Al-Mahaidi R (2006) Coupled flexural–shear retrofitting of RC beams using CFRP straps. Compos Struct 75:457–464. https://doi.org/10.1016/J.COMPSTRUCT.2006.04.037

Anania L, Badalà A, Failla G (2005) Increasing the flexural performance of RC beams strengthened with CFRP materials. Constr Build Mater 19:55–61. https://doi.org/10.1016/J.CONBUILDMAT.2004.04.011

Anil Ö, Kaya N, Arslan O (2013) Strengthening of one way RC slab with opening using CFRP strips. Constr Build Mater 48:883–893. https://doi.org/10.1016/J.CONBUILDMAT.2013.07.093

Benjeddou O, Ouezdou M Ben, Bedday A (2007) Damaged RC beams repaired by bonding of CFRP laminates. Constr Build Mater 21:1301–1310. https://doi.org/10.1016/J.CONBUILDMAT.2006.01.008

Ceroni F (2010) Experimental performances of RC beams strengthened with FRP materials. Constr Build Mater 24:1547–1559. https://doi.org/10.1016/J.CONBUILDMAT.2010.03.008

Chajes MJ, Thomson TA, Januszka TF, Finch WW (1994) Flexural strengthening of concrete beams using externally bonded composite materials. Constr Build Mater 8:191–201. https://doi.org/10.1016/S0950-0618(09)90034-4

Costa IG, Barros JAO (2010) Flexural and shear strengthening of RC beams with composite materials – The influence of cutting steel stirrups to install CFRP strips. Cem Concr Compos 32:544–553. https://doi.org/10.1016/J.CEMCONCOMP.2010.03.003

Ebead UA, Marzouk H (2004) Fiber-Reinforced Polymer Strengthening of Two-Way Slabs FEM Analysis for UHP-FRC subject blast loading View project Thin Laminated Cement-Based Composites for Rehabilitation and Strengthening Existing Structures View project. ACI Struct J 101:

Esfahani MR, Kianoush MR, Tajari AR (2007) Flexural behaviour of reinforced concrete beams strengthened by CFRP sheets. Eng Struct 29:2428–2444. https://doi.org/10.1016/J.ENGSTRUCT.2006.12.008

Gao B, Leung CKY, Kim JK (2005) Prediction of concrete cover separation failure for RC beams strengthened with CFRP strips. Eng Struct 27:177–189. https://doi.org/10.1016/J.ENGSTRUCT.2004.09.007

Kim HS, Shin YS (2011) Flexural behavior of reinforced concrete (RC) beams retrofitted with hybrid fiber reinforced polymers (FRPs) under sustaining loads. Compos Struct 93:802–811. https://doi.org/10.1016/J.COMPSTRUCT.2010.07.013

Li L, Guo Y, Liu F (2008) Test analysis for FRC beams strengthened with externally bonded FRP sheets. Constr Build Mater 22:315–323. https://doi.org/10.1016/J.CONBUILDMAT.2006.08.016

Rafi MM, Nadjai A, Ali F, Talamona D (2008) Aspects of behaviour of CFRP reinforced concrete beams in bending. Constr Build Mater 22:277–285. https://doi.org/10.1016/J.CONBUILDMAT.2006.08.014

Smith ST, Kim SJ (2009) Strengthening of one-way spanning RC slabs with cutouts using FRP composites. Constr Build Mater 23:1578–1590. https://doi.org/10.1016/J.CONBUILDMAT.2008.06.005

Starossek U, Falah N, Lohning T (2010) Numerical analyses of the force transfer in concrete-filled steel tube columns. Structural engineering and mechanics : An international journal 35:241–256

Toutanji H, Zhao L, Zhang Y (2006) Flexural behavior of reinforced concrete beams externally strengthened with CFRP sheets bonded with an inorganic matrix. Eng Struct 28:557–566. https://doi.org/10.1016/J.ENGSTRUCT.2005.09.011

Wenwei W, Guo L (2006) Experimental study and analysis of RC beams strengthened with CFRP laminates under sustaining load. Int J Solids Struct 43:1372–1387. https://doi.org/10.1016/J.IJSOLSTR.2005.03.076

Wael S. Hameedi (1988) MSc structural engineer at Budapest University of Technology and Economics. Currently pursuing his Ph.D. studies at the Department of Structural Engineering, Budapest University of Technology and Economics. Research fields: Strengtheneing of structural members using FRP's composites, and bolt connections between reinforced concrete beams. A member of the Iraq Engineers Association. E-mail: wael.hameedi@edu.bme.hu

István K. Völgyi He made his MSc and Ph.D. at the Budapest University of Technology and Economics, Hungary, where he serves as an associate professor. He is a member of the *fib* and standardization committees of MSZT and MAÚT. E-mail: volgyi.istvan@emk.bme.hu

Waleed S. Hameedi (1985) MSc Architecture Design at University of Technology-Malaysia. Currently pursuing his Ph.D. studies at the Department of Architecture, University of Technology-Malaysia. Research fields: Environmental engineering and sustainable design approaches. A faculty member of the collage of engineering - University of Al-Qadisiyah and member of Iraq Engineers Association.

COMPARING THE EUROPEAN STANDARDS AND THE AMERICAN STANDARDS FOR TESTING CONCRETE MECHANICAL PROPERTIES

Ahmed M. Seyam – Rita Nemes

Europe and the United States have a worldwide significance in the field of concrete control and construction, as well as the cleared and specified standards, according to many countries adopted their standards and regulations in the field of concrete quality control and assurance as proof of the Europe and US strong standards and due to lack of their regulations. This research compares the European standards, the American Society for Testing and Materials (ASTM) and American Concrete Institute (ACI) standards for testing the mechanical properties of concrete. The research focuses on compressive strength, flexural tensile strength, shear strength, and modulus of elasticity as key properties for assessing the quality and performance of concrete. The study found variations in the specimen size, preparation, and curing requirements, as well as testing procedures and acceptance criteria among the European, ASTM and ACI standards. The research also compared the specimen preparation and curing standards among the different standards. The research highlights the importance of following the appropriate standards and testing procedures to ensure the test results' reliability and accuracy. Proper specimen preparation and curing are also critical to obtain accurate and representative test results. The research concludes that by following the relevant standards and procedures, it is possible to obtain consistent and reliable results that can be used to assess the quality and performance of concrete in various construction applications. This research provides a useful guide for engineers, contractors and researchers involved in the construction industry to understand and apply the standards for testing the mechanical properties of concrete.

Keywords: *ACI, ASTM, European standards, mechanical properties, testing*

1. INTRODUCTION

Concrete is the most used material worldwide, surpassed only by water consumption. Concrete production greatly impacts the global economy (Gavilan & Luiz Carlos, 2018). (Miller et al., 2016) calculated the annual concrete consumption of 10,058 million cubic meters. The production of high-quality concrete requires specific knowledge and abilities. From the careful selection of constituent materials and their compatibility through production, placement, and work hardening, a lengthy procedure of trial and testing leads to the conformance evaluation. Depending on the material's nature, laboratories for building materials undertake these tests with varying characteristics, functions, and limits. The mechanical and durability properties of concrete mixtures can be adjusted to meet the design specifications of construction. The compressive strength of concrete is the most common performance measure used by engineers to determine if the concrete is structurally acceptable or not. After the concrete has hardened, it is typically required to examine the structure to verify if it is sufficient for its intended use. Various tests and examinations could be made to check this acceptability. Concrete mechanical properties play the primary control role in concrete quality control and assurance regarding bearing capacity, lifetime and durability. Concrete strength tests are performed for several reasons (Mindess et al., 2003a). For research purposes, physical laws and properties investigation. During construction, an estimate of the in-situ strength of concrete may be desired for determining the safe time to strip forms or to proceed with further work. The adequacy of mix proportions may need to be verified. And for quality control, part of the quality aspect is the determination of the acceptability of concrete (Neyestani, 2011).

Testing the mechanical properties of concrete is an essential aspect of evaluating the quality and performance of concrete mixes. The mechanical properties of concrete, such as compressive strength, flexural tensile strength, shear strength and modulus of elasticity, are related to the performance and durability of concrete structures and are used to ensure that concrete meets the required specifications. The importance of standardization in concrete testing cannot be overstated. A number of standards have been developed by organizations such as the European Union (EU), the American Society for Testing and Materials (ASTM), and the American Concrete Institute (ACI) to ensure consistency and accuracy in concrete testing. These standards specify the procedures and tolerances for testing the mechanical properties of concrete and are widely adopted in many regions worldwide. European and American consumptions correspond to approximately 9% of this total amount, but their regulations are widely

adopted in many other countries worldwide. Despite the widespread adoption of these standards, comparative studies related to concrete strength testing codes, standards, and specifications are uncommon in the available literature. While several studies have highlighted the European or American standards, with a comparison of testing results, a few studies have considered the difference between those standards, the specimen shapes, the testing conditions, procedures, and the special considerations.

This paper discusses the main variations and differences between testing the compressive strength, flexural tensile strength, and modulus of elasticity of concrete according to EU, ASTM, and ACI standards. It will provide an overview of the testing procedures and requirements specified in each standard and compare the differences and similarities between the standards. Understanding these variations and differences is essential for professionals in the construction industry who use these standards to evaluate the quality of concrete mixes and design concrete structures.

2. TESTING OF THE MOST COMMON MECHANICAL PROPERTIES

2.1 Specimens preparations

The preparation of concrete specimens is a crucial step in evaluating the mechanical properties of concrete and ensuring compliance with the relevant standards. In this regard, several standards have been established as the ASTM C192 (ASTM international, 2002), the ACI 308 and the EN 12390-1 (European Standards, 2003a). These standards outline the procedures and tolerances for the preparation of concrete specimens in the laboratory or on-site, ensuring consistency and reliability in the testing process. Adhering to these standards guarantees accurate evaluation of the properties of the concrete mix and compliance with the relevant specifications for the specific application. Failure to adhere to these standards may result in variations in the preparation of concrete specimens, leading to inconsistent and unreliable test results and potentially the use of substandard concrete in construction. One main difference between these standards is the type of curing methods allowed, with ASTM and ACI allowing for the use of moist rooms, water tanks, and membranes. At the same time, the EU standard also allows for the use of curing compounds and the application of heat. Another difference is the minimum curing time and temperature requirements, with ACI specifying more stringent requirements than the other two standards.

2.2 Curing

Concrete curing is the process of maintaining a moist and favourable environment for the newly placed concrete to allow it to harden properly and gain strength. Several standards specify the procedures and tolerances for concrete curing, including the American Society for Testing and Materials (ASTM), the American Concrete Institute (ACI), and the European Union (EU).

ASTM C31/C31M (ASTM International, 2010) is the standard practice for making and curing concrete test specimens in the laboratory. It covers the procedures for preparing, moulding, curing, and storing concrete specimens and includes provisions for the use of moist rooms, water tanks, or membranes for curing.

ACI 308 (ACI Committee 308, 1998) is the standard for curing concrete in the United States. It includes recommendations for the curing of concrete, including the use of moist rooms, water tanks, or membranes for curing, as well as the use of curing compounds and the application of heat. The standard also specifies the minimum curing time and temperature requirements for different types of concrete (ACI Committee 308, 2016).

The EU standard for curing concrete is EN 12390-2 (European Standards, 2003b). This standard is similar to ASTM C31 and ACI 308, but it includes additional provisions for curing specimens made from lightweight and high-strength concrete.

Despite these differences, all three standards provide a consistent and reliable method for curing concrete. They are widely used in the construction industry to ensure that concrete achieves the required strength and durability. Proper curing is essential for developing the desired properties of concrete, including strength, density, and durability(Felippe & Andrade, 2003; Hamada et al., 2022; Tang et al., 2017).

There are several differences between European standards, (ASTM), and (ACI) standards in the curing specifications for concrete. Some of the differences include the following:

- Curing temperature: European standards generally specify lower minimum curing temperatures compared to ASTM and ACI standards. For example, the European standard EN 206-1 (European Standards, 2013) specifies that concrete should be cured at a minimum temperature of 10 °C (50 °F) for the first 24 hours after casting and that the concrete should not be subjected to freezing temperatures for at least the first 72 hours. On the other hand, ASTM C31 (ASTM International, 2010) Standard Specification for Making and Curing Concrete Test Specimens in the Laboratory and ASTM C192/C192M (ASTM international, 2002) Standard Practice for Making and Curing Concrete Test Specimens in the field specifies that concrete should be cured at a minimum temperature of 16 °C (60 °F) and 23 °C (73.5 °F) respectively for the first 48 hours after casting. The American Concrete Institute (ACI) standard for curing temperature is ACI 308R-01 (ACI Committee 308, 1998), Guide to Curing Concrete, which states that concrete should be cured at a minimum temperature of 20 °C (68°F) for the first 7 days after casting. The concrete curing temperature is important because it affects the rate of hydration and the development of strength in the concrete. The lower the curing temperature, the slower the rate of hydration and the slower the development of strength. High temperatures can cause excessive drying and can also cause cracking. Therefore, it is important to maintain proper curing temperatures in order to achieve the desired strength and durability of the concrete.

- Curing duration: The European standard EN 206-1 specifies that concrete should be cured for at least 28 days before it is subjected to any mechanical loading, this is to ensure that the concrete has reached its maximum strength and that the structure is safe to use. On the other hand, the ACI 308R-01, stated that concrete should be cured for a minimum of 7 days before being subjected to mechanical loading. ASTM C31 and ASTM C192, do not specify any minimum curing duration for concrete before it is subjected to mechanical loading, but provide guidelines for making and curing concrete test specimens in the laboratory and field, respectively.

The curing duration is important because of the

concrete strength gained during the curing period, it is also important for the development of the concrete's microstructure and also for reducing the risk of cracking. The more the curing duration, the more strength gained and the more the development of the concrete's microstructure. Proper curing is crucial to achieve the desired strength and durability of the concrete.

- Curing methods: The European standard EN 206-1 provides several options for curing concrete, it allows for curing using various methods such as: keeping the concrete wet using water, covering the concrete with water-retaining materials such as plastic sheets, covering the concrete with wet burlap or other water-retaining materials, continuously misting the surface of the concrete or using any other method that will effectively keep the concrete surface moist and at a temperature above 10 °C. On the other hand, ASTM C31 and ASTM C192/C192M, do not specify any specific curing methods, but they do require that the concrete be cured in a moist condition, either by ponding or by covering the concrete with a moisture-retaining material, such as plastic sheeting. The ACI 308R-01 stated that concrete should be cured in a moist condition, either by ponding or by covering the concrete with a moisture-retaining material, such as plastic sheeting or by maintaining a humidity chamber around the concrete, it also allows for the use of curing compounds, which are liquid-applied or spray-applied materials that can be applied to the surface of freshly placed concrete to form a barrier that slows or prevents the evaporation of water from the concrete surface, which promotes the hydration process of the cement.

- Acceptance criteria: The European standard EN 206-1 specifies several acceptance criteria for cured concrete, including strength, density, air content, workability, and durability. The standard also establishes requirements for surface quality, such as allowable tolerances for surface defects and requires the concrete to be free from harmful substances that could negatively impact the properties of the concrete over time. On the other hand, ASTM C31 and ASTM C192, provide specific requirements for compressive strength, air content, workability, density and durability of the concrete, but do not include specific requirements for surface quality. The acceptance criteria are standards ACI 308R-01, stated that concrete should be inspected and tested to ensure that it has achieved the desired strength and durability properties, it also specifies a compressive strength requirement and air content requirements but does not specify other requirements for surface quality and durability as the European standards do.

2.3 Compressive strength

Compressive strength tests for concrete are essential for evaluating the quality and performance of concrete mixes. Additionally, the grading of concrete often relies on its characteristic compressive strength e.g. C20/25 (Tam et al., 2017). By emphasizing the compressive strength as the nominal way to characterize concrete, it highlights the significance of this property in assessing the quality and performance of the material. These tests determine the compressive strength of concrete, which measures the material's ability to resist compressive loads. The compressive strength of concrete is a critical property for determining the structural suitability of the material for its intended use (Aghda & Baniasadizade, 2013; Mindess et al., 2003a; G. B. Neville, 2012; Neyestani, 2011).

Compressive strength tests are performed on cylindrical or cubic concrete specimens of a specific size and shape. The specimens are typically made from fresh concrete and cured in a controlled environment before testing. The compressive strength of the concrete is determined by applying a compressive load to the specimen until it reaches failure. The compressive strength of concrete is directly related to the performance and durability of concrete structures. A concrete mix with high compressive strength will withstand greater loads and be more durable over time than a mix with lower compressive strength. This is important for ensuring that concrete structures are safe and will perform as intended over their intended lifespan. In addition, the compressive strength of concrete is used to evaluate the material's suitability for different types of construction projects. Different types of projects have different requirements for the compressive strength of concrete, and compressive strength tests are used to ensure that the concrete mix meets these requirements. For example, the compressive strength of concrete used in high-rise buildings or bridges must be much higher than that of concrete used in sidewalks or residential foundations.

Compressive strength tests are also used to verify the adequacy of mix proportions (Talaat et al., 2021) and to estimate the in-situ strength of concrete during construction (Gavilan & Luiz Carlos, 2018). This information is used to make decisions about when it is safe to strip forms or proceed with further work on a structure. It also provides insight on the quality control of the concrete and the acceptance criteria for the concrete mixture. The concrete industry relies heavily on the results of concrete compressive strength tests to determine the adequacy of as-delivered or in-place concrete. Compressive strength tests provide a good and straightforward indication of assessing the property of the concrete in its hardened state. Specimens of various shapes and sizes are used to determine the compressive strength of the concrete (Abd & Habeeb, 2014; *Comparison of Test Methods of Evaluation of Concrete Durability in the Persian Gulf Environment*, 2013; Kumar et al., 2016). The specimen size and shape are different in the available authorized standards. Several standards specify the methods and tolerances for this type of testing, including the (ASTM), the (ACI), and the European Union (EU).

ASTM C39/C39M (ASTM International, 2018) is the standard test method for determining the compressive strength of cylindrical concrete specimens. The test involves placing a cylindrical concrete specimen in a compression-testing machine and applying a compressive load to the specimen until it fractures. The compressive strength is calculated by dividing the maximum load achieved during the test by the cross-sectional area of the specimen.

ACI 318 is the standard for the design and construction of reinforced concrete in the United States. It includes provisions for determining the compressive strength of concrete, including cylinders and cubes. The standard specifies the size, shape, and manufacture of the specimens, as well as the testing procedure and the calculation of the compressive strength.

In the EU, the standard for testing the compressive strength of concrete is EN 12390-3 (European Standards, 2019a). This standard is similar to ASTM C39 (ASTM International, 2018) and ACI 318 (ACI 318, 2020; ACI Committee 311, 2004a), but it includes additional provisions for preparing, curing, and testing specimens made from lightweight and high-strength concrete.

One main difference between these standards is the size

and shape of the specimens used for testing. ASTM and ACI specify the use of cylinders, while the EU standard allows for cylinders or cubes. Another difference is the size of the specimens, with the EU standard allowing for larger specimens than ASTM and ACI, as explained in the following.

There are several differences in the compressive strength testing procedures and acceptance criteria specified by European and American standards. Some of the differences include the following:

- Testing frequency: European standards generally specify a higher testing frequency than American standards. For example, European standards for concrete specify that compressive strength testing must be performed at 7 and 28 days after the concrete is poured, while American standards typically only require testing at 28 days. This means that the concrete's strength is checked twice in Europe but only once in the US. This difference in testing frequency may be due to the fact that European standards tend to place a greater emphasis on ensuring the quality and safety of construction materials, while American standards may focus more on cost-effectiveness and efficiency (Technical Activities Committee, 2022). It's worth noting that this is just one example, and the specific testing requirements can vary depending on the product or material and the standard being used (ACI Committee 311, 2004a).

- Test specimen size: European and American standards specify different sizes for the concrete test specimens used for compressive strength testing. European standards generally define smaller test specimens compared to American standards. According to European standards (European Standards, 2019a), the concrete test specimens for compressive strength testing are generally cylindrical in shape with a diameter of 150 mm and a height of 300 mm, as shown in *Fig 1*, or cubes with 150 mm side size as shown in *Fig 2*. On the other hand, American standards generally define slightly larger concrete test specimens for compressive strength testing. According to American standards, the concrete test specimens are cylindrical in shape with a diameter of 6 inches (152.4 mm) and a height of 12 inches (304.8 mm). These specimens are referred to as 6x12 inches cylinders (ASTM international, 2009) It is important to note that the size of the test specimens can affect the compressive strength test results. Smaller test specimens generally have lower compressive strength values compared to larger specimens. This is because smaller specimens are more susceptible to variations in their manufacturing process and have less material to average out any variations in the strength of the concrete (Abd & Habeeb, 2014; Domagala, 2020; A. M. Neville, 2012; Sudin & Ramli, 2014; To et al., 2005).

- Testing machine capacity: European standards generally specify lower capacities for the testing machines compared to American standards. According to European standards, the capacity of the testing machine for compressive strength testing of 150 mm concrete cubes should be at least 2,500 kN (560,000 lbs). This capacity is sufficient to test concrete cubes with compressive strength up to around 150 MPa (22,000 psi). While American standards generally specify higher capacities for the testing machines. According to American standards, the capacity of the testing machine for compressive strength testing of 6x12 inches of concrete cylinders should be at least 11,000 kN (2,500,000 lbs). This capacity is sufficient to test concrete cylinders with compressive strength up to
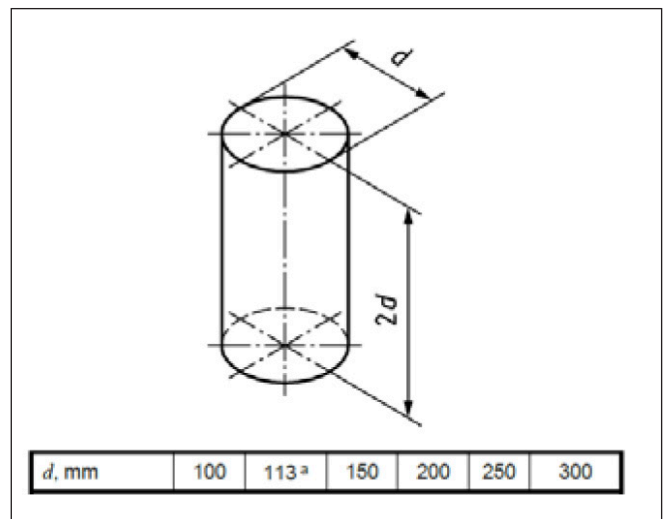
Fig 1: Standard cylindrical specimen shape size (European Standards, 2019a)
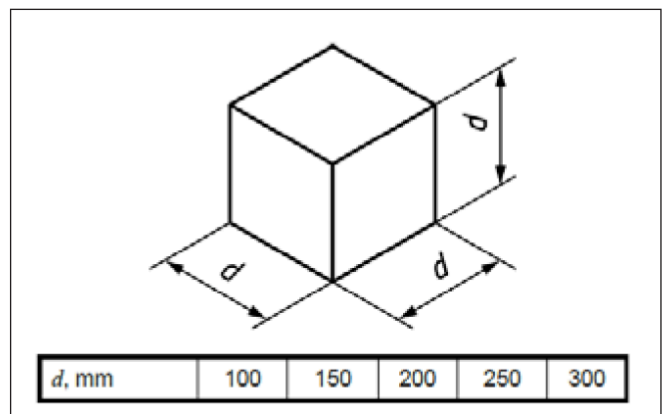
Fig 2: Standard cubic shape size (European Standards, 2019a)

around 150 MPa (22,000 psi). It's important to note that the capacity of the testing machine is a critical factor in determining the accuracy of compressive strength test results (Kumar et al., 2016; Talaat et al., 2021). A testing machine with a lower capacity than the maximum strength of the specimen will not be able to accurately determine the compressive strength of the specimen. The difference in testing machine capacities between European and American standards can be attributed to the different sizes of the concrete test specimens used in the two regions. As previously mentioned, European standards generally define smaller test specimens compared to American standards, and thus lower capacity testing machines are sufficient for testing these smaller specimens.

- Acceptance criteria: European standards generally define higher minimum compressive strength values for normal-weight concrete compared to American standards. According to European standards, the minimum compressive strength for structural concrete should be at least 20 MPa (2,900 psi) and at least 25 MPa (3,600 psi) for precast and prestressed concrete. These values apply to concrete that has reached 28 days of age and is cured under standard curing conditions. Comparing with the American standards, which define lower minimum compressive strength values for normal-weight concrete. According to American standards, the minimum compressive strength for residential and non-residential construction should be at least 2,500 psi (17 MPa) and at least 3,500 psi (24 MPa) for bridges and other infrastructure. These values also apply to concrete that has reached 28 days of age and is cured under standard curing conditions.

2.4 Flexural tensile strength

Flexural strength, also known as bending strength, is an important mechanical property of concrete that measures its ability to resist bending loads. It measures the concrete's ability to resist bending loads; when a load is applied to the top of the beam, the bottom will bend. The flexural strength of concrete is crucial for determining the suitability of the material for construction projects that involve beams or slabs that are subject to bending loads (Mindess et al., 2003b; A. M. Neville, 2012; G. B. Neville, 2012). Flexural strength tests are typically performed on beam-shaped concrete specimens of a specific size and shape. The specimens are typically made from fresh concrete and cured in a controlled environment before testing. The flexural strength of the concrete is determined by applying a load to the top of the beam and measuring the bending of the bottom of the beam (Carpinteri, 1992; Popovics, 1992; Shetty & Jain, 2019). Its also a significant property for evaluating the durability of concrete structures. Concrete structures subjected to repeated loading and bending can experience cracking and deterioration over time if the concrete's flexural strength is insufficient. Therefore, it's crucial to have appropriate flexural strength to ensure the safety and longevity of the structure (Wang & Gupta, 2021). In addition, flexural strength tests are also used to verify the adequacy of mix proportions, estimate concrete's in-situ strength during construction, and evaluate the material's suitability for different types of construction projects (Seyam & Nemes, 2022a). The results of flexural strength tests and other mechanical properties are used in the design and construction of concrete structures to ensure that they can withstand the loads to which they will be subjected. Several standards specify the procedures and tolerances for flexural strength testing, including the American Society for Testing and Materials (ASTM), the American Concrete Institute (ACI), and the European Union (EU).

ASTM C78 (ASTM International, 2016) is the standard test method for flexural strength testing of concrete. It involves using a three-point bending test on a concrete beam specimen with a span length of at least twice the depth. The flexural strength is calculated by dividing the maximum bending moment achieved during the test by the beam's section modulus; in addition, ACI 318 (ACI 318, 2020; ACI Committee 311, 2004b)is the standard for the design and construction of reinforced concrete in the United States. It includes provisions for determining concrete's flexural strength, including the three-point bending and four-point bending tests. The standard specifies the specimens' size, shape, and manufacture, as well as the testing procedure and the calculation of the flexural strength. In the EU, the standard for testing the flexural strength of concrete is EN 12390-5 (British Standards Institution (BSI), 2019). This standard is similar to ASTM C78 and ACI 318, but it includes additional provisions for preparing, curing, and testing specimens made from lightweight and high-strength concrete. One main difference between these standards is the size and shape of the specimens used for testing. ASTM and ACI specify the use of beams, while the EU standard allows for the benefit of beams or prisms. Another difference is the type of test used, with ACI allowing for both three-point and four-point bending tests, while the EU standard only provides for three-point bending.

There are notable differences among the European, ASTM, and ACI standards regarding the flexural strength testing of concrete. Some of the differences include the following:

- Test specimen size: European, ASTM, and ACI standards specify different sizes for the concrete test specimens used for flexural strength testing. European standards generally specify smaller test specimens compared to ASTM and ACI standards. European standards, such as those set by the European Committee for Standardization (CEN), generally specify smaller test specimens compared to ASTM and ACI standards. The size of the test specimens used in European standards is typically 150 mm x 300 mm x 600 mm (length x width x height). These smaller test specimens are often used in the laboratory, rather than in the field, to determine the flexural strength of concrete. On the other hand, ASTM (American Society for Testing and Materials) and ACI (American Concrete Institute) standards typically specify larger test specimens, such as 150 mm x 150 mm x 700 mm or 150 mm x 150 mm x 900 mm. These larger test specimens are often used in the field to determine the flexural strength of concrete in situ. It is important to note that the flexural strength of concrete, also known as the modulus of rupture, measures the material's ability to resist failure in bending. The size and shape of the test specimen can affect the measured flexural strength, so it is important to use the appropriate specimen size and shape when conducting flexural strength tests to ensure that the results are accurate and comparable.

- Testing machine capacity: European standards, such as those set by the European Committee for Standardization (CEN), generally specify lower capacity for testing machines than ASTM and ACI standards. For example, the European standard EN 12390-4 specifies a capacity of 2000 kN for testing machines used to determine the flexural strength of concrete. This lower capacity is sufficient for testing the smaller test specimens typically used in European standards. On the other hand, ASTM and ACI standards typically specify higher capacities for testing machines, such as 4000 kN or 6000 kN. These higher capacities are often required to test the larger test specimens typically used in ASTM and ACI standards.

  It is important to note that the capacity of a testing machine refers to the maximum force it can apply to a test specimen. The capacity of the testing machine should be greater than the expected strength of the specimen being tested, to ensure that the results are accurate and reliable. Also, the codes and standards have different requirements for the capacity of the testing machine depending on the requirements for the test and the type of specimen used.

- Testing procedures: European, ASTM, and ACI standards specify different methods for conducting flexural strength testing. For example, European standards may specify the use of a three-point bend test, while ASTM standards may specify the use of a four-point bend test. The European standard for flexural strength testing is EN 12390-5 (British Standards Institution (BSI), 2019), which specifies the use of a two-point loading bend test. In this test, a beam specimen is supported on two rollers that are located at a fixed distance apart, and a load is applied from the top by two loading point as shown in *Fig 3*, the EN 12390-5 standards added the center point loading to their specification, where a beam specimen is supported on two rollers that are located at a fixed distance apart and loaded by a third point, usually at the midpoint of the specimen as shown in *Fig 4*. The load is applied in such a way that it bends the specimen in a single plane. The flexural strength of the specimen is determined by measuring the maximum load that the specimen can withstand before it fails in a brittle manner.
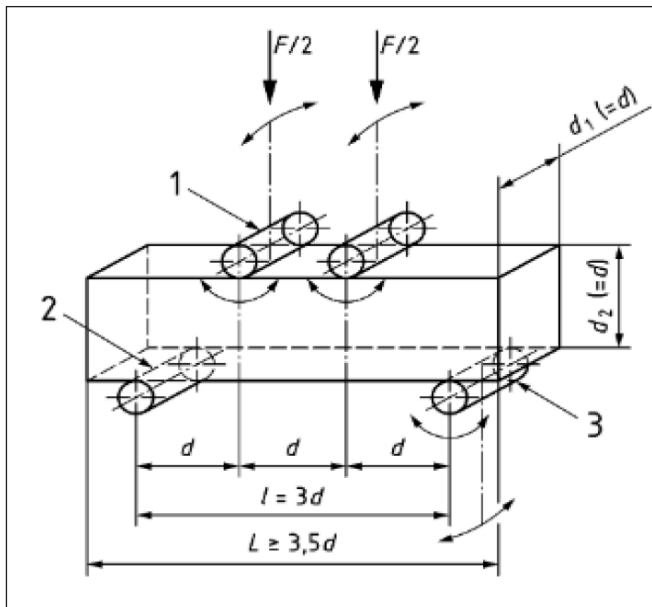
Fig 3: *Two point loading for flexure test of concrete based on European standards (European Standards, 2019b)*
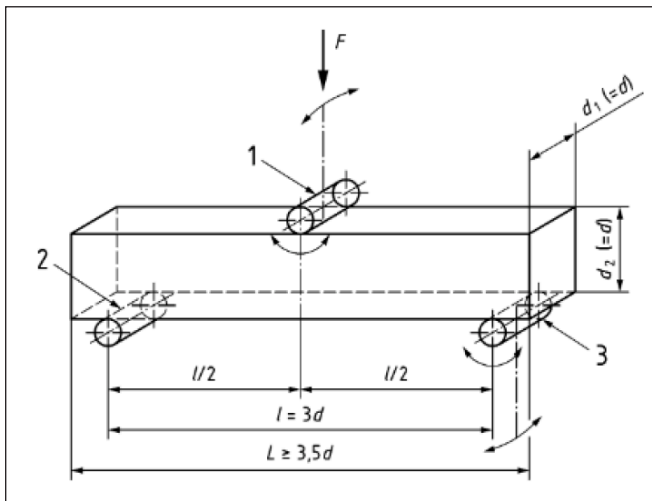

Fig 4: *Central point loading for flexure test of concrete based on European standards (European Standards, 2019b)*

The American Society for Testing and Materials (ASTM) has several standards for flexural strength testing, including ASTM C78, ASTM C293, and ASTM C496. ASTM C78 standard specifies the use of a four-point bend test, shown in *Fig 5*, in which a beam specimen is supported on two points at one end and two points at the other end. A load is applied at the midpoint of the specimen, in such a way that it bends the specimen in a single plane. As the test is done with 4 points of support, it is more accurate in a case where there are some non-uniformities in the sample.

The American Concrete Institute (ACI) standard for flexural strength testing is ACI 318-19. The standard describes two methods for determining the flexural strength of concrete: the simple beam with centre-point loading and the modified two-span beam test. The simple beam test is similar to the three-point bend test described in the European standard, while the modified two-span beam test is similar to the four-point bend test described in the ASTM standard. It's worth mentioning that each standard can have several variations in procedure, but the general principle of testing is the same.

Despite these differences, all three standards provide a consistent and reliable method for determining the flexural strength of concrete. They are widely used in the construction industry to ensure that materials meet the required strength
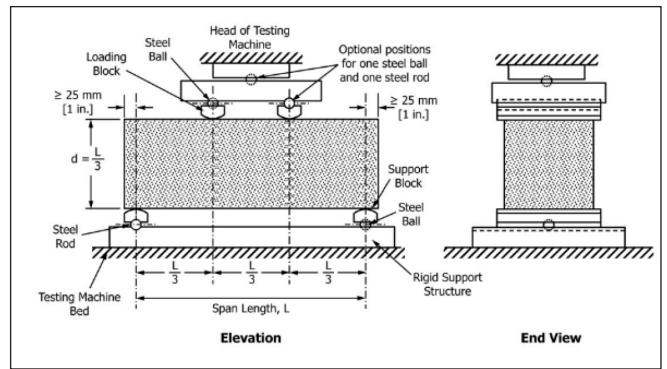

Fig 5: *Apparatus for Flexure Test of Concrete based on ASTM C78 (ASTM International, 2016)*

requirements and to evaluate the quality of concrete mixes. The flexural strength of concrete is an essential factor in the design of structures, as it determines the material's ability to resist cracking and deformation under load.

2.5 Shear strength

Shear strength, also known as the transverse strength of concrete, is an important mechanical property that measures a concrete's ability to resist shear loads (Lamond & Pielert, 2006; Popovics, 1992). It is the ability of the concrete to withstand forces that are applied perpendicular to the main axis of the material he shear strength of concrete is a critical property for determining the structural suitability of the material for certain types of construction projects, particularly those that involve the use of beams or slabs that are subject to shear loads. Shear strength tests are typically performed on concrete beams, typically by applying a transverse load to the beam, and measuring the deformation of the beam. Several methods can be used to test the shear strength of concrete, such as the beam shear test, the diagonal compression test, or the direct shear test. The shear strength of the concrete is determined by the ratio of the applied load to the beam's shear deformation (G. B. Neville, 2012; Ozyildirim & Carino, 2006; Popovics, 1992; Shetty & Jain, 2019). Shear strength also plays an important role in the durability and safety of concrete structures. Concrete structures that are subjected to repeated loading and shear forces can experience cracking and deterioration over time if the shear strength of the concrete is not sufficient. The shear strength is an essential property to ensure the safety and longevity of the structure. In addition, shear strength tests are also used to verify the adequacy of mix proportions and estimate concrete's in-situ strength during construction (Seyam & Nemes, 2022b) There are several methods for testing the shear strength of concrete, including the direct shear test, the beam shear test, and the diagonal compression test (Slater et al., 1926). The American Concrete Institute (ACI) 318-19, Building Code Requirements for Structural Concrete, provides provisions for the design of members and systems that resist shear forces, but it doesn't provide methodologies or procedures for testing the shear strength of concrete. The American Society for Testing and Materials (ASTM) does not have any specific standard for shear strength testing of concrete. EN standards as well as does not have a specific standard for shear strength testing of concrete. Different countries or regions may have different standards and codes for shear strength testing of concrete.

2.6 Modulus of Elasticity

The modulus of elasticity, also known as Young's modulus, is a key mechanical property of concrete that measures a
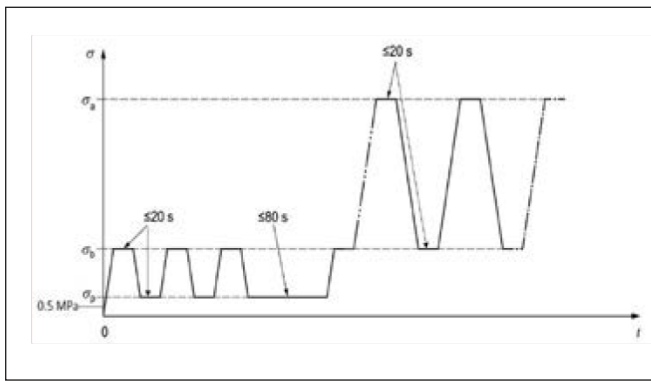
Fig 6: *Cycle for the determination of the modulus of elasticity based on Method A (European Standads, 2013)*
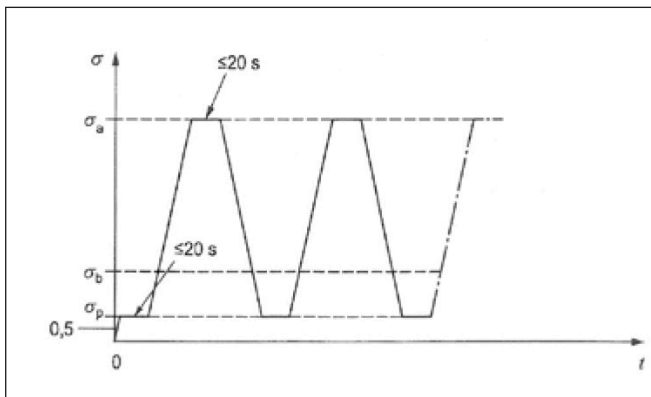

Fig 7: *Cycle for the determination of the modulus of elasticity based on Method B (European Standads, 2013)*

material's ability to resist deformation under load. It is used in the design of concrete structures to calculate the amount of deformation or strain that will occur under a given load. To determine the modulus of elasticity of concrete, American standards ASTM provide a standards C468/468M (ASTM international, 2014), while the European standards EN 12390-13 (European Standads, 2013) describe the modulus of elasticity methods, tests are typically conducted on concrete cylinders or beams in both compression and tension modes. In compression testing, a load is applied to the cylinder axially to measure the deformation. In tension testing, the load is applied to the end of a concrete beam to measure the deformation. The modulus of elasticity is then calculated as the ratio of the applied load to the corresponding deformation.

A higher modulus of elasticity indicates a higher quality concrete that is less prone to deformation under load. According to (ACI) and (ASTM) standards (ASTM international, 2014), the static modulus of elasticity of concrete is typically determined using cylindrical specimens, while in the European standards, the specimen can be a cylindrical or prismatic shape (Vu et al., 2021), and calculated using the formula $E = P/\Delta$, where E is the modulus of elasticity, P is the applied load, and Δ is the measured deformation. However, neither ACI nor ASTM standards specify a minimum modulus of elasticity for concrete. Similarly, European standards do not specify a minimum modulus of elasticity for normal-weight or lightweight concrete. However, EN 12390-13 standard accepts two methods for the determination of concrete modulus of elasticity: Method A shown in *Fig 6*. and Method B, shown in Fig 7. Method A is a more detailed and accurate method for determining the modulus of elasticity of concrete. The main difference between Method A and Method B is the manner in which the load is applied. In Method A, the load is applied at a constant rate, while in Method B, the load is applied at a constant rate of deformation. This means

that in Method A, the load is applied at a constant rate until failure occurs, while in Method B, the load is applied until a specified amount of deformation is reached (Domagała & Dobrowolska, 2018).

In addition to static modulus of elasticity, the dynamic modulus of elasticity of concrete can be determined by conducting a resonant frequency test or a pulse velocity test (Trifone, 2017). In the resonant frequency test, the frequency of a vibrating concrete specimen is measured to calculate the modulus of elasticity. In the pulse velocity test, the speed of a pulse of energy transmitted through the concrete specimen is measured to calculate the modulus of elasticity (Henrique Alves & Lucas BarcelosOtani, 2022). These tests are similar to the methods specified in ASTM standards but are not specified in European standards.

3. CONCLUSION

In conclusion, this research has compared the European standards, the American Society for Testing and Materials (ASTM) and American Concrete Institute (ACI) standards for testing the mechanical properties of concrete. The study has highlighted the importance of compressive strength, flexural tensile strength, shear strength, and modulus of elasticity as key properties for assessing the quality and performance of concrete. The research has also revealed that there are variations in the specimen size, preparation, and curing requirements, as well as testing procedures and acceptance criteria among the European, ASTM and ACI standards. The research concludes that it is essential to follow the appropriate standards and testing procedures to ensure the test results' reliability and accuracy. Proper specimen preparation and curing are also critical to obtain accurate and representative test results. By following the relevant standards and procedures, it is possible to obtain consistent and reliable results that can be used to assess the quality and performance of concrete in various construction applications.

4. REFERENCES

Abd, M. K., & Habeeb, Z. D. (2014). *Effect of specimen size and shape on compressive strength of self-compacting concrete.*

ACI 318. (2020). *Building Code Requirements for Structural Concrete (ACI 318-19): An ACI Standard; Commentary on Building Code Requirements for Structural Concrete (ACI 318R-19).* https://www.concrete.org/store/productdetail.aspx?ItemID=318U19&Language=English&Units=US_Units

ACI Committee 308. (1998). *ACI 308.1 Standard Specificationfor Curing Concrete.*

ACI Committee 308. (2016). *Guide to external curing of concrete.*

ACI Committee 311. (2004a). *ACI 311.5-04 Guide for Concrete Plant Inspection and Testing of Ready-Mixed Concrete.*

ACI Committee 311. (2004b). *ACI 311.5-04 Guide for Concrete Plant Inspection and Testing of Ready-Mixed Concrete.*

Aghda, S. T. T., & Baniasadizade, M. (2013). Comparison of test methods of evaluation of concrete durability in the Persian Gulf environment. *Proceedings of the 4rd International Conference on Concrete and Development (4ICCD).* https://doi.org/10.13140/RG.2.1.4414.3128

ASTM international. (2002). *C192/C192M-02: Standard Practice for Making and Curing Concrete Test Specimens in the Laboratory.*

ASTM international. (2009). C470/470M: Standard Specification for Standard Specification for Molds for Forming Concrete Test Cylinders Vertically Molds for Forming Concrete Test Cylinders Vertically. *ASTM International.* https://doi.org/10.1520/C0470_C0470M-09

ASTM International. (2010). *C31/C31M – 10: Standard Practice for Making and Curing Concrete Test Specimens in the Field.* https://doi.org/10.1520/C0031_C0031M-10

ASTM international. (2014). *Standard Test Method for Static Modulus of Elasticity and Poisson's Ratio of Concrete in Compression.*

ASTM International. (2016). C78/C78M: Standard Test Method for Flexural Strength of Concrete (Using Simple Beam with Third-Point Loading). *ASTM International.* https://doi.org/10.1520/C0078_C0078M-16

ASTM International. (2018). ASTM C39/C39M-18 standard test method for compressive strength of cylindrical concrete specimens. *ASTM International, West Conshohocken, PA. ASTM, AI (2018)." ASTM C*, *192*. https://doi.org/10.1520/C0039_C0039M-14

British Standards Institution (BSI). (2019). *BS EN 12390-5:2009: Testing hardened concrete - Part 5: Flexural strength of test specimens*. BSI.

Carpinteri, A. (1992). *Applications of fracture mechanics to reinforced concrete*. CRC Press.

Comparison of test methods of evaluation of concrete durability in the Persian Gulf environment. (2013). https://doi.org/10.13140/RG.2.1.4414.3128

Domagala, L. (2020). Size effect in compressive strength tests of cored specimens of lightweight aggregate concrete. *Materials*, *13*(5). https://doi.org/10.3390/ma13051187

Domagała, L., & Dobrowolska, J. (2018). The influence of an applied standard test method on a measurement of concrete stabilized secant modulus of elasticity. *MATEC Web of Conferences*, *163*. https://doi.org/10.1051/matecconf/201816307001

European Standads. (2013). *EN 12390-13 -2014-06 Testing hardened concrete - Part 13 Determination of secant modulus of elasticity in compression*.

European Standards. (2003a). *EN 12390-1 Testing hardened concrete-Part 1: Shape, dimensions and other requirements for specimens and moulds*.

European Standards. (2003b). *EN 12390-2 Testing hardened concrete. Part 2, Making and curing specimens for strength tests.* BSI.

European Standards. (2013). *EN 206:2013: Concrete - Specification, performance, production and conformity*. British Standards Institution (BSI).

European Standards. (2019a). *EN 12390-3:2019 Testing hardened concrete - Part 3: Compressive strength of test specimens*. BSI.

European Standards. (2019b). *EN 12390-5:2019 Testing hardened concrete - Part 5: Flexural strength of test specimens*.

Felippe, A. P., & Andrade, R. S. (2003). Influence of the curing temperature on the compressive strength of concrete. *Cement and Concrete Research*, *33*(10), 1589–1594.

Gavilan, S., & Luiz Carlos, L. C. P. (2018). Variations of in situ concrete strength by European Standard and American Code. *Structural Concrete*, *19*(4), 1185–1194. https://doi.org/10.1002/suco.201700115

Hamada, H., Alattar, A., Tayeh, B., Yahaya, F., & Almeshal, I. (2022). Influence of different curing methods on the compressive strength of ultra-high-performance concrete: A comprehensive review. *Case Studies in Construction Materials*, *17*. https://doi.org/10.1016/j.cscm.2022.e01390

Henrique Alves, & Lucas BarcelosOtani. (2022). *Determination of elastic moduli of concrete by Impulse Excitation Technique*. www.sonelastic.com

Kumar, S., Mukhopadhyay, T., Waseem, S. A., Singh, B., & Iqbal, M. A. (2016). Effect of Platen Restraint on Stress–Strain Behavior of Concrete Under Uniaxial Compression: a Comparative Study. *Strength of Materials*, *48*(4), 592–602. https://doi.org/10.1007/s11223-016-9802-z

Lamond, J. F., & Pielert, J. H. (2006). *Significance of Tests and Properties of Concrete and Concrete-Making Materials STP 169D*. https://doi.org/10.1520/STP169D-EB.

Miller, S.A., Horvath, A., & Monteiro, P. J. M. (2016). Readily implementable techniques can cut annual CO_2 emissions from the production of concrete by over 20%. *Environmental Research Letters*, *11*(7). https://doi.org/10.1088/1748-9326/11/7/074029

Mindess, S., Young, J. F., & Darwin, D. (2003a). *Concrete* (2nd ed.). Prentice Hall, Pearson Education, Inc. .

Mindess, S., Young, J. F., & Darwin, D. (2003b). *Concrete* (2nd ed.). Prentice Hall, Pearson Education, Inc. .

Neville, A. M. (2012). *Properties of concrete* (Fifth Edition 2011). John Wiley & Sons, Inc.

Neville, G. B. (2012). The Strength of Concrete. In *Concrete Manual* (pp. 23–27). ICC.

Neyestani, B. (2011). Specified Tests for Concrete Quality. *SSRN Electronic Journal*. https://doi.org/10.2139/ssrn.2950019

Ozyildirim, C., & Carino, N. J. (2006). Concrete strength testing. *ASTM Special Technical Publication*, *169 D-STP*, 125 – 140. https://www.scopus.com/inward/record.uri?eid=2-s2.0-33745660603&partnerID=40&md5=8e104142dc755361cadd4e41d74e9002

Popovics, S. (1992). *Concrete materials: Properties, specifications, and testing*. William Andrew. https://doi.org/10.1016/B978-0-8155-1308-7.50009-0

Seyam, A. M., & Nemes, R. (2022a). Impacts of Aggregate Type and Elevated Temperature on Flexural Tensile Strength of Concrete. In M. di Prisco, A. Meda, & G. L. Balazs (Eds.), *Proceeding of the 14th fib International PhD Symposium in Civil Engineering*.

Seyam, A. M., & Nemes, R. (2022b). Shear Strength Behavior for Lightweight Aggregate Concrete Subjected to Elevated Temperature. In Stokkeland Stine & Braarud Henny Cathrine (Eds.), *6th fib International Congress, Concrete Innovation for Sustanbaility* (pp. 595–603).

Shetty, M. S., & Jain, A. K. (2019). *Concrete Technology (Theory and Practice), 8e*. S. Chand Publishing.

Slater, W. A., Lord, A. R., & Zipprodt, R. R. (1926). *SHEAR TESTS OF REINFORCED CONCRETE BEAMS* (Issue 314). https://doi.org/10.6028/nbst.8631

Sudin, M. A. S., & Ramli, M. (2014). Effect of Specimen Shape and Size on the Compressive Strength of Foamed Concrete. *MATEC Web of Conferences*. https://doi.org/10.1051/matecconf/20141002003.

Talaat, A., Emad, A., Tarek, A., Masbouba, M., Essam, A., & Kohail, M. (2021). Factors affecting the results of concrete compression testing: A review. In *Ain Shams Engineering Journal* (Vol. 12, Issue 1, pp. 205–221). Ain Shams University. https://doi.org/10.1016/j.asej.2020.07.015

Tam, C. T., Babu, D. S., & Li, W. (2017). EN 206 Conformity Testing for Concrete Strength in Compression. *Procedia Engineering*, *171*, 227–237. https://doi.org/10.1016/j.proeng.2017.01.330

Tang, Y., Su, H., Huang, S., Qu, C., & Yang, J. (2017). Effect of Curing Temperature on the Durability of Concrete under Highly Geothermal Environment. *Advances in Materials Science and Engineering*, *2017*. https://doi.org/10.1155/2017/7587853

Technical Activities Committee, A. (2022). *An ACI Manual Technical Committee Manual Reported by the ACI Technical Activities Committee*. www.concrete.org

To, S., By Dennis Vandegrift, P., & Anton Schindler, J. K. (2005). *The Effect of Test Cylinder Size on the Compressive Strength of Sulfur Capped Concrete Specimens*.

Trifone, L. (2017). *A Study of the Correlation Between Static and Dynamic Modulus A Study of the Correlation Between Static and Dynamic Modulus of Elasticity on Different Concrete Mixes of Elasticity on Different Concrete Mixes* [Benjamin M. Statler College of Engineering and Mineral Resources]. https://researchrepository.wvu.edu/etd

Vu, C.-C., Weiss, J., Plé, O., & Amitrano, D. (2021). The potential impact of size effects on compressive strength for the estimation of the Young's modulus of concrete. *Materials and Structures*. https://doi.org/10.1617/s11527-021-01795-7

Wang, B., & Gupta, R. (2021). Performance of repaired concrete under cyclic flexural loading. *Materials*, *14*(6). https://doi.org/10.3390/ma14061363

Ahmed M Seyam (1989), Civil engineer (MSc in structural engineering), PhD candidate in civil engineering, at Department of Construction Materials and Technologies of Budapest University of Technology and Economics (BME). His Main fields of interest: concrete technology, aggregate influence in concrete, fire resistance and fire design, durability, FRC, recycling and sustainability. Budapest University of Technology and Economics, Műegyetem rkp 3. Budapest H-1111, Hungary, E-mail: seyam.ahmed@emk.bme.hu.

Rita Nemes, Civil engineer (MSc), postgraduate degree in concrete technology, PhD, associate professor at the Department of Construction Materials and Technologies, Budapest University of Technology and Economics. Main fields of interest: concrete technology, ceramics, non-destructive testing of concrete, supplementary cementing materials for concrete, bond in concrete, fiber reinforced concrete, lightweight concrete, shrinkage of concrete, durability measurement, waste materials as aggregates. Member of the Hungarian Group of *fib* and the Scientific Society of Silicate Industry. Budapest University of Technology and Economics, Műegyetem rkp 3. Budapest H-1111, Hungary, E-mail: Nemes.rita@emk.bme.hu.

A REVIEW IN TECHNOLOGIES, DEFINITIONS, PROPERTIES AND APPLICATIONS OF ULTRA HIGH-PERFORMANCE CONCRETE (UHPC)

Ahmed M. Seyam – György L. Balázs

Concrete technology has changed dramatically during the last decades, where the high-strength concrete concept has gone from 30 MPa to well over 100 MPa. In this paper, a review study has been conducted on ultra high-performance concrete (UHPC), however, researchers have a lot of definitions for this term, but all of them agreed that (UHPC) which refers to cement-based materials exhibiting superior properties, including compressive strength higher than 150 MPa with high ductility, and excellent durability. This paper reviews the theoretical principles of UHPC, definitions, raw materials, mixture design methods, successful mixture components with the required properties, challenges, and some of the successful applications of UHPC, focusing on bridge applications. The paper concluded by summarizing the benefits of using UHPC, the future of this superior concrete, current challenges and some recommendations for wider use.

Keywords: *UHPC, UHPC definitions, UHPC mixtures, UHPC applications*

1. INTRODUCTION

Since Roman times, concrete has been the most used material in construction; construction materials development does not stop, day by day, concrete expresses new applications and an advanced improvement in the construction industry, one of the quanta leaps in concrete structures achieved by developing the ultra-high performance concrete technology (UHPC), UHPC is the new concrete technology provide a high level of qualities that had never been possible before. During the 20th century, the development of concrete technology was significant. In 1950, concrete with 34 MPa 28-day compressive strength was considered a high-strength material. At present, these values can reach well over 200 MPa. A timeline of concrete development is shown in Table 1 (Buitelaar, 2004; EFNARC, 2005).

The significance of this paper is to review and present the crucial components and characteristics of ultra-high performance concrete (UHPC); highlighting the UHPC definitions, design methodologies, features, challenges, and some successful applications in construction. *(Table 1)*

2. UHPC DEFINITIONS

Researchers defined the term UHPC in different forms; definitions have been given to UHPC according to their major components, Farzad et al. (2019) define ultra-high-performance concrete as a cement-based material created with an enhanced gradation of granular components, with less than 0.2 water-to-cement ratio (w/c) and significant internal portions of fibre. Azmee & Shafiq (2018) mentioned that UHPC is a fibre-reinforced, super plasticized, silica fume-cement mixture with a very low water-to-cement ratio, with a presence of fine quartz sand instead of the coarse aggregate. Mishra & Singh (2019) concluded that UHPC is a particular

type of concrete consisting of a high fine-grained reactive admixture, including fine quartz and silica fume, fibres and superplasticizers while having low w/b ratio and a high binder content. Ahmad et al. (2016) define the UHPC as a concrete mixture produced using high cement contents, silica fume, superplasticizer, and very fine quartz, quartz powder, and fibres without coarse aggregate. Nematollahi et al. (2012) also define the term of ultra-high-performance concrete with a cement-based composite material with less than 0.25 water-cement ratio, which consisting fine materials with optimized grading curves and very high strength discrete micro steel fibres.

In the other hand, a lot of researchers defined the UHPC based according to its superior durability and mechanical properties. Bajaber & Hakeem (2021), defines UHPC as a new generation of cement-based material which has very high compressive strength, high ductility, and sustainability based on the optimization of fine and ultrafine aggregates (such: the silica fume and sand), low water to cement ratio with added superplasticizer, and reinforced by a high strength steel fibre. Li, J. et al. (2020) defined the UHPC term as an innovative composite material that can be a potential candidate for concrete structures exposed to aggressive environments. Aroraa et al. (2019) define the UHPC as a multi-scale microstructure material tailored for high mechanical properties, i.e., very-high compressive strength, high flexural tensile strength, and high ductility material compared with ordinary concrete. Moreover, some of the researchers adopt comprehensive definitions combining both characteristics. For example, the Association Francaise de Genie Civil (AFGC) defines UHPC as a material with a cement matrix and a characteristic compressive strength in excess of 150 MPa and containing steel fibres in order to achieve ductile behaviour. The Japan Society of Civil Engineers (JSCE) defines the UHPC as a type of cementitious composite

Table 1: *Development of concrete materials (in terms of strength)*

Year	History
1824	Portland cement is first developed.
1849	Reinforced concrete evolves with the addition of metallic reinforcement.
1950	Concrete with 34 MPA strength was considered as high strength.
1960	High-strength concrete developed in the laboratory reached 80 MPa.
1980	Army Corps of Engineers for the United States were the first user of UHPC in the 1980s, though UHPC did not become commercially available in the U.S. High-performance concrete for use mainly in security and defence applications was developed in Denmark compressive strength 100 Mpa.
1985	The first research program was conducted on the application of UHPC.
1997	The first bridge partly composed of UHPC was constructed in Canada
2002	First recommendations for using UHPC were published in France.
2005 and forward	Many research programs are looking at the use of UHPC in different structures worldwide. At least 90 bridges have been built and the use of UHPC has been implemented in many other types of structures.

reinforced by fibres with characteristic values more than 150 MPa in compressive strength, a minimum first cracking strength of 4 MPa. ACI 239R (2018) defines UHPC as a fibre-reinforced concrete that has a minimum compressive strength of 22 Ksi (150 MPa) with high durability, tensile ductility, and compliance with the toughness requirements.

3. UHPC MATERIALS

The general formulation of UHPC consists of a high binder content, including Portland cement, the essential factor in achieving better UHPC is optimizing the mixture's micro and macro characteristics. Cement, silica fumes, and sand grain size distributions must be tuned to create high capacity and, hence, a thick matrix with extremely low permeability (Salahi et al., 2021). Materials are carefully selected to ensure mechanical homogeneity, maximum particle packing density and minimum size of flaws (Balázs, G. L., 2015); (Schmidt et al., 2005); (Vernet, 2004); (Shah, Weiss, 1998); (Wille et al., 2011); (Shi et al., 2015). Thus gravel or coarser aggregate is usually replaced in UHPC mixes to avoid the formation of high voids and to create a densified interfacial transitional zone around the aggregates, thus, eliminating the weakest region within the matrix (Morcus, Akhnoukh, 2007), (Akcaoglu et al., 2004).

3.1 Binders

Generally, Portland cement is used as the primary binder to produce UHPC. For UHPC, cement content is usually (about/ more than 700 kg/m^3), about double the cement amount in the normal strength concrete. Cement was chosen for many reasons, the low C3A content, which minimizes the water demand of cement, ettringite formation, and heat of hydration, as indicated by De Larrard (1994) and Richard, Cheyrzy (1995). It also has low alkali content, low to medium fineness, and availability.

3.2 Fillers and aggregates

Fine sand and coarser aggregates are generally inexpensive inert materials used as fillers when making concrete. In concrete technology, especially UHPC concretes grading fillers and aggregates, maximum and minimum sizes are crucial. Quartz sand is used in the mix because of the high hardness, good paste aggregate interfaces, and chemical inactivity in the cement hydration reaction (Koh et al., 2018). The mean particle size is often smaller than 1 mm. Right proportions will result in a denser, more packed mix with a lower water demand due to fewer free inter-particle spaces, eliminating the coarse aggregates and improving the durability of UHPC. The optimization will yield a higher compressive strength, better rheology and lower water demand, which are essential characteristics of UHPC properties.

Using inert materials and coarser fillers will also decrease the concrete's shrinkage since the cement paste's volume is smaller, resulting in lower autogenous shrinkage and, thus, lower cracking risk (Wu et al., 2017).

3.3 Micro fillers

The most commonly used micro fillers are silica fume which reacts with CH (Calcium hydroxide) through pozzolanic reaction, and quarts fillers, which can be activated when exposed to high curing temperatures. Other micro fillers investigated and used are pulverized fly ash, lime-stone, metakaolin or micronized, and phonolite (Cwirzen, Panttala, 2006).

The smallest component, with a 0.2 µm diameter, serves three basic functions in UHPC, it fills voids between cement grains, forms hydration products by pozzolanic activity, and enhances the rheological characteristics. Silica fume reacts with the cement hydration product of portlandite ($Ca(OH)_2$) and water, which forms calcium silicate hydrates (C–S–H), this formation known as the pozzolanic (Oertel et al., 2014). The pozzolanic reaction makes the cement matrix denser, ultimately enhancing and improving the mechanical properties of UHPC (Zhang et al. 2016).

3.4 Fibres

UHPC behaves in a linear-elastic manner along the largest part of the stress-strain curve under loading and has a failure mode with very limited post-crack behaviour, which causes a rigid failure. The incorporation of fibres mainly aims to bridge forming cracks and transfer loads to induce ductile behaviour and to increase flexural strength (Cwirzen, Panttala, 2006). Seyam et al. (2020) mentioned that incorporating 16% of steel fibres and 0.75% polypropylene fibres according to cement weight increased the compressive strength by 28%

and the flexural strength by 58%. Shehab et al. (2016) mentioned that longer fibres (length to diameter (l/d)=50) increased compressive and flexural strengths slightly more than shorter fibres (l/d=30) with the same diameter of the fibre. Shin et al. (2021) studied the effect of the shape of steel fibres and mentioned that the twisted steel fibres had a greater pull-out resistance than straight steel fibres with a circular cross-section, and its efficacy increased as the number of ribs increased. In comparison, the straight steel fibre demonstrated the best flexural behaviour in both uniaxial and biaxial stress states, but the six-times twisted steel fibre displayed the poorest flexural behaviour due to the composites' high bond strength.

One of the more significant problems related to using fibres in concrete is ensuring correct fibre orientation and an even distribution within the binder matrix. When poured, fibres tend to orient themselves in the direction of the concrete flow, which, if done improperly, can cause the fibres to orient themselves in unfavourable directions leading to worse mechanical properties (Schmidt, 2005).

3.5 Chemical admixtures

The UHPC mixtures require a relatively high dosage of chemical admixtures, specially high-range water reducers (HRWR), HRWR commercially known as superplasticizers (Akhnoukh, Buckhalter, 2021). Superplasticizers are long-chain polymers or co-polymers with negative charges used as high-range water reducers in the concrete mixture. It's a material used to disperse cement particles and silica fume, which improves the workability of UHPC mixes (Voo, Foster, 2010). Adding superplasticizers not only improves concrete workability or flowability but also the particle dispersion homogenizes the concrete material significantly (Zhu et al., 2021).

Thus, superplasticizers facilitate the achievement of using a lower water/binder (w/b) ratio without affecting the workability of the mixture. In the case of UHPC, the optimum amount of superplasticizer is relatively high and its dependent on the w/c with a solid content that is approximately 1.6% of the cement content (Ghafari et al. 2016).

3.6 Water

UHPC effectiveness mix could be made not by minimizing water content but by maximizing the relative density (Tayeh, Abu, 2013). The minimum w/b ratio for a workable concrete mixture is about 0.08 (Ghafari et al. 2016). By increasing the w/b ratio to above 0.08 to about 0.13, air will be replaced by water without increasing the volume of the mixture. In case of increasing the water-to-binder ratio beyond 0.13, the volume increases due to the additional water and as a result, the density of the mixture decreases dramatically. Thus, the optimum w/b ratio should be practically tested and selected to be slightly toward the higher values of the w/b ratio to ensure that the w/b ratio of the real mix is slightly higher than the theoretical optimum (Graybeal, 2006).

Richard and Cheyrezy (1995) found that the optimum w/b ratio is 0.14 as the optimal for UHPFRC, which is almost the same conclusion for De Larrard and Sedran (1994) study, where a solid suspension model was used. The result also agrees closely with that of Gao et al. (2005), where an optimum w/b ratio of 0.15. As mentioned, most of UHPC's previous mixes standed to trial mixes, which could achieve superior performance by a higher w/b ratio in the presence of additive materials.

3.7 UHPC mix design

One of the most significant aspects of UHPC manufacturing is the mix design. It focuses on improving the qualities of fresh and hardened concrete and optimizing the concrete properties. Optimizing particle packing density for the granular components of UHPC has been regarded as the essential idea for mix design in improving workability, strength, and durability (Schmidt and Fehling, 2005). When fibres are added to UHPC to improve its ductility and energy absorption capability, but negatively affects the workability.

In general, compressive strength of UHPC is higher than 150 MPa; the specific mix design procedures are not commercially available as they are for conventional concrete. Most researchers have provided mixture proportions of UHPC after many trials with no specific design procedures reported (Yu et al., 2014), (Shi et al., 2015).

In reality, trial and error modification of current UHPC recipes from the accessible literature is widespread for UHPC mix creation. This practice's success is hampered by the fact that the input materials come from a variety of sources. Several difficulties are associated with initiating a UHPC design utilizing area market materials. Figures 1 and 2 show the mixing proportions for UHPC mixes, which succeeded in producing concrete with compressive strength 150 MPa and more.

The procedure of defining the concrete mixture proportion is different for every researcher, but most of them have the same concept, for example, Richard and Cheyrezy (1995), Alkaysi and El Tawil (2016), Seyam et al. (2020), Habel et al. (2006), Aoude et al. (2015), Deeb et al. (2012). Azad and Hakeem (2013), Ma et al. (2002) and Wille (2013) go to the same way of replacing the coarse aggregates by fine aggregates with a high amount of binder and low b/w content. Table 2 shows the range of UHPC constituents materials used in various studies to produce UHPC successfully.

Table 2: *UHPC components (Ghafari et al., 2015)*

Components	Weight (kg/m³)	Volumetric (%)
Binder / Cement	693-1114	22-35
Sand	733-1340	28-51
Crushed quartz	0-208	0-9
Silica fume	116-273	5-13
Fibres	79-234	1-3
Superplasticizer	14-40	1.4-4
Water	140-240	14-24

4. UHPC APPLICATIONS

The increased strength and durability of UHPC are primarily attributable to improved particle gradation, which results in a highly densely packed mix, a very low water-to-powder ratio, and the utilization of steel fibres. UHPC is a desirable material due of its unmatched strength and durability and it became an attractive material for bridges construction, In 1997, a brave application was made in Canada, the very first prestressed hybrid pedestrian bridge over the Magog River in Sherbrooke was built using UHPC, this use for UHPC opens the door for using this superior concrete in bridges. In 2001 France constructed Bourg-les-Valence bridge made for cars and trucks, a year after South Korea built a bridge with a main span of 120 m using UHPC, in 2003 Japan also joining
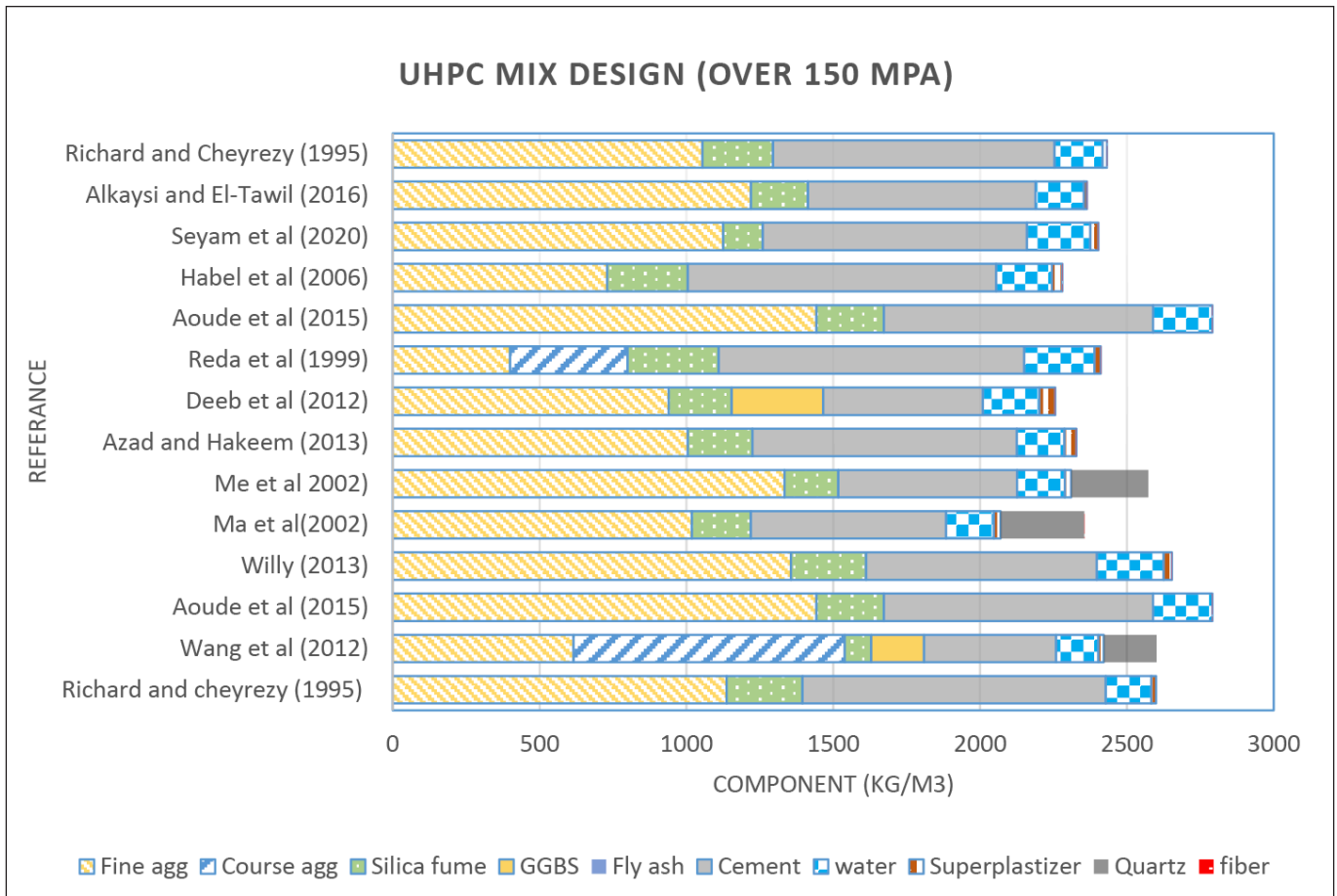
Fig. 1: UHPC materials and mixture proportions
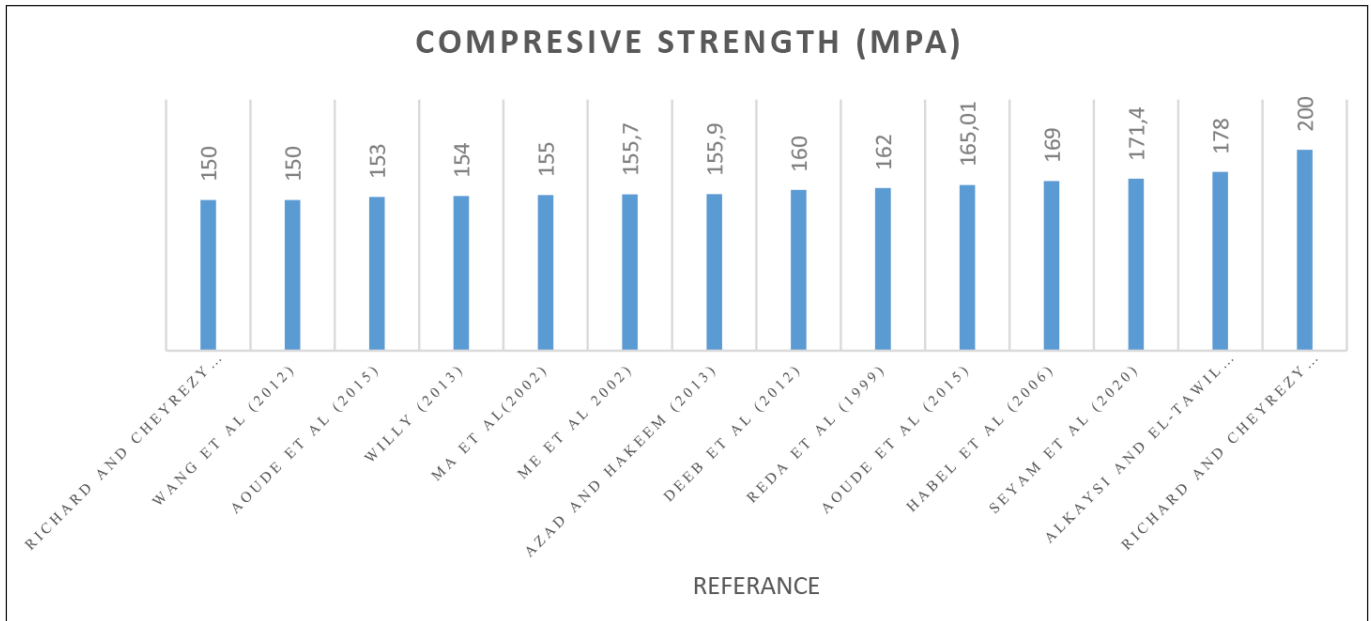
Fig. 2: The compressive strength of each researcher's mix

the UHPC world, by constructing Sakata-Mirai footbridge with 50 m span. Following the success of UHPC bridge construction, in 2005 the construction of four bridges started at the same time, the Papatoetoe footbridge in New Zealand, the Shepherds Gully Creek Bridge in Australia, the Bourdles-Valence bridge in France, and the Horikoshi C-ramp bridge in Japan. Since then UHPC application in bridges became more and more popular around the world. In 2013, 55 bridges in total have been built using UHPC in United states and Canada in addition to around 22 in Europe and 27 in Asia and Australia and more recent bridges mentioned in *Table 3*.

UHPC can be used as beams, girders, deck panels,

protective layers, field-cast joints between different components, etc. (Tirimanna, 2013), (Graybeal, 2013), (Musha et al., 2013), (Park et al., 2013), (Brugeaud, 2013), (Kim et al., 2013). Compared to standard reinforced concrete bridges, most bridges constructed using UHPC components or joints have a slender shape, a considerable reduction in volume and self-weight, a speedier construction process, and increased durability (Graybeal, 2006). The majority of UHPC constructions need less than half the section depth of conventional reinforced or pre-stressed concrete components, resulting a huge weight reduction (Perry, 2006). This lighter-weight construction and materials efficiency used in UHPC

structures lead to a sustainable structure through its lower carbon footprints (Voo, 2010).

The application of UHPC is not limited to bridges; UHPC is recommended for tunnel construction owing of its greater strength and fire resistance, which are critical characteristics for this type of building. UHPC's strength and durability make it an appropriate material for seismic columns as well. This is a novel method of designing earthquake-resistant columns; UHPC components are also employed in green energy, where they are used to build larger wind turbine towers. By increasing the strength and reducing the section size of the towers, we can enhance their production and create more renewable energy.

UHPC is the solution to concerns regarding the degradation, maintenance, and replacement of highway infrastructure. Due to its longer life and reduced lifetime cost, it is the ideal material for repairing and replacing existing roads and bridges.

5. UHPC CHALLENGES

UHPC is used in many applications around the world, but this use is still very limited compared with ordinary concrete, a lot of challenges still face the UHPC for wider implementation, as the benefits of this innovative material are still not well known.

Key challenges that must be addressed to provide a higher level of convenience to stakeholders, designers, contractors, and manufacturers to successfully implement UHPC in the field including, developing a logical and accurate method for optimizing UHPC components and mixture design to ensure the successful development and implementation of UHPC on a larger scale, some properties of UHPC affected by the fibre orientation in the mixture like the flexural tensile strength, therefore, it is necessary to develop a reliable method that allows efficient distribution of fibres in its concrete matrix in the desired direction, especially when the work with small sizes elements.

The shrinkage strains in UHPC mixes are much greater than those in conventional concrete. As a result, specific additives or preventive measures are required to address dimensional stability difficulties, particularly in large-scale structures.

The high strength properties of UHPC's and durability are heavily dependent on heat treatment. As a result, unique measures for on-site and precast heat treatment of the building should be investigated.

Due of the UHPC's extremely low w/c ratio, high-power mixers are necessary to adequately mix its constituents. Additionally, many adjustments to off-site mixers are necessary for the effective manufacture of precast UHPC parts.

The generally acknowledged, simple, and reasonable design requirements for UHPC (reinforced and unreinforced) should be designed to provide the design engineer confidence in the effective application of the UHPC's high strength and other special qualities.

6. CONCLUSION

Ultra high-performance concrete, the new generation for wider concrete applications and solutions, it has a superior level of qualities that had never been thought possible before. After reviewing the subject thoroughly, the following conclusions were found:

Table 3: Applications in Bridge engineering

Year	Location	Name
2017	China	Yuan Jiahe Bridge
2015	China	Fuzhou University Land-scape Bridge
2013	United States and Canada	55 bridges using UHPC have been built or are under construction
2013	Czech Republic	Celakovice Pedestrian Bridge
2010	Austria	WILD Bridge
2010	Malaysia	Kampung Linsum Bridge
2009	SouthKorea	Office Pedestrian Bridge
2008	United States	Cat Point Creek Bridge
2008	United States	Jakway Park Bridge
2008	France	Pont du Diable Pedestrian Bridge
2008	Japan	GSE Bridge
2007	Canada	Glenmore Pedestrian Bridge
2007	France	Pinel Bridge
2007	Germany	Friedberg Bridge
2006	United States	Mars Hill Bridge
2006	China	Luan Bai trunk Railway Bridge
2005	Japan	Horikoshi C-ramp bridge
2005	France	PS3, Bridge (Bourd-les-Valence bridge)
2005	Australia	Shepherds Gully Creek Bridge
2005	New Zealand	Papatoetoe footbridge
2003	Japan	Sakata-Mirai footbridge
2002	South Korea	Peace Bridge (Seonyu foot-bridge)
2001	France	Bourg-les-Valence bridge
1997	Canada	Sherbrooke Overpass

It was clear that the majority of researchers at the state-of-the-art highlighted that UHPC exceeds all expectations in terms of mechanical and environmental performance, emphasizing the possibility of more fantastic applications in building.

The mechanical properties of the UHPC are greatly superior to the properties of ordinary concrete. These incomparable values are a function of water to binder ratio, ultrafine powders, optimized packing of particles, method of curing, and microstructural reinforcement.

This technique enables the construction of buildings that are lighter, bigger, or have a greater span than conventional

designs. Due to its exceptional workability, new concrete may be cast in irregular or extremely thin forms to create structures with an exceptionally aesthetic look or finish.

7. REFERENCES

ACI 239R-18,2018. committee-ultra High performance Concrete: An Emerging Technology Report. American Concrete Institute. USA

Ahmad, S., Hakeem, I., & Maslehuddin, M. (2016). Development of an optimum mixture of ultra-high performance concrete. *European Journal of Environmental and Civil Engineering*, 20(9), 1106-1126. https://doi.org/10.1080/19648189.2015.1090925

Akçaoğlu, T., Tokyay, M., & Çelik, T. (2004). Effect of coarse aggregate size and matrix quality on ITZ and failure behavior of concrete under uniaxial compression. *Cement and concrete composites*, 26(6), 633-638. https://doi.org/10.1016/S0958-9465(03)00092-1

Akhnoukh, A. K., & Buckhalter, C. (2021). Ultra-high-performance concrete: Constituents, mechanical properties, applications and current challenges. *Case Studies in Construction Materials*, 15, e00559 https://doi.org/10.1016/j.cscm.2021.e00559.

Alkaysi, M., & El-Tawil, S. (2016). Effects of variations in the mix constituents of ultra high performance concrete (UHPC) on cost and performance. *Materials and Structures*, 49(10), 4185-4200. https://doi.org/10.1617/s11527-015-0780-6

Aoude, H., Dagenais, F. P., Burrell, R. P., & Saatcioglu, M. (2015). Behavior of ultra-high performance fibre reinforced concrete columns under blast loading. *International Journal of Impact Engineering*, 80, 185-202. https://doi.org/10.1016/j.ijimpeng.2015.02.006.

Arora, A., Yao, Y., Mobasher, B., & Neithalath, N. (2019). Fundamental insights into the compressive and flexural response of binder-and aggregate-optimized ultra high performance concrete (UHPC). *Cement and Concrete Composites*, 98, 1-13. https://doi.org/10.1016/j.cemconcomp.2019.01.015

Association of Civil Engineers of France, "Ultra High Performance Fibre-Reinforced Concrete Recommendations", France, June 2013.

Azad, A. K., & Hakeem, I. Y. (2013). Flexural behavior of hybrid concrete beams reinforced with ultra-high performance concrete bars. *Construction and Building Materials*, 49, 128-133. https://doi.org/10.1016/j.conbuildmat.2013.08.005

Azmee, N. M., & Shafiq, N. (2018). Ultra-high performance concrete: From fundamental to applications. *Case Studies in Construction Materials*, 9, e00197. https://doi.org/10.1016/j.cscm.2018.e00197

Bajaber, M. A., & Hakeem, I. Y. (2021). UHPC evolution, development, and utilization in construction: A review. *Journal of Materials Research and Technology*, 10, 1058-1074. https://doi.org/10.1016/j.jmrt.2020.12.051

Balázs, G. L. (2015). Material and Structural Properties for Creating High Performance Concrete Structures. In *Key Engineering Materials* (Vol. 629, pp. 21-27). Trans Tech Publications Ltd. https://doi.org/10.4028/www.scientific.net/KEM.629-630.21

Behloul, M., Ricciotti, R., Ricciotti, R. F., Pallot, P., & Leboeuf, J. (2008). Ductal pont du diable footbridge, France. In *Proceedings of the fib symposium "tailor made concrete structures* (pp. 335-338). https://doi.org/10.1201/9781439828410.ch58

Bierwagen, D., & Abu-Hawash, A. (2005, August). Ultra high performance concrete highway bridge. In *Proc. of the 2005 Mid-Continent Transportation Research Symposium, Ames, Iowa* (pp. 1-14).

Blais, P. Y., & Couture, M. (1999). PRECAST, prestressed pedestrian BRIDGE-WORLD'S first reactive powder concrete bridge. *PCI journal*, 44(5). https://doi.org/10.15554/pcij.09011999.60.71

Brugeaud, Y. (2013). Express bridge deck and light duty bridge. In *Toutlemonde F, Resplendino J, eds. Proceedings of International Symposium on Ultra-High Performance Fibre-Reinforced Concrete. Marseille, France* (pp. 389-394).

Buitelaar, P. (2004). Heavy reinforced ultra high performance concrete. In *Proceedings of the Int. Symp. on UHPC, Kassel, Germany* (pp. 25-35).

Chen, B. C., Huang, Q. W., & Wang, Y. Y. (2016). Design and construction of China's first ultra high performance concrete (UHPC) arch bridge. *Journal of China & Foreign Highway*, 36(01), 67-71.

Concrete, S. C. (2005). The European guidelines for self-compacting concrete. *BIBM, et al*, 22, 563.

Cwirzen, A., & Penttala, V. (2006). Effect of increased aggregate size on the mechanical and rheological properties of RPC. In *Proceedings of Second International Symposium on Advances in Concrete through Science and Engineering, Quebec, Canada*. https://doi.org/10.1617/2351580028.049

De Larrard, F., & Sedran, T. (1994). Optimization of ultra-high-performance concrete by the use of a packing model. *Cement and concrete research*, 24(6), 997-1009. https://doi.org/10.1016/0008-8846(94)90022-1

De MATTEIS, D., Marchand, P., Petel, A., Thibaux, T., Fabry, N., & Chanut, S. (2008). The new Pinel Bridge in Rouen, the fifth French road bridge using ultra high performance fibre-reinforced concrete components. In *17th Congress of IABSE. Creating and Renewing Urban Structures International Association for Bridge and Structural Engineering*. https://doi.org/10.2749/222137908796292821

Deeb, R., Ghanbari, A., & Karihaloo, B. L. (2012). Development of self-compacting high and ultra high performance concretes with and without steel fibres. *Cement and concrete composites*, 34(2), 185-190. https://doi.org/10.1016/j.cemconcomp.2011.11.001

El-Din, H. K. S., Mohamed, H. A., Khater, M. A. E. H., & Ahmed, S. (2016, July). Effect of steel fibres on behavior of ultra high performance concrete. In *International Interactive Symposium on Ultra-High Performance Concrete* (Vol. 1, No. 1). Iowa State University Digital Press. https://doi.org/10.21838/uhpc.2016.11

Farzad, M., Shafieifar, M., & Azizinamini, A. (2019). Experimental and numerical study on bond strength between conventional concrete and Ultra High-Performance Concrete (UHPC). *Engineering Structures*, 186, 297-305. https://doi.org/10.1016/j.engstruct.2019.02.030

Fehling, E., Bunje, K., Schmidt, M., Tue, N. V., Schreiber, W., & Humburg, E. (2007). Design of first hybrid UHPC-steel bridge across River Fulda in Kassel, Germany. In *IABSE Symposium: Improving Infrastructure Worldwide, Weimar, Germany, 19-21 September 2007* (pp. 328-329). https://doi.org/10.2749/222137807796158165

Gao, R., Liu, Z. M., Zhang, L. Q., & Stroeven, P. (2006). Static properties of plain reactive powder concrete beams. In *Key Engineering Materials* (Vol. 302, pp. 521-527). Trans Tech Publications Ltd.

Ghafari, E., Costa, H., Júlio, E., Portugal, A., & Durães, L. (2012, March). Optimization of UHPC by adding nanomaterials. In *Proceedings of the 3rd International Symposium on UHPC and Nanotechnology for High Performance Construction Materials, Kassel, Germany* (pp. 71-78).

Graybeal, B. (2013). UHPC in the US highway infrastructure: Experience and outlook. In *Toutlemonde F, Resplendino J, eds. Proceedings of International Symposium on Ultra-High Performance Fibre-Rein-forced Concrete. Marseille, France* (pp. 361-370). https://doi.org/10.1002/9781118557839.ch15

Graybeal, B. A. (2006). *Material property characterization of ultra-high performance concrete* (No. FHWA-HRT-06-103). United States. Federal Highway Administration. Office of Infrastructure Research and Development.

Graybeal, B. A. (2006). *Material property characterization of ultra-high performance concrete* (No. FHWA-HRT-06-103). United States. Federal Highway Administration. Office of Infrastructure Research and Development.

Habel, K., Viviani, M., Denarié, E., & Brühwiler, E. (2006). Development of the mechanical properties of an ultra-high performance fibre reinforced concrete (UHPFRC). *Cement and Concrete Research*, 36(7), 1362-1370. https://doi.org/10.1016/j.cemconres.2006.03.009

Japan Society of Civil Engineers (JSCE) (200.6), "Recommendations for Design and Construction of Ultra High Strength Fibre Reinforced Concrete Structures (Draft)", JSCE Guidelines for Concrete No 9.

Jun-feng Tan (2007), Application of reactive powder concrete (RPC) in railway prefabricated beam engineering, Shanghai Railway Sci. Technol., 2, pp. 54-55, https://doi.org/10.3969/j.issn.1673-7652.2007.02.027

Kim, B. S., Kim, S., Kim, Y. J., Park, S. Y., Koh, K. T., & Joh, C. (2013). Application of ultra high performance concrete to cable stayed bridges. In *Toutlemonde F, Resplendino J, eds. Proceedings of International Symposium on Ultra-High Performance Fibre-Reinforced Concrete. Marseille, France* (pp. 413-422).

Koh, K. T., Park, S. H., Ryu, G. S., An, G. H., & Kim, B. S. (2018). Effect of the Type of Silica Fume and Filler on Mechanical Properties of Ultra High Performance Concrete. In *Key Engineering Materials* (Vol. 774, pp. 349-354). Trans Tech Publications Ltd. https://doi.org/10.4028/www.scientific.net/KEM.774.349

Koukolík, P., Vítek, J. L., Brož, R., Coufal, R., Kalný, M., Komanec, J., & Kvasnička, V. (2015). Construction of the first footbridge made of UHPC in the Czech Republic. In *Advanced Materials Research* (Vol. 1106, pp. 8-13). Trans Tech Publications Ltd. https://doi.org/10.4028/www.scientific.net/AMR.1106.8

Lee, C. D., Kim, K. B., & Choi, S. (2013). Application of ultra-high performance concrete to pedestrian cable-stayed bridges. *Journal of Engineering Science and Technology*, 8(3), 296-305.

Li, J., Wu, Z., Shi, C., Yuan, Q., & Zhang, Z. (2020). Durability of ultra-high performance concrete–A review. *Construction and Building Materials*, 255, 119296. https://doi.org/10.1016/j.conbuildmat.2020.119296

Ma, J., Dietz, J., & Dehn, F. (2002). Ultra high performance self compacting concrete. *Lacer*, 7, 33-42.

Mishra, O., & Singh, S. P. (2019). An overview of microstructural and material properties of ultra-high-performance concrete. *Journal of Sustainable Cement-Based Materials*, 8(2), 97-143. https://doi.org/10.1080/21650373.2018.1564398

Morcous, G., & Akhnoukh, A. (2007). Reliability analysis of NU girders designed using AASHTO LRFD. In *New Horizons and Better Practices* (pp. 1-11). https://doi.org/10.1061/40946(248)81 Musha, H., Ohkuma, H., & Kitamura, T. (2013, October). Innovative UFC structures in Japan. In *Proceedings of International Symposium on Ultra-High Performance Fibre-Reinforced Concrete* (pp. 17-26).

Nematollahi, B., Saifulnaz, R. M., Jaafar, M. S., & Voo, Y. L. (2012). A review on ultra high performance›ductile›concrete (UHPdC) technology. *International Journal of Civil and Structural Engineering*, *2*(3), 994. https://doi.org/10.6088/ijcser.00202030026

Nguyen, K., Freytag, B., Ralbovsky, M., & Rio, O. (2015). Assessment of serviceability limit state of vibrations in the UHPFRC-Wild bridge through an updated FEM using vehicle-bridge interaction. *Computers & Structures*, *156*, 29-41. https://doi.org/10.1016/j.compstruc.2015.04.001

Oertel, T., Helbig, U., Hutter, F., Kletti, H., & Sextl, G. (2014). Influence of amorphous silica on the hydration in ultra-high performance concrete. *Cement and Concrete Research*, *58*, 121-130. https://doi.org/10.1016/j.cemconres.2014.01.006

Park, S. Y., Kim, S. T., Cho, J. R., Lee, J. W., & Kim, B. S. (2013, October). Trial construction of UHPC highway bridge. In *Proceedings of the RILEM-fib-AFGC international symposium on ultra-high performance fibre-reinforced concrete (UHPFRC 2013). International Union of Laboratories and Experts in Construction Materials, Systems and Structures (RILEM), Marseille, France* (pp. 1-3).

Perry, V. (2006). Ductal®-A Revolutionary New Material for New Solutions. Association of Professional Engineers and Geoscientists of the Province of Manitoba (APEGM).

Perry, V. H., & Seibert, P. J. (2008, March). The use of UHPFRC (Ductal®) for bridges in North America: The technology, applications and challenges facing commercialization. In *Proceedings of Second International Symposium on Ultra High Performance Concrete, University of Kassel, Germany* (pp. 815-822).

Rebentrost M., Wight G. (208). Experience and Applications of Ultra-High Performance Concrete in Asia, Kassel University Press, Kassel, Germany, pp. 19-30.

Richard, P., & Cheyrezy, M. (1995). Composition of reactive powder concretes. *Cement and concrete research*, *25*(7), 1501-1511. https://doi.org/10.1016/0008-8846(95)00144-2

Rouse, J., Wipf, T. J., Phares, B., Fanous, F., & Berg, O. (2011). *Design, construction, and field testing of an ultra high performance concrete pi-girder bridge* (No. IHRB Project TR-574). Iowa State University. Institute for Transportation.

Salahi, A., Dehghan, A. N., Sheikhzakariaee, S. J., & Davarpanah, A. (2021). Sand production control mechanisms during oil well production and construction. *Petroleum Research*, *6*(4), 361-367, https://doi.org/10.1016/j.ptlrs.2021.02.005

Schmidt, S. R., Katti, D. R., Ghosh, P., & Katti, K. S. (2005). Evolution of mechanical response of sodium montmorillonite interlayer with increasing hydration by molecular dynamics. *Langmuir*, *21*(17), 8069-8076. https://doi.org/10.1021/la050615f

Seyam, A. M, Shihada, S., & Nemes, R. (2020). Effects of polypropylene fibres on ultra high performance concrete at elevated temperature. *Concrete Structures*, *21*, 11-16. https://doi.org/10.32970/CS.2020.1.2

Seyam, A. M., Shihada, S., & Nemes, R. (2020). Effects of using polypropylene and steel fibres on Ultra High Performance Concrete subjected to elevated temperatures. 13th edition of the fib International PhD Symposium in Civil Engineering, 25-32. Paris.

Shah, S., & Weiss, W. (1998). Ultra high strength concrete; Looking toward the future. In *ACI Special Proceedings from the Paul Zia Symposium Atlanta, GA*.

Shi, C., Wu, Z., Xiao, J., Wang, D., Huang, Z., & Fang, Z. (2015). A review on ultra high performance concrete: Part I. Raw materials and mixture design. *Construction and Building Materials*, *101*, 741-751. https://doi.org/10.1016/j.conbuildmat.2015.10.088

Shin, H. O., Kim, K., Oh, T., & Yoo, D. Y. (2021). Effects of fibre type and specimen thickness on flexural behavior of ultra-high-performance fibre-reinforced concrete subjected to uniaxial and biaxial stresses. *Case Studies in Construction Materials*, *15*, e00726. https://doi.org/10.1016/j.cscm.2021.e00726

Tanaka, Y., Maekawa, K., Kameyama, Y., Ohtake, A., Musha, H., & Watanabe, N. (2009). Innovation and application of UFC bridges in Japan. *Proceedings of UHPC*, 112-120

Tayeh, B. A., Bakar, B. A., Johari, M. M., & Voo, Y. L. (2013). Evaluation of bond strength between normal concrete substrate and ultra high performance fibre concrete as a repair material. *Procedia Engineering*, *54*, 554-563. https://doi.org/10.1016/j.proeng.2013.03.050

Tirimanna, D., & Falbr, J. (2013). FDN modular UHPFRC bridges. In *Proceedings of international symposium on ultra-high performance fibre-reinforced concrete* (pp. 0395-0404).

Vernet, C. P. (2004). Ultra-durable concretes: structure at the micro-and nanoscale. *MRS bulletin*, *29*(5), 324-327. https://doi.org/10.1557/mrs2004.98

Voo, Y. L., & Foster, S. J. (2008). Shear Strength of Steel Fibre Reinforced Ultra-High Performance Concrete Beams Without Stirrups, 5th Int'l Specialty Conference on Fibre Reinforced Materials.

Voo, Y. L., & Foster, S. J. (2010). Characteristics of ultra-high performance 'ductile'concrete and its impact on sustainable construction. *The IES Journal Part A: Civil & Structural Engineering*, *3*(3), 168-187. https://doi.org/10.1080/19373260.2010.492588

Wille, K. (2013). "Development of non-proprietary ultra-high performance concrete for use in the highway bridge sector." Rep. No. PB2013- 110587, National Technical Information Service, Springfield, VA.

Wille, K., Naaman, A., & Montesinos, G. (2011). Ultra-high performance concrete with compressive strength exceeding 150 MPa (22 ksi): a simpler way. *ACI Materials Journal*, *108*(1), 46–54. https://doi.org/10.14359/51664215

Wu, L., Farzadnia, N., Shi, C., Zhang, Z., & Wang, H. (2017). Autogenous shrinkage of high performance concrete: A review. *Construction and Building Materials*, *149*, 62-75. https://doi.org/10.1016/j.conbuildmat.2017.05.064

Yu, R., Spiesz, P., & Brouwers, H. J. H. (2014). Mix design and properties assessment of ultra-high performance fibre reinforced concrete (UHPFRC). *Cement and concrete research*, *56*, 29-39. https://doi.org/10.1016/j.cemconres.2013.11.002

Zhou, M., Lu, W., Song, J., & Lee, G. C. (2018). Application of ultra-high performance concrete in bridge engineering. *Construction and Building Materials*, *186*, 1256-1267. https://doi.org/10.1016/j.conbuildmat.2018.08.036

Zhu, W., Feng, Q., Luo, Q., Bai, X., Lin, X., & Zhang, Z. (2021). Effects of PCE on the dispersion of cement particles and initial hydration. *Materials*, *14*(12), 3195. https://doi.org/10.3390/ma14123195

Ahmed M. Seyam (1989), civil engineer (M.Sc) in design and rehabilitation of structures, Ph.D. student at Department of Construction Materials and Technologies, Budapest University of Technology and Economics. Main field of interest: concrete technology, fibre reinforced concrete, fire design and improving construction materials. Member of the Palestinian Association of Engineers and the Hungarian Group of *fib*. E-mail: seyam.ahmed@emk.bme.hu

György L. Balázs (1958), Civil Engineer, PhD, Dr.-habil., Professor of structural engineering at the Department of Construction Materials and Technologies of Budapest University of Technology and Economics (BME). His main fields of activities are experimental investigation and modeling of RC, PC, FRC, FRP, HSC, HPC, LWC, fire resistance and fire design, durability, sustainability, bond and cracking. He is chairman of several commissions and task groups of *fib*. He is president of Hungarian Group of *fib*, Editor-in-chief of the Journal "Concrete Structures". He was elected as President of *fib* for the period of 2011-2012. Since then, he is Honorary President of *fib*. Chairman of *fib* Com 9 Dissemination of knowledge. E-mail: balazs.gyorgy@emk.bme.hu

FIRE PERFORMANCE OF RECYCLED AGGREGATE CONCRETE: CHALLENGES AND FUTURE PROSPECTS

Zubair Yousuf - Viktor Hlavička

The substantial amount of building and demolition waste that is produced worldwide and that is frequently disposed of by dumping and landfilling, which causes social and environmental problems, is discussed in the article. In order to address this issue, recycling technology for C&D trash has been created, and waste from the construction and demolition industries is turned into recycled aggregate that is then used to create recycled aggregate concrete. This strategy might aid in addressing the raw material shortage, cutting waste, and promoting environmentally friendly building methods. The effectiveness of recycled aggregate concrete (RAC) against fire is also explored in the research. The combination of components used, as well as their quality and manufacturing, might affect how fire-resistant RAC is. Because RAC is made of a solid, inert material with less water than traditional concrete, it has been shown to have excellent fire-resistant qualities overall. However, compared to conventional aggregate concrete, RAC may show more spalling and suffer a larger decrease in strength when subjected to high temperatures. The impact of variables like moisture content and compressive strength on the danger of spalling is also highlighted in the paper. According to the study, sustainable concrete built with RAC may, with proper design, meet specified fire design goals, although it may function mechanically less well at extremely high temperatures than conventional concrete.

Keywords: Construction and demolition debris, sustainable concrete, fire resistance, spalling, mechanical performance, traits that prevent fires.

1. INTRODUCTION

Concrete the most common construction material in the world represents the main component of construction and demolition waste (Xiao, Lu, and Ying, 2013). The rapid urbanization in the world has resulted in a significant amount of construction and demolition (C&D) waste, which is commonly disposed of through dumping and landfilling. This leads to social and environmental issues, such as safety problems and pollution of soil and water. To combat this, recycling technology for C&D waste has been developed, and concrete and brick waste are recycled into recycled aggregate for use in preparing recycled aggregate concrete (Vázquez et al., 2014). The construction industry is identified as a major contributor to this issue, the European Union generating approximately 850 million tons of waste per year, or about 31% of overall production (Thomas et al., 2013). However, some researchers have found that the CDW accounts for over 35% of all waste produced in the EU, generating about 1000 million tons of waste per year (Hu et al., 2018). The construction activities in Europe have been growing at an increasing rate due to the increasing demand for raw materials and aggregate production and importation are no longer sufficient to provide all the needed raw materials, and lead to the depletion of natural aggregate resources. In France, quarries are being protected, and aggregate producers are struggling to find

workable sites. On the other hand, demolition sites generate significant waste, which is often not reused and limited to road construction. The paper suggests recycling demolition waste as construction materials for structural concrete as a promising alternative, provided that the recycled materials meet the necessary mechanical standards. This approach could help to address the shortage of raw materials, reduce waste, and promote sustainable construction practices (Yuan et al., 2023). Using waste materials in construction aligns with the principles of sustainable development and numerous environmentally friendly production technologies incorporate waste materials as fillers or additions to concrete and other construction materials, such as asphalt. Among the options available, the use of concrete made with recycled aggregates from construction and demolition waste is particularly relevant. This approach has a dual benefit, as it reduces waste accumulation in landfills and limits the consumption of natural aggregates, indirectly controlling the environmental impact of opening new quarries. By reusing waste materials in construction, it is possible to promote sustainable practices and contribute to the circular economy, which can have positive environmental and economic effects (Adessina et al., 2019). However, the direct use of recycled aggregates (RAs) in making concrete is inefficient due to the high-water absorption and porosity of old mortar layer on recycled aggregate. Further, the interfacial transition zones (ITZs) in RAC are different from those of natural aggregate concrete

(NAC). In other words, the amount of RA utilized in RAC is one of the critical factors affecting its mechanical properties (Guo et al. 2018). Recycle aggregate concrete RCA has some distinct differences from natural aggregates (NA), including higher water absorption, higher Los Angeles wear, lower bulk and particle density, and more irregular geometry, which can be attributed to the mortar adhered to the aggregates. However, the rough texture and high porosity of RCA can lead to densification of the interfacial zone and improved performance in concrete (Thomas et al., 2013). Furthermore, concrete being a brittle material composed of aggregates and mortar, which has many microcracks and other defects. Visible cracks propagate from microcracks under load during the service life, reducing the load capacity of the structure at ambient temperature, the use of RAC in high-temperature conditions, such as during a fire, needs further study to ensure its bearing capacity and promote its use as a sustainable construction material (Guo et al., 2018). Fire performance is a critical factor that needs to be considered in RAC structures due to the material's brittleness. Therefore, further studies are necessary to promote the use of RAC in construction (Yuan et al., 2023).

2. PROPERTIES OF RECYCLED AGGREGATE CONCRETE

The ability to explain why RAC can differ significantly when used in concrete can be improved by having a better grasp of how the aggregate transforms after being used in concrete. The study involves discussion on various types of concrete and evaluating their physical characteristics such as absorption, density, porosity, and water permeability, as well as their mechanical properties including compression, tensile strength, Young's modulus, shrinkage, and creep, freezing and thawing etc.

2.1 Mechanical properties of recycled aggregate concrete, factors affecting the mechanical properties

Concrete consists of aggregate, which makes up 70-80% of its volume and is crucial for determining its properties. Coarse aggregate forms the framework of particles that bear the load in a concrete structure, while fine aggregate and cement paste fill in the voids between these particles, affecting the density, cement mortar amount, and performance of the concrete (Bui, Satomi and Takahashi, 2017). The greatest distinguishing aspect of RA is that, in contrast to NA, it is made up of original aggregate and attached mortar. The adhering mortar content tends to be inversely related to specific gravity and proportional to water absorption. The method of manufacturing, the strength of the parent concrete, and the quantity of uses all have an impact on the quality of RA. The mechanical characteristics and durability of RAC are influenced by the RA quality, and when the RA quality is poor or the replacement rate rises, RAC's performance suffers. The main distinction between RA and NA is that the former is composed of attached mortar and original aggregate. The content of the adhering mortar often correlates with water absorption and has an inverse relationship with specific gravity (Kim, 2022). Recycled aggregate concrete is not as strong or durable as natural aggregate concrete because the surface of the recycled aggregate sticks to the mortar, which

changes its properties and creates a weak interface between the binder and the aggregate. This weak point depends on the relative strength of old and new mortar, as well as the mass of the interfacial transition zone. The recycled aggregate also has a "wall effect" that leads to a higher water-cement ratio, more pores and cracks, and weaker concrete. Nano silica has been found to accelerate hydration and improve the mechanical properties of the interfacial transition zone, resulting in stronger and less porous concrete. However, excessive use of nano silica can cause problems such as expansion of the silicate polymer, reduced compressive strength, and increased shrinkage and creep (Zheng, Zhuo, and Zhang, 2021). it was observed that the strength decreases as the proportion of recycled concrete aggregate in the mix increases. Specifically, there is an average drop of 13% in compressive strength when using 20% recycled concrete aggregate replacement, and a drop of 32% for 100% replacement. The compressive strength of recycled aggregate concrete is influenced by various factors, such as the amount of free water, cement content, and properties of the recycled concrete aggregate. Generally, replacing natural aggregate with recycled concrete aggregate is expected to decrease both compressive strength and elasticity modulus of the concrete, which may be due to lower strength of the recycled concrete aggregate or defects in the interfacial transition zones between the old and new mortar (Guo et al., 2018). The recycled aggregate typically consists of virgin aggregate with old cement mortar attached, which determines its properties along with the type and quality of the virgin aggregates, unbound stone, and any impurities present such as bricks, tiles, glass, asphalt, plastic, wood, and gypsum. The old cement mortar attached to recycled aggregate is often considered the primary reason for its poorer properties compared to natural aggregate, as it results in higher water absorption, porosity, crushing value, and Los Angeles abrasion value, and lower specific gravity. Compared to natural aggregates, the RAs exhibited lower density and 10% fines values. It appears that 10% fines value (TFV) is a more sensitive indicator of recycled aggregate strength than aggregate crushing value. A strong correlation exists between the density of concrete and the specific gravity of the aggregates used, with all correlation coefficients (R^2) exceeding 0.85. The compressive strength of concrete made with recycled aggregates was mostly lower than that made with natural aggregates, regardless of the water-to-cement ratio used. However, the strength of both types of concrete increased with age. Thus, high-quality RAs can be used to produce concrete with similar strength to natural aggregates. This increase in strength may be attributed to the attached cement mortar, which enhances the bonding between the RA and new cement paste, and the rough surface of the RAs, which improves the microstructure of the interfacial transition zone (Duan and Poon 2014). The presence of old mortar and contaminants, recycled aggregates often had worse characteristics than NA. The strength of the concrete is impacted by the presence of attached mortar in recycled aggregate. Nevertheless, silica fume solution impregnation and ultrasonic cleaning improve the strength properties of RAC by 15% and 7%, respectively. Treating RA giving beneficiation and improves its characteristics. Treatment of recycled aggregates primarily entails removing mortar that has clung to the aggregate's outer layer. The aggregate surface qualities were enhanced, and loose and weakly adherent mortar was eliminated as much as possible from treated aggregates. The compressive strength of treated recycled

aggregate concrete was increased by 8–18% at the age of 28 days compared to untreated RAC due to better contact at the interfacial transition zone between treated RA and fresh cement paste. The latter age of prepared recycled aggregate concrete was shown to have good strength development. The surface treatment technique successfully eliminated the loose mortar particles, greatly enhancing the qualities of RA (Saravanakumar, Abhiram, and Manoj 2016). The most important property of concrete is its compressive strength, which impacts its mechanical strength, durability, and other characteristics. As the replacement rate of recycled aggregate increases, regardless of the type or quality of the aggregate, the compressive strength of concrete decreases. It is 95% likely that recycled aggregate concrete containing 100% coarse recycled concrete aggregate will have compressive strengths about 0.766 times lower than those of corresponding NAC specimens. However, in some cases, RAC exhibits similar or even slightly greater strength, especially when it contains RCA. This may be because the bond strength in the interface transition zone (ITZ) between the old, attached mortar and new cement paste is improved for some reason (*Fig*. 1). Overall, increasing the amount of RA used in concrete is generally unfavourable to its compressive strength, but incorporating a small proportion of recycled aggregate can sometimes increase strength. Like ordinary concrete, the compressive strength of RAC decreases with an increase in the water-cement ratio, and it varies greatly at lower ratios. To achieve similar compressive strength values as NAC, the water-cement ratio of RAC should be 0.05-0.1 lower, which is due to the low water utilization ratio of the ITZs between old, adhered mortar and aggregate. While the performance of RAC is generally inferior to NAC, simple and low-cost approaches such as adjusting the water-cement ratio, aggregate water content, mixing method, and admixture can improve its quality to some extent. It is not practical to remove old, adhered mortar to improve the properties of RAC (Bai et al., 2020). The remaining mortar and ITZs in RCA with extended service times are weaker, resulting in reduced compressive strength of the final concrete. However, the "internal curing effects" brought on by the saturated RCA may increase the compressive strength of recycled concrete. A model was created using the two-phase composite material theory to estimate the RAC elastic modulus by linking it to the NAC elastic modulus and taking residual mortar content into account. With a linear coefficient of 0.972 and a correlation coefficient (R^2) of 0.850, the projected values were found to be in fair agreement with the equivalent experimental results. The crucial parameter impacting the shrinkage behaviour of RAC was found to be residual mortar content (Geng et al., 2019).

When RAC's and NAC's indirect shear strengths are contrasted, In RAC and NAC, the indirect shear strength at 56 days was, on average, 8% and 5% greater than it was at 28 days. When comparing the growth of the compressive and indirect shear strengths, it can be seen that the compressive strength grew more quickly in the next two weeks after the indirect shear strength did in the first two. The average of the coefficient of variation values for the five mixtures was 2.73% for RAC and 2.60% for NAC. This difference is negligible, probably as a result of the aggregate's few sources being recycled. If concrete is obtained from various sources, this observation could not be valid. The comparison takes into account the compressive strengths of cubes, cylinders, and indirect shear. The strength of the RAC cube was, on average, 88.4% more than that of normal concrete. In a similar vein, RAC's cylinder compressive strength and indirect shear strength were, respectively, 92.2% and 87.7% of those of NAC. When recycled coarse aggregates are utilized, the strength often decreases by 10%. The large variation in strength reduction illustrates the impact of several elements, including the recycled aggregate's source, and highlights the necessity of testing local materials to determine their true behavior. In general, for RAC and NAC, respectively, the 56-day cube strength was 5% and 3% higher than the 28-day strength on average. Like to NAC, RAC can have its strength boosted by reducing the water-to-cement ratio if water reducers are used to provide sufficient workability. The strength of the crushed concrete used to create the recycled aggregates does not limit the compressive strength of RAC (Rahal 2007). When compared to natural aggregate with the same particle size, it was discovered that recycled aggregate considerably absorbs more water. This is due to the fact that broken limestone is less capable of absorbing water than the old, connected mortar in recycled aggregate. The physical characteristics of recycled aggregate (density and water absorption) were inferior to those of natural aggregate. The strength of recycled concrete decreased with an increase in recycled aggregate percentage when it ranged from 0% to 66.7%. The strength of recycled concrete improved as the percentage of recycled aggregate grew, which was greater than 66.7%. In other words, concrete with a single type of coarse aggregate (0% and 100%) had a better strength than concrete with both recycled and natural material. This was due to the fact that, as compared to other replacement levels of concrete, the difference between the physical properties of aggregate groupings for concrete (0% and 100%) was less. Also, it was investigated. With a larger aggregate size, recycled concrete performed compressively better. This was mostly caused by the decreased amount of adhering mortar in the larger aggregate size (Kang and Weibin 2018). Other researchers observed the improvement of the mechanical properties even from a 50% RCA dosage (Abed and Nemes 2019). It was found that as the substitution ratio of crushed recycled concrete aggregate (CRCA) increased, the cracks on the non-loaded surface of concrete during compression failure decreased, while the tensile and shear failure sections of concrete became rougher and accompanied
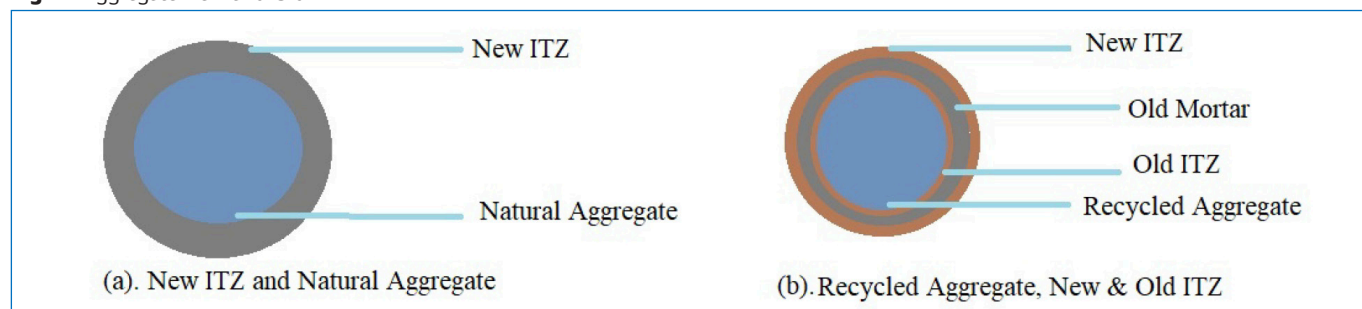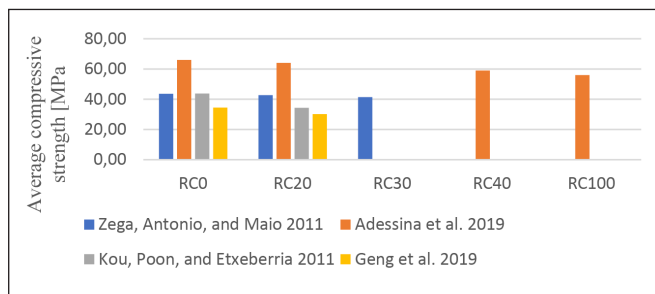
Fig. 1: *Aggregate New and Old ITZ*

(a). New ITZ and Natural Aggregate

(b). Recycled Aggregate, New & Old ITZ

Effect of replacement rate of recycled coarse aggregate on residual compressive strength at the age of 28 days of concrete

Research	Replacement rate of recycled coarse aggregate				
	RC0	RC20	RC30	RC40	RC100
Zega, Antonio, and Maio 2011	43.6	42.7	41.4	-	-
Adessina et al. 2019	66	64	-	59	56
Kou, Poon, and Etxeberria 2011	43.8	34.3	-	-	-
Geng et al. 2019	34.5	30.2	-	-	-

Fig. 2: *Effect of replacement rate of recycled coarse aggregate on residual compressive strength at the age of 28 days of concrete (Adessina et al. 2019) (Zega, Antonio, and Maio 2011), (Kou, Poon, and Etxeberria 2011), (Geng et al. 2019)*

by more concrete fragments, which were not affected by the substitution ratio of CRCA. Additionally, as the size of the concrete specimen increased, the integrity of concrete after compression failure increased. When the side length of the concrete cube was 150 mm, the substitution ratio of CRCA had the least impact on the compression failure of concrete. Moreover, as the substitution ratio increased, the peak compressive stress and peak tensile stress of RAC gradually decreased, the splitting limit displacement decreased, and the splitting tensile modulus slightly increased. As the substitution ratio of CRCA increased, the impact of the size effect on the peak compressive stress of concrete decreased gradually. The influence of size effect on the compressive strength of RAC was higher than that of ordinary concrete. Specifically, when the substitution ratios were 0% and 100%, the peak compressive stresses of RAC were reduced by up to 18.97% and 8.53%, respectively, due to the influence of the size effect (Du et al., 2021). When examined the relationship between the compressive strength of recycled aggregate concrete RAC and conventional concrete CC over three experimental phases, which were aged for 28 (a), 180 (b), and 365 (c) days, and also considered the effective water-to-cement (w/c) ratio. The results indicated that using 20% recycled aggregate RA content did not significantly impact the compressive strength of the concrete compared to CC after 28 days. However, with 100% RA substitution, there was a significant decrease in compressive strength, and to maintain similar strength levels, it was necessary to reduce the w/c ratio by 0.05. Additionally, after 180 days, the difference between the compressive strength of CC and RAC was more significant for stronger concretes (Thomas et al., 2013). A new method for combining RA in concrete, which replaces only large-sized RA particles with NA in the coarse aggregates. This method was compared to the conventional method, which replaces the entire coarse aggregate mixture or fine aggregate combined with all particle sizes of NA. The results showed that compressive strength increased as the RA replacement percentage decreased, and the new combination method yielded significantly higher compressive strengths at 7 days compared to the conventional method. This was attributed to the angular and rougher surface texture of RA,

which improved bonding and interlocking with the cement paste at an early age. At 28 days, the compressive strength of RAC with 100% RA decreased by 38% compared to that of natural aggregate concrete (NAC). However, the new method showed considerable increases in compressive strength at all replacement levels compared to the conventional method, with a maximum increase of 22.7% for 50% RA content. In general, the compressive strength of RAC using the new method was similar to that of NAC, with a maximum difference of 5.6% at 50% RA content. The splitting tensile strength of RAC was slightly affected by the replacement proportion of RA and combination method, with the new method yielding slightly higher strengths of approximately 5% compared to the conventional method. Overall, the study suggests that the new combination method is more effective in accelerating the compressive strength of RAC than the conventional method and recommends using up to 50% RA content with the new method (Bui et al., 2017). The above all discussion can be understood from the illustrated graph plotted below, this graph is the final combined results of several literatures and is plotted between the compressive strength of RCA after 28 days and the proportional replenishment rate of natural aggregate by recycled coarse aggregate, It is observed that the compressive strength of the recycled aggregate concrete increases as the replenishment rate of the recycled coarse aggregate increases but similarly shows some decrease in compressive strength at 100% replenishment rate of NA by RA which is admissible. This phenomenon of increase in strength of the RCA is because of the adhered mortar on the recycled aggregate and presence of the double ITZ in RCA. The given *Table 1. and Fig. 2* summarizes the results of the previous experiments.

2.2 Durability

The fundamental durability traits of recycled aggregate concrete, such as water absorption, chloride permeability, porosity, freezing and thawing, were covered in this review paper. A crucial aspect of concrete's long-term durability is its capacity to function in all challenging circumstances, including extreme heat. Furthermore, covered is concrete's performance at high temperatures, which is a crucial factor.

2.2.1 Chloride permeability

Chloride ingress is the primary form of environmental attack on reinforced concrete exposed to chlorine salt environments, leading to corrosion of reinforcing steel bars and a reduction in durability. There are two commonly used tests to measure the chloride permeability of concrete: the conventional chloride diffusion test and the accelerated chloride diffusion test. The majority of NAC diffusion coefficients fall within the range of 110×10^{-12} m²/s, with the upper limit of chloride diffusivities increasing with w/c. RAC diffusion coefficients, on the other hand, range from 116×10^{-12} m²/s, showing larger variability than NAC, likely due to the influence of old attached mortar

and old ITZ, which vary more than new mortar and new ITZ. The replacement percentage of RCA also has a linear impact on chloride penetrability, with recycled aggregates slightly increasing the coefficient of permeability and chloride diffusion coefficient but remaining within acceptable values for durable concrete. The resistance of chloride ion penetrability can be improved by using fly ash as a partial replacement of cement and recycled aggregate concrete displays greater resistance as curing age increases. Reducing the w/c ratio can also improve chloride impermeability (Xiao et al., 2013), indicating that in a chloride environment, RAC (recycled aggregate concrete) prepared with a low w/c (water-to-cement) ratio performs better than NAC (natural aggregate concrete). This may be due to the higher presence of C-S-H (calcium silicate hydrate) gels in RAC, which facilitate binding with chloride. The binding of chloride in concrete can occur through a chemical reaction between chlorides and hydrated cement aluminates, or through physicochemical adsorption in the CSH. Chlorides from an external source can be bound by the new cement paste in the RAC, as well as the old mortar adhered to the RCA. The use of a new method for mix proportioning in RAC leads to comparable diffusion performance for chlorides, similar to that of NAC and conventional RAC, while significantly reducing the cement content of the mix. This represents a noteworthy advancement in terms of sustainability (Vázquez et al., 2014). The substitution of NA in recycled aggregate concrete (RAC) had a greater effect on reducing chloride penetration as the w/c ratio in the RAC mix increased. This suggests that the w/c ratio used in RAC plays a role in enhancing the RCA's diffusivity (Yuan et al., 2023). The recycled aggregate size ranging from 5-10 mm offers greater resistance to chloride permeability (Duan and Poon, 2014). Demonstrates that the amount of recycled concrete, in the microstructure affects the ability of the sample to resist chloride penetration. When the recycled aggregate contains more mortar, the resulting concrete is more porous, leading to a rapid increase in cumulative chloride concentration. The replacement rate is also related to an increase in the chloride diffusion coefficient, which is influenced by the porosity of the recycled concrete. the new mortar has a higher diffusion coefficient than the reconstructed attached mortar, which is primarily due to the content and lack of damage of the reconstructed mortar. However, it is important to note that the real chloride diffusion coefficient of the attached mortar in the recycled concrete aggregate is expected to be higher than that of the reconstructed attached mortar due to the presence of micro-cracks and interface effects (Adessina et al., 2019). It is suggested there is approximately a 95% probability that the total accumulated charge of Recycled Aggregate Concrete (RAC) with 100% coarse Recycled Aggregate (RA) content exceeds that of Normal Aggregate Concrete (NAC) by a factor of about 2.07. The influence of fine RA on chloride penetration is more noticeable than that of coarse RA because of the greater amount of adhered mortar and clay content. Like regular concrete, the chloride penetration resistance of RAC decreases as the w/c ratio increases and increases with curing age. When compressive load is applied, the chloride diffusion coefficient of RAC initially decreases and then increases as the compression load increases. The maximum reduction in the chloride diffusion coefficient of RAC was approximately 40% at stress ratio of 0.51, which is more responsive to compressive loading compared to NAC (which was 25%) due to the higher porosity of RA. RAC made with RA sourced from higher-strength concrete

showed lower chloride penetration than the concrete made with lower strength RA due to its lower water absorption (Guo et al., 2018). In general the durability of recycled aggregate concrete (RAC) used in construction needs special attention, especially regarding chloride penetration. Since the distribution of recycled coarse aggregates (RCA) is random, a five-phase RAC model is suggested to predict the effective diffusion coefficient of chlorides in RAC. This model includes new mortar, adhering old mortar, new interfacial transition zone (ITZ), old ITZ, and original natural coarse aggregates. It focuses on critical factors such as the volume fraction of RCA, the adhesion ratio of old mortar, the chloride diffusivity of adherent old mortar, the thicknesses of old and new ITZs, and the chloride diffusivity of old and new ITZs, and how they affect each phase and the effective diffusion coefficient of chlorides in RAC. Results show that the effective diffusion coefficient varies depending on the quality of adherent old mortar, the adhesive ratio of old mortar, the thickness of ITZs, and the chloride penetration resistance of ITZs. However, the model is only applicable to fully replaced RCA concrete since the model's multilayer spherical approximation (MLSA) cannot accurately predict the smear effect between RCA and natural aggregates (NA) in concrete with both RCA and NA (Hu et al., 2018).

2.2.2 Porosity

There is a connection between the open spaces within RAC and control concrete (CC), and this was investigated in three experimental phases over the course of 28, 180, and 365 days, as well as the effective water-to-cement (w/c) ratio. Generally, the RAC's accessible spaces, in contrast to CC, increases with a higher w/c ratio and substitution degree. Using RA has a negative effect on the durability of non-compact cement paste concretes. Furthermore, incorporating RA leads to an increase in porosity that is dependent on the w/c ratio and degree of substitution (Thomas et al. 2013). Both normal aggregate concrete and recycled aggregate concrete using two different sources of recycled coarse aggregate RA (one obtained from crushed granite and another crushed concrete rubble from demolished building), exhibited similar levels of porosity after 28 days of curing. However, significant variations in porosity were observed among the different types of concrete after 5 years of water curing. The concrete made entirely from crushed concrete aggregate had the lowest porosity after 5 years of curing, with a 45% reduction in porosity compared to 28 days. In contrast, concrete made with recycled aggregate containing mainly natural stone (granite) had the highest porosity after 5 years of curing, with only a 7% reduction in porosity compared to 28 days. The use of crushed concrete in the recycled aggregate significantly enhanced the long-term interfacial properties of the new concrete, most likely due to the extended self-cementing effects of the old cement mortar and the interaction between the new cement paste and the old cement mortar (Kou et al. 2011). It was found that the total porosity measured by X-ray computed tomography (XCT) increased with the ratio of substitution due to the adhered mortar of the aggregate, but the increase was different for saturated and dry aggregate. The increase in porosity was more significant for the saturated recycled aggregate, where the water absorbed increased the water/cement ratio, resulting in reduced mechanical properties. The recycled aggregate concrete made with saturated recycled aggregate had a higher number of larger pores and an open microstructure. The macro porosity of recycled aggregate concrete, shows an increase

in macropore density with the height of the specimens, an exponential trend of the number of pores with their size, and a higher increase in the number of small pores and also larger pores in the perimeter of the sample, which increased with the substitution ratio were also observed (Thomas et al., 2019). It appears that at substitution rates of 20%, 30%, and 60%, there is no significant change in porosity (2%, 4%, and 11% respectively) when compared to the original mixture (NAT). Compared to natural aggregates, RA are more porous and have old cement paste attached to their surface, resulting in a different microstructure of the Interfacial Transition Zone (ITZ) in RAC than that of traditional concrete. As the RA content increases, the total and average porosity diameter of the concrete increases (Arredondo-Rea et al., 2019) The RCs' replacement factor r, which refers to the pore radius, is associated with both total volume and pore size. Its impact is more pronounced in younger concrete and diminishes as it ages. The reason for this effect is attributed to the creation of new products that reduce the number and size of pores. Given the wide range of pore sizes in concretes ranging from 1 nm to 1 cm. The most significant differences observed in the samples analyzed were related to two parameters, the first being the threshold for a larger pore radius, which increases as the replacement of NA by RCA increases, and the second being the detection of areas with major quantitative changes, where the pore volume from pores with a radius less than 30 nm increases (Smart and Jerman 2002). As the temperature exposure increased, the mortars' porosity and average pore diameter increased. The RA concrete had higher porosities than natural aggregate concrete before being exposed to high temperatures, likely due to the presence of old mortars. Concrete made with Portland cement had lower porosities than those made with 55% GGBS55 (ground granulated blast furnace slag) and 35% FA, but the average pore sizes of Portland cement concrete were higher than those of GGBS55 and FA concretes. After exposure to 300 °C, the increase in porosity of FA and GGBS concrete was lower than that of Portland cement concrete, possibly due to the pozzolanic reactivity of FA and GGBS, resulting in generally smaller average pore diameters (Eckert and Oliveira, 2017).

2.2.3 Water Absorption

The presence of pores in aggregates means that dry particles can absorb some water. The amount of water absorbed depends mainly on the number and continuity of the pores, while the rate of absorption is influenced by pore size and continuity, as well as particle size. When using aggregates in a concrete mix, any unsaturated aggregate will absorb some of the mixing water, while free moisture on the surface of the particles will also contribute to the mix. To calculate the effective water/cement ratio and mix proportions by weight, the saturated surface dry condition is used as a reference point. However, recycled aggregates can be challenging to work with because their irregular shape makes it difficult to eliminate all free water after soaking. To measure the water absorption coefficient over time for both natural and recycled aggregates, it is best to observe the rate of capillary rise and measuring the change in mass of the sample over time but the standard 24-hour soaking time is insufficient for measuring water absorption in recycled aggregates, as it only accounts for 60-70% of the total absorption obtained after longer soaking periods (Materials, 2017). The ability of water to pass through a material increases as the ratio of water to cement (w/c) increases and as the proportion of Recycled

Aggregate used in the material increases. The absorption coefficient of RAC increases with both the w/c ratio and the extent of recycled aggregate (RA) substitution. For instance, when the w/c ratio is 0.65 and the RAC contains 100% RA, the absorption coefficient increases from 6.2% to 8.4% compared to the CC. This represents a 35% increase in absorption (Thomas et al., 2013). The water absorption rate of RAC concretes is 15% greater than that of CC, but the water absorption rate of concretes made with varying amounts of recycled fine aggregates remains the same. Therefore, it can be inferred that the coarse aggregate has a significantly greater impact on this characteristic (Zega et al. 2011). The ability of recycled aggregate concrete (RAC) to resist water penetration is mainly influenced by factors such as the content of recycled aggregate (RA), the ratio of water to cement (w/c), the original strength of the waste concrete, the age of curing, and the presence of mineral admixtures. When the proportion of RA in RAC increases, its water resistance decreases. This is because the attached mortar and cracks in the waste concrete can provide a pathway for water to penetrate the RAC, and as the w/c ratio increases, the water absorption of RAC also increases. The impermeability of RAC is also affected by the particle size of the RA. Larger coarse aggregates have less surface area and attached mortar content, which reduces the water required for concrete and improves its strength. However, larger particles can also increase defects within the RAC. Mineral admixtures have been utilized to enhance the impermeability of RAC by filling the pores and creating a mesoscale pozzolanic reaction. So, incorporating a specific quantity of mineral additive is a successful approach for enhancing the interface composition and overall functionality of RAC (Guo et al., 2018). The water absorption in RCA within 24 hours is a combination of two factors, the capillary absorption of any leftover cement paste and the initial absorption of the natural aggregates. The two samples of RCA with the same 24-hour absorption rate can have significantly different absorption kinetics, which can impact the slump loss of concrete made with dry RCA. This behavior is strongly linked to the porosity of the paste, which is similar to the capillary absorption of regular concrete (Habert and Roussel, 2014). The absorbent qualities of aggregate depend on the degree of particle porosity or the average value of a mixture of high and low absorption materials. Coarse aggregate has a higher water absorption rate due to the higher absorption rate of cement mortar attached to the aggregate particles. Recycled aggregate is typically more absorptive than natural aggregate, with water absorption rates ranging from 3-10% and less than 1-5%, respectively. Therefore, it is crucial to understand the water absorption rates of recycled aggregate during the mix design stage. British Standards Institution (BSI) for measuring water absorption of aggregate is prominent. The BSI approach requires surface-drying the aggregate with a cloth or towel, which may detach some cement paste sticking to the surface of the aggregate, leading to a significant reduction in the oven-dried mass of aggregate and a less accurate testing result. To overcome these issues, the author proposes a new approach called real-time assessment of water absorption (RAWA), which provides a simpler and more accurate way to obtain water absorption rates at different time intervals without the need to soak and dry the recycled aggregate sample. RAWA avoids the removal of cement paste during the soaking and drying process of the recycled aggregate sample and provides a more genuine water absorption rate. The method has been tested and proven to be a good

alternative for measuring water absorption of recycled aggregate (Tam et al., 2008). increasing the amount of Recycled Aggregate in concrete leads to a rise in water absorption and a decrease in density. The measured difference in water absorption between NAC and RAC is similar to the calculated difference, indicating that the cement slurry couldn't decrease the aggregate absorption capacity by sealing the pores. However, there is a noticeable difference between the measured and calculated densities. The calculated density decrease from NAC to RAC is on average 45% higher than the measured ones, suggesting that the mortar seals some superficial pores of the aggregates, especially in lower density aggregates. Concretes durability is linked to water absorption, and hence RAC should be protected from moisture in harsh environments. The water flow capacity in the hardened state allows internal curing via saturated aggregates, reducing shrinkage cracking. It is worth mentioning that low aggregate density has positive effects on concrete structures, such as reducing the dead weight of the structure, thermal conductivity, and thermal bridges, which improves the insulation capacity of the building. The staged mixing approach can be followed to decrease the ITZ water flow of RAC to a negligible amount in its fresh state. Incorporating extra water during the two-staged mixing approach for RAC can mitigate the adverse effects of recycled aggregate water absorption in concrete technology, provided the pre-wetting time is 5 min. However, these procedures are not recommended for natural aggregates since significant swelling in the slump test was found, which breaks the bonds and increases the effective w/c ratio (Eckert and Oliveira, 2017). The absorption of water by recycled aggregates (RAs) depends on the effective water to cement ratio (w/c), which affects the workability of the concrete mix and the performance of the hardened concrete. The size of the RAs affects the rate at which water is absorbed due to the different specific surfaces. There are two stages of water absorption, a rapid stage and a slow stage. During the first stage, the rate of absorption increases as the size of the RAs decreases. The three-dimensional Terzaghi capillary water rise model can be used to express the rapid water absorption stage, which ends when the wetting front reaches the center of the RAs particles. The slow water absorption in the second stage is caused by air bubbles not being separated from the opening of large pores in a timely manner, which increases the buoyancy force of the sample, and water-air displacement in the large pores slowing down due to a decrease in capillary pressure. The difference in capillary pressure between small and large permeable pores drives the water absorption of RAs immersed in water, and the capillary pressure in large pores can usually be ignored due to their diameters being several orders of magnitude larger than the most probable value of the RAs pores' diameters. The size of the RAs affects the rate of water absorption due to the different specific surfaces (Liang et al., 2021). The water permeability of recycled aggregate concrete (RAC) is weak compared to natural aggregate concrete (NAC), with a value of around 10-20 m². Self-healing may also play a role in reducing water permeability and improving durability in real conditions, making it a potential factor for assessment (Zaharieva et al., 2003). Moreover, after being exposed to temperatures below 500 °C, the capillary absorption coefficients of recycled aggregate concrete (RAC) were found to be higher than those of natural aggregate concrete with all types of binders used. This is most likely because the RA has higher porosity and a larger amount of total mortar. However, when exposed to 800 °C, the concrete prepared with 100% RA had a lower water absorption coefficient than natural aggregate concrete due to the more suitable CTE (coefficient of thermal expansion) of the RA with the new cement paste-mortar, resulting in less cracking. Additionally, regardless of the type of binder used, the concrete mixtures made with 100% RA showed the smallest increase in capillary absorption coefficient (compared to 25 °C), followed by those with 50% RA and natural aggregates (Cong, Sun, and Etxeberria, 2014).

2.3 Freeze and Thaw Resistance

One of the harshest and most damaging environmental effects on concrete is exposure to freeze-thaw cycles. A critical issue that can result in significant concrete deterioration is the harm that freezing and thawing cycles have on concrete structures in cold climates. Many physical characteristics, including matrix porosity and aggregate qualities, affect how resistant concrete is to freezing and thawing. In freeze-thaw cycles, the water initially enlarges within the pores after freezing, and if the necessary volume is greater than the available space, the surplus water is expelled by expansion pressure when the pressure is greater the material resistance, which causes local cracks to develop. Nonetheless, continuous freeze-thaw cycles in a humid atmosphere cause water to enter fractures during the thaw stage and freezes again later, leading to increasing degradation over time. This shows that it is possible to build RAC that provide equivalent workability in comparison to traditional concrete mixture including only natural aggregates. Taking into account the RCAs' water absorption capacity (which accounts for 50% of the total absorption value) and individually determining each proportion. These findings support compressive packing approach's superior ability to forecast the compressive strength of various recycled and natural concrete of different strength group. The mechanical and physical performance of normal strength concretes are more affected by the degradation cycles than are high strength combinations. The key mechanical parameters following freeze-thaw degradation (compressive strength, elastic modulus, and tensile strength) are proposed as a function of the initial open porosity of the concrete by way of a freeze-thaw degradation-law for RAC. Compressive strength after cycles separated by reference and its relationship Compressive strength is a function of the concrete's initial open porosity, and this relationship holds true for elastic modulus and tensile strength as well. According to research, the presence of mortar that is affixed to concrete generates a "delta" of increased degradation after 300 cycles. The distinction between natural and recycled concrete's ITZs (between aggregate and new paste) can be explained (one between aggregate and new paste and another between old paste and original aggregate). More damage occurs in RACs than NACs as a result of having more ITZs (Rangel et al., 2020). The deterioration of recycled concrete specimens constantly exposed to up to 56 freeze-thaw cycles (with freezing performed at 18 °C in air and thawing in water at 20 °C until the core temperature reached 6 °C), the concrete's initial strength determines its capacity to withstand the hydrostatic pressures produced by the degradation process. This describes how the type of RCA, their quality, and any potential processing procedure affect the performance of RAC as a result. For instance, treated RCA (RCA that has been cleaned before mixing) produces RAC that is more durable than untreated concrete mixtures, which, according to the authors' view, is due to a higher initial strength (and compactness). This is advantageous in reducing damage brought on by freeze-thaw cycles (Richardson,

Coventry, and Bacon 2011). The interior structure of RAC remains generally tight with few micropores and cracks during the initial freeze-thaw interval (100 cycles). On the other hand, after 400 cycles, there were more pores and microcracks present, and the link between the aggregates and mortar weakened. It was no longer feasible to differentiate the ITZs within the mixture when samples failed in the late freeze-thaw interval 800 cycles, indicating that the concrete had become exceedingly porous (Zhu et al. 2019). The existing microcracks tend to grow as concrete is repeatedly subjected to free-thaw cycles after examining the mechanical properties of concretes with 30 MPa compressive strength subjected to different freeze-thaw cycles (0, 5, 15, 30, 50, 75, and 100 cycles). In addition, both the lowest freezing temperature and the number of free-thaw cycles have a detrimental effect on the residual compressive strength (Wang et al., 2020). Partially substituting fly ash for cement does not improve the freeze-thaw resistance of RCA concrete. It is anticipated that when the curing time is extended, the qualities of the mixes containing fly ash will become more favorable. It is crucial to stress that lower readings in specimens with additional cementitious materials do not necessarily indicate that these specimens are more susceptible to freeze-thaw assault. However, RCA-concrete mixes proportioned by the traditional mix design approach (100% RCA content) or by the EMV method (63.5% and 74.3% RCA content for RCA-concrete prepared with RCA-MO and RCA-VA, respectively) have strong resistance against freeze and thaw when used as a performance indicator. However, the EMV technique provides concrete with greater resilience to freeze-and-thaw action than RCA-concrete proportionate by conventional mix design method (Abbas et al. 2009). As the water/cement ratio fell, the weight loss reduced significantly and very consistently, with 50% recycled material and 50% saturation, the specimens showed remarkably good performance. Most of the RCA-containing mixes outperformed the control mix. The fact that the RCA encouraged the creation of a denser and more solid contact may be one factor in this performance's success. Semi-saturation of the 50% RCA had the greatest results among the groups including RCA, while full saturation and semi-saturation of the 50% RCA improved the concrete's durability. These numbers were remarkably similar to those seen in the control group. These results were also supported by the mechanical tests conducted for this investigation. The efficacy of concrete containing RCA was approximately equivalent to that of cement concrete only virgin aggregate after exposure to 300 freeze-thaw cycles, particularly for mixtures containing 50% RCA at a 50% saturation point (Yildirim, Meyer, and Herfellner, 2015).

3. FIRE PERFORMANCE OF RECYCLED AGGREGATE CONCRETE

In this review paper, the critical fire performance of recycled aggregate concrete was also covered. RCA's fire performance can change based on the precise combination of materials utilized as well as the RCA's quality and processing. Due to its construction from a solid, inert substance, RCA has generally been found to have strong fire-resistant qualities. Moreover, RCA often contains less water than conventional concrete, which can aid in reducing the risk of spalling and other types of damage during a fire (Dong et al., 2014). High temperatures frequently result in aggregate damage, a softening of the cement paste-aggregate bond, a softening of the cement paste because of higher porosity

upon dehydration, a partial break - down of the calcium silicate hydrate the principal of cement hydration, and the development of cracking. Recycled aggregate should be utilized in the design mix rather than natural aggregate since it absorbs water more quickly. Recycled aggregate with a high crush value and resistance to abrasion may be a clear sign of weaker concrete. Concrete loses a considerable portion of its strength quickly when subjected to high temperatures, and recycled aggregate concrete exhibits this loss of strength earlier than natural aggregate concrete. With late-aged concrete compared to early-aged concrete, the percentage loss in concrete strength caused by high temperatures is less. Recycled aggregate concrete does suffer a greater loss than natural aggregate concrete, though. Recycled aggregate concrete has an excellent resistance to strength deterioration brought on by thermal stress, and its value is only 5% to 10% lower than ordinary aggregate concrete's (Kim, 2022). According to a statistical analysis of cracks, normal strength concretes primarily experienced cracking along interfaces, such as those between old paste and new paste or between old paste and natural aggregate. Nonetheless, it was noted that certain cracks in high strength matrix concretes crossed through the aggregate. According to the chemical studies, the hydration reactions in the old mortar at the LRCA were not quite finished. As a result, extra hydration reactions with the LRC concretes may have strengthened the existing mortar and provided more crack resistance. Due to higher moisture concentrations in the aggregates, Industrial recycled concrete aggregate (IRCA) concretes showed more mass loss after exposure to high temperatures and the possible cause is because of presence of impurities. The *Fig. 3* shows the crack pattern at high temperature for three different types of concrete viz, (a) IRC 0.6 concrete at 750 °C, (b) IRC 0.3 concrete at 450 °C, IRC 0.3 concrete at 450 °C respectively.

Spalling is the fundamental issue when analyzing the fire behavior of concrete structures. This phenomenon involves the violent or nonviolent separation of concrete particles from a concrete member's surface. Fire spalling can have a significant impact on the structural performance depending on the extent of the damage because it decreases the cross - sections and may even exposes steel rebars to the fire. This may result in a decrease in load-bearing capability, thermal insulation, and fire resistance. The overall weight loss of the sample (% of the initial mass of the sample), the spalled volume (percentage of the starting volume of the sample), the mean spalling depth (mm), and the maximum spalling depth were the four indicators used to assess the spalling after the fire (mm). Compared to NA-made concrete, RCA-made concrete showed more spalling. The degree of spalling increased slightly as the compressive axial stress increased. Spalling indicators (volume and maximum depth) showed strange behavior in relation to the replacement rate. First, the volume and depth of the spalling grew from 0% to 40%. The spalling signs were steady from 40% to 100%. The general behavior was not significantly altered by the replacement approach (direct replacement or strength-based replacement). Several characteristics, like the water content and compressive strength, that may increase the danger of spalling are impacted by the presence of RCA. Since concrete mixes with relatively low strength displayed a notably increased spalling, the compressive strength of concrete prepared with RCA had no effect on the spalling risk. Since mixes with a high-water content had greater spalling depths and volumes, the water content affected the spalling damage. More water content and less thermal cracking may be linked to an increased likelihood of spalling. The improvement in the mechanical characteristics of the concrete due to the smaller thermal mismatch may also be associated with a potential reduction in the probability of spalling (Fernandes et al., 2022).
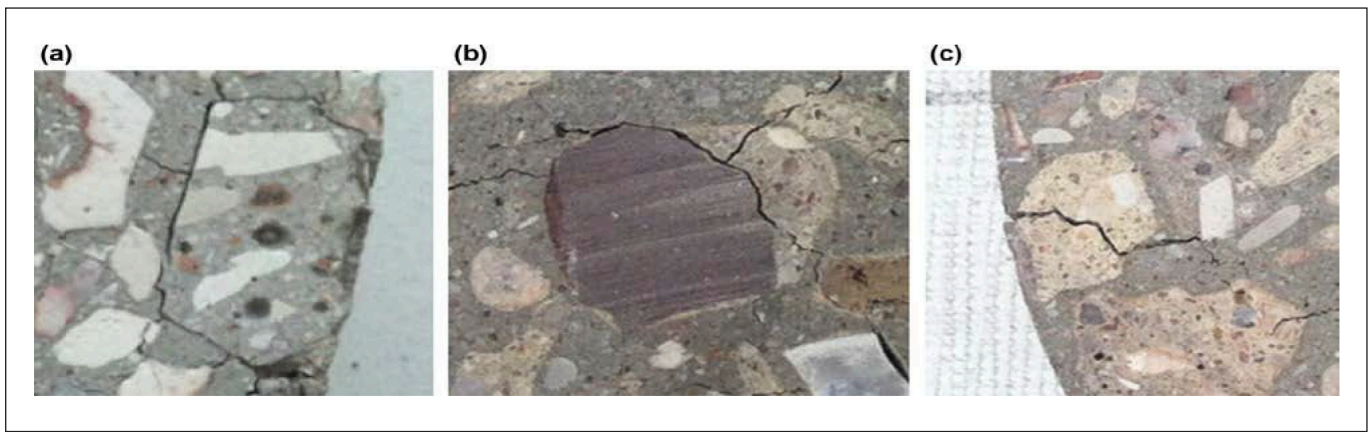
Fig. 3: *Crack patterns observed after heating: (a) at ''new paste–old paste'' interface at 750 ℃, (b) between siliceous aggregate and old paste at 450 ℃, (c) through a calcareous aggregate at 450 ℃. (Laneyrie et al., 2016)*

For mechanical properties post-fire, sustainable concrete using coarse recycled concrete aggregate has received little attention to far (heated, cooled, and then loaded at-ambient temperature). It was found that the sustained strength and elasticity of the concretes under consideration decreased proportionally as the temperature rose. Moreover, the only discernible change across the concrete was a slight rise in strength as RCA concentration increased. The higher strength of the original RCA source and the higher curing conditions resulting from retained moisture in the source aggregate were both used to explain this behavior. This has significant ramifications for the practitioner since it makes it more difficult to identify probable mechanical property losses at high temperatures. In general, the thermal strain coefficient values were comparable. The main finding was that sustainable concrete with RCA had much lower mechanical performance at rising temperatures than conventional concrete. This does not imply that the sustainable concrete was ineffective, either. Even with a full RCA replacement, all sustainable concretes behaved above 35 MPa at 500 °C, exceeding the required 40 MPa strength of the concrete mix design. This observation shows that sustainable concretes with RCA might be able to achieve particular fire design goals with a good design (Gales et al., 2016). If the replacement amount is kept between 0% and 40% and done with hydrated old concrete, it is inferred that concrete with recycled coarse aggregate in it will behave similarly to natural aggregate concrete when exposed to temperatures between 25°C and 800°C. For dry conditions and saturated surface dry conditions, the average particle densities of natural coarse aggregate are 2895 kg/m^3 and 2935 kg/m^3, respectively, while for dry conditions and saturated surface dry conditions, the average particle densities of recycled aggregate are 2311 kg/m^3 and 2446 kg/m^3, respectively. As a result, recycled coarse aggregate (RCA) is lighter than natural coarse aggregate, which may be due to the addition of low-density cement paste to RCA. The volume % of leftover mortar will increase as the recycle aggregate particle size is increased; this invariably results in a decrease in the specific gravity and density of the aggregate particles. With rising temperatures, the densities of concrete containing granite (virgin aggregates) and recycled aggregates rise. Regardless of the % substitution of the virgin coarse aggregate (granite) with the recycled ones. It is believed that the relatively weak interfacial bond between the RCA and the solidified paste within the concrete matrix is what caused the initial reduction in strength from 25 °C through 100 °C and 200 °C. At temperatures between 200 °C and 400 °C, strength increased continuously. From 200 °C to 400 °C, the strength continued to gradually rise. The strength of the control samples gradually rose up to roughly 30%, but those with 15% and 30% RCA replacements showed 36% and

35% increases in strength, respectively. There may have been dehydration and heat expansion of the concrete. After then, the strength of the concrete cube began to decline steadily once more as the temperature approached 600 °C. In contrast to samples with 15% and 30% RCA replacements, which showed 5% and 2% strength reductions respectively, control samples gradually decreased by roughly 13%. The temperatures were approaching 600 °C when the fissures were discovered. Generally speaking, nothing changed until the temperature was well above 100 °C. There was an initial drop in strength from 100 °C to 200 °C which is suspected to be due to the relative weak interfacial bond between the RCA and hardened paste within the concrete matrix; a gradual increase in strength continued from 200 °C to 450 °C and steady drop occurred again after that up to 600 °C. Also, with temperatures higher than 400 °C the cubes showed further loss in weight and increased visibility and higher density of cracks. Beyond 600 °C, deterioration was relatively more severe and the mechanical properties of concrete (such as compressive strength) were largely affected by the temperature. The *Fig. 4* shows the crack lines formed on 15% recycled concrete after tempering for 2 hours at 400 °C (Salau, Oseafiana, and Oyegoke, 2015).

All concrete compositions' compressive strength declined as exposure temperature rose. The greater amount of recycled mortar used to adhere the recycled aggregates is what is contributing to the rise in the residual compressive strength for recycled aggregate concrete. Subsequently improving the thermal expansion characteristics of the cement paste and aggregates. Although the residual compressive strength of concrete mixes made with recycled aggregates was somewhat lower at 200 °C and 400 °C than that of the control mixture, the ratios of residual to early compressive strength increased for concrete mixtures that contained 20% extra materials in place of OPC, especially at greater exposure temperatures of 400 °C and 600 °C. The increase in residual compressive strength of blended concrete containing marble powder and rice husk ash was mainly due to pozzolanic reaction that result in the formation of supplementary hydration products. The production of additional hydration products as a result of the pozzolanic reaction increased the residual compressive strength of concrete mixtures comprising marble powder and rice husk ash. At high temperatures, recycled aggregate concrete's residual compressive strength was satisfactory and on par with the control mixture. When recycled aggregate concrete was subjected to elevated temperatures, there was no spalling or fragmentation. demonstrating the recycled aggregates' sufficient thermal compatibility with cement paste. When contrasted with the control mix, concrete mixtures containing a 30% substitution of recycled aggregates had splitting tensile strengths that were over 35% higher. Even

Fig. 4: *Crack lines formed on 15% recycled concrete after tempering for 2 hours at 400 °C (Salau et al., 2015)*

though the splitting tensile strength was reduced as recycled aggregates were added, the final strength was equivalent to that of the control mix. With 100% recycled aggregate concrete, the use of marble powder and rice husk ash as a 20% cement replacement resulted in a decrease in both compressive and breaking tensile strengths. When compared to 100% recycled aggregate conventional concrete without steel wires, the mixtures with 0.5% waste steel wires demonstrated higher splitting tensile strength and compressive strength. (Salahuddin et al. 2019). The compressive strength decreased by 6 to 8% when recycled material was used in place of natural aggregate. The excess cement paste in recycled aggregate, which led to a weak interface zone and lower density, has been recognized by Mehta in 1986 as the cause of these reductions in splitting tensile strength, which decreased by 8 to 12%. For concretes made using river gravel, crushed limestone, and recycled aggregate. When the various concretes were subjected to temperatures of 250 °C and 500 °C, there were no apparent cracks. However, the river gravel concrete specimens that surviving the exposure had several deep, wide fissures. This can be due to the river gravel concrete's high quartzite content, which was discovered by mineralogical investigation. The neighboring cement paste is typically thermally incompatible with the quartzite because it typically has a greater coefficient of thermal expansion. With fewer, smaller cracks, all the RCA and crushed limestone specimens withstood the exposure to 750 °C. The extremely slight cracks in the RCA concrete examples were shallower and narrower than those in the crushed limestone specimens. Because RCA contains a significant amount of mortar, it is expected that its coefficient of thermal expansion is similar to that of cement paste. In order to strengthen the physical bond between the cement paste and the aggregate, it also features a rough surface roughness. Generally speaking, it has been shown that concrete created from recycled concrete aggregate performs well at high temperatures and is equivalent to other types of concrete. When RCA concrete was heated to 750 °C, unlike river gravel concrete, no spalling or disintegrating was seen. Compressive and flexural strength as well as elastic modulus of concrete constructed using recycled concrete aggregate frequently decreased with temperature. For all raised temperatures, the residual to starting compressive and tensile strength ratios of concrete built using recycled concrete aggregate were higher than those of river gravel concrete. Comparing RCA concrete to crushed limestone concrete heated to 500 °C or higher revealed the same pattern. With the exception of RCA concrete at 500°C, all concretes' residual moduli of elasticity displayed similar tendencies (Sarhat and Sherwood 2011). The main factor influencing the features of the aggregates and the factor anticipated to influence the final

properties of the RAC is the adhering mortar content inside the RCAs particles, thermal shock and image analysis, were used on concrete samples made with red binders and coarse RCAs to assess the adherent mortar content for the used coarse RCAs. In both situations, the volume of adhering mortar was roughly 48%. The mechanical performance that was still present after exposure to high temperatures show that RCAs can be used in place of natural aggregates. The data reported revealed how residual mechanical performance are not harmed throughout the heating procedures, but residual physical performance are influenced by the presence of RCAs. This makes it easier for water and vapour to migrate, which can lessen the likelihood of the spalling phenomenon (Beatriz da Silva, Pepe, and Toledo Filho 2020). The integration of recycled concrete coarse aggregates have no effect on the material's thermal responsiveness, despite the increased porosity and altered thermal characteristics of the matrix-aggregate interface when compared to reference concrete. Upon exposure to high temperatures, recycled concrete coarse aggregate showed variations in the studied residual mechanical parameters (compressive strength, splitting tensile strength, and elasticity modulus) that were roughly comparable to those shown by reference concrete. As a result, it appears that there is no correlation between the rate at which natural coarse aggregates (natural concrete aggregate) degrade and the rate at which recycled concrete coarse aggregate replaces them for the various exposure temperatures examined. As a result, when compared to ordinary concrete, the structural use of recycled concrete coarse aggregate has no restrictions in terms of post-fire residual mechanical qualities. As a result, when compared to ordinary concrete, the structural use of recycled concrete coarse aggregate has no restrictions in terms of post-fire residual mechanical qualities. As with conventional concrete, the mechanical properties of concrete are significantly decreased after exposure to high temperatures with growing replacement levels of natural concrete aggregate by recycled concrete coarse aggregate. The highest decreases of residual effectiveness took place for exposure temperature of 800 °C: 12.2% for compressive strength. As a function of the exposure temperature, reduction factors were proposed to assess the remaining mechanical properties of recycled concrete coarse aggregate (Vieira, Correia, and De Brito 2011). On reviewing the several literature results and plotting the graph between the rate of substitution of NA and post fire compressive strength. On comparing these graphs, it is observed that the compressive strength of recycled aggregate concrete is comparable to the natural aggregate concrete only when the substitution rate of natural aggregate by the recycled coarse aggregate is up to 30% and the fire resistance of the recycled aggregate concrete is admissible up to the temperature of 400 °C.

Fig. 5 summarizes the results of the previous experiments.

4. CONCLUSIONS

Recycled aggregate (RA) often contains adhered old cement mortar, which can alter its properties. This prior mortar can improve the adhesion between RA and fresh cement paste, contributing to increased strength. Additionally, the coarse surface of RAs can also contribute to this strength enhancement.

When 20% RA is used in concrete, it has a minimal impact on its compressive strength compared to traditional concrete or conventional concrete (TC/CC). However, when 100% RA is employed, there is a noticeable reduction in strength due to the inherent weaknesses and porosity of recycled aggregates.

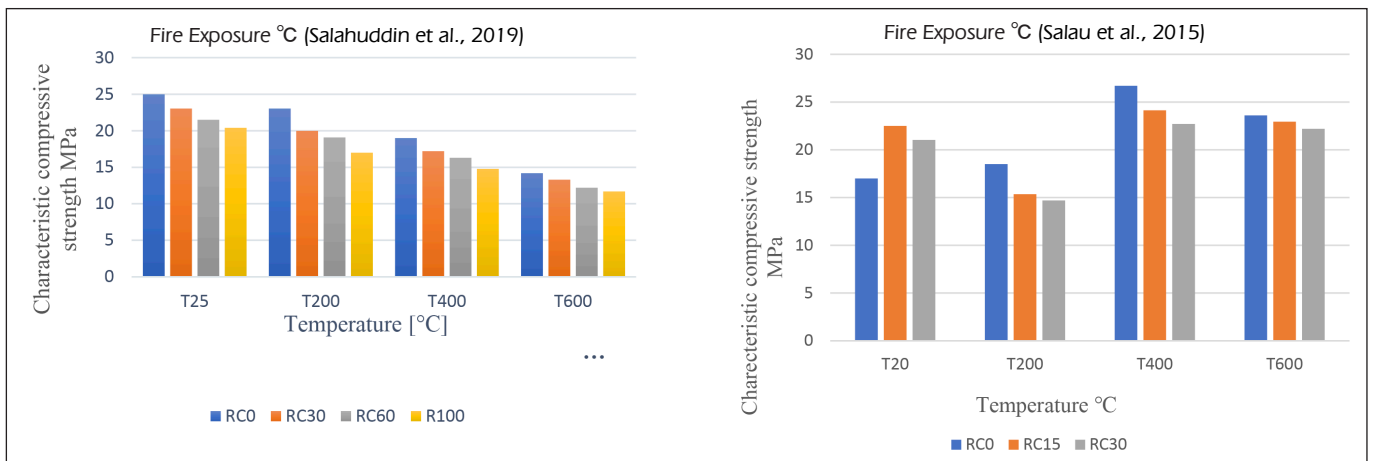The use of nano silica can boost the performance of

Fig. 5: *Effect of replacement ration of coarse recycled aggregate on characteristic compressive strength after being exposed to elevated temperatures.*

recycled concrete by expediting hydration and enhancing the interfacial transition zone (ITZ). Nonetheless, an excessive usage of nano silica can lead to problems such as reduced compressive strength.

Adjusting factors like the water-cement ratio, aggregate water content, mixing technique, and admixture can enhance the quality of recycled aggregate concrete (RAC). The water-cement ratio for RAC should be slightly lower than that for natural aggregate concrete (NAC) to attain equivalent compressive strength.

The quality of RA is influenced by manufacturing methods, the strength of the parent concrete, and its usage history. High-quality RA can slow down the deterioration of RAC, and up to 30% RA can be used as a replacement.

Recycled aggregates can elevate permeability and chloride diffusion coefficients, yet these values still remain within acceptable ranges for durable concrete. The degree of substitution with recycled coarse aggregates (RCA) has a linear effect on chloride penetrability.

In a chloride environment, RAC with a low water-cement ratio performs better than NAC, owing to the higher concentration of C-S-H gels.

The incorporation of crushed concrete in recycled aggregate significantly enhances the long-term interfacial qualities of new concrete.

RAC exhibits least water tightness due to its higher water absorption coefficient, which escalates with the water-to-cement ratio and the level of RCA substitution.

The absorption of free water by irregularly shaped recycled aggregates can influence the actual water-cement ratio and mix proportions.

The resistance to freezing and thawing in RAC is determined by matrix porosity and aggregate quality. During the initial freeze-thaw cycles, the internal structure remains tight, but it deteriorates over time.

The link between cement paste and aggregates can be damaged, the cement paste can become softer, and cracks can form as a result of high temperatures having a negative impact on concrete. Although its absorption rate and crush value must be taken into account to prevent weaker concrete, recycled aggregate is a potential choice for concrete mix design. Recycled aggregate concrete exhibits good resilience to thermal stress, it loses strength more quickly in high temperatures than natural aggregate concrete. Although recycled aggregate concrete experiences a larger overall strength loss than natural aggregate concrete, the percentage loss is still rather small. Compared to early-aged concrete, late-aged concrete loses less strength as a result of high

temperatures. The enduring strength and flexibility of concretes both decrease as temperatures rise, though higher concentrations of RCA can marginally boost strength.

The mechanical properties of concrete at high temperatures can be impacted by RCA and other additives like marble powder and rice husk ash, which enhance hydration and residual compressive strength.

RCA concrete maintains its mechanical performance even after exposure to high temperatures, supporting its application as an alternative to natural aggregates and reducing the risk of spalling.

Incorporating recycled concrete coarse aggregates has no effect on the thermal responsiveness of concrete and does not restrict post-fire residual mechanical properties. Nonetheless, concrete does experience a decline in its mechanical characteristics at high temperatures.

5. ACKNOWLEDGEMENT

6. REFERENCES

Abbas, A., Fathifazl, G., Isgor, O. B., Razaqpur, A. G., Fournier, B., & Foo, S. (2009). Durability of recycled aggregate concrete designed with equivalent mortar volume method. *Cement and Concrete Composites*, *31*(8), 555–563. https://doi.org/10.1016/j.cemconcomp.2009.02.012

Abed, M., & Nemes, R. (2019). Mechanical Properties of Recycled Aggregate Self-Compacting High Strength Concrete Utilizing Waste Fly Ash, Cellular Concrete and Perlite Powders. *Periodica Polytechnica Civil Engineering*. https://doi.org/10.3311/PPci.13136

Adessina, A., Ben, A., Barthélémy, J., Chateau, C., & Garnier, D. (2019). Cement and Concrete Research Experimental and micromechanical investigation on the mechanical and durability properties of recycled aggregates concrete. *Cement and Concrete Research*, *126*(June), 105900. https://doi.org/10.1016/j.cemconres.2019.105900

Bai, G., Zhu, C., Liu, C., & Liu, B. (2020). An evaluation of the recycled aggregate characteristics and the recycled aggregate concrete mechanical properties. *Construction and Building Materials*, *240*, 117978. https://doi.org/10.1016/j.conbuildmat.2019.117978

Beatriz da Silva, J., Pepe, M., & Toledo Filho, R. D. (2020). High temperatures effect on mechanical and physical performance of normal and high strength recycled aggregate concrete. *Fire Safety Journal*, *117*(August). https://doi.org/10.1016/j.firesaf.2020.103222

Bui, N. K., Satomi, T., & Takahashi, H. (2017). Improvement of mechanical properties of recycled aggregate concrete basing on a new combination method between recycled aggregate and natural aggregate. *Construction and Building Materials*, *148*, 376–385. https://doi.org/10.1016/j.conbuildmat.2017.05.084

Cong, S., Sun, C., & Etxeberria, M. (2014). Cement & Concrete Composites

Residue strength , water absorption and pore size distributions of recycled aggregate concrete after exposure to elevated temperatures. *CEMENT AND CONCRETE COMPOSITES*, *53*, 73–82. https://doi.org/10.1016/j.cemconcomp.2014.06.001

Dong, H., Cao, W., Bian, J., & Zhang, J. (2014). The fire resistance performance of recycled aggregate concrete columns with different concrete compressive strengths. *Materials*, *7*(12), 7843–7860. https://doi.org/10.3390/ma7127843

Du, Y., Zhao, Z., Xiao, Q., Shi, F., Yang, J., & Gao, P. (2021). *Experimental Study on the Mechanical Properties and*. 1–19.

Duan, Z. H., & Poon, C. S. (2014). Properties of recycled aggregate concrete made with recycled aggregates with different amounts of old adhered mortars. *Materials and Design*, *58*, 19–29. https://doi.org/10.1016/j.matdes.2014.01.044

Eckert, M., & Oliveira, M. (2017). Mitigation of the negative effects of recycled aggregate water absorption in concrete technology. *Construction and Building Materials*, *133*, 416–424. https://doi.org/10.1016/j.conbuildmat.2016.12.132

Fernandes, B., Carré, H., Mindeguia, J. C., Perlot, C., & La Borderie, C. (2022). Spalling behaviour of concrete made with recycled concrete aggregates. *Construction and Building Materials*, *344*, 168–174. https://doi.org/10.1016/j.conbuildmat.2022.128124

G, J. M., & G, D. C. (n.d.). *applied sciences Durability Parameters of Reinforced Recycled Aggregate Concrete : Case Study*. https://doi.org/10.3390/app9040617

Gales, J., Parker, T., Cree, D., & Green, M. (2016). Fire Performance of Sustainable Recycled Concrete Aggregates: Mechanical Properties at Elevated Temperatures and Current Research Needs. *Fire Technology*, *52*(3), 817–845. https://doi.org/10.1007/s10694-015-0504-z

Geng, Y., Wang, Q., Wang, Y., & Zhang, H. (2019). Influence of service time of recycled coarse aggregate on the mechanical properties of recycled aggregate concrete. *Materials and Structures/Materiaux et Constructions*, *52*(5), 1–16. https://doi.org/10.1617/s11527-019-1395-0

Guo, H., Shi, C., Guan, X., Zhu, J., Ding, Y., & Ling, T. (2018). Durability of recycled aggregate concrete - A review. *Cement and Concrete Composites*, *89*, 251–259. https://doi.org/10.1016/j.cemconcomp.2018.03.008

Habert, P. B. G., & Roussel, M. T. N. (2014). *Cement paste content and water absorption of recycled concrete coarse aggregates*. 1451–1465. https://doi.org/10.1617/s11527-013-0128-z

Hu, Z., Mao, L. X., Xia, J., Liu, J. Bin, Gao, J., Yang, J., & Liu, Q. F. (2018). Five-phase modelling for effective diffusion coefficient of chlorides in recycled concrete. *Magazine of Concrete Research*, *70*(11), 593–594. https://doi.org/10.1680/jmacr.17.00194

Kang, M., & Weibin, L. (2018). Effect of the aggregate size on strength properties of recycled aggregate concrete. *Advances in Materials Science and Engineering*, *2018*. https://doi.org/10.1155/2018/2428576

Kim, J. (2022). Influence of quality of recycled aggregates on the mechanical properties of recycled aggregate concretes: An overview. *Construction and Building Materials*, *328*(September 2021), 127071. https://doi.org/10.1016/j.conbuildmat.2022.127071

Kou, S., Poon, C., & Etxeberria, M. (2011). Cement & Concrete Composites Influence of recycled aggregates on long term mechanical properties and pore size distribution of concrete. *Cement and Concrete Composites*, *33*(2), 286–291. https://doi.org/10.1016/j.cemconcomp.2010.10.003

Laneyrie, C., Beaucour, A. L., Green, M. F., Hebert, R. L., Ledesert, B., & Noumowe, A. (2016). Influence of recycled coarse aggregates on normal and high performance concrete subjected to elevated temperatures. *Construction and Building Materials*, *111*, 368–378. https://doi.org/10.1016/j.conbuildmat.2016.02.056

Liang, K., Hou, Y., Sun, J., Li, X., Bai, J., & Tian, W. (2021). Theoretical analysis of water absorption kinetics of recycled aggregates immersed in water. *Construction and Building Materials*, *302*(February), 124156. https://doi.org/10.1016/j.conbuildmat.2021.124156

Materials, B. (2017). *Determining the water absorption of recycled aggregates utilizing hydrostatic weighing approach. February 2012*. https://doi.org/10.1016/j.conbuildmat.2011.08.018

Rahal, K. (2007). Mechanical properties of concrete with recycled coarse aggregate. *Building and Environment*, *42*(1), 407–415. https://doi.org/10.1016/j.buildenv.2005.07.033

Rangel, C. S., Amario, M., Pepe, M., Martinelli, E., & Filho, R. D. T. (2020). Durability of structural recycled aggregate concrete subjected to freeze-thaw cycles. *Sustainability (Switzerland)*, *12*(16), 1–21. https://doi.org/10.3390/su12166475

Richardson, A., Coventry, K., & Bacon, J. (2011). Freeze/thaw durability of concrete with recycled demolition aggregate compared to virgin aggregate concrete. *Journal of Cleaner Production*, *19*(2–3), 272–277. https://doi.org/10.1016/j.jclepro.2010.09.014

Salahuddin, H., Nawaz, A., Maqsoom, A., Mehmood, T., & Zeeshan, B. ul A. (2019). Effects of elevated temperature on performance of recycled coarse aggregate concrete. *Construction and Building Materials*, *202*, 415–425. https://doi.org/10.1016/j.conbuildmat.2019.01.011

Salau, M. A., Oseafiana, O. J., & Oyegoke, T. O. (2015). Effects of elevated temperature on concrete with Recycled Coarse Aggregates. *IOP Conference Series: Materials Science and Engineering*, *96*(1). https://doi.org/10.1088/1757-899X/96/1/012078

Saravanakumar, P., Abhiram, K., & Manoj, B. (2016). Properties of treated recycled aggregates and its influence on concrete strength characteristics. *Construction and Building Materials*, *111*, 611–617. https://doi.org/10.1016/j.conbuildmat.2016.02.064

Sarhat, S. R., & Sherwood, E. G. (2011). The behaviour of recycled aggregate concrete at elevated temperatures. *Proceedings, Annual Conference - Canadian Society for Civil Engineering*, *2*(April), 1475–1485. https://doi.org/10.13140/RG.2.1.4867.7285

Smart, D., & Jerman, J. C. (2002). nc or Pr o or ed Pr o. 93, 1–11.

Tam, V. W. Y., Gao, X. F., Tam, C. M., & Chan, C. H. (2008). *New approach in measuring water absorption of recycled aggregates*. 22, 364–369. https://doi.org/10.1016/j.conbuildmat.2006.08.009

Thomas, C., Setién, J., Polanco, J. A., Alaejos, P., & Juan, M. S. De. (2013). Durability of recycled aggregate concrete. *Construction and Building Materials*, *40*, 1054–1065. https://doi.org/10.1016/j.conbuildmat.2012.11.106

Thomas, C., Setién, J., Polanco, J. A., de Brito, J., & Fiol, F. (2019). Micro- and macro-porosity of dry- and saturated-state recycled aggregate concrete. *Journal of Cleaner Production*, *211*(November), 932–940. https://doi.org/10.1016/j.jclepro.2018.11.243

Vázquez, E., Barra, M., Aponte, D., Jiménez, C., & Valls, S. (2014). *Improvement of the durability of concrete with recycled aggregates in chloride exposed environment*. 67, 61–67. https://doi.org/10.1016/j.conbuildmat.2013.11.028

Vieira, J. P. B., Correia, J. R., & De Brito, J. (2011). Post-fire residual mechanical properties of concrete made with recycled concrete coarse aggregates. *Cement and Concrete Research*, *41*(5), 533–541. https://doi.org/10.1016/j.cemconres.2011.02.002

Wang, Y., Liu, Z., Fu, K., Li, Q., & Wang, Y. (2020). Experimental studies on the chloride ion permeability of concrete considering the effect of freeze–thaw damage. *Construction and Building Materials*, *236*, 117556. https://doi.org/10.1016/j.conbuildmat.2019.117556

Xiao, J., Lu, D., & Ying, J. (2013). Durability of recycled aggregate concrete: An overview. *Journal of Advanced Concrete Technology*, *11*(12), 347–359. https://doi.org/10.3151/jact.11.347

Yildirim, S. T., Meyer, C., & Herfellner, S. (2015). Effects of internal curing on the strength, drying shrinkage and freeze-thaw resistance of concrete containing recycled concrete aggregates. *Construction and Building Materials*, *91*, 288–296. https://doi.org/10.1016/j.conbuildmat.2015.05.045

Yuan, W., Mao, L., & Li, L. (2023a). Science of the Total Environment A two-step approach for calculating chloride diffusion coefficient in concrete with both natural and recycled concrete aggregates. *Science of the Total Environment*, *856*(October 2022), 159197. https://doi.org/10.1016/j.scitotenv.2022.159197

Yuan, W., Mao, L., & Li, L. (2023b). Science of the Total Environment A two-step approach for calculating chloride diffusion coefficient in concrete with both natural and recycled concrete aggregates. *Science of the Total Environment*, *856*(October 2022), 159197. https://doi.org/10.1016/j.scitotenv.2022.159197

Yuan, W., Mao, L., & Li, L. (2023c). Science of the Total Environment A two-step approach for calculating chloride diffusion coefficient in concrete with both natural and recycled concrete aggregates. *Science of the Total Environment*, *856*(October 2022), 159197. https://doi.org/10.1016/j.scitotenv.2022.159197

Zaharieva, R., Buyle-Bodin, F., Skoczylas, F., & Wirquin, E. (2003). Assessment of the surface permeation properties of recycled aggregate concrete. *Cement and Concrete Composites*, *25*(2), 223–232. https://doi.org/10.1016/S0958-9465(02)00010-0

Zega, C. J., Antonio, Á., & Maio, D. (2011). Use of recycled fine aggregate in concretes with durable requirements. *Waste Management*, *31*(11), 2336–2340. https://doi.org/10.1016/j.wasman.2011.06.011

Zheng, Y., Zhuo, J., & Zhang, P. (2021). A review on durability of nano-SiO 2 and basalt fiber modified recycled aggregate concrete. *Construction and Building Materials*, *304*(September), 124659. https://doi.org/10.1016/j.conbuildmat.2021.124659

Zhu, P., Hao, Y., Liu, H., Wei, D., Liu, S., & Gu, L. (2019). Durability evaluation of three generations of 100% repeatedly recycled coarse aggregate concrete. *Construction and Building Materials*, *210*, 442–450. https://doi.org/10.1016/j.conbuildmat.2019.03.203

Zubair Yousuf Construction Technology MSc., He is currently pursuing his PhD in Budapest University of Technology and Economics. His research interest focuses on use of sustainable material in construction and to investigate the post fire behaviors of sustainable construction materials. E-mail: zubair.yousef@edu.bme.hu

Viktor Hlavička (1987), Structural Engineer MSc, PhD, concrete technologist, fire safety engineer, Assistant Professor of Department of Construction Materials and Technologies, Budapest University of Technology and Economics. His main fields of interest are experimental investigation and modelling of fastening systems in concrete and thermally damaged concrete. He is a member of the Hungarian Group of ***fib***, e-mail: hlavicka.viktor@emk.bme.hu

EXPERIMENTS ON INCREASED LOADBEARING CAPACITY OF CONFINED FRP REINFORCED BEAMS

Bálint Somlai - Sándor Sólyom

Fibre Reinforced Polymers (FRP) have been in use in aerospace engineering since the 1940s in military aircraft. Later as manufacturing technology developed it became available to other sectors. The use of FRPs in concrete construction can offers a variety of advantages over steel reinforcement. For the technology to be employable on a wider scale related research needs to address certain disadvantages and other properties of FRP rebars. One area that needs further discussion is the brittle failure of FRP reinforced concrete elements. There are several methods proposed aiming to modify the behaviour of elements in bending, among them is the utilization of concrete crushing failure and confinement to achieve a more ductile failure.

Keywords: *FRP, Confinement, Strengthening, Structural elements*

1. INTRODUCTION

The use of Fibre Reinforced Polymer (FRP) rebars, for reinforcing concrete is an alternative to steel. There are advantages to using them such as higher tensile strength, corrosion resistance, electromagnetic neutrality and ease of deconstruction (fib, 2007; Sólyom et al. 2018). This makes them preferable to steel in certain cases such as maritime structures and other aggressive environments, temporary structures, outdoor structures where self weight or thickness matter and special cases such as magnetic levitation trains or MRI rooms (ACI, 2015). However, certain properties of FRP reinforcements are different to that of steel. Due to this the design and construction of structures utilizing the technology need to take into account these differences (Mohammed et al. 2022; Sólyom et al. 2018). These include among others, the lack of plastic deformations before failure, the lower elastic moduli of most FRP rebars or the lack of bendability after production (JPCI, 2021; AFGC, 2023).

The subject of this paper is the elastic-brittle behaviour of FRP rebars. The plastic behaviour of steel reinforcement is utilized in the design of structures where plastic hinges can form and large deformations can occur without failure. But it also provides a visual indication of damage that anyone can understand without expertise in structural mechanics, importantly while the structure still maintains plastic capacity before collapse. In case of conventionally designed structures built with FRP rebars once they reach their ultimate stress capacity, the structure fails. There are multiple proposed ways to circumvent this problem, among them are the use of both FRP and steel reinforcements (Bencardino et al. 2016), the utilization of different fibre types, and the change from tension controlled to compression controlled failure. The implementation of steel-FRP and hybrid material systems results in higher costs, while the approach using concrete crushing as the primary mode of failure does not have a direct effect on cost. This has been proposed by multiple studies and recent model codes have taken care to includes sections on compression controlled failure (ACI, 2015; fib, 2007).

The design structural elements in bending with concrete crushing in mind is uncommon and there is room to refine and improve methods (Vu et al. 2009). One method proposed to enhance the load bearing capacity and ductility of concrete is the use of confinement, where reinforcement is used to restrict the deformations of a concrete section. The method is commonly used in elements subjected to large normal forces such as columns. This method can enhance loadbearing capacity, but further research needed before practical application can be achieved with confidence (Gouda, Asadian & Galal, 2022; Renic, 2022).

2. RESEARCH OVERVIEW

The aim of this research is to determine how certain parameters of confinement effect the load bearing capacity, ultimate deflection, crack pattern and mode of failure of reinforced concrete beams. To accomplish this, we conducted experiments on beams with varying reinforcements ratio and type, and supplemented the results with finite element analysis based on the experiments. The first set of experiments were carried out on rectangular beams of dimensions 2200 × 200 × 100 mm (length × height × depth), which were subjected to four point bending tests. The aim was to determine the influence the degree of confinement has. To achieve this, the central section of the beams, subjected to constant bending moment, was reinforced with varying number of stirrups. In order to assess the maximum achievable effect we also used external textile reinforcement to confine the entire middle section of a beam. Two specimens with steel longitudinal reinforcement were also produced with the same reinforcing ratio as the FRP reinforced ones as control.

There were seven beams produced in total with three 150 mm concrete cubes per beam to determine concrete strength.
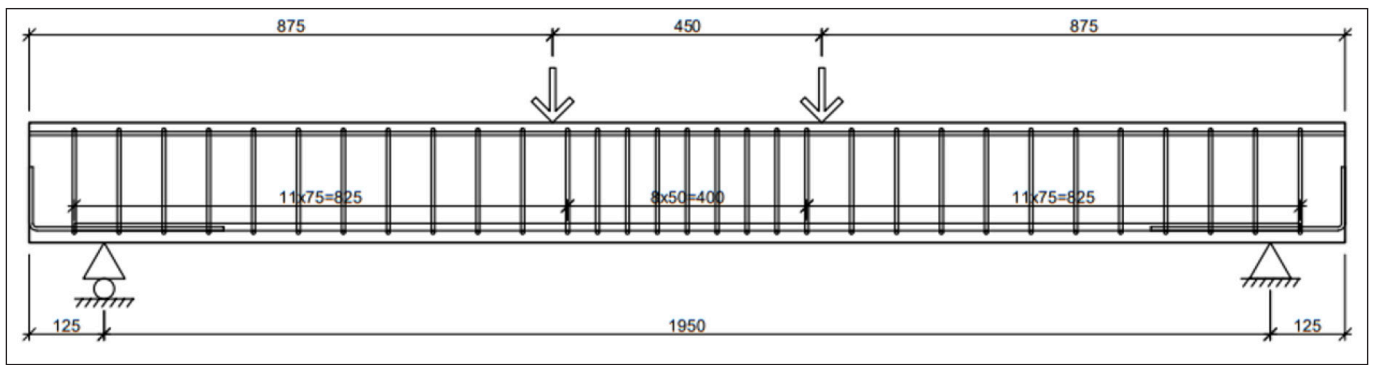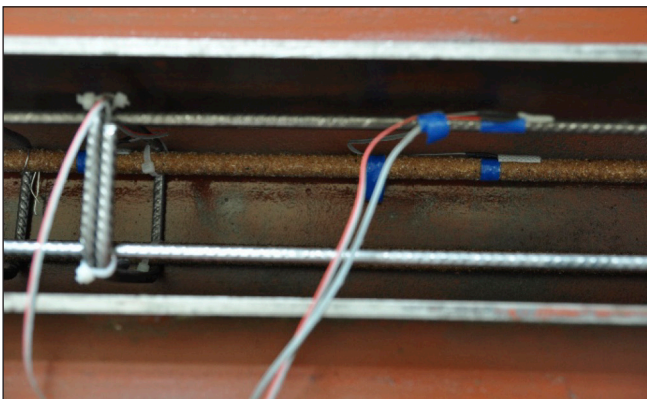
Fig. 1: *Reinforcement plan of beam 5*

All the beams were reinforced with two 12 mm diameter steel or Glass FRP (GFRP) on the tension side and two 8 mm steel rebars on the compression side. For the sake of clarity the beams reinforced longitudinally in tension with FRP rebars will be referred to as FRP reinforced and the ones with an entirely steel reinforcement will be referred to as steel reinforced. The tensile longitudinal reinforcement was chosen to be this size so that if made with steel the beam would fail in tension while if made with FRP the beam would fail in compression. Each specimen is divided into three zones by the four point bending test configuration (*Fig. 1*). The middle portion (under constant bending moment) is 450 mm and it is subject to the varying stirrup configuration and on one beam, textile wrapping. The outer sections of each beam measure 875 mm in length and are reinforced with twelve stirrups each with 75 mm spacing. Beams 1 and 2 are reinforced identically without stirrups in the constant moment zone. Beam 1 is the control specimen reinforced with steel longitudinally, while beam 2 is reinforced with GFRP rebars. Beams 3 through 5 are reinforced with progressively more stirrups 200, 100 and 50 mm spacing, respectively. Beams 6 and 7 are identical to beam 4 in their stirrup spacing, but 6 is reinforced with steel longitudinally while 7 is the only beam confined with the CFRP wrap. CFRP was chosen because it provides confinement while having minimal effect on the bending moment resistance directly like a steel wrapping would. The wrap was applied to the middle section of the beam, where the edges were grinded down in order to avoid damage to the wrap. A primer, a foundation layer and two adhesive layers (one before and one after application of the wrap) were used in the application following the instructions outlined in the manufacturers product catalogue (Mapei Kft. n.d.). The purpose of beam 6 was to demonstrate that increased confinement does not effect the loadbearing capacity or behaviour of steel reinforced elements failing in tension. The list of beams and their respective reinforcement can be seen in *Table 1*.

Symbol	Tensile reinforcement		Stirrup spacing in middle section [mm]				CFRP wrap	
	Steel	GFRP	-	200	100	50	Yes	No
Beam 1	X		X					X
Beam 2		X	X					X
Beam 3		X		X				X
Beam 4		X			X			X
Beam 5		X				X		X
Beam 6	X				X			X
Beam 7		X			X		X	

Table 1: *List of beams and the type of reinforcements in them*

The experimental setup included multiple LVDTs (linear variable differential transformers) to collect data regarding the deflections and crack openings in multiple positions. We also utilized multiple strain gauges applied to both the concrete and the reinforcement (*Fig. 2*). This formed the basis of numerical model calibration later. The load was applied by an Instron electromechanic testing machine with a capacity of 600 kN (*Fig. 3*). The load was applied in one phase at a rate of 1 mm/minute until first crack, when the LVDTs measuring crack openings were applied. From then onwards loading was applied in 15 kN increments until failure. At every step the crack pattern was marked and the first nine cracks were photographed with a handheld microscope.

The collected data was the following (*Fig. 4*):
1. Strain gauge at the top of the compression zone, in the centre, on concrete
2. LVDT measuring the first crack opening
3. LVDT measuring the second crack opening
4. Deflection below the force on one side
5. Deflection at the middle of the beam on one side
6. Deflection at the middle of the beam on the other side
7. Strain gauge on the compressed longitudinal reinforcement

Fig. 3: *Test setup with LVDTs and load measuring cell*

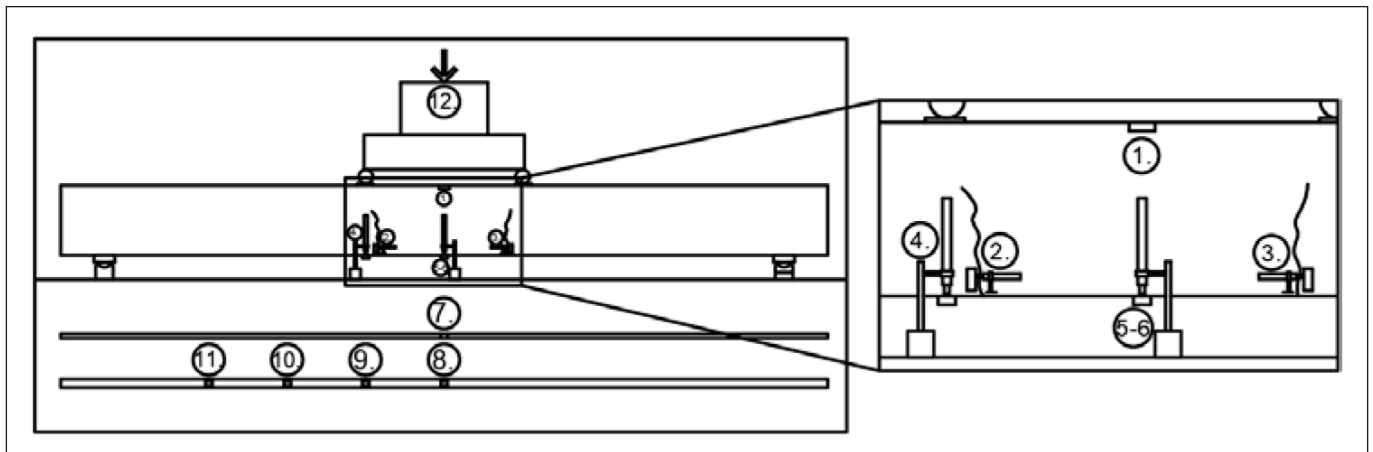**Fig. 2:** *Strain gauges on the reinforcement cage in the formwork*
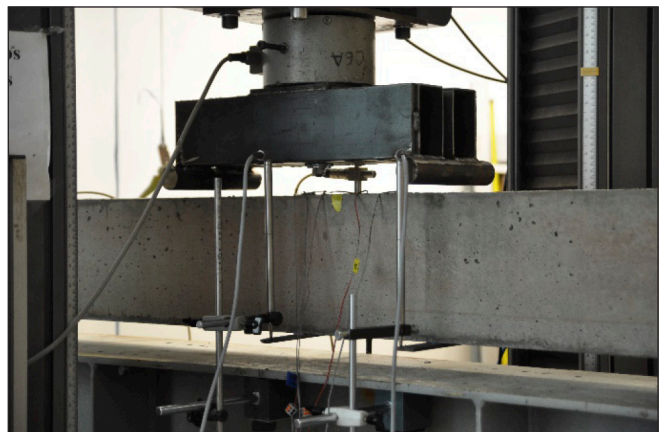
Fig. 4: Data collected during experiments

8. Strain gauge on the tensile longitudinal reinforcement at the centre
9. Strain gauge on the tensile longitudinal reinforcement at the force
10. Strain gauge on the tensile longitudinal reinforcement at 225 mm form force
11. Strain gauge on the tensile longitudinal reinforcement at 450 mm from force
12. Load .

The concrete mix used was designed to achieve at least 50 MPa compressive strength at testing. Every beam and the corresponding three test cubes were made with a new mixture due to the capacity limit of the mixing equipment. The reinforcement was pre-assembled and the strain gauges were installed in place. The beams were removed from the formwork one day after pouring the concrete and were subsequently wrapped in plastic to prevent dehydration and accelerate aging (*Fig. 5*). This was also necessary as the storage of the beams was only possible outdoors. The wrap was removed one day before testing and the specimen were brought indoors. The concrete cubes were subjected to the same treatment before testing. The tests were conducted seven days after pouring the concrete for both the beam and cube specimen.

Fig. 5: Beams before testing with some still wrapped in plastic (left) CFRP wrapping on beam 7 (right)

3. EXPERIMENTAL RESULTS

The first results indicated the load-deflection diagrams (Fig. 6). They indicate the degree to witch the confinement resulted in an increase of loadbearing capacity. There are several important details to note. Most of the FRP reinforced beams have failed at similar load levels. This can be attributed to multiple causes, but the exploration of these is left to after all the results have been discussed. Another notable result is the load-deflection behaviour of Beam 7. The CFRP wrap reinforced beam displayed a significantly increased loadbearing capacity as well as a more ductile behaviour with larger deformations before failing. The capacity of the beam increased by approximately 10 kN and the maximum deflection by approximately 20 mm. The mode of failure in this case was concrete crushing next to the applied load, outside of the wrapped area. It is also notable that the two steel reinforced beams both failed at a similar, lower load level compared to the FRP reinforced ones. This demonstrates the increased load-bearing capacity of FRP reinforcements and confirms that confinement has no significant impact on load-deflection behaviour as anticipated.

Although the confinement did not noticeably effect the loadbearing capacity of the beams, it influenced the failure zone. On Beam 1 and 2, which were not constructed with confinement, the crushed concrete zone is triangular in shape. Beam 3 failed similarly but the depth of the failure zone is shallower than that of beams 1 and 2. Compared to these however, beams 4 and 5 failed with a layer of concrete on the top splitting from the rest. This indicates that the confinement did have an effect on the way the beams failed, but the effect can only be achieved under specific circumstances. The mode of failure of beams 4 and 5 seems to indicate that the
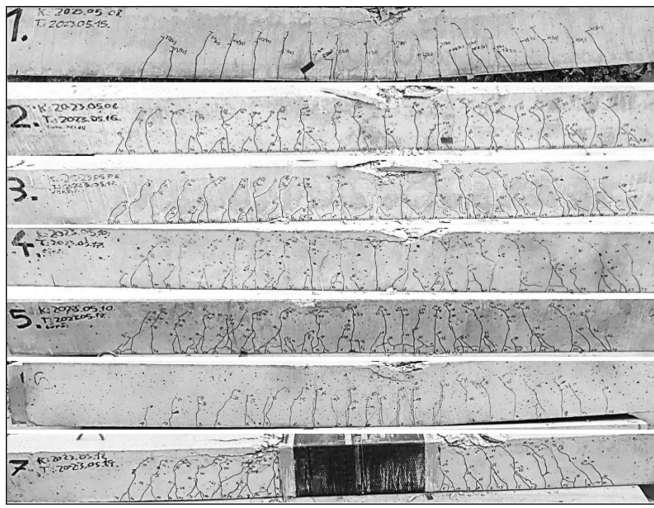
Fig. 6: Load-deflection diagram of all seven beams
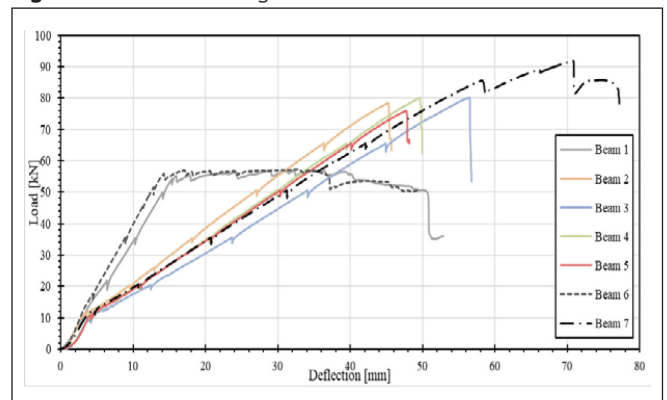
Fig. 7: *The beams laid out after testing, their crack patterns and failure zones visible*
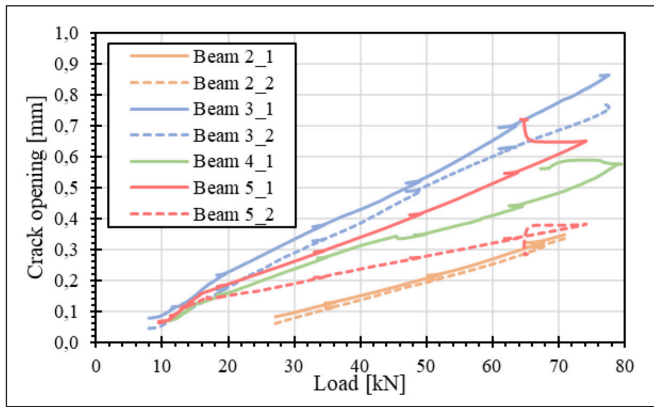

Fig. 8: *Crack opening – load diagram of the first two cracks of beams 2-5 as measured by LVDTs put on after the first crack formation*
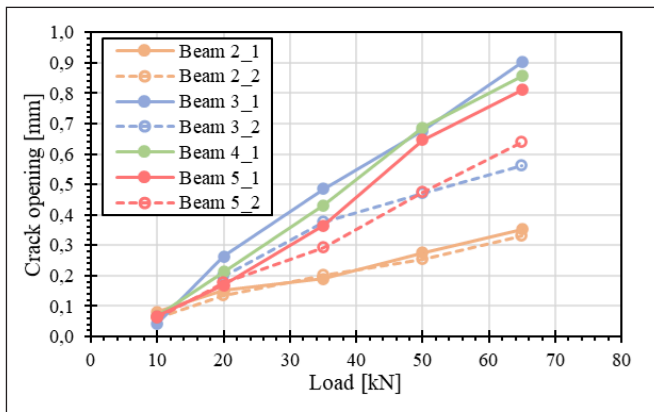

Fig. 9: *Crack opening - load diagram of the first two cracks of beams 2-5 as measured on the pictures taken by hand held microscope*

compressed concrete cover used was too large. However further experimentation is needed to properly understand the limitations of using stirrups to achieve confinement in structures subjected to bending. It should be noted that beam 7, which had GFRP and CFRP wrapping for reinforcement, showed a similar failure mode. The section where concrete crushing occurred was reinforced with stirrups with spacing of 75 mm.

Multiple methods were employed in order to observe the crack patterns and crack openings. However, neither the crack patterns nor the crack openings showed any remarkable change relating to the degree of confinement. The crack patterns in general are in line with expectations, the beams reinforced with GFRP rebars show development of cracks at earlier load levels, with overall smaller crack openings

at failure. The crack patterns of beam 7 shows similarities with other GFRP reinforced beams, with the pattern even showing through the CFRP wrap. *Fig. 7* shows the crack patterns of all seven beams. The difference between steel and GFRP reinforced beams is observable, while any difference between the GFRP reinforced ones is hardly discernible. It is also visible that beams 1 and 6 have suffered permanent deformations while the rest have retained their shape. This demonstrates that the beams failed in compression and the FRP rebars did not fail.

Fig. 8 shows the first two opening cracks on every FRP reinforced beam, as measured by LVDTs. Although the results show a range of openings there in no trend that can be attributed to confinement. beams 2 and 3 showed the smallest and largest cracks respectively, while beams 4 and 5 fall between the two. These results indicate that crack opening does not seem to be influenced by the increase in confining reinforcement. The pictures taken with handheld microscope were used to measure the crack openings at set load levels (*Fig. 8 and 9*). The cracks were on the opposite side to the LVDTs, thus they did not provide the same exact data. Similar results to the LVDT measurements can be observed. This trend reinforces the observations based on the other crack opening measurements.

The strains measured on the surface of the reinforcement were implemented to try to gauge the degree of confinement and to monitor the GFRP rebars. *Figs. 10 and 11* show the strain measurements on the concrete surface, on the compressed longitudinal reinforcements and the tensile reinforcements. As the beams failed at the same load level, the values measured at the concrete surface were expected to be similar to each other. This has largely proven to be true, with the exception of beam 3, which showed larger strain levels throughout loading, even compared to beam 7. Similar results were measured on the compressive reinforcements. Comparing the strain values of beam 7, that

Fig. 10: *Concrete strain – Load diagram of beams 1-4 and 7 (beam 5's strain gauge failed)(top) Compressed reinforcement strain – Load diagram of beams 1-5 and 7 (bottom)*
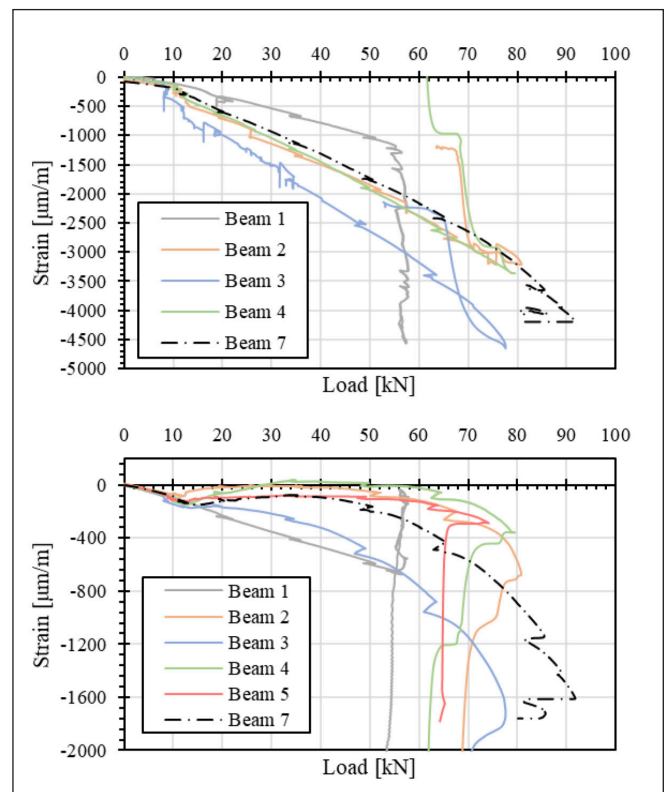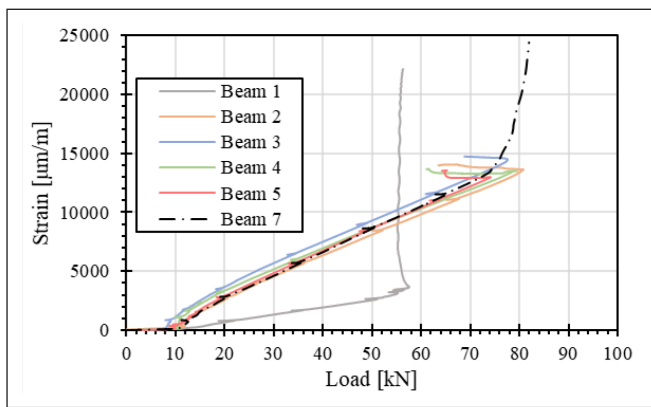
Fig. 11: *Tensile reinforcement strain – Load diagram of beams 1-5 and 7 (bottom)*

was in confinement, to the other FRP reinforced beams it is observable that the behaviour is similar to the other beams. This I also observable on the strain values measured at the tensile reinforcements. These results show that these methods were not adequate to measure confinement. They also show that the effect of confinement can mostly be observed near failure.

4. CONCLUSIONS

The goal of this research was to determine to what extent confinement can be utilized to strengthen FRP reinforced concrete beams. The experiments have proven that confinement can significantly increase the maximum deflection and loadbearing capacity of beams. The majority of the test specimens confined only with stirrups however did not indicate confinement effecting them. This is confirmed by the measurements of crack openings, strains of the reinforcement and the concrete. The exact reason behind this is not known, further testing has to be conducted in order to determine the cause. The failure zones of beams 4 and 5 indicate that the possible reason confinement could not take effect is that the concrete cover was too large, thus when it failed the loadbearing capacity of the remaining cross section was not enough to support the load. From the measurements taken, strains of the compressed and tensile longitudinal reinforcement are suitable to measure confinement.

In further testing strain of stirrups could be measured to obtain a better indicator. Furthermore, in addition to spacing of stirrups, variation on concrete cover, longitudinal reinforcement on the compressive side and size of beams has to be considered as variables. The results of our tests prove that confinement cannot be used in all circumstances to increase the loadbearing capacity of beams, further testing needs to be conducted in order to assess the parameters affecting it, and what values these parameters can take to reliably produce the desired results.

The aim of this research was to study the effect confinement can have on FRP reinforced beams in bending, designed for compressive failure. To achieve this we have conducted experiments on seven beams reinforced with varying tensile and confinement reinforcement. The results of these tests have proven that an approximately 13% increase of loadbearing capacity and an approximately 40% increase of deflection at

failure can be achieved using confinement. This was achieved with wrapping a beam with CFRP textile. The beams produced with FRP reinforcement and a varying number of stirrups showed no sign of confinement. This is possibly to be caused by the compressed concrete cover of being too large. Further testing is needed to determine under what circumstances confinement can be used reliably to increase loadbearing capacity. The measurement of strains of reinforcement can be used to monitor confinement, but further testing is needed to assess other possible monitoring options. In light of these results the usage of confinement on beams designed to fail in compression, is only recommended if it can be reliably achieved, for example by wrapping. However, using stirrups as a confining method is not recommended without further research determining variables affecting confinement.

5. REFERENCES

ACI Committee 440 (2015), "*Guide for the Design and Construction of Structural Concrete Reinforced with Fiber Reinforced Polymer (FRP) Bars*", American Concrete Institute. Report number: ACI 440.1R-15

fib Task Group 9.3 (2007) "*FRP reinforcement in RC structures*",. Report: *fib* bulletin 40

Francesco Bencardino, Antonio Condello & Luciano Ombres (2016), "Numerical and analytical modeling of concrete beams with steel, FRP and hybrid FRP-steel reinforcements. *Composite Structures*. 140, 53-65. https://doi.org/10.1016/j.compstruct.2015.12.045

Japan Prestressed Concrete Institute (2021), "*Recommendations for design and construction of concrete structures using fibre reinforced Polymer (FRP)*", Japan prestressed institute. Accessed: 2023.10.05.

Mapei Kft. (n.d.) "*MapeWrap*" C UNI-AX, MAPEWRAP C UNI-AX, műszaki adatlap | Mapei

Mohammed Abed, Zaher Alkurdi, Jan Fořt, Robert Černý, Sándor Sólyom (2022), "*Bond behavior of FRP bars in lightweight SCC under direct pull-out conditions: experimental and numerical investigation*", Materials, pp.1-15, 15(10), 3555; https://doi.org/10.3390/ma15103555

Omar Gouda, Alireza Asadian, Khaled Galal (2022), "Flexural and Servicability Behavior of Concrete Beams Reinforced with Ribbed GFRP Bars", *Journal of Composites for Construction*. 26(5). https://doi.org/10.1061/(ASCE)CC.1943-5614.0001253

Sándor Sólyom, Matteo Di Benedetti, Anna Szijártó, György L. Balázs (2018), „*Non-metallic reinforcements with different moduli of elasticity and surfaces for concrete structures*", ACEE - The Journal of "Architecture Civil Engineering Environment", Vol. 11/2, pp. 79-88, https://doi.org/10.21307/ACEE-2018-025

Tvrtko Renić (2022), "Duktilnost betonskih greda sfrp armaturom i ovijenim tlačnim područjem", PhD dissertation, University of Zagreb

Working group: Use of FRP (Fibre Reinforced Polymer) rebars for reinforced concrete structures of AFGC (2023), "*Recommendations for the use of FRP (Fibre Reinforced Polymer) rebars for reinforced concrete structure*", Association Francaise de Génie Civil. Accessed: 2023.10.05.

Xuan Hong Vu, Yann Malecot, Laurent Daudeville & Eric Buzaud (2009), "Experimental analysis of concrete behavior under high confinement: Effect of the saturation ratio", *International Journal of Solids and Structures*. 46(5), 1105-1120. https://doi.org/10.1016/j.ijsolstr.2008.10.015.

Bálint Somlai: Civil and structural engineer working on his PhD at BME, while working in the industry as an active bridge engineer. His previous research topics include corrosion resistant concrete testing, textile reinforced concrete structures and FRP reinforced structures. He participated and won multiple student research competitions and assisted in multiple research projects at the Department of Construction Materials and Technologies. E-mail: somlai.balint@edu.bme.hu

Sándor Sólyom: Assistant professor at the Department of Construction Materials and Technologies, Faculty of Civil Engineering, Budapest University of Technology and Economics. Research interest: FRP (Fibre Reinforced Polymer), FRC (Fibre Reinforced Concrete), bond of reinforcement to concrete, 3D concrete printing, concrete technology and durability. E-mail: solyom.sandor@emk.bme.hu

IMPACT AND BLAST RESISTANCE OF SLURRY INFILTRATED FIBER CONCRETE (SIFCON): A COMPREHENSIVE REVIEW

Wisam K. Tauma – György L. Balázs

The construction field developed Slurry Infiltrated Fiber Concrete (SIFCON) to improve mechanical properties considerably. The durability and ductility of this unique kind of concrete have significantly improved as well, and it has a higher energy absorption capacity. SIFCON differs from other fiber-reinforced concretes because it is produced in a different process, and finally, it contains a significant quantity of fiber, up to 20% or even more. In recent years, several research studies have been conducted on SIFCON, mainly focusing on the performance under impact and blast loading. Although this type of concrete is currently being utilized for significant structures, such as energy plants and military buildings, little is known about how it will respond to blast loads. The aim of this study is to analyze the research findings on enhancing the characteristics and toughness of SIFCON during impact and explosion situations. The review provides essential details about SIFCON that specialists in this field would need to know.

Keywords: *Slurry Infiltrated Fiber CONcrete, SIFCON, impact, blast resistance, fibers*

1. INTRODUCTION

Since the 1970s, fiber-reinforced cementitious composite (FRCC) has advanced significantly. It is well recognized that FRCC improves the properties of normal concrete, such as its tensile strength, stiffness, and fracture resistance. These benefits have led to the use of FRCC in civil engineering construction. Slurry infiltrated fiber concrete (SIFCON), a variation of traditional FRCC, was created by Lankard in 1984. The mechanical properties of SIFCON and its applications have been the subject of several investigations (Naaman and Najm, 1992; Naaman et al., 1993; Wang and Maji, 1994; Shannag et al., 2001; Mohammed et al., 2009; and Farnam et al., 2010). According to these studies, SIFCON is more ductile and capable of absorbing more energy than traditional FRCC. Due to these qualities, SIFCON is utilized for significant constructions such as military complexes, runway precast pavements, and underground shelters.

Steel fibers are covered with a slurry of Portland cement, fine sand, pozzolanic products, water, and superplasticizer to make SIFCON. SIFCON contains a high-volume ratio of fibers (up to 20%), significantly higher than that of regular steel FRCC (containing less than 2%), which sets it apart from conventional steel FRCC (Pang et al., 2013).

Many concrete buildings are frequently subjected to impact loads throughout their service lives. Today, much civil infrastructure is subject to impact loads, which can seriously harm the buildings. Therefore, extra consideration must be given to safety and technical solutions so that these structures can withstand impact loads. The kinds of impact situations include vehicular accidents on concrete systems, ships crashing into bridges, falling objects impacting concrete slabs, planes taking off and landing on airport runways, constructions exposed to wind and explosions, etc. (Bambach et al., 2008; and Abirami et al., 2019).

Due to the significant growth in nuclear power plants, terrorist threats, and military threats over the past few decades, the behavior of building materials under blast loading has become a topic of growing interest. With the abovementioned features, SIFCON has much potential as a blast-proof material. However, because of the complexity of blasting experiments, relatively few investigations have been reported on the behavior of SIFCON during blast loading (Pang et al., 2013).

Blast-resistant constructions must be strong to ensure switch load ways in the event of localized failures. If the structural details cannot function as intended, toughness may not be feasible to guarantee. It has been demonstrated that structural features have a considerable behavioral impact on buildings subjected to blast loads. Therefore, it is essential to better understand how structural details behave when subjected to blast stresses. Several sources (Baker et al., 1983; American Society of Civil Engineers, 1985; HQ Dept. of Army, 1986; Drake et al., 1989; Department of Army, 1990; Department of Energy, 1992; and Krauthammer, 1999) contain a lot of details on this subject.

In this review, we attempt to summarize what has been discussed in earlier studies related to the resistance of SIFCON to the impact and blast and the materials used to increase its strength to the influence of those loads.

2. REVIEW OBJECTIVES

This review explores the properties of slurry infiltrated fiber concrete when subjected to the influence of impact and

blast. This study focuses on two main themes: (1) the impact response of SIFCON and (2) the blast resistance of SIFCON.

Emphasis is placed on studying how SIFCON is affected by impact load and explosion compared to other types of concrete. Previous studies and their summary of how to enhance the properties of SIFCON to resist blast and collision are also discussed.

3. IMPACT RESPONSE OF SIFCON

For concrete constructions like bridges, ordinary buildings, and other secure structures, strength against impact is necessary. Examples include an airplane landing impact on a runway, a highway barrier against a random vehicle hit, an accidental ship impact on a bridge pier, a boulder falling on a concrete building, and an offshore structure affected by a sea wave (Murali and Ramprasad, 2018). Because of this, there is an increasing demand for the development of building materials, especially concrete, vulnerable to impact loads. The distortion in regular concrete is nonetheless low. The insufficient impact energy absorption capacity makes it difficult to guarantee the safety of buildings that are subject to impact loads (Li et al., 2020). Several procedures can improve the resistance of concrete to impact loads and significantly reduce damage. Among these techniques, adding fibers to concrete can improve its tensile properties and ability to absorb impact energy compared to ordinary concrete (Abid et al., 2020). Steel fibers can efficiently prevent fracture development and spread, increase energy absorption, and enhance ductile behavior in concrete (Nili and Afroughsabet, 2010).

This section discusses previous research dealing with the SIFCON response to impact load. As well as the types of mineral admixtures used in SIFCON and the range of their influence on this aspect. Also, the extent of the action of impact load is explored through a comprehensive review of the previous literature to gain the most benefit from this study and save effort for researchers in this field. In most previous studies, the drop weight impact testing setup has been fabricated following the guidelines of ACI Committee 544.2R-89.

Table 1. presents details on the number of blows required to cause the first crack (N1) in SIFCON and other types of concrete specimens under impact loading tested in past investigations. Additionally, the number of blows required to cause the ultimate failure stage (N2) was documented.

The same table also includes a comparison of total energy-absorption capacities at the first crack (E1) and ultimate impact strength stages (E2). The energy absorption is obtained by using the following formula (Sudarsana et al., 2010):

$$E = m \cdot g \cdot h \cdot N, \qquad (1)$$

where:

E is the energy absorption capacity.
m is the mass of the ball (kg),
g is the acceleration due to gravity (9.81 m/s^2),
h is the height of falling (mm), and
N is the number of blows.

Based on the results of *Table 1.* SIFCON specimens were highly effective against the impact load compared to other types of concrete. SIFCON was more intact because it has a higher fiber content. Its property of increasing tensile strength and ductility when loaded beyond the elastic limit caused energy dissipation in the slab and increased the stiffness of the specimens against the impact load.

Table 2. shows the figures of failure patterns for the tested specimens. Note from it an improvement in the impact resistance of the specimens using SIFCON compared with other types of concrete.

4. BLAST RESISTANCE OF SIFCON

In recent times, terrorism and explosion accidents have been increasing worldwide. The design of blast-resistant structures is a challenge in modern days. With the latest research in the field of fiber-reinforced concrete, SIFCON is now considered one of the best materials. The need for reinforced concrete buildings as physical protection grows as the threat of international terrorism increases. The protection systems must endure sudden dynamic loads, such as explosion strikes, terrorist attacks, and military accidents.

Fiber-reinforced concrete is now regarded as one of the best materials due to recent industry studies, and it is better to use it in this field (Haekook et al., 2017).

This section discusses previous research dealing with the SIFCON resistance to blast loading. The details of the type of fibers and mineral admixtures used, explosive material (type, quantity, and location for the tested specimen), and the damages (crater diameter or fragment weight in the tested specimen) under blast loading for SIFCON and other types of concrete specimens tested in previous investigations are presented in *Table 3*.

The results of the blast behavior of SIFCON for many previous papers were recorded in *Table 3,* investigated, and compared to other types of concrete. A series of blasting tests was conducted with varying amounts of explosive materials. It was found that SIFCON has much higher blast resistance than other types of concrete.

During the test, it was observed that the SIFCON specimens expanded, proving the superior ductility and energy absorption of SIFCON. It is considered that these characteristics are due to the bridging effect of steel fibers in SIFCON, which transfers the stress across cracks.

Table 4. shows the failure patterns of the samples subjected to blasting. The SIFCON concrete proved its effectiveness in resisting blasting compared to the other concrete types, which were completely destroyed in some cases. Therefore, SIFCON is suitable for structures that may be subject to blast loading. These achievements will help us to design and provide safer structures with SIFCON.

5. CONCLUSIONS AND FUTURE RESEARCH NEED

The purpose of the current study was to critically analyze relevant papers in the published literature on the two factors that directly influence of slurry infiltrated fiber concrete (SIFCON). The impact loading and resistance of SIFCON to blast are discussed. This comprehensive review leads to the following conclusions:

1. When compared to other types of concrete, SIFCON specimens were more efficient against the impact load. Because SIFCON has more fibers, it was less damaged (see *Table 1*). SIFCON achieved high results in energy absorption compared to conventional FRC and other special types of concrete.

Table 1: Summary of impact response of SIFCON

No.	Type of concrete	Dimension of specimens (cm)			Type of fiber	Volume fiber fraction Vf. (%)	Type of mineral admixtures	Number of blows		Energy absorption (kJ)		References
		L	W	T				N1	N2	E1	E2	
1	SIFCON	60	60	5	Steel D=1 mm L=50 mm	8	--	7516	40700	169	915	(Sudarsana et al., 2010)
						10		13750	67466	309	1517	
						12		26950	82133	606	1848	
	SIFCON with steel bar					8		94600	162800	2128	3663	
						10		111100	192500	2499	4331	
						12		137500	242000	3093	5445	
	FRC with steel bar					2		213	40150	4	903	
	FRC					2		100	7406	2	166	
	RCC				--	--		27	11550	0.600	259	
	PCC							--	10	--	0.220	
2	SIFCON	--			Hooked end steel D=1 mm L=30 mm	10	--	246	1005	4.988	20.355	(Elavarasi, and Saravana, 2018)
							SF-15%	273	1032	5.527	20.894	
							GGBS-30%	303	1112	6.130	22.512	
	SIFCON with steel bar						--	715	2364	14.491	47.854	
							SF-15%	742	2572	15.031	52.101	
							GGBS-30%	836	2740	16.918	55.457	
	RCC				--	--	--	10	117	--	--	
	PCC							--	10			
3	SIFCON	Cylindrical disc, D=150 mm H=64 mm			Hooked end steel D=0.9 mm L=60 mm	10	--	619	2074	--		(Abirami et al., 2019)
	FRC					1.5		172	374			
	TSFRC					5		428	1358			
	LFRC					T, M, B 2, 1, 2		450	1394			
4	FRC	Cylindrical disc, D=152 mm H=63 mm			Hooked end steel D=0.7 mm L=35 mm	2	--	33	127	2396	9220	(Manolia et al., 2020)
	SIFCON					11	--	200	923	14519	67004	
							SF-10%	365	1385	26497	100543	
							SF-10% FA-20%	470	1508	34120	109472	
5	FRC	50	50	4	Micro steel L/D = 65	2	--	44	133	2158	6524	(Nadia et al., 2020)
	SIFCON					6	SF-10% FA-20%	430	1327	21091	65089	
6	SIFCON	Cylindrical disc, D=152 mm H=63.5 mm			Hooked end steel D=0.5 mm L=30 mm	8	--	74	614	--		(Ramakrishnan et al., 2021)
					Polypropylene D=0.8 mm L=45 mm			43	480			
	PAFC					2.5		32	241			
					Hooked end steel D=0.5 mm L=30 mm			46	450			
	PAC				--	--		15	17			
7	SIFCON	--			Hooked end steel D=1 mm L=30 mm	10	--	--	--	605	1130	(Sumathi et al., 2022)

No	Type				Fiber	Code	Additive					Reference
8	SIFCON	50	50	5	Hooked end steel D=0.55 mm L=35 mm	6-S	SF-10%	135	800	7457	44190	(Ali and Nada, 2022)
						4-S,2-P		95	770	5248	42533	
					Polyolefin D=0.9 mm L=60 mm	4-P,2-S		67	650	3701	35904	
						6-P		30	150	1657	8286	
9	SIFCON	Cylindrical disc, D=100 mm H=64 mm			Hooked end steel D=0.6 mm L=35 mm	4	--	--	--	--	2329	(Shelorka and Jadhao, 2022)
							MK-10%				3863	
							FA-10%				3540	
10	SIFCON	90	90	6	Hooked end steel D=0.55 mm L=35 mm	6	SF-10%		1086		--	(Mohammed et al., 2023)
					Micro steel D=0.2 mm L=13 mm				1075			
					Hybrid fiber Hooked end steel + Micro steel				1324			
	NSC				--	--	--		580			

Remark: Data should be evaluated according to varying parameters such as mixture proportions, curing conditions, and mechanical properties

2. SIFCON has shown much higher blast resistance than other types of concrete (see Table 3). Samples of concrete types, such as HSC and NSC, were destroyed compared to the fragmentation of very small parts of SIFCON samples.
3. The failure patterns of the samples that were subjected to blast and impact loading show that SIFCON is more successful at withstanding against them than other concrete types, some of which were destroyed (see Tables 2 and 4).
4. For future research, a few studies have examined how SIFCON is affected when exposed to various factors that reduce its service life, specifically when SIFCON is subjected to blasts and impact loads. Nevertheless, there is a need for more studies on the resistance of SIFCON to impact and blast resistance and the use of fibers of different lengths or different aspect ratios in it.

6. TERMINOLOGY

SIFCON	slurry infiltrated fiber concrete
NSC	normal strength concrete
HSC	high strength concrete
FRCC	fiber reinforced cementitious composite
FRC	fiber reinforced concrete
RCC	reinforced cement concrete
PCC	plain cement concrete
TSFRC	two stage fiber reinforced concrete
LFRC	layered fiber reinforced concrete
PAFC	preplaced aggregate fibrous concrete
PAC	preplaced aggregate concrete
HPFRCC	high performance fiber reinforced cementitious composite
UHPFRC	ultra high-performance fiber reinforced concrete
SF	silica fume
GGBS	ground granulated blast furnace slag
FA	fly ash
MK	metakaolin

7. REFERENCES

Abid S., Abdul Hussein M., Ali S., and Kazem A., (2020). "Suggested modified testing techniques to the ACI 544-R repeated drop-weight impact test." Construction and Building Materials. 244, 118321. https://doi.org/10.1016/j.conbuildmat.2020.118321

Abirami, T., Loganaganandan M., Murali G., Roman F., Sreekrishna R., Vignesh T., Januppriya G., and Karthikeyan K. (2019). "Experimental research on impact response of novel steel fibrous concretes under falling mass impact." Construction and Building Materials 222, 447-457. https://doi.org/10.1016/j.conbuildmat.2019.06.175

ACI Committee 544.2R-89. "Measurement of properties of fiber reinforced concrete."

Ali H., and Nada M., (2022). "The effect of using different fibers on the impact-resistance of slurry infiltrated fibrous concrete (SIFCON)." Journal of the Mechanical Behavior of Materials, 31:135-142. https://doi.org/10.1515/jmbm-2022-0015

American Society of Civil Engineers, Manual 42 (1985). "Design of structures to resist nuclear weapons effects."

Baker WE et al., (1983). "Explosion hazards and evaluation." Elsevier Scientific Publishing Company.

Bambach, M.R., Jama, H., Zhao, X.L., Grzebieta, R.H., (2008). „Hollow and concrete-filled steel hollow sections under transverse impact loads." Eng. Struct. 30 (28) 59-70. https://doi.org/10.1016/j.engstruct.2008.04.003

Department of Army, DC, TM 5-1300, (1990). "Structures to resist the effects of accidental explosions."

Department of Energy, Report No. DOE/TIC-11268, US, (1992). "A manual for the prediction of blast and fragment loading on structures."

Drake JL et al., (1989). "Protective construction design manual." (8 Vols), Final Report, ESL-TR-87-57, Air Force Engineering & Services Center, Engineering & Services Laboratory, Tyndall Air Force Base, FL.

Drdlová M., Bibora p., and Čechmánek R., (2018). «Blast resistance of slurry infiltrated fiber concrete with hybrid fiber reinforcement.» Materials Science and Engineering 379, 012024. https://doi.org/10.1088/1757899X/379/1/012024

Elavarasi D., Saravana K., (2018). "On low-velocity impact response of SIFCON slabs under drop hammer impact loading." Construction and Building Materials 160, 127-135. https://doi.org/10.1016/j.conbuildmat.2017.11.013

Farnam, Y., Moosavi, M., Shekarchi, M., Babanajad, S. K. and Bagherzadeh, A., (2010). "Behavior of Slurry Infiltrated Fiber Concrete (SIFCON) under triaxial compression." Cement and Concrete Research, 40(11), 1571-1581. https://doi.org/10.1016/j.cemconres.2010.06.009

Haekook J., Sangin P., Seungwon K., Chelwoo P., (2017). "Performance of SIFCON based HPFRCC under Field Blast Load." 6th International Workshop on Performance, Protection & Strengthening of Structures under Extreme Loading, PROTECT2017, 11-12.

HQ Dept. of the Army, TM 5-855-1, (1986). "Fundamentals of protective design for conventional weapons."

Krauthammer, T., (1999). "Blast-resistant structural concrete and steel

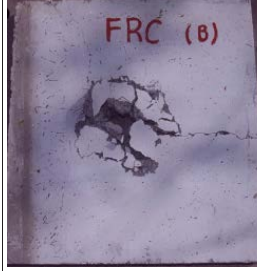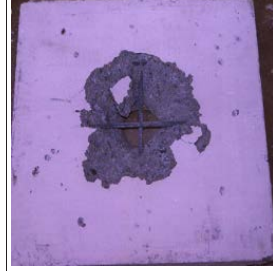**Table 2:** Failure patterns for the impact-tested specimens
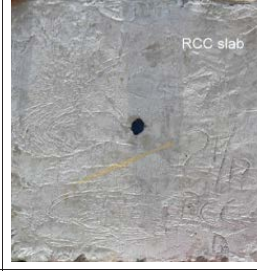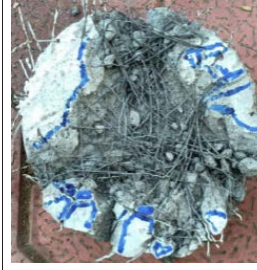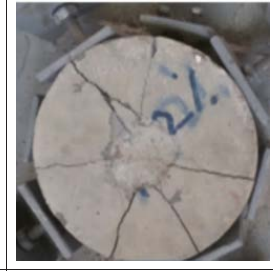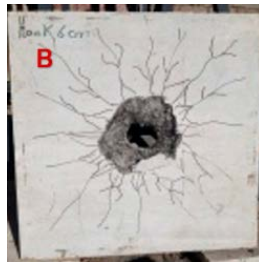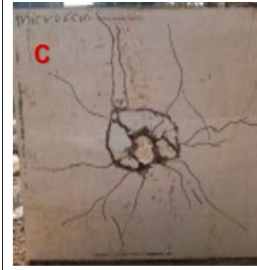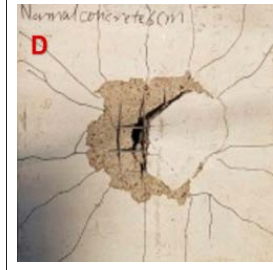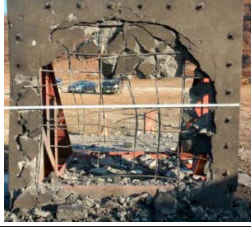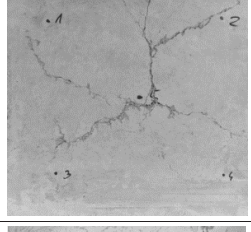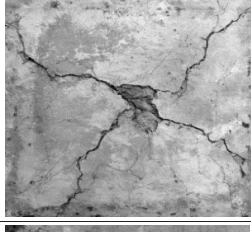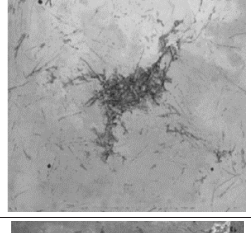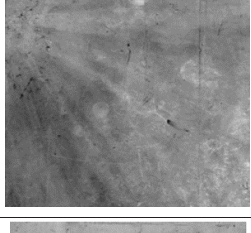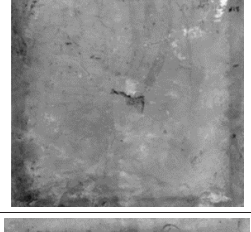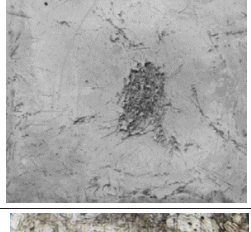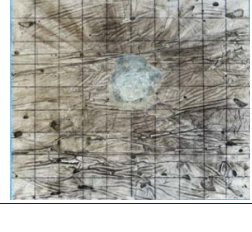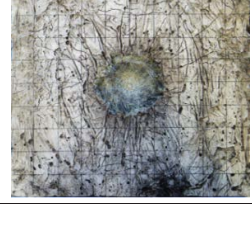
No.	Figures of specimens of all concrete types after the impact test				References
1	SIFCON with steel bars and 8% fibers	SIFCON with 12% fibers	FRC with 2% fibers	RCC	(Sudarsana et al., 2010)
2	SIFCON with steel bars, 10% fibers, and 30% GGBS	SIFCON with 10% fibers and 15% SF	RCC	PCC	(Elavarasi, and Saravana, 2018)
3	SIFCON	LFRC	TSFRC	FRC	(Abirami et al., 2019)
4	SIFCON with 6% fibers	SIFCON with 8.5% fibers	SIFCON with 11% fibers	FRC with 2% fibers	(Manolia et al., 2020)
5	SIFCON with hybrid steel fibers	SIFCON with hooked-end steel fibers	SIFCON with microsteel fibers	NSC	(Mohammed et al., 2023)

Table 3: Summary of blast load resistance of SIFCON

No.	Type of concrete	Dimension of specimens (cm)			Type of fiber	Volume fiber fraction Vf. (%)	Type of mineral admixtures	Explosive material			The damages: A- Crater diameter (cm) or B- Fragment weight (g)	References
		L	W	T				Type	Quantity (g)	Place		
1	SIFCON	50	50	30	Steel D=0.5 mm L=30 mm	9	--	Gelignite	3	Inside the center of slab	A/8.82	(Pang et al., 2013)
									27		A/21.38	
	HSC				--	--	FA GGBS		3		A/22.2	
									9		Destroyed	
2	SIFCON based HPFRCC	190	190	10	Steel D=0.75 mm L=60 mm	5	SF	TNT	100000	5 m of away	Remained intact, but some permanent damage was observed	(Haekook et al., 2017)
					Basalt sheet (surface wrapping)	--						
	NSC				--	--	--				Destroyed	
3	SIFCON	50	50	4	Waste steel fibers from tires	10	SF	Semtex 10	150	1 m of away	B/23.9	(Martina et al., 2018)
					Steel D=0.5 mm L=30 mm	10					B/84	
	UHPFRC					4					B/232	
4	SIFCON	50	50	40	Steel D=0.8 mm L=50 mm	9	SF	Semtex 10	150	1 m of away	B/192	(Drdlová et al., 2018)
					Aramid D=12 μm L=1 mm	0.5 + 9 steel					B/20	
					AR glass D=12 μm L=1.3 mm	0.7 + 9 steel					B/50	
					Polypropylene D=15 μm L=2.2 mm	0.5 + 9 steel					B/166	
					Carbon PAN D=12 μm L=2 mm	0.5 + 9 steel					B/30	
					Wollastonite D=9 μm L=0.3 mm	2 + 9 steel					B/126	
5	SIFCON	50	50	8	Steel D=0.62 mm L=30 mm	11.5	GGBS	SEP	130	Inside the center of slab	A/14.7	(Shintaro et al., 2020)
					Polypropylene D=0.53 mm L=30 mm	10.5					A/18.4	
					Polyethylene D=0.7 mm L=30 mm	15					A/22.2	

Remark: Data should be evaluated according to varying parameters such as mixture proportions, curing conditions, and mechanical properties

Table 4: Failure patterns for the blast-tested specimens
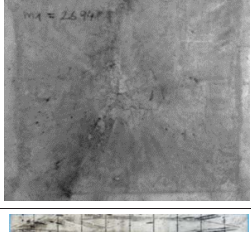
No.	Quantity of explosive material (g)	Figures of specimens of all concrete types after the blasting test				References
		Concrete specimens 1		Concrete specimens 2		
		Types	Figures	Types	Figures	
1	3	SIFCON		HSC		(Pang et al., 2013)
	9	SIFCON		HSC		
2	100000	SIFCON based HPFRCC		NSC		(Haekook et al., 2017)
3	150	SIFCON with Waste steel fibers from tires		UHPFC		(Martina et al., 2018)
4	150	SIFCON with 9% steel fibers		SIFCON with 9% steel + 0.5% Aramid fibers		(Drdlová et al., 2018)
		SIFCON with 9% steel + 0.7% AR glass fibers		SIFCON with 9% steel + 0.5% Polypro-pylene fibers		
		SIFCON with 9% steel + 0.5% Carbon PAN fibers		SIFCON with 9% steel + 2% Wollast-onite fibers		
5	130	SIFCON with 11.5% steel fibers		SIFCON with 15% Polyethy-lene fibers		(Shintaro et al., 2020)

connections." International Journal of Impact Engineering, 22, 887-910. https://doi.org/10.1016/S0734-743X(99)00009-3

Li N., Long G., Li W., Ma C., Zeng X., Xie Y., Li H., Ya H., (2020). „Designing high-impact resistance self-compacting concrete by addition of asphalt-coated coarse aggregate." Construction and Building Materials. 253, 118758. https://doi.org/10.1016/j.conbuildmat.2020.118758

Manolia A., Shakir A., Qais J., (2020). "Study the behavior of Slurry infiltrated fibrous concrete (SIFCON) under impact loading." IOP Conf. Series: Materials Science and Engineering 737, https://doi.org/10.1088/1757-899X/737/1/012069

Martina D., Oldřich S., Petr B., Miloslav P., René C., (2018). "Blast Resistance of Slurry Infiltrated Fibre Concrete with Waste Steel Fibres from Tires." MATEC Web of Conferences 149, 01060. https://doi.org/10.1051/matecconf/201814901060

Mohammed H., Mohammed M., Watheq G., (2023). "Development of an Engineered Slurry-Infiltrated Fibrous Concrete: Experimental and Modelling Approaches." Infrastructures, 8, 19. https://doi.org/10.3390/infrastructures8020019

Mohammed, A. E., Hamed, M. S., Ahmed, M. F. and Ashraf, H. E., (2009). "Use of Slurry Infiltrated Fiber Concrete in Reinforced Concrete Corner Connections Subjected to Opening Moments." Journal of Advanced Concrete Technology, 7(1), 51-59. https://doi.org/10.3151/jact.7.51

Murali G., Ramprasad K., (2018). "A feasibility of enhancing the impact strength of novel layered two-stage fibrous concrete slabs." Eng. Struct. 175, 41-49. https://doi.org/10.1016/j.engstruct.2018.08.034

Naaman, A. E., Otter, D. and Najm, H., (1992). "Elastic modulus of SIFCON in tension and compression." ACI Materials Journal, 88(6), 603-613. https://doi.org/10.14359/1197

Naaman, A. E., Reinhardt, H. W., Fritz, C. and Alwan, J., (1993). "Non-linear analysis of RC beams using a SIFCON matrix." Materials and Structures, 26, 522-531. https://doi.org/10.1007/BF02472863

Nadia M., Husein A., Huda Z., (2020). "Investigation of the Behavior of Slurry Infiltrated Fibrous Concrete" Journal of Advanced Research in Fluid Mechanics and Thermal Sciences 65, Issue 1,109-120

Nili M., Afroughsabet V., (2010). "The combined effect of silica fume and steel fibers on concrete's impact resistance and mechanical properties." Int. J. Impact Eng. 37, 879-886 https://doi.org/10.1016/j.ijimpeng.2010.03.004

Pang-jo Chun, Sang Ho Lee, Sang Ho Cho, and Yun Mook Lim, (2013). "Experimental Study on Blast Resistance of SIFCON." Journal of Advanced Concrete Technology Vol. 11, 144-150. https://doi.org/10.3151/jact.11.144

Ramakrishnan K., Depak S., Hariharan K., Sallal R., Murali G., Daiane C., Roman F., Mugahed A., Hakim S., Jamal M., (2021). "Standard and modified falling mass impact tests on preplaced aggregate fibrous concrete and slurry infiltrated fibrous concrete." Construction and Building Materials 298,123857. https://doi.org/10.1016/j.conbuildmat.2021.123857

Shannag, M. J., Barakat, S. and Jaber, F., (2001). "Structural repair of shear-deficient reinforced concrete beams using SIFCON." Magazine of Concrete Research, 53(6), 391-403. https://doi.org/10.1680/macr.2001.53.6.391

Shelorkar A., Jadhao P., (2022). "Empirical Relationship between the Impact Energy and Compressive Strength for Slurry Infiltrated Fibrous Concrete (SIFCON)." ASPS Conference Proceedings 1: 1199-1202. https://doi.org/10.38208/acp.v1.640

Shintaro M., Makoto Y., Soshiro S., Shinji K., and Teppei S., (2020). "Effects of Fiber Type on Blast Resistance of Slurry-Infiltrated Fiber Concrete Under Contact Detonation." Journal of Advanced Concrete Technology Vol. 18, 157-167. https://doi.org/10.3151/jact.18.157

Sudarsana H., Vaishali G., Ramana N., Gnaneswar K., (2010). "Response of SIFCON two-way slabs under impact loading." International Journal of Impact Engineering 37, 452-458. https://doi.org/10.1016/j.ijimpeng.2009.06.003

Sumathi A., Elavarasi D., Saravana R., (2022). "Experimental studies on slurry infiltrated fibrous concrete (SIFCON) using m-sand." Romanian Journal of Materials, 52 (1), 90 - 96

Wang, M. L. and Maji, A. K., (1994). "Shear properties of slurry-infiltrated fiber concrete (SIFCON)." Construction and Building Materials, 8(3), 161-168. https://doi.org/10.1016/S0950-0618(09)90029-0

Wisam K. Tuama (1987), a Ph.D. student at the Department of Construction Materials and Technologies, Budapest University of Technology and Economics. Researcher at Scientific Research Center, Al-Ayen University, Thi Qar, Iraq. Finished his Bachelor's (2010) in Civil Engineering at the College of Engineering, Thi Qar University in Iraq, and finished his master studies (2019) Master of Science in Construction Materials Engineering at the College of Engineering, Babylon University in Iraq. Research areas: Fiber Reinforced Concrete, durability of concrete, Mechanical Properties of concrete. He is a member of the Hungarian Group of *fib*. E-mail: wisamkamiltuamaalzweehm@edu.bme.hu

György L. Balázs (1958), Civil Engineer, PhD, Dr.-habil., Professor of structural engineering at the Department of Construction Materials and Technologies of Budapest University of Technology and Economics (BME). His main fields of activities are experimental investigation and modeling of RC, PC, FRC, FRP, HSC, HPC, LWC, fire resistance and fire design, durability, sustainability, bond and cracking. He is chairman of several commissions and task groups of *fib*. He is president of Hungarian Group of *fib*, Editor-in-chief of the Journal "Concrete Structures". He was elected as President of *fib* for the period of 2011-2012. Since then, he is Honorary President of *fib*. Chairman of *fib* Com 9 Dissemination of knowledge. E-mail: balazs.gyorgy@emk.bme.hu

MULTIAXIAL STRENGTH AND DEFORMATIONS OF CONCRETE, FAILURE MODES AND A NEW FAILURE CRITERION

Andor Windisch

The multiaxial strength of concrete, the associated stress-strain relationships, the failure modes and the failure criteria are again and again in the interest of researchers. After a historical review the most important bi- and triaxial experiments loading through brushes are analyzed. Based on the principal strengths and the loading path-concept a new, transparent type of presentation of the ultimate strength surface (USS) is introduced. For concrete classes ≤ C100 simplified relative strength-increase values are proposed. The difficulties of deformation measurements are reviewed. The outlines of future bi- and triaxial tests are discussed. Two failure modes are appointed. Stress failure criterion of biaxial state of stress are presented. Instead of the Modified Mohr-Coulomb failure criterion Extended Rankine-type failure criteria are proposed. Further systematic tests are necessary to detect the rate of participation of the loading equipment.

1. INTRODUCTION, HISTORICAL OVERVIEW

The failure models developed until the 1960ies were defined by the testing equipment: the triaxial loading cell which was developed at the beginning of the last century by von Kármán[1]. The axial loading was performed with a solid metallic loading plate, the central-symmetric transverse loading through hydraulic pressure. Therefore, the characterization of the failure surface with the octahedral stresses without any reference to deformations was a logical consequence.

Hilsdorf (1965) proposed a brush-type loading equipment. Using brushes Kupfer (1973) carried out his well-known biaxial loading tests which made possible the characterization of concrete strength by means of the principal stresses. Ottosen (1977) applied in his model for multiaxial strength of concrete the tensor invariants. The same did CEB in its Bulletin d'Information N°. 156 (1983).

Van Mier (1984) applied brushes and proposed a triaxial representation of strength increase using principal stresses and contour lines. He emphasized that all experiments, also the uniaxial ones, are/must be essentially considered as triaxial. Based on his test data he concluded that the physical processes underlying the prepeak and postpeak stress-strain responses were basically different and should be treated separately in material models.

The fib Model Code for Concrete Structures 2010 (2013) returned to the Ottosen model and declared concrete as frictional material. "The multiaxial criteria should depend not only on shear stresses, but also on the first invariant I_1 of the stress tensor to consider the influence of the hydrostatic pressure on the ductility of the material."

As it will be shown, concrete is not a "frictional material". Especially in case of higher class concretes when the prin-cipal stresses reach the ultimate strength the concrete loses dramatically its load bearing capacity, accordingly its behavior does not allow for a treatment as a "plastic material" either. Any transformation of the non-linear stress-strain curve into a linear-elastic-"plastic" working diagram (even if with retaining the area under them) falsifies the real character of concrete.

Based on the principal stresses a new, transparent (and physically really sound) form of representation of the failure surface (USS) showing the strength increase due to bi- and triaxial loading is presented.

2. TESTS UNDER MULTIAXIAL STATES OF STRESS

2.1 Van Mier´s tests

Van Mier (1984) tested specimens made of concretes with strengths between 35 and 40 N/mm² using brush-type loading equipment. His strength-envelops for bi- and triaxial experiments in the coordinate system of principal stresses (*Fig. 1*) are very transparent and informative.

Making use of the sense of these strength envelopes, the following dimensioning and control tasks can be followed (the envelopes of the relevant concrete class must be known):

− Dimensioning: in case of a given concrete class the strength $f_c^* > f_c'$ shall be reached. $f_c^* > f_c'$ can be achieved along the line $\sigma_1 = f_c^*$ parallel to the σ_2-axis. It must be checked what kind of constrictions perpendicular to the direction of f_c^* (i.e. σ_2/σ_1 and σ_3/σ_1) are given/possible. σ_2/σ_3 means the steepness of a line in the σ_2-σ_3 plane through the origo; σ_3/σ_1 is the coordinate of the elevation contour line of the failure surface parallel to the σ_1-σ_2 plane. The intersection of
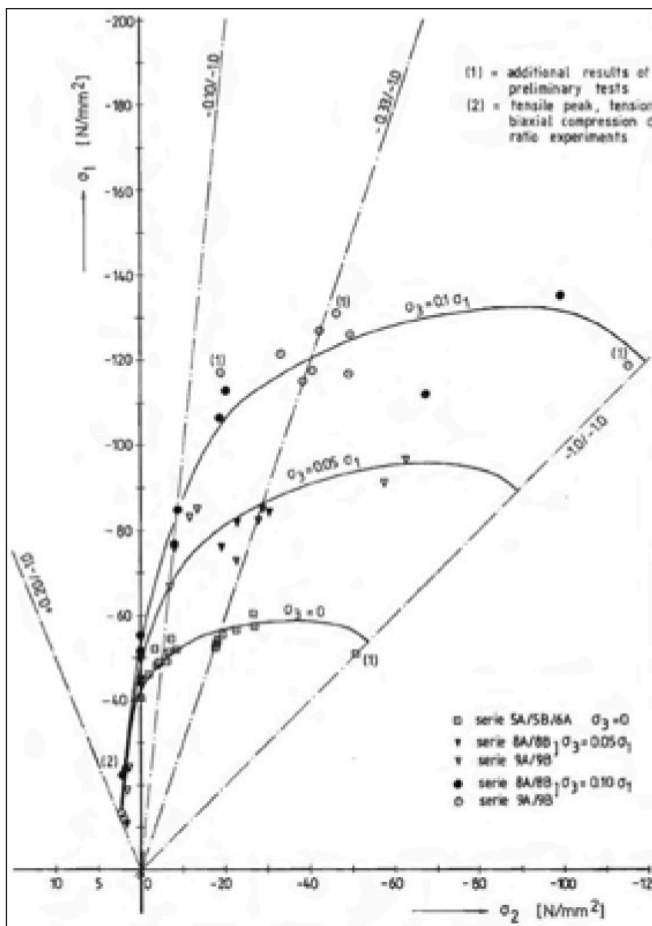
Fig. 1: *Strength-envelopes for the bi- and triaxial experiments of van Mier (1984). (The tensile axis σ₂ is drawn at a larger scale!) Authorized reprint of Fig. 5.8 of a PhD thesis elaborated at TU Eindhoven.*

the $\sigma_1 = f_c{}^*$ –line with the line with the steepness of σ_2/σ_3 in relation to the next two σ_3/σ_1-contours along the σ_2/σ_3-line gives the necessary rate of confinement in the direction of σ_3. (Note: the numbering of the principal axis is acc. to van Mier, it differs from that used later in this paper.)

- Control: concrete class, σ_1/σ_3 and σ_2/σ_3 are given. The position of the point along the σ_2/σ_3-line corresponding to the σ_1/σ_3-ratio shall be determined. The σ_3 ordinate of the intersection is the achievable strength, $f_c{}^*$. If $\sigma_3 \geq f_c{}^*$ then the strength criterion is fulfilled, otherwise
  - either the rate/s of confinement shall be changed or
  - a higher concrete class shall be chosen.

As in the tests

- the most possible endeavor was made to have the principal axis parallel with the sides of the cubic specimens,
- as the principal components are the most fundamental characteristics of any state of stress
- as concrete (and the specimens, too) are never isotropic (at least the direction of compaction has some significant impacts)

hence any transition to the invariants of the deviatoric stress tensor is rather meaningless.

An important statement of van Mier is: "From the statistical analysis of both, the bi- and triaxial series no effect of cyclic or monotonic loading on the envelope curve was observed. The stress-strain curves for concrete seem to be unique, and all stress- and strain conditions within the envelope-curve may exist."

The Author means that whereas the minor compressive- or maximum tensile principal stress is the 'basic' influencing factor for the size of the failure strength, the intermediate principal stress is the more important variable. This can be easily realized: in case of the biaxial compression test the 'basic' factor is $\sigma_1=0$. The size of the intermediate stress σ_{2u} defines the size of σ_{3u}! In case of a constant $\sigma_1 > 0$ principal stress the size of σ_2 governs σ_3. Two comments:

- All failure models ignoring the direct reference to intermediate principal stress must fail. This means that neither the Mohr- nor the Coulomb-failure criteria or any of their modifications can be applied for the proper characterization of concrete.
- Models based on the invariants do not allow for a clear understanding of the impact of the intermediate principal stress.

Van Mier reported that the direction of the loading with regard to the direction of casting had a significant influence on strength and deformational response of the specimens. This doubts further whether the description of the failure surface using the tensor invariants could be correct?

Due to its normal method of manufacture (pouring and compaction) concrete is not isotropic.

The role of the highest (i.e. smallest compressive) principal stresses in triaxial compression tests is similar as specified for σ_2 in the biaxial tests.

2.2 Tests of Speck

Speck (2007) carried out bi- and triaxial loading tests in compression using brush-type loading equipment. She tested 100 mm cubes made of high and ultrahigh strength concretes, also with fibers. In this paper her results with BI (f_c'=56 N/mm²), BII (f_c'=85 N/mm²) and BIII (f_c'=93 N/mm²) concretes without fibers will be considered. The specimens in the triaxial tests for uniaxial compressive strength were loaded parallel to the direction of pouring/compaction whereas in the biaxial tests perpendicular to it. Speck found a pronounced influence of the direction of compaction on the uniaxial compressive strength: parallel loaded the strength was ~10% higher than loaded in transverse direction. Nevertheless the data do not confirm this. Van Mier (1984) did not observe a similar effect.

Speck developed an Ottosen-type failure criteria with improvements related to the brittleness of the UHPCs (this will not be treated here).

2.3 Tests of Ritter

For testing UHPC specimens containing fibers primarily in tension-compression-compression loadings in the triaxial loading equipment at TU Dresden Ritter (2014) developed a new type of tensile load transmission.

3. NEW TYPE OF PRESENTATION OF ULTIMATE STRENGTH SURFACE

3.1 Fundamentals

The most important basic statement: All experiments, also the uniaxial ones must be essentially considered as triaxial.

Concrete obeys principal stresses only. Concrete does not have any shear strength. Shear stress is the consequence of our hugging to the global coordinate system only.

All possible combinations of stresses which correspond to an ultimate stress state can be expressed in terms of principal

stresses normalized to the uniaxial compressive strength as an Ultimate Strength Surface (USS).

The stress state in a point is characterized with the three principal strength values and the direction of the principal axes. The stresses are ordered as follows: $\sigma_1 \geq \sigma_2 \geq \sigma_3$. Compressive stresses and strains are negative, the tensile ones are positive. (The uniaxial compressive strength is considered as a positive value.)

The following notations are introduced:
- σ_1 and σ_2 are related to σ_3, accordingly $\sigma_{1u} = \gamma \sigma_{3u}$ and $\sigma_{2u} = \lambda \sigma_{3u}$.
- The loading occurs along a "loading path", i.e. during loading the ratios γ and λ remain constant, the triade $[\gamma, \lambda, 1]$ characterizes a stress-loading path. (Note: plastic theory is valid in case of one-parametric loading only!)
- σ_{3u} is the most negative strength at failure along any stress-loading path
- The invariants of the stress and of the strain tensors remain – as non-transparent and misleading quantities – ignored. Accordingly the hydrostatic axis, the deviatoric plane, the requirement for the (not realistic) three-fold symmetry and the convexity of the polar figures disappear, too.
- The hydrostatic stress and strain and the octahedral shear stress and strain, which hinder the direct examination of the impact of the three (maximum, intermediate and minimum) principal stresses and strains on the failure surface, disappear.
- Notions as "equibiaxial" and "equitriaxial" tensile strengths disappear as well: in an equibiaxial tensile test the tensile failure will occur according to the actual direction-dependent scatter of the tensile strength, independent of each other in the two other directions. The same is valid for the equitriaxial tensile tests. The reason is, that –in contrary to the compressive loading, where in transverse direction to the compressive stresses micro- and later discrete macro-cracks occur which influence the actual strength there- the tensile failure occurs in a 'thin' region only perpendicular to the direction of tensile force hence does not influence the tensile strength in the two other directions (See Fictitious Crack Model of Hillerborg et al. (1976)).
- The results of the bi- and triaxial tests (σ_{3u}) will be displayed in the coordinate system γ, λ as $\sigma_{3u} = \Phi (\gamma, \lambda)$. Advantages of this display are:
  o The direct impact of the minimum and medium principal stresses, resp. can be perceived,
  o USS is a continuous, smooth, convex, single-valued surface,
  o As $\gamma \leq 1$, $\lambda \leq 1$ hence USS is always limited, no extra "cap function" as in case of the octahedral strength function is needed.
  o The $-\sigma_{3u}/f_c$' values along the [0, 0] to [1, 1] diagonal correspond to the "compressive meridian", whereas along the [0, 1] to [1, 1] line correspond to the "tensile meridian".
  o If the pouring direction coincides with the $-\sigma_{3u}/f_c$'-axis then the $-\sigma_{3u}/f_c$'-surface is axisymmetric to the [0, 0] – [1, 1]-diagonal.

It should be recognized that for each concrete class only two failure configurations characterized with the triade $[\gamma, \lambda, 1]$ exist: i) the direction of σ_{3u} coincides with the direction of the pouring/compaction, ii) it does not coincide. This means that each failure surface displayed in the (σ_1, σ_2, σ_3) coordinate system is single-valued over the (σ_1, σ_2)- or (γ, λ)-planes.

The description using the octahedral stress components suggests an axis-invariance which in the case of concrete (if only because of the direction set by the compaction) might lead to faulty assumptions as due to its production technology concrete is not isotropic.

In case of three dimensional representations (relative increase of strength) the two horizontal axis correspond to the γ and λ values and the vertical one to the $\Phi = -\sigma_{3u} / f_c$'-values.

The renunciation from the hydrostatic- and deviator-related representation yields a
i. clear and transparent understanding of the influence of the minor (γ)- and intermediate- (λ) stress levels resp.,
ii. deviating from the compulsory three-fold symmetry with respect to the hydrostatic axis the figures meet the non-isotropic characteristics of the concrete which is the direct consequence of concrete production technology (pouring). It is even more pronounced in case of the fiber-reinforced and printed concretes which are more and more coming.

3.2 Ultimate strengths in triaxial state of stress

Van Mier's (1984) test results in the proposed form of representation can be seen in *Fig. 2*. With increasing γ the $-\sigma_{3u}/f_c$' values increase whereas in case of $\lambda = 1$ the $-\sigma_{3u}/f_c$' values are less than in case of $\lambda = 0.6$.

Fig. 3 shows a level-type representation of relative strength-increase measured by Speck (2007) at her BII concrete.

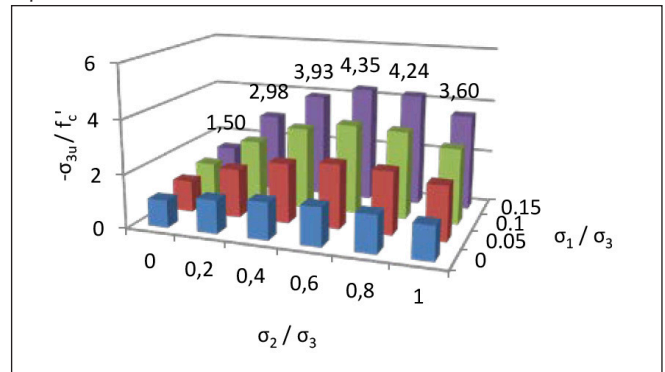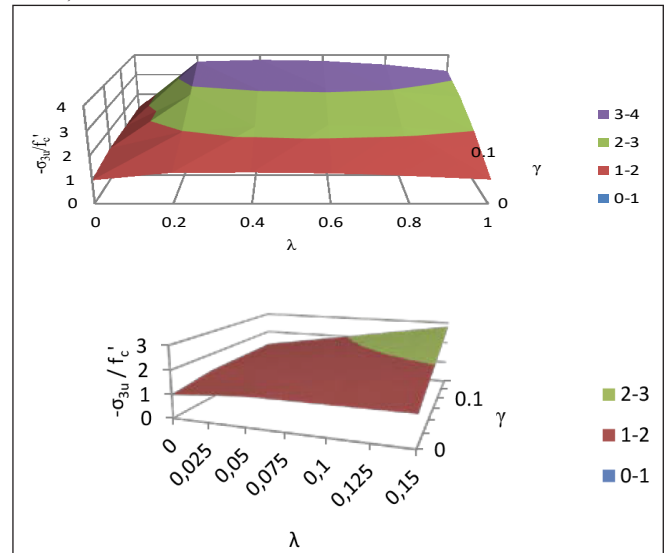**Fig. 2:** *Van Mier's tri-axial test results in the new form of representation*

Fig. 3: *Level-type representation of 3D strength of Speck's BII (f_c' = 71 N/mm²) concrete: a) the whole tested field, b) the symmetrical region $\gamma \leq 0.15$, $\lambda \leq 0.15$*
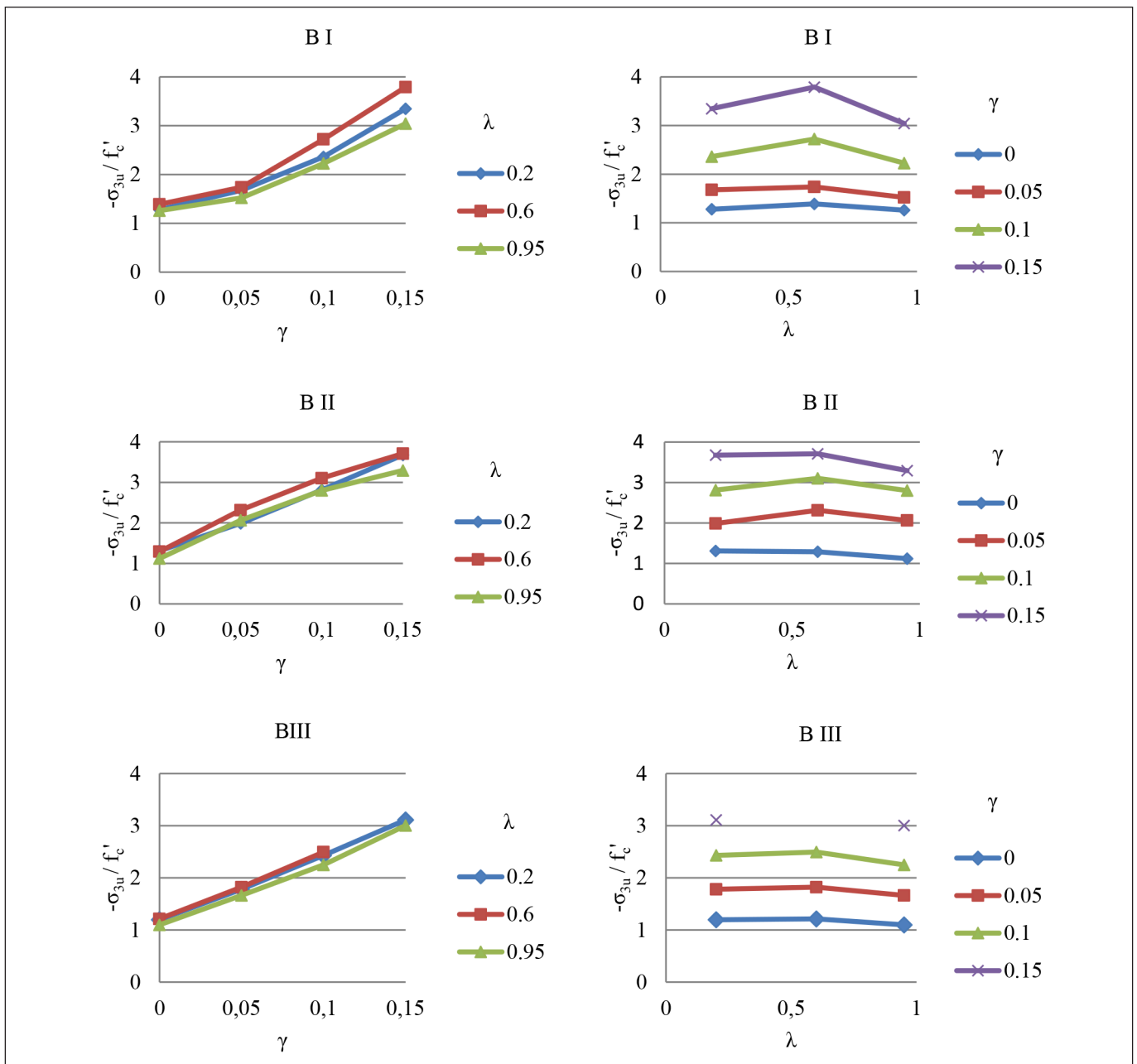
Fig. 4: *Segments of the USS for concretes tri-axially tested by Speck for a)* λ = const, *b)* γ = const.

Fig. 4a) and b) show the sections along the λ = const. and γ = const. lines of the 3D ultimate strength surfaces for concretes tested by Speck. The courses in *Fig. 4a)* imply that –at least within the tested region 0 ≤ γ ≤ 0.15– no tendency for a downward, slowing growth of the normalized strength increase can be detected.

Fig. 5 shows the relative strength increase of the three concretes tested by Speck (2007) for the three λ-values as function of γ. As a matter of fact the differences between the courses of the relative strength-increases for the three concrete classes along the λ = const. lines are within the possible scatters of the tests, no characteristic differences can be detected. Even the order of the increasing concrete strengths cannot be discerned. This can be interpreted that at least in case of concrete classes < C100 generally valid -σ_{3u}/f_c' values as linear function of γ can be defined hence no further test-series are needed. At γ = 0.15 -σ_{3u}/f_c'-values could be 3.5 (for λ = 0.2), 3.7 (for λ = 0.6) and 3.3 (for λ = 0.95). The sections along the λ=const. lines up to the tested γ ≤ 0.15 ratio do not yield enough information for estimation of a convex course or even a limit value of the hydrostatic compressive strength

of these concretes. *Fig. 2 to 5* reveal the advantages of the proposed new type of presentation.

4. PROBLEMS AND DIFFICULTIES AT DEFORMATION MEASUREMENTS

Deformation measurement is complicated when brush-type bearing platens are used. Four or all six surfaces of the specimen are "occupied" with the brushes. On the free surface DMS or optical sensors can be applied. Here the limited sensor length might cause a problem: the failure procedure occurs through development of discrete cracks from microcracks. If the discrete crack occurs outside the sensor length, then the measured deformation is not characteristic. The transversal deformation perpendicular to the free specimen surfaces can be measured mechanically in a discrete point (Kupfer (1973) has chosen two points in 4 cm distance from the corners of the 20*20 cm² specimen). Here once more the question arises whether the deformation in this point is typical for the whole
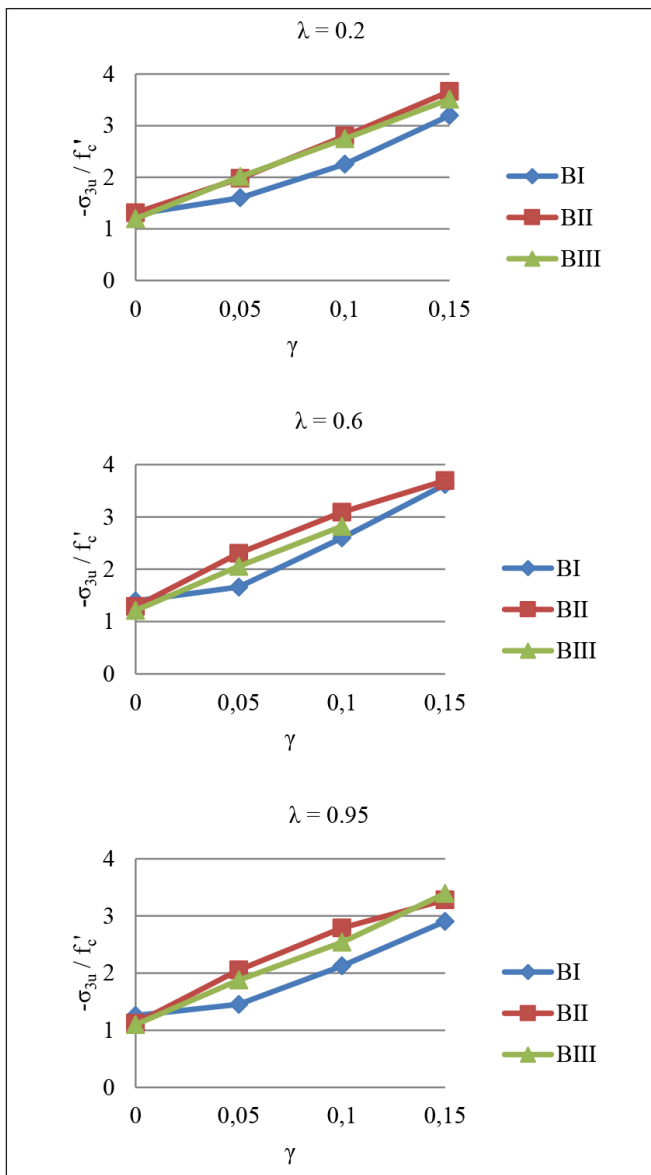
Fig. 5: *Normalized ultimate strength increase of the three classes of concrete tested by Speck[8]*

specimen? Measuring elements can be put into the specimen: Ritter (2014) applied tetrahedron shaped wire-scaffolds mounted with optical sensors. Here the gauge or its carrier causes discontinuity in the specimen influencing its behavior. Another possibility is to measure the deformations between two elements of the brush (van Mier (1984), Speck (2007)). Here the question arises whether the brush correctly follows the deformation of the specimen's surface (eventual slip).

The strain values published by Speck (2007) are mean values of up to six measurements (which were made with the greatest possible care). Nevertheless, mean values may sometimes deform/obscure the real physical relationships. Speck reports in detail on the problems that were arisen from the additional forces caused by the flexural rigidity of the brush-teeth. This measuring method cannot detect discrete cracks which develop during the loading procedure.

The conclusion of van Mier (1984) is pointing the way: the results are well within the 'engineering accuracy' (but not more). He reports that the outer parts of the cubic specimens behaved/deformed in a different way as the central parts: the deformation of the brush-rods and the specimen results in a spherical loading surface. Van Mier mentions that cracks developed in the descending branch of the stress-strain curve, which is important for the evaluation of the deformations.

5. ULTIMATE STRAINS IN MULTIAXIAL TESTS

Fig. 6 shows the courses of the mean values of the measured failure strains in the biaxial tests ($\gamma = 0$, **compression-compression sector**) of normal concretes measured by Kupfer (1973) ($f_c' = 19$ N/mm², 32 N/mm²), high strength concretes tested by Speck (2007) BI ($f_c'=56$ N/mm²), BII ($f_c'=85$ N/mm²) and BIII ($f_c'=93$ N/mm²) and Ultra High Performance concrete by Ritter (2014) ($f_c' = 171$ N/mm²) as function of λ.

The following general observations can be made for each concrete class:

- the ε_{3u} strains (in the direction of the major compressive stress) remain around -3‰ as λ increases
- the ε_{2u} strains (direction of the intermediate stress) decrease continuously linearly (from positive to negative parallel with the increasing, relative compressive loading in direction 2) unless they arrive at the same value as in the minimum strength direction (with scatter).
- the tensile strain ε_{1u} (deformation in the unloaded transverse direction) continuously increases with the increasing relative compressive loading in direction 2, the elongation exceeds very soon the strain limit assigned to the very limited uniaxial tensile strength of concrete. The measured elongations cannot detect the discrete cracks,
  - the max. value of ε_{3u} is not less than -4‰, nevertheless, no real trend between concrete strength and deformation can be detected, this means that the deformation in the most loaded direction cannot be considered as singular failure criterion,
  - beyond that the tensile strains, ε_{1u}, increase with increasing λ, no regularity can be detected either,
  - for simplicity reasons at the development of the stress-strain curves at different λ-values a linearity between the relevant ε-values measured under the uniaxial- and the biaxial loading can be considered.

Fig. 7 shows the ε_{1u} and ε_{3u} strains for BII concrete as function of γ, measured in triaxial tests, published by Speck (2007). It is conspicuous that the ε_{1u}-value for $\gamma = 0$ is not compatible with the following values for $\gamma > 0$ values. The range of the tested γ-values does not allow any sensible extrapolation for the further course of the strains.

The following trends can be diagnosed:

- ε_{1u} increases far beyond the strain related to the uniaxial tensile strength (in case of $\gamma = 0.05$ up to 2.49 ‰, of $\gamma = 0.10$ up to 4.72 ‰, and of $\gamma = 0.15$ up to 6.11 ‰). This means that not negligible compressive stresses ($\lambda\sigma_{3u}$) must be transferred despite/across the numerous macrocracks. Here the large-scale influence of the loading equipment (its lateral stiffness) shall be investigated in the future.
- ε_{3u} continuously increases (i.e. shortening decreases), at the same time (in case of $\gamma = 0.05$ from ~ -2 ‰ up to -1.75 / -1.6 ‰, of $\gamma = 0.10$ from -4.73 ‰ up to -4.23 ‰, and of $\gamma = 0.15$ from -8.28 up to -5.12 ‰).

The course of the maximum strains in direction of the lowest (ε_{1u}) and of the highest (ε_{3u}) compressive stresses, resp. as function of λ (at $\gamma = 0.05$) **for a wide range of concrete classes**, presented in *Fig. 8*, shows that both deformations have a decreasing tendency at increasing concrete strengths.

At all observations and conclusions the normal scatter due to the very different concrete compositions, strain measuring methods etc. must be considered.

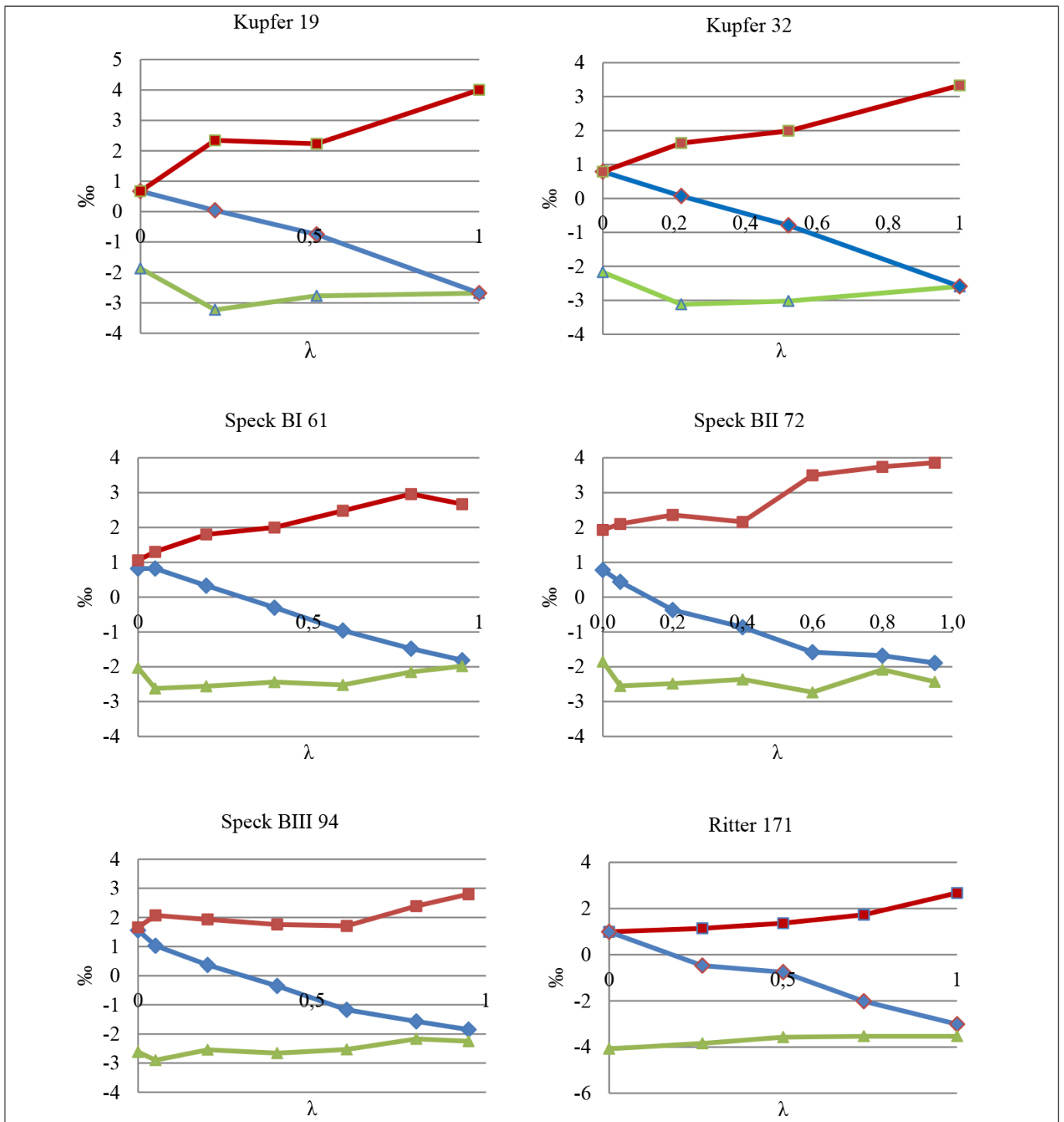The experimental studies have shown that the deformation

Fig. 6: Ultimate strains measured in biaxial tests   Legend: red – ε_{1u}, blue – ε_{2u}, green – ε_{3u}

characteristics and the ultimate strength of concrete subjected to uni-, bi- or triaxial stresses are controlled by the development and propagation of microcracks. These microcracks are mainly oriented in a perpendicular direction to the direction of the smallest principal compressive stress or the largest principal tensile stress. (It is one more reason to leave the octahedral stress-type representation.)

6. FUTURE OF 3D-TESTS

The history of bi- and triaxial tests with HPC- and UHPC-specimens reveals that the capacity of the loading brushes restricts the applicable γ- and λ-ranges. *Fig. 9* gives useful information: as higher is the concrete strength, as lower is the relative strength increase. Similar tendency can be detected in *Figure 10*: the relative triaxial strength increases measured
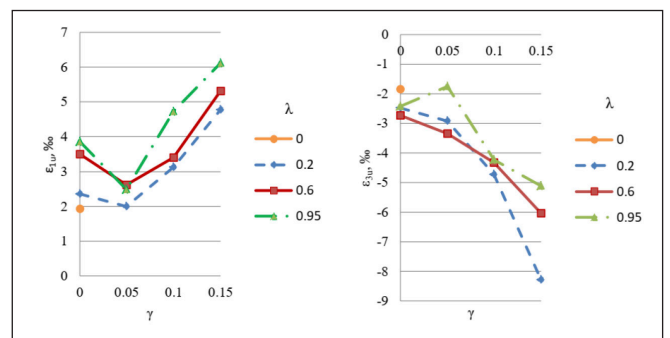
Fig. 7: Development of the strains a) ε_{1u} and b) ε_{3u} under tri-axial loading of BII specimens, measured by Speck

at γ = 0.027 (very low) and different λ-values for Ultra High Strength concrete (Ritter (2014)) are regularly smaller than those in case of High Strength concretes (Speck (2007)).

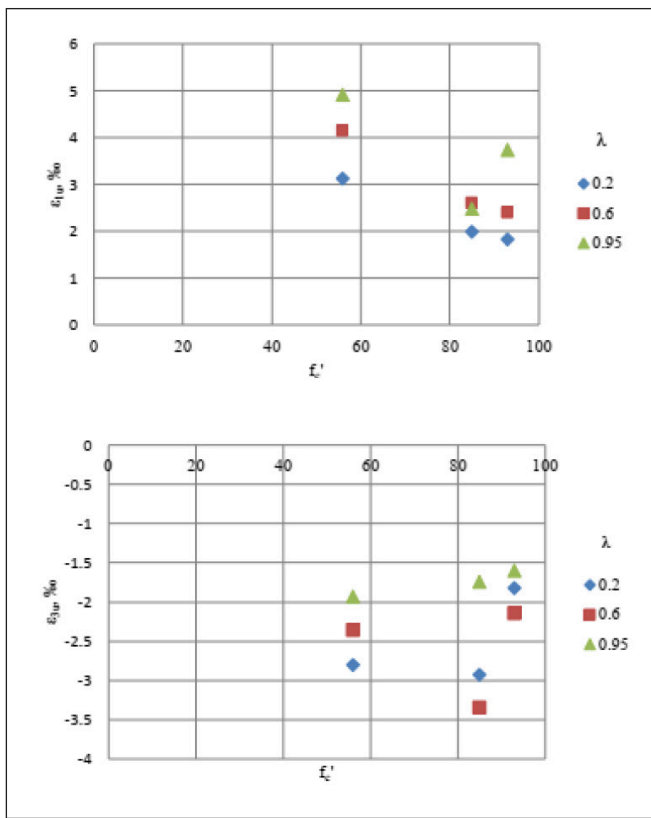This means that using an existing (brush-type) loading

Fig. 8: Courses of strains ε_{1u} and ε_{3u} as function of the uniaxial concrete strength at $\gamma = 0.05$
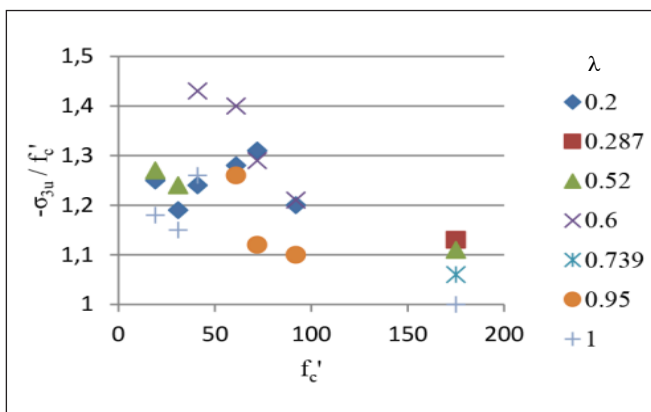

Fig. 9: Relative increase of relative ultimate biaxial compressive strength of different concrete classes ($f_c' = \sim40 - 175$ N/mm²) as function of λ
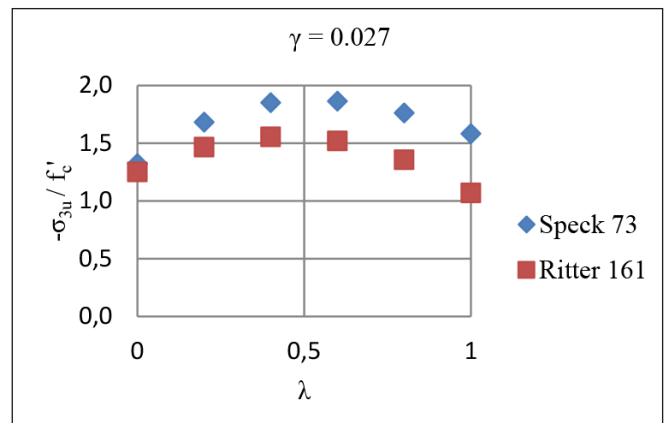

Fig. 10: Comparison of relative increase of tri-axial strengths of High and Ultra High Strength Concretes

limited number of cracks develop, which are approximately parallel with the medium principal stress and perform an angle approx. 20-30° to the smallest principal stress

5. crushing failure: the internal structure of concrete is destroyed, the pores fail, many cracks without orientation develop.

Comparing the modes 1-3 it can be realized that in each of these modes the tensile deformation capacity was exhausted. Referring to failure mode 4 we recall to van Mier's (1984) hints: "According to investigations carried out by Newman et al. (1965), this "shear-plane" fracture mode should be attributed to a non-uniform stress-distribution within the concrete. This is the result of a rotation of one of the loading plates, when an experiment is carried out with one end effectively fixed and the other end effectively pinned. The effect may even become more significant when non-homogeneous specimen is tested." In van Mier's investigation the prisms were loaded perpendicular to the direction of pouring, which implies that one side of the prism could be weaker. The specimen's neutral axis did not coincide with the loading axis. The prisms failed with cracks running more or less parallel to the direction of loading. "The difference in fracture mode of specimen did not seem to influence the macroscopic stress-strain curve. Probably the rotation of the upper loading platen is reflected by unevenness in the descending branch and the effect is not pronounced when perpendicular loading (i.e. to the direction of pouring) is applied." Conclusion: failure mode 4 (if it occurs) is an anomaly. This conclusion can be confirmed with reference to the contradiction between the geometrical boundary conditions (plane end of the loading brush and support plate) and the relative displacements necessary for the development of the wedges corresponding to the shear failure (wedges must undergo a mutual shifting) these are not compatible with each other.

Failure mode 5 is used by the cement chemists to squeeze pore water from very small concrete probes, i.e. it is not relevant for structural engineers.

The 'hugging' to the shear stress oriented failure criterions like Mohr-Coulomb can be understood/excused as due to the axial loading through the rigid steel plates (friction) and the dumpy test specimens (h/d ≤ 2): in all cases the failure patterns showed inclined 'shear' failure planes, similar to those at uniaxial compressive tests on cubes and dumpy cylinders.

All 'shear band ruptures' must be regarded as reminiscences and tribute to the aforementioned inclined shear failure planes seen in former imperfect tests. Van Mier (1984) reports that some of the shear-band type failures were caused through the spherical deformation of the loading brush: Shear

equipment with given load bearing capacity and following a [$\gamma > 0.15$; λ; σ_{c3u}] (or similar) loading path, specimens with increasing compressive strengths should be loaded up to failure. The smallest value of the measured $-\sigma_{c3u}/f_c'$-values yields an upper limit of the possible $-\sigma_{c3u}/f_c'$-values for all higher strength concretes.

Certainly the impact of the rigidity of the loading brushes should be systematically investigated and taken into account.

7. FAILURE MODES

In the literature five failure modes are listed:
1. tensile failure: main crack perpendicular to highest principal stress
2. compression failure: the specimen fails to columns parallel with the highest compressive stress
3. splitting failure: the specimen fails to slices perpendicular to the smallest compression stress
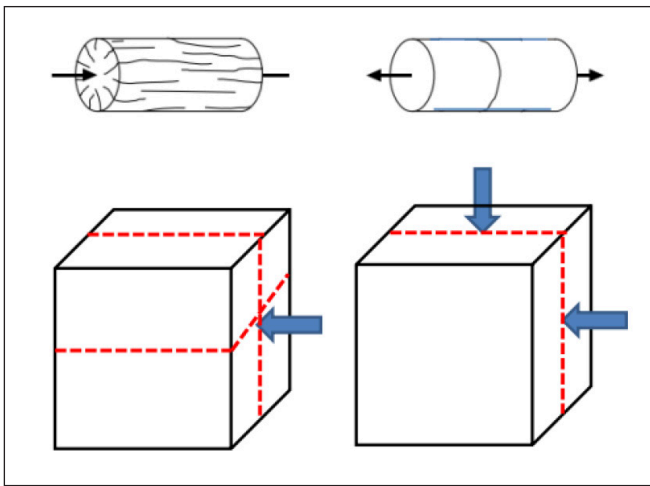4. shear failure: with inclined failure surfaces, where only a

Fig. 11: *Macrocracks (schematic representation) in specimens loaded in a) cylinder in uniaxial compression, b) uniaxial tension, c) cubes in uni- and biaxial compression*

plane fracture was observed for four of the eight prism tests. This means, that in four of eight cases neither the loading brush deformed nor the specimen performed "prefabricated" weak planes: the four shear plane fractures are the "abnormal" ones.

The 'cone-like' rupture elements are formed when a shear-band develops through an array of initial parallel tensile micro-cracks. This tensile crack-array was visualized by Stroeven (1973) using the fluorescenting technique.

In fact two fracture patterns for concrete with only one single inherent cause exist: microcracks occur in plane(s) parallel with the major compressive load or perpendicular to the maximum tensile load. In the section with the weakest tensile strength microcracks form a macrocrack (*Fig. 11*). In case of compressive loading the parts formed by the cracks might continue to carry the compressive loading, whereas in case of tension the first crack stops the loading procedure, unless the stiffness of the loading brushes takes over some tensile stresses.

Similar fracture pattern was observed in high-performance concrete for all tested stress ratios and all concrete classes by Speck (2007). Crack formed, which run parallel to the unloaded surface. In the uniaxial tests and partly under the stress ratio λ = 0.05, cracks appeared in two planes, parallel to the unloaded surfaces and parallel to the slightly loaded surface. For all other biaxial stress conditions, there was the crack plane quite parallel to the free surface. The specimen was split into several slices. The parallelism of the crack planes with regard to the unloaded surface increased beyond λ = 0.6 in the second load axis and with increasing concrete class.

An interesting issue should be mentioned: the authors of the different fracture criteria operating with meridians argue over the shape of the meridians and their closure resp. at high hydrostatic loading, i.e. on the size of the 'cap' value. Considering the possible failure modes in case of the loading path $[1, 1, \sigma_{c3u}]$ we must conclude that only a full crushing of the concrete texture can occur as the concrete chemists squeeze the pore water for their investigations. A 'cap' strength value is difficult to assign.

8. FAILURE CRITERIA

Three types of criteria could be considered:
- Strength(s) or their combination at failure
- Strain(s) or their combination at failure
- a combination of both.

With regard to strength, reference is made to Section 3.2.

What about the strain(s)? Figure 7a shows the development of the ε_{1u} strains (elongation) as function of γ, measured in the triaxial loading tests (compression-compression sector) of Speck (2007). It is conspicuous that despite of the considerable elongations, compressive stresses up to 45 N/mm² can/must be transmitted in this direction. This must be understood as "contribution" of the loading system, and makes any statement about a failure criterion rather questionable.

Van Mier (1984) diagnosed: "The tests show clearly the interaction between stress- and deformation." "It seems more appropriate to describe the specimen response as 'structural' rather than as 'material property'."

Due to the problems and difficulties at deformation measurements (as discussed in chapter 4) no reliable failure criteria referring to strains can be defined.

As a conclusion it must be discovered, that due to the unknown degree of participation of the different loading brushes, for the time being neither the measured strengths nor the published strains are correct characteristics of the failure of the tested concretes.

In order to quantify the rate of participation of the loading equipment further systematic tests are necessary: following identical and characteristic loading paths specimens of the same concrete strength must be tested with significantly different stiff loading brushes!

Thereafter it can be tried to formulate a reliable failure criteria for multiaxially loaded concrete.

8.1 Ottosen's Model

Ottosen (1977) lists as advantage of the description of his failure criterion (surface) as function of the invariants: (1) only four parameters are used; (2) makes determination of the principal stresses unnecessary; (3) the surface is smooth and convex with the exception of the vertex; (4) the meridians are parabolic and open in the direction of the negative hydrostatic axis; (5) the trace in the deviatoric plane changes from nearly triangular to circular shape with increasing hydrostatic pressure; (6) it contains several earlier proposed criteria as special cases, in particular, the criterion of Drucker and Prager (1952) and of van Mises.

The four parameters can be determined with tedious calculations from the uniaxial tensile strength, uniaxial compressive strength, equibiaxial compressive strength and an ultimate strength on the compressive meridian. Advantage (2) does not exist: the invariants are composed from the principal stresses nevertheless the invariants make the failure criterion extremely non-transparent. The influence of the distinct principal stresses and trace the load path cannot be perceived.

8.2 CEB Bulletin No. 156

In the CEB Bulletin No. 156 (1983) the description of "the Ultimate Strength Surface (USS) is based on the following technical considerations and rational reasoning:

a. USS is to be described by invariants of the stress tensors or by expressions derived from it

b. For an isotropic material without any history, the USS in the deviatoric plane (polar figure) is three-fold symmetric with respect to the hydrostatic axis.

c. Theory of plasticity and more recent fracture mechanics

studies require the polar figures to be convex.

d. For a material whose uniaxial compressive strength differs from its tensile strength we have to distinguish between a triaxial compression curve and a triaxial tension curve."

Comments

To a): already Kármán (1910) wrote in 1910: "If the principal stresses are considered as spatial coordinates then each point in the space corresponds to a certain state of stress. The points corresponding to the limit of elasticity form a surface, which encloses that portion of space where purely elastic deformations occur. This surface is called limit surface of elasticity. Another surface corresponds to the maximum stress states which act just before failure occurs." As it is well known, the sense of invariants of a tensor (here the stress tensor) is that it does not change with rotation of the coordinate system. (But this is its single sense.) The description of USS by invariants makes the stress state non-transparent and less practical. Much better is to transfer any stress state into its principal stresses with the corresponding directions. Concrete "perceives" principal stresses only. The description by hydrostatic normal and octagonal shear stress was essential as at the early experiments in the triaxial cells only the longitudinal principal stress was explicit; all perpendicular directions were "principal" directions. The octagonal stress components "helped" to overcome this 'inconvenience'.

To b): due to its production technology (pouring), concrete is not isotropic. In the era of the high capacity computers there is no reason to adhere to this not existing isotropy.

To c): recent test series (van Mier (1984), Speck (2007)) revealed that -especially in case of concretes beyond C40- the upper bound theory of plasticity cannot be applied to concrete. The "plasticity" of RC slabs results from the "residual elasticity" of the concrete compression zone of slightly reinforced cross sections. This plasticity attributed to the concrete compression zone "results" of the difference between the depth of compression zone calculated assuming perfect bond between rebars and concrete, and the real behavior of the cracked RC section, provided that low amount, moderate diameter rebars are applied.

To d): the triaxial compression curve (or meridian) and the triaxial tension curve are direct "results" of the physical possibilities of the ancient triaxial cells: the stresses in the transversal directions were always identical, which corresponds to the definition of these meridians. In a description of the USS in the coordinate system of principal stresses these meridians are meaningless.

8.3   MC2010

Among several acceptable formulations MC2010 (2013) has chosen the constitutive equation of Ottosen (1977) as "it is not too difficult to use and agrees well with test data".

The mean value of strength under multiaxial states of stress may be estimated from the failure criterion

$$\alpha \, \frac{J_2}{f_{cm}^2} + \lambda \frac{\sqrt{J_2}}{f_{cm}} + \beta \, \frac{I_1}{f_{cm}} - 1 = 0$$

where

$$\lambda = c_1 \cdot \cos\left[\tfrac{1}{3} \cdot arccos(c_2 \cdot cos3\theta)\right]$$

$$\cos 3\theta = \frac{3\sqrt{3}}{2} \cdot \frac{J_3}{J_2^{3/2}}$$

The material parameters α, β, c_1 and c_2 depend on the uniaxial compressive strength f_{cm}, the uniaxial tensile strength f_{ctm}, the biaxial compressive strength f_{c2cm} and the triaxial compressive strength at one point of the compressive meridian ($\sigma_1 = \sigma_2 > \sigma_3$) described by σ_{com} and τ_{com}. In order to determine these coefficients five additional parameters have to be calculated. It must be diagnosed that the Ottosen model is not transparent.

8.4   Multiaxial states of stress: recommendations in MC2010

MC2010 (2013) writes: "Basically, yield functions f can be chosen based on multiaxial failure criteria for concrete. These criteria should depend not only on shear stresses, but also on the first invariant I_1 of the stress tensor to consider the influence of the hydrostatic pressure on the ductility of the materials. Thus, formulations as

- the Rankine criterion, where tensile failure occurs when the maximum principal stress reaches the uniaxial tensile strength,
- Drucker-Prager criterion, which is modification of von Mises criterion including the influence of hydrostatic pressure on yielding,
- Mohr-Coulomb criterion, where the maximum shear stress is the decisive measure of yielding, and the critical shear stress value depends on hydrostatic pressure, and
- modifications or combinations of them

can be used in concrete plasticity models. Concrete is a frictional material."

Some comments:

- Rankine criterion is valid not only in tension-tension sector but in all other sectors, too. Extended Rankine-type failure criteria for concrete was proposed recently by the Author (2022).
- Mohr's model does not consider the influence of the intermediate principal stress.
- Concrete is not a frictional material. The failure in compression, too, occurs in form of discrete tensile cracks, relative displacements which could induce friction stresses do not occur at all, or at a 'late' stage of the load- and deformation state only where the crack widths are already so large that only very limited frictional stresses can occur.

Here elementary further research is still needed!

9.   STRESS FAILURE CRITERION FOR BIAXIAL STATE OF STRESS

9.1   Ratio of Compressive to Tensile Strength

In MC2010 (2013) the mean value of uniaxial tensile strength f_{ctm} in [MPa] is defined as

$$f_{ctm} = 0.3 \, (f_{ck})^{2/3} \ \text{ for concrete grades} \leq C50 \tag{1}$$

$$f_{ctm} = 2.12 \cdot \ln(1 + 0.1 \cdot (f_{ck} + 8)) \quad \text{for concrete grades} > C50. \tag{2}$$

Windisch (2021) defined the ratio
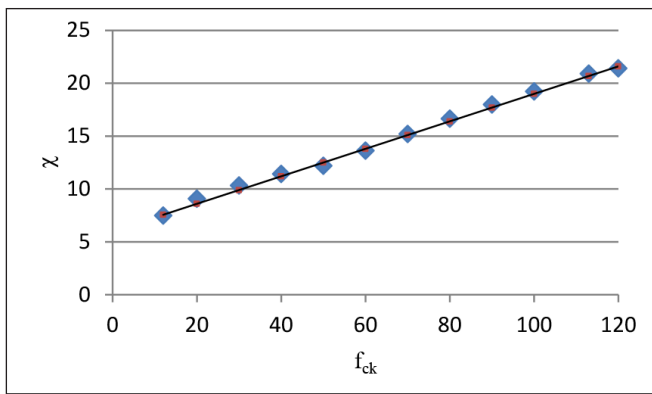
$$\chi = f_{ck}/f_{ctm} \tag{3}$$

Fig. 12: Ratio of compression strength to tensile strength (χ) as function of f_{ck}

i.e. the mean value of uniaxial tensile strength f_{ctm} as function of the characteristic compressive strength, f_{ck} (*Fig. 12*).

Fig. 12 reveals that the simple linear function

$$\chi = 0.13\, f_{ck} + 6 \tag{4}$$

describes quite exactly the interrelation of tensile to compressive strengths hence $f_{ctm} = f_{ck}\,/\,\chi$.

9.2 Compression-tension-, tension-tension sectors

Here the criteria deduced empirically by Kupfer is the most known one. An elliptical relationship between the two (principal) stresses σ_1 and σ_2 is proposed by Kupfer in case of high transversal compressive stresses, a parabola in case of low ones.

Fig. 13a shows the original figure of Kupfer about the strength development in the compression-tension- and tension-tension sectors. As the vertical axis is made dimensionless with σ_1/β_p, the three concrete grades yield three different curves. With reference to the proposed χ-ratio defined in Chapter 9.1 the dimension of the vertical axis is changed to f_{ct}^* / f_{ct}. Figure 13b shows the curves for the two lower strength concretes. The courses of the two curves can be quite well described with

$$\left(\frac{f_c'^*}{f_c'}\right)^2 + \left(\frac{f_{ct}^*}{f_{ctm}}\right)^2 = 1 \tag{5}$$

Applying Eq. (5)

$$\left(\frac{f_c'^*}{f_c'}\right)^2 + \left(\frac{\chi \cdot f_{ct}^*}{f_c'}\right)^2 = 1 \tag{5a}$$

or
$$(f_c'^*)^2 + (\chi \cdot f_{ct}^*)^2 = f_c'^2 \tag{5b}$$

Ritter tested Ultra High Performance concretes (with short, 2.5% Vol%, 15 mm long steel fibers) having cube (100mm) strength between 170 and 180 N/mm². Figure 13c shows his test results (with very low γ) values.

A comparison of the test results gained on specimens with extreme different strengths let conclude that Eq. (5) describes fairly well the 2D compression-tension behavior of all types of concrete.

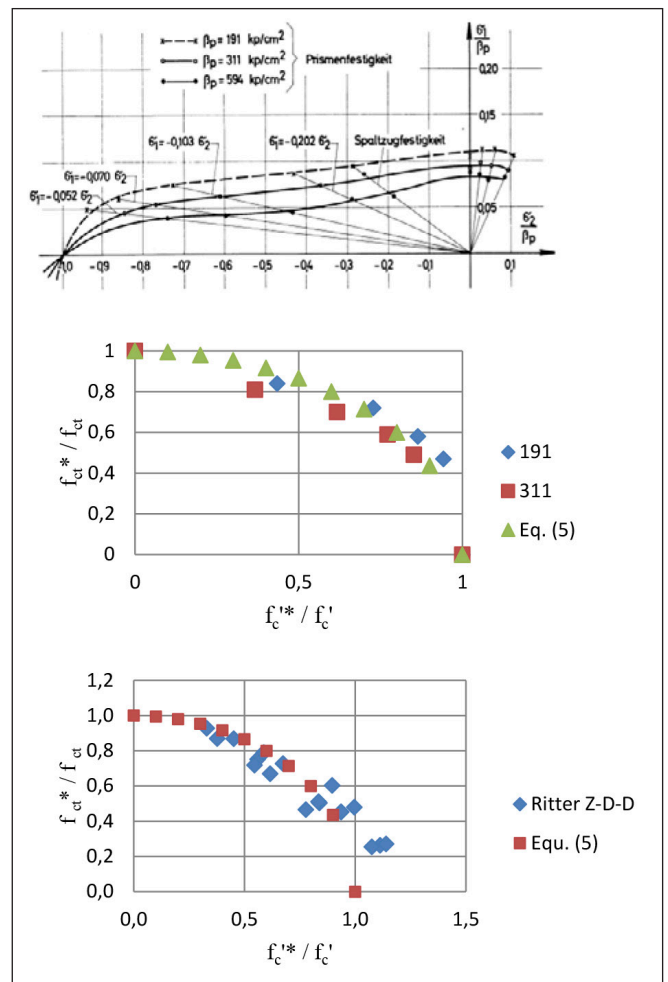Note: The question arises whether at transition from the

Fig. 13a Mean values of Kupfer′s test results in compression-tension and tension-tension sectors (with permission of DAfStb, Berlin)
Fig. 13b New type representation of Kupfer′s test results
Fig. 13c New type representation of Ritter′s test results in tension-compression sector (γ ~0.01 – 0.075)

sector compression-tension into compression-compression the curve should be smooth or might have a kink. As shown in *Fig. 13a*, Kupfer (1973) suggests a smooth transition. Nevertheless, as the types of failure in these two sectors are fundamentally different, there must be a kink.

In biaxial tension-tension tests the direction with the lower actual tensile strength fails. Here too, the tensile failure patterns pertaining to the two directions are completely independent of each other hence failure occurs in that direction where first the actual tensile strength is reached. "Biaxial tensile strength" does not exist (Lemnitzer et al. (2008)).

9.3 BIAXIAL COMPRESSIVE LOADING

The impending failure of the concrete body in the hydraulic loading equipment is recognized by the fact that, if the amount of hydraulic oil flowing through the valve per unit time is not changed then with less-and-less increasing load increasing deformations occur: the stiffness of the specimen more-and-more decreases. The decrease of the stiffness occurs due to development of more and more microcracks which merge to discrete macrocracks.

The different crack patterns 'produce' different elongated, slim concrete elements which fail at slightly different strengths.

In biaxial compression the discrete macrocracks develop in a prismatic specimen mostly perpendicular to the stress free principal axis and also perpendicular to the axis of the intermediate compressive stress-loading (in case of low transverse loading rate, i.e. $\lambda \leq 0.4$)

In biaxial loading tests the biggest ultimate compressive strength was found around the size $\lambda \approx 0.4$ of the intermediate loading. The explanation can be given on the basis of the measured relative deformations (Kupfer (1973), Speck (2007), Ritter (2014)) as shown in *Fig. 6*.

The course of the intermediate ε_{2u} relative deformations changes its sign around $\lambda \approx 0.4$. In case of $0 \leq \lambda \leq 0.4$ the rate of the transverse (Poisson-type) elongations due to the intermediate loading perpendicular to the axis 1 decreases, i.e. the achievable compressive strength in direction 3 increases. Beyond $\lambda \approx 0.4$ the relative deformations (shortenings) in direction of the intermediate loading increase which more and more contributes to the tensile deformations (development of micro- and discrete macrocracks) perpendicular to the axis 1, therefore the achievable compressive strength, σ_{3u}, decreases again.

10. THE PROPOSED EXTENDED RANKINE FAILURE CRITERIA

After recognizing of the fundamental importance of the principal stresses and that the failure behavior of concrete makes no reference to any friction-type behavior an Extended Rankine Failure Criteria (ERFC) was proposed by the Author (Windisch (2022)).

Rankine (1868) stated in his in 1876 published model that a body fails when any of the three principal stresses exceeds the ultimate tensile strength, regardless of the magnitude of the other principal stresses. It was obvious to extend this criterion to the compressive principal stresses, as well:

- the greatest (> 0) principal stress, σ_1, cannot be greater than the actual tensile strength (its size depends on the size of the σ_2 and σ_3 principal stresses, resp. if at least one of them is compressive stress. (In case of the original Rankine criterion one (fix) tensile strength governed.)
- the triple of the compressive principal stresses $\sigma_3 = \Phi(\sigma_1, \sigma_2)$ cannot be smaller than the actual smallest principal strength, σ_3, which is function of the two other principal stresses,

$$\sigma_3 = \Phi (\sigma_1, \sigma_2) \tag{6}$$

Fig. 14 shows the local ordinates of normalized $-\sigma_3/f_c' = \Phi (\sigma_1/f_c', \sigma_2/f_c')$ function as deduced from the bi- and triaxial tests measured by Speck (2007) on $f_c' = 72$ N/mm² test specimens.

Fig. 15 presents the Ultimate Strength Surface, USS, in another form: the abscissa is $\gamma = \sigma_1 / \sigma_3$, the ordinate is $\lambda = \sigma_2 / \sigma_3$. The USS increases monotonic in the γ-direction, whereas increases up to $\lambda = 0.4 \sim 0.6$ then decreases moderately.

Having determined the relevant failure causing principal stresses the corresponding normal- and shear stress components in the global coordinate system can be determined using Mohr-circles or the tensor calculus. Note: the global shear stress components calculated from the failure causing principal stresses refer by no means to any shear failure!

11. CALIBRATION OF THE STRENGTH FAILURE CRITERIA IN MC 2010

Following the proposals of Ottosen (1977), MC 2010 (2013) uses four strength values for calibration: the uniaxial tensile strength, the uniaxial compressive strength (point on the compressive meridian), the biaxial compressive strength (point on the tensile meridian), and a triaxial compressive strength at one point on the compressive meridian ($\sigma_1 = \sigma_2 > \sigma_3$) described by the octahedron stresses. The red arrows in *Fig. 14* mark these strength values revealing that they are not suitable for describing the USS.

Note: Kupfer's biaxial strength curves reveal that even the uni- and biaxial strength values are absolute not representative for the course. Also the strength values along the compressive meridian are of very limited informative value. The maximum strength increase could be anticipated with $\gamma = \lambda = 0.5 \sim 0.6$. With her very advanced test equipment Speck achieved $\gamma = \lambda = 0.15$ only. The double-curved surface of the USS does not allow any reliable extrapolation relying on $\gamma = \lambda = 0$ and $\gamma = \lambda = 0.15$ values. Here further tests are necessary.

Fig. 14: *Local ordinates of normalized $-\sigma_3/f_c' = \Phi(\sigma_1/f_c', \sigma_2/f_c')$ function as deduced from the bi- and triaxial tests measured by Speck (2007) on $f_c' = 72$ N/mm² test specimens*
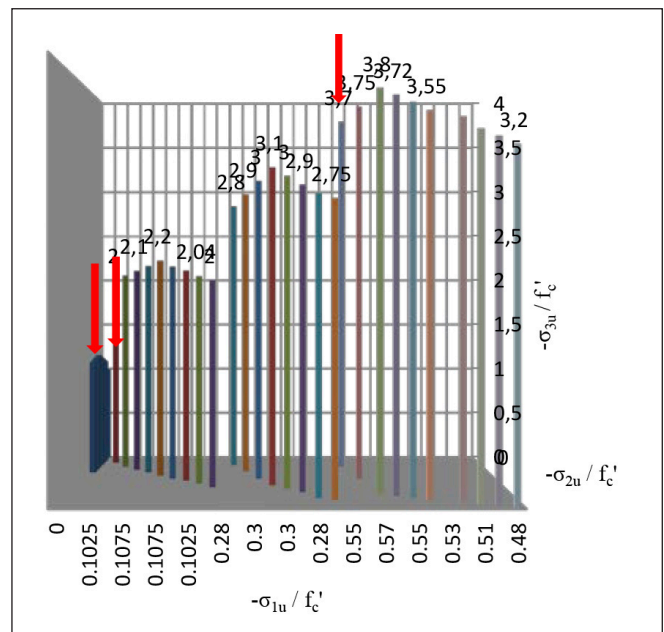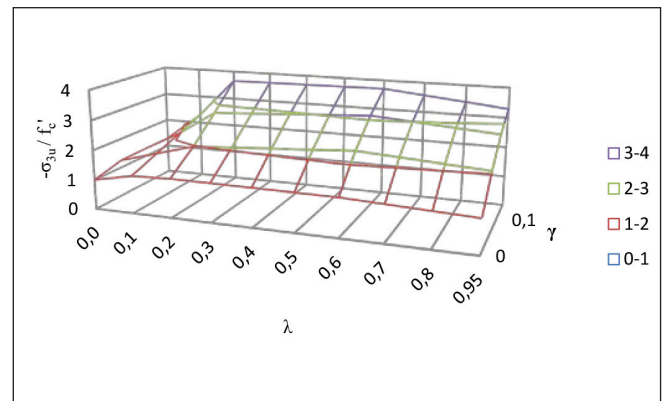

Fig. 15: *The Ultimate Strength Surface compiled from the data measured by Speck (2007)*

12. CONCLUSIONS

The development of the failure models corresponds to the possibilities of the testing equipment and follows the achievements of the numerical calculation methods.

All experiments, also the uniaxial ones, are/must be essentially considered as tri-axial. Concrete knows/obeys principal stresses only. Concrete does not have any shear strength. Shear stress is the consequence of our hugging to the global coordinate system only.

Based on the principal stresses and their relationship i.e. the loading paths as independent variables, a new, transparent (and physically really sound) form of representation of the failure surface (USS) showing the strength increase due to bi- and triaxial loading is presented. This paper focus on the increasing branch of the stress-strain curve up to the peak stress only.

Any target triaxial ultimate strength can be reached following the loading path only: with a biaxial loading an increase of maximum 10-20% can be achieved only. Beyond this level loading/strain restriction in the third direction is necessary to let increase the maximum compressive strength in the 'main/leading' direction. Simplified relative strength increasing factors for concrete classes $\leq$ C100 are presented.

Problems and difficulties at deformation measurements are discussed. At evaluation of the strength- and strain values the impact of the loading equipment and the measuring methods must be considered: the elongations refer to development of pronounced discrete cracks, nevertheless remarkable compressive loading is transmitted perpendicular to this (these) cracks. Further systematic tests are necessary.

Reference is made that due to intense development of discrete cracks rules of continuum mechanics shall be applied with reservation. As failure modes the tensile failure and compression failure after splitting are identified. The 'shear' failure occurs due to deviations in the loading system only. A simple stress failure criterion is proposed for biaxial compression-tension loading. The tensile strengths in the three principal directions are independent from each other.

Extended Rankine Failure Criteria is presented: i) the greatest (> 0) principal stress, σ_1, cannot be greater than the actual tensile strength, ii) the triple of the compressive principal stresses $\sigma_3 = \Phi(\sigma_1, \sigma_2)$ cannot be smaller than the actual smallest principal strength, σ_3, which is function of the two other principal stresses. The calibration of the strength failure criteria in MC2010 is discussed.

Further systematic tests are needed before more reliable failure criteria could be formulated for multiaxial loaded concrete.

13. REFERENCES

Comité Euro-international du Béton, (1983) Bulletin d'information N° 156: Concrete under multiaxial states of stress. "Constitutive equations for practical design ». Contribution à la 23e Session plenière du C.E.B. Prague – Octobre 1983, Juin 1983, p. 149.

Drucker, DC, Prager, W., (1952), "Soil Mechanics and Plasticity Analysis of Limit Design". Quarterly of Applied Mathematics, 1952; Vol. 10, No. 2, 157-165. https://doi.org/10.1090/qam/48291

fib Model Code for Concrete Structures 2010 (MC2010), (2013), Fédération international du béton, Oct. 2013, Ernst & Sohn, Berlin, p. 434. https://doi.org/10.1002/9783433604090

Hillerborg, A., Modéer, M., Peterson, P.E. (1976), "Analysis of crack formation and crack growth in concrete by means of fracture mechanics and finite elements", Cement and Concrete Research, 1976; Vol. 6, 773-782. https://doi.org/10.1016/0008-8846(76)90007-7

Hilsdorf, H., (1965) Versuchstechnische Probleme beim Studium der zweiachsigen Festigkeit des Betons. Sonderdruck, 1965; Heft 173 der Schriftenreihe des Deutschen Ausschusses für Stahlbeton.

Kármán von, Th., (1910), "What determines the stress-strain behavior of materials?" (In Hungarian: Mitől függ az anyag igénybevétele?), Journal of the Society of Hungarian Engineers and Architects, 1910; Vol. XLIV, No. X, 212–226

Kupfer, H. (1973), „Das Verhalten des Betons unter mehrachsiger Kurzzeitbelastung unter besonderer Berücksichtigung der zweiachsigen Beanspruchung", Deutscher Ausschuss für Stahlbeton, 1973; Heft 229, Ernst und Sohn, Berlin, p. 105.

Newman, K, Siqvaldason, OT. (1965), "Testing machine and specimen characteristics and their effect on the mode of deformation, failure and strength of materials". Proc. Inst. Mech. Engrs., 1965-66, Vol. 180, part 3A, pp. 399-410. https://doi.org/10.1243/PIME_CONF_1965_180_048_02

Lemnitzer, L, Eckfeldt, L, Lindorf, A, Curbach, M., (2008), "Biaxial strength of concrete – answers from statistics in Tailor Made Concrete Structures" – Walraven & Stoelhorst (eds). 2008; ISBN 978-0-415-47535-8, pp. 1101-1002.

Ottosen, NS., (1977), "A Failure Criterion for Concrete". Journal of Engineering Mechanics, Div. ASCE, 1977; Vol 103, EM4. https://doi.org/10.1061/JMCEA3.0002248

Rankine, WJM, (1868) A Manual of Applied Mechanics. 1868; London

Ritter, R. (2014), „Verformungsverhalten und Grenzflächen von Ultrahochleitsungsbeton unter mehraxialer Beanspruchung", Dissertation, 2014; TU Dresden, p. 280.

Speck, K., (2007), „Beton unter mehraxialer Beanspruchung. Ein Materialgesetz für Hochleistungsbetone unter Kurzzeitbelastung, Concrete under multiaxial loading conditions. A Constitutive Model for Short-Time Loading of High Performance Concretes". Dissertation, 2007; TU Dresden, p. 224.

Stroeven, P., (1973), "Some aspects of the micromechanics of concrete". Dissertation, 1973; Delft.

Van Mier, JGM. (1984), "Strain-Softening of Concrete under Multiaxial Loading Conditions", Dissertation, TH Eindhoven, 1984; p. 363.

Windisch A, (2021).." The tensile strength: the most fundamental mechanical characteristics of concrete". Concrete Structures, 2021; Vol. 22, pp. 1-4. https://doi.org/10.32970/CS.2021.1.1

Windisch, A., (2022), "Extended Rankine Failure Criteria for Concrete". Concrete Structures, 2022; Vol. 23, pp. 4-10, https://doi.org/10.32970/CS.2022.1.2

NOTATIONS

I_1	first invariant of the stress tensor;
J_2, J_{2c}, J_3, J_{3c}	second and third invariants of the stress deviators
f	yield function (MC2010)
f_c'	concrete compressive strength
f_c^*, f_{ct}^*	compressive and tensile stresses in 2D and/or 3D loading
f_{ck}	characteristic concrete compressive strength
f_{cm}, f_{ctm}	mean compressive and tensile strength, resp.
f_{c2cm}	biaxial compressive strength
α, β, c_1 and c_2	material parameters (Ottosen)
β	prism strength (Kupfer)
$\varepsilon_{1u}, \varepsilon_{2u}, \varepsilon_{3u}$	ultimate strains in principal directions 1 to 3
$\gamma = \sigma_1 / \sigma_3$	loading parameter
ε_i	strain measured in test
ε_{iu}	ultimate strain measured in test in i^{th} principal direction
$\lambda = \sigma_2 / \sigma_3$	loading parameter
Φ	relative ultimate strength as function of the loading path
$\chi = f_{ck}/f_{ctm}$	ratio of characteristic concrete compressive strength to mean tensile strength
$\sigma_1, \sigma_2, \sigma_3$	principal stresses ($\sigma_1 \geq \sigma_2 \geq \sigma_3$)
σ_{3u}	ultimate strength measured in test
σ_{com}	hydrostatic normal stress
τ_{com}	octahedral shear stress
$[\gamma, \lambda, 1]$	stress-loading path
$[1, 1, \sigma_{c3u}]$	ultimate hydrostatic normal strength (cap value)

Andor Windisch PhD, Prof. h.c. retired as Technical Director of DYWIDAG-Systems International in Munich, Germany. He made his MSc and PhD at Technical University of Budapest, Hungary, where he served 18 years and is now Honorary Professor. Since 1970 he is member of different commissions of FIP, CEB, *fib* and ACI. He is author of more than 190 technical papers. Andor.Windisch@web.de

BME, Dept. of Construction Mats. and Techns.
Head of Dept. for the period of 1999-2018 (19y)

Közlekedéstud.
Egyesület (KTE)

Magyar
Szabványügyi
Testület (MSZT)

fib Hungary
fib HU Head 1998 – (26y)
fib President (2011-2012)

Editor-in-Chief 1999- (25y)

Initiator of the Int. PhD Symp.
in Civil Eng. 1996-   (27y),
supported by CEB then *fib*

Editor-in-Chief 2000-   (24y)

CONCRETE TOWARDS A SUSTAINABLE FUTURE
KORSZERŰ BETONELEMEK A FENNTARTHATÓ JÖVŐ ÉRDEKÉBEN
on the occasion of
Prof. György L. Balázs 65th birthday
*BME, **fib** Honorary President*

PROGRAM

2023. ápr. 28. (p) – *28 April 2023 (Friday)* – **BME K 1st Floor, Room 3 Díszterem + Online**
H-1111 Budapest, Műegyetem rkp., 3
Co-ordinator: Dr. Sándor Sólyom
Technical editor: András Biró, PhD student
Registration - Jelentkezés: https://forms.gle/WDbKThXBzhsCTWzCA
Online Teams Code: https://tinyurl.com/5473cwpv, Meeting ID: 339 886 675 535

Kövér szedés mutatja az előadás nyelvét – ***Bold** charachters indicates language of the presentation*
Konferencia részvétel ingyenes, de regisztrációt igényel. *Conference is free, just needs registration*

Levező elnök - Chairmen: Assoc. Prof. Olivér Fenyvesi and Szabolcs Szinvai, PhD student, fib-HU YMG Chair

9:00-9:10 CEST	**Prof. Levendovszky János,** Vice-Rector for Science and Innovation (BME)	BME Tudományos és innovációs rektorhelyettesi megnyitó	**Opening by the Vice-Rector for Science and Innovation of BME**
9:10-9:20	**Assoc. Prof. Szabolcs Rózsa,** Dean of Fac. of Civil Engineering (BME)	Az Építőmérnöki Kar dékánjának megnyitója	**Opening by the Dean of Faculty of Civil Engineering at BME**
9:20-9:30	**Prof. László Kollár,** Secretary General of Hungarian Academy of Sciences (MTA), Head of PhD School in Civ. Eng.	Doktori kutatások elősegítése fiatal kutatók számára	**Supporting PhD research for young engineers**
9:30-9:50	**h. Prof. Andor Windisch** (BME) - online	Tapadás és repedések – összekapcsolnak bennünket több, mint 40 éve	**Bond and cracking – link us since more than 40 years**
9:50-10:10	**Dr. Akio Kasuga, Executive Vice President, *fib*** President 2021-2022 (Sumitomo Mitsui Construction Co.)	A jövő megoldásai az előregyártott vasbeton szerkezeteeknél	**Possibilities in the Future of Precast Construction**
10:10-10:30	**Prof. em. Harald S. Müller, *fib*** President 2015-2016 (Karlsruhe Institute of Technology, SMP Eng.)	Környezetvédő betonok - a tervezés alapelvei szerkezeti anyagok és elemek vonatkozásában	**Green concretes – Principle design approaches for materials and members**
10:30-10:45	**Prof. Konrad Bergmeister** (University of Natural Resources, Vienna)	Hidak tervezésének új módszerei – a lehetséges legegyszerűbb, de nem annál is egyszerűbb módszer	**Novel concrete bridge design - as simple as possible, but not simpler**
10:45-11:00	**Prof. Marco di Prisco** (Politecnico di Milano)	SFRC in EC2-ben és a MC 2020-ban	**SFRC in EC2 and in MC 2020**
11:00-11:15	**Prof. Jan Vítek** (Czech Techn. University in Prague)	UHPC fejlesztés és alkalmazás Csehországban	**Development and application of UHPC in Czechia**

| 11:15-11:25 | | Hozzászólások – *Discussion* | | |
| 11:25-11:45 | | Kávészünet / Coffee break | | |

11:45-12:00	**Gordon Clark,** *fib* President 2013-2014, (Ramboll retired) - online	Az utófeszítés története vasbeton hidak esetében	**History of Post-Tensioning in Concrete Bridges**
12:00-12:10	**Prof. Sherif Yehia,** Univesity of Sharjah (UEA) - online	Újrafelhasznált adalékanyaggal készülő beton szerkezeti alkalmazások céljából	**Concrete with Recycled Aggregate for Structural Applications**
12:10-12.25	**Dr. David Fernandez-Ordonez** (EPFL Lausanne), *fib* Secretary General	Fenntarthatóság the *fib* Model Code 2020-ban	**Sustainability in the *fib* Model Code 2020**
12:25-12:40	**Prof. Tamás Nagy-György** (Politechnica Univ. Timisoara)	Szerkezetek megerősítése szálerősítésű polimerekkel – temesvári emlékek, eredmények	**Use of FRP composites for structural strengthening – Results from Timisoara**
12:40-12:55	**Assoc. Prof. Zsuzsa Szalay,** Deputy Head of Dept. BME)	Építőanyagok és épületek környezeti hatásának értékelése	**Environmental assessment of building materials and buildings**
12:55-13:10	**Assoc. Prof. Éva Lublóy** (BME)	**Anyagvizsgálati lehetőségek a számítógépes tomografiával**	**Possibilities in material testing by Computed Tomograpy**

| 13:10-13:45 Rövid köszöntések – Short greetings (3 min each) | **Assoc. Prof. Kovács Tamás**, *fib* Secretary (*fib* HU) (BME) **Dr. Sólyom Sándor,** *fib* Deputy Head of Delegation (*fib* HU) (BME) **Magyar János,** műszaki igazgató, *fib* PR (A-Híd Zrt.) (*fib* HU) **Dr. Madaras Gábor,** former *fib* Deputy Head of Delegation (*fib* HU) **Prof. Köllő Gábor,** elnök (EMT) **Nyiri Szabolcs**, elnök (MAÚT) **Sitku László**, elnök (Hidászokért Egyesület) **h. Assoc. Prof. Arany Piroska,** retired (BME) **h. Prof. Józsa Zsuzsanna,** retired (BME) **Prof. Kiss Rita**, tanszékvezető, Depart. of Mechatronics, Optics and Mechanical Eng. Informatics (BME) **Dr. Szabó Zsombor,** former PhD student (Maroshévíz) **Bedics Antal**, Hídiroda igazgató (Uvaterv Zrt.) **Dubrovszky Gábor** (Ferrobeton Zrt.) **Spránitz Ferenc**, betonüzem vezető (Dolomit Kft.) **Polgár László**, Senior Technical Consultant (Consolis, ASA Ép.ip. Kft.) **Dr. Galaskó Gyula**, (MAFC Vitorlás Szakosztály) **Czintos Csongor**, technikai igazgató (PERFYCOMP Zrt.) – online **Bernáth Csaba**, szakreferens MSZT 107 Bizottság (MSZT) – online **Kolozsi Gyula** (Singapur) – online **Dr. Czoboly Olivér**, former PhD student, termék portfólió vezető (BTC) **Dr. Naser Alimrani**, former PhD student (Sherbrook University, Canada) … | | |

| 13:45-13:55 | | Hozzászólások – *Discussion* | | |
| 13:55-14:40 | | Ebédszünet / Lunch break | | |

Levezető elnök - Chairman: Assoc. Prof. Nehme Salem

14:40-15:00	**Assoc. Prof. Nehme Salem,** Head of Dept. (BME)	**Tanszéki barangolásaim Balázs L. Györggyel**	My journeys together with György L. Balázs in technical fields
15:00-15:15	**Prof. em. Patonai Dénes** (BME)	**Építészek és mérnökök egymásra utaltsága**	Need for cooperation of architects an civil engineers
15:15-15.30	**Prof. Gálos Miklós,** retired (BME)	**Betonadalékanyag – minek nevezzelek?**	Concrete aggregate – what should I call you?
15.30-15:45	**h. Prof. Kausay Tibor** (BME)	**Képek az OC-görbe megismeréséről és egyebekről…**	Bilder über Erkenntnisse der OC-Kurve und andere…”
15:45-16:00	**Assist. Prof. Árpád Cseh** (Univ. Novi Sad, Fac. of Civil Engineering, Subotica)	**Nagy teljesítőképességű beton mezőgazdasági épületekhez**	Towards the implementation of UHPC in agricultural buildings
16:00-16:15	**Assoc. Prof. Orbán Zoltán** (PTE)	**Történeti épületek és hidak állapotvizsgálata roncsolásmentes diagnosztika felhasználásával**	Condition assessment of historic buildings and bridges using non-destructive diagnostics
16:15-16:40	**Assoc. Prof. Nemes Rita** (BME) **Assoc. Prof. Kovács Tamás** (BME)	**Könnyűbeton hídgerendák lehetőségei és kérdései**	Ligweight concrete bridge girders – potentials and questions
16:40-16:55	**Assoc. Prof. Fenyvesi Olivér** (BME)	**Hulladékok és másodnyersanyagok felhasználása az építőiparban**	Use of waste and secondary raw materials in the construction industry
16:55-17:10	**Assoc. Prof. Paládi-Kovács Ádám** (BME)	**Építészet és beton**	Architecture and concrete

| 17:10-17:20 | *Hozzászólások – Discussions* |

| **17.10-17.20 Prof. Balázs L. György (BME):** **A konferencia nap zárása – *Summary. Conclusions. Closing of the conference.*** |

Előadások publikálásra benyújthatók a VASBETONÉPÍTÉS folyóirathoz: ***http://fib.bme.hu/kiadvanyok.html***

The written form of the contribution can be submitted to CONCRETE STRUCTURES Journal for publication:
http://fib.bme.hu/kiadvanyok.html

LÁBATLANI VASBETONIPARI ZRT.

Since 1942

Member of the RAILONE GROUP
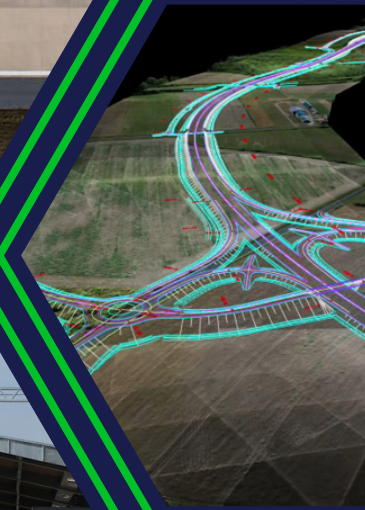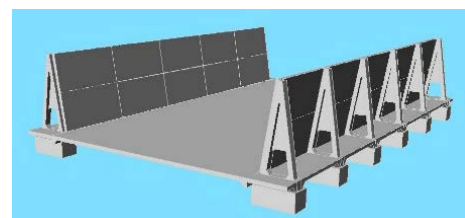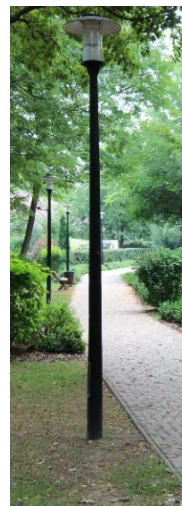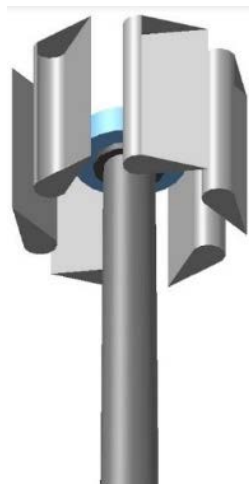
#railway sleepers #turnout sleepers #narrow gauge sleepers #platform elements #panel elements for urban transit #composite sleepers #lighting poles #upperline poles #wind generator poles #energy poles #agricultural elements #fence elements #statue pedestal and other unique products

Lábatlani Vasbetonipari Zrt. www.railone.hu